Engineering Geological Investigation of the Lake Coleridge Rock Avalanche Deposits, Inland Canterbury

---

A thesis
submitted in partial fulfilment
of the requirements for the degree
of
Master of Science in Engineering Geology
at the
University of Canterbury
By

Jenny Alice Lee

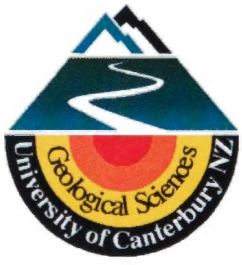

Department of Geological Sciences
University of Canterbury
December 2004

Frontispiece

View of Carriage Drive and adjoining Cottons Sheep Range from the Harper Road in the early morning. An ephemeral pond provides a mirror image of the Lake Coleridge Rock Avalanches' source basin.

Abstract

The Lake Coleridge Rock Avalanche Deposits (LCRADs) are located on Ryton Station in the middle Rakaia Valley, approximately 80 km west of Christchurch. Torlesse Supergroup greywacke is the basement material and has been significantly influenced by both active tectonics and glaciation. Both glacial and post-glacial processes have produced large volumes of material which blanket the bedrock on slopes and in the valley floors. The LCRADs were part of a regional study of rock avalanches by WHITEHOUSE (1981, 1983) and WHITEHOUSE and GRIFFITHS (1983), and a single rock avalanche event was recognised with a weathering rind age of 120 years B.P. that was later modified to 150 ± 40 years B.P. The present study has refined details of both the age and the sequence of events at the site, by identifying three separate rock avalanche deposits (termed the LCRA1, LCRA2 and LCRA3 deposits), which are all sourced from near the summit of Carriage Drive.

The LCRA1 deposit is lobate in shape and had an estimated original deposit volume of 12.5 x 10^6 m^3, although erosion by the Ryton River has reduced the present-day debris volume to 5.1 x 10^6 m^3. An optically stimulated luminescence date taken from sandy loess immediately beneath the LCRA1 deposit provided a maximum age for the rock avalanche event of 9,720 ± 750 years B.P., which is believed to be realistic given that this is shortly after the retreat of Acheron 3 ice from this part of the valley. Emplacement of rock avalanche material into an ancestral Ryton riverbed created a natural dam with a ~17 M m^3 lake upstream. The river is thought to have created a natural spillway over the dam structure at ~557 m (a.s.l), and to have existed for a number of years before any significant downcutting occurred. Although a triggering mechanism for the LCRA1 deposit was poorly constrained, it is thought that stress rebound after glacial ice removal may have initiated failure. Due to the event occurring c.10,000 years ago, there was a lack of definition for a possible earthquake trigger, though the possibility is obvious.

The LCRA2 event had an original deposit volume of 0.66 x 10^6 m^3, and was constrained to the low-lying area adjacent to the Ryton River that had been created by river erosion of the LCRA1 deposit. Further erosion by the Ryton River has reduced

the deposit volume to 0.4 x 10^6 m^3. A radiocarbon date from a piece of mānuka found within the LCRA2 deposit provided an age of 668 ± 36 years B.P., and this is thought to reliably date the event. The LCRA2 event also dammed the Ryton River, and the preservation of dam-break outwash terraces downstream from the deposit provides clear evidence of rapid dam erosion and flooding after overtopping, and breaching by the Ryton River. Based on the mean annual flow of the Ryton River, the LCRA2 lake would have taken approximately two weeks to fill assuming that there were no preferred breach paths and the material was relatively impermeable. The LCRA2 event is thought to have been coseismic with a fault rupture along the western segment of the PPAFZ, which has been dated at 600 ± 100 years B.P. by SMITH (2003).

The small LCRA3 event was not able to be dated, but it is believed to have failed shortly after the LCRA2 event and it may in fact be a lag deposit of the second rock avalanche event possibly triggered by an aftershock. The deposit is only visible at one locality within the cliffs that line the Ryton River, and its lack of geomorphic expression is attributed to it occurring closely after the LCRA2 event, while the Ryton River was still dammed from the second rock avalanche event.

A wedge-block of some 35,000 m^3 of source material for a future rock avalanche was identified at the summit of Carriage Drive. The dilation of the rock mass, combined with unfavourably oriented sub-vertical bedding in the Torlesse Supergroup bedrock, has allowed toppling-style failure on both of the main ridge lines around the source area for the LCRADs. In the event of a future rock avalanche occurring within the Ryton riverbed an emergency response plan has been developed to provide a staged response, especially in relation to the camping ground located at the mouth of the Ryton River. A long-term management plan has also been developed for mitigation measures for the Ryton riverbed and adjacent floodplain areas downstream of a future rock avalanche at the LCRAD site.

Acknowledgements

Tim Davies (principal supervisor) thank you for your continued support this year and all the really interesting talks. You have an exceptionally interesting field of study and you also have a fabulous ability to ask questions of which I don't know the answers to! Thank you for all your help.

David Bell (secondary supervisor) thank you for your invaluable contribution to my work and for all the help over the years. You're an extremely busy person but with a bit of persuasion you never failed to provide incredibly valuable constructive criticism of my work. And your red pen usage to mark drafts has become legend. The financial aid you gave to my project was also most appreciated. Thank you very much for all your help.

Mike and Karen Mears (Ryton Station owners), thank you for allowing me to carry out my fieldwork on your property and for the trench excavations – much appreciated Mike.

Margaret and Bruce Lee (mum and dad), thank you so much for your immense support over the years I've been up here at university. It's been a huge support and relief knowing that you're only an hour away. Particularly for this year, thanks for allowing me to use your prized truck dad, and for the huge meals mum when I arrived from the field unexpected. Thank you to both of you – it's been a long five years but we have all made it and I wouldn't have changed a single thing. To my sisters Janine and Cherie and also my Gran, thank you very much for your interest and support.

The technicians are a wonderful attribute to this department. Cathy Knight (Engineering Geology technician) thank you for your help and patience in teaching me how to use gear (particularly the GPS) at short notice and for giving me gear I needed for my fieldwork. Rob Spiers, the same goes for you, and you're a superb cabinet maker! John Southward (the electronic and computer technician), thanks for all your assistance with the technical trouble that I undoubtedly ran into. Arthur Nicolas, for your help with drafting diagrams and for the outstanding driving reviews that nobody could quite believe! Jane Guise, thank you so much for your help with grain size analysis towards the end, much appreciated. I feel very fortunate to have gotten to know you guys over the years here and will miss you all very much when I'm finished.

I would really like to thank the administrative staff within the department. Both Julie-Ann and now Pat and also Janet have all been a fantastic help. Their knowledge of the bureaucracy within the department quite often fast tracked many things that could have taken a lot longer. Thank you so much for all your help, I really appreciated it. Also a huge thank you to Alison Johnston (librarian at the Central Library) for all your help and for your sixth sense at finding books and journals within the library when no one else can.

Academics which also contributed to my project: Dr Mauri McSaveney and his wife Dr Eileen McSaveney for taking time out of your busy schedule to come up and see my site. Phil Tonkin for your help in the field and helpful advice on soils and loess. Jamie Schulmeister and Henrik Rother for your glacial chats. Nigel Newman for

organic matter identification. Jocelyn Campbell, for your structural chats and Jarg Pettinga for structural references and papers. Thank you.

Fellow postgraduates: Guyon Smith for all your initial help and passing down of knowledge and for help out in the field (especially those nasty trench logging episodes). You were a huge all-round help that really kick started my project, thank you very much. Tim Nash thank you for providing me with numerous references. Leah Bateman thank you for accompanying me out in the field for the first of many bush-bashing expeditions through the matagouri. Joyce Seale thank you for also accompanying me out into the field to GPS and carry gear back and forth to various sites and for all the pep talks. Jeff and Joshu, thank you for your field assistance. And Perla J. Delos Reyes for formatting help.

I would also like to thank Scott and Fiona Hussey, managers (till early 2004) at Lake Coleridge Station. Thank you for the initial accommodation at the cookshop (which I soon abandoned and took refuge at my parents after having possums the size of small children running around in the attic on a nightly basis!).

And I've met some fabulous people while I've been in the department so thank you to my geology friends including: Leah, Jeni, James, Aaron, Andy, Alina, Kelly, Neil, Tom, Joyce and my office buddies P.J., Olivia and Katie. These people always acted interested about my project and humoured me when I got carried away discussing it – both good and bad. I'm going to really miss you guys and hope that we can all keep in touch in the future. I'd also like to thank my flatmates Chris, Elizabeth and Andrew. You guys have been fabulous to live with over the last two years.

Finally, I'd like to say thank you to Andrew, for your support and belief in me through these last and ultimately trying years at university. Your understanding that university took *a lot* of time out of my life allowed me to spend countless hours here guilt free! I couldn't have done it without you, you've been my anchor, and you could say my rock. Thank you also to your family for their support, encouragement, editing and employment over the years. I am incredibly indebted that I had the fortune of meeting you because you have brought sunshine to my life.

Table of Contents

List of Figures

CHAPTER 4

CHAPTER 5

List of Tables

Chapter 1

Introduction

1.1 Project Background

The middle Rakaia Valley has undergone significant changes in the past, predominantly from mountain building (orogenic) episodes and glaciations. Periodically earthquakes have rattled the mountain peaks which have not only given rise to the mountains that make up the Southern Alps through uplift, but also triggered landslides and massive rock avalanche events. Glaciations in the Late Pleistocene were the last to have effected the Lake Coleridge area in the middle Rakaia Valley, in the process eroding most of the previous glacial and geomorphological deposits away. Since the glacial retreat, extensive erosional and paraglacial processes have reshaped the landscape again. The geomorphology of the Lake Coleridge area reflects the last Late Pleistocene glaciation in the form of moraines, kettle lakes, striations, varve silts and lake beaches. On a larger scale roches moutonnées and extensive "U" shaped valleys signify glacial action in the past. The geomorphology of the last 10,000 years shows changing fluvial processes both during and after ice retreat, fan development, and most importantly from this project's perspective, large rock mass failures in the form of rock avalanche deposits.

Rock avalanches represent the large end member of a continuum of landslide types. They are large gravity driven landslides that fail catastrophically and are often coseismic. Travelling at extremely high velocities (~50 m/sec) they tend to break-up and fragment while they flow downslope. Numerous studies, particularly in the Southern Alps of New Zealand, (e.g. WHITEHOUSE (1981, 1983); WHITEHOUSE and GRIFFITHS (1983); PREBBLE (1995); ORWIN (1998)) have highlighted the fact that rock

avalanches are a significant natural process and due to their catastrophic nature and size, are an important geomorphic feature within the region.

The volume of debris displaced during rock avalanche events can be great. EISBACHER and CLAGUE (1984) note that the minimum threshold volume at which free tumbling rocks from a rockfall changes into a flowing stream of disintegrating rock mass of a rock avalanche is believed to range from 0.1×10^6 m^3 to 1×10^6 m^3. However in most studies the minimum volume described for forming rock avalanches is 1×10^6 m^3 (WHITEHOUSE and GRIFFITHS, 1983), with the deposits riding over valley floor topography and commonly up opposing valley slopes. A common consequence of rock avalanche deposit emplacement is the instantaneous delivery of sediment to drainage networks (BESCHTA, 1983; HOVIUS *et al.*, 1997). A relatively recent focus of rock avalanche research has been the sediment flux in alpine rivers and associated sediment yields (e.g. KORUP *et al.*, 2004; PEARCE and WATSON, 1986). Geomorphic impacts from rock avalanches include valley floor destruction, channel alteration, large-scale fanhead avulsions (KORUP *et al.*, 2004), and the creation of natural dams (e.g. ADAMS, 1981; SCHUSTER, 1983; NASH, 2003).

The Lake Coleridge Rock Avalanche Deposit (LCRAD) is located near the mouth of the Ryton River, adjacent to eastern shores of Lake Coleridge in inland Canterbury (figure 1.1). The source is a small dislocated summit of the Cottons Sheep Range called Carriage Drive which takes its name from the wide fault scarp of the Carriage Drive Fault that crosses the northeastern slope. The LCRAD is located ~350 m north of the Ryton Homestead on Ryton Station, and is one of the rock avalanche deposits identified in a large-scale study in the Southern Alps (WHITEHOUSE and GRIFFITHS, 1983). On closer inspection there are three separate rock avalanche deposits (as identified in this study) that are all or partly superimposed on each other. Unless otherwise stated, the term LCRAD refers to all three rock avalanche deposits.

The trigger mechanism for the LCRAD failures is considered to be seismic shaking during regional earthquake events, and this hypothesis has been investigated in the present study. This is based on the working model that rock avalanches occur during earthquakes and fail in regional "clusters" (e.g. WHITEHOUSE and GRIFFITHS, 1983; ORWIN, 1998 and SMITH, 2003). Rock avalanches can also occur following glacial ice

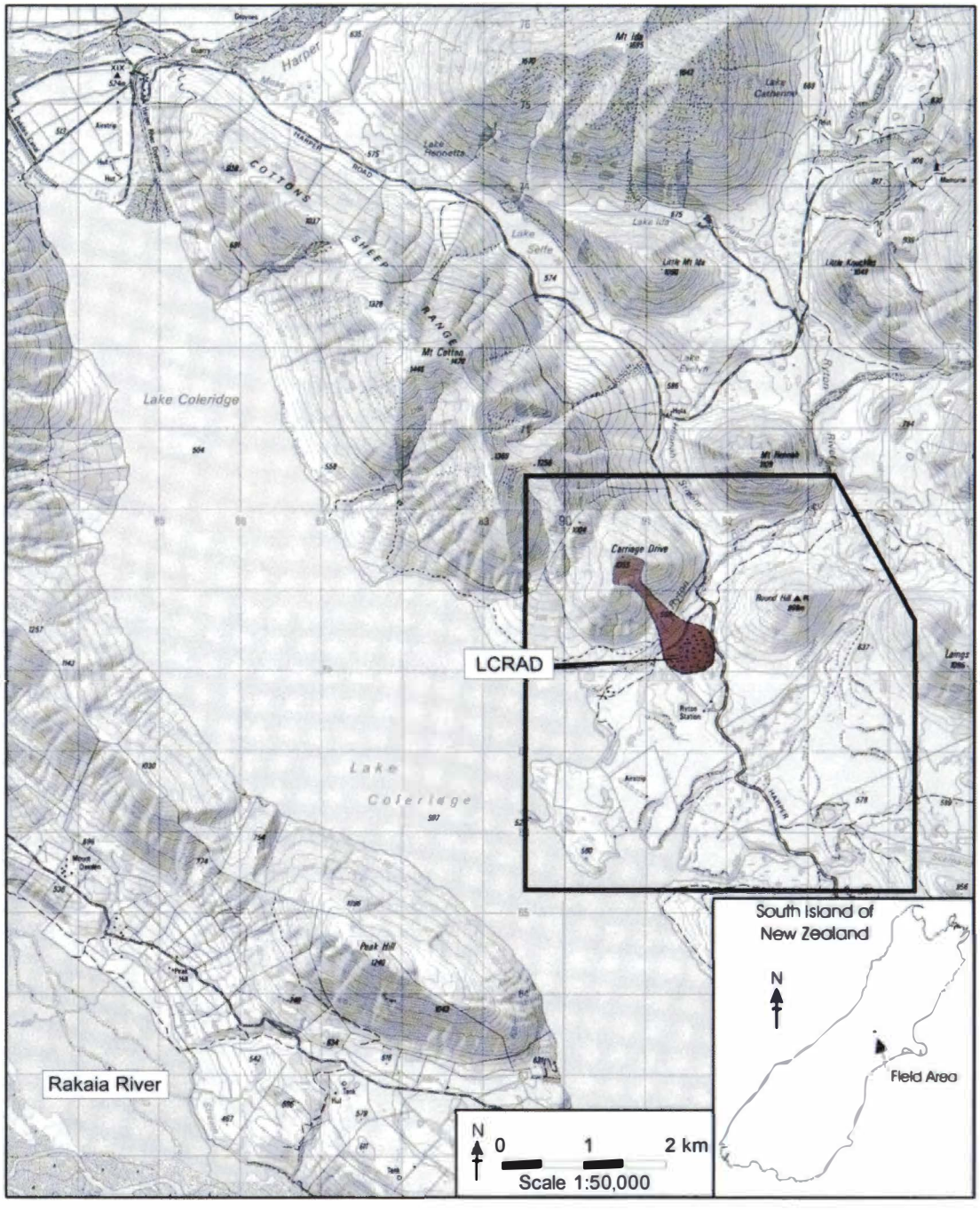

Figure 1.1: Location of study area. The Lake Coleridge Rock Avalanche Deposit (LCRAD) is located geographically below Carriage Drive on the south-eastern side of Ryton River (see shaded zone in boxed area). Source: NZMS 260, sheet K35 (scale 1:50,000).

retreat with debuttressing of the valley walls. However, it is understood that rock avalanches can occur without any obvious trigger, such as the 1991 Mt Cook (HANCOX *et al.*, 1991) and the 1999 Mt Adams events (DAVIES, 2002). Rainstorms are also a known trigger. A very important aspect of determining whether earthquake events were responsible for initiating the three rock avalanches of the LCRAD is the ability to place reliable dates on the failures, and to be able to correlate these with dated fault ruptures and/or other rock avalanche events within the region.

1.1.1 Previous Studies within the Lake Coleridge Area

Previous studies in this region have focused on reconstructing the Late Pleistocene glacial sequences within the valley. SOONS (1963) undertook an extensive study of the glacial deposits and landforms of the Rakaia Valley, while there have been numerous other researchers discussing the glacial sequences with the valley (e.g. SPEIGHT, 1926, 1933; COX, 1926; CARRYER, 1967). Studies have also included the geological structure and seismic implications of major active faults controlling the uplift of the surrounding mountain ranges (e.g. ELVY, 1999; COWAN, 1992; HOWARD, 2001; NICOL, 2001; SMITH, 2003). An adjacent field of study to seismicity is the study of rock avalanches, including their occurrence, frequency, location, age and triggering mechanism (e.g. WHITEHOUSE and GRIFFITHS, 1983; ORWIN, 1998; SMITH, 2003).

1.2 Thesis Aims and Objectives

The main aim of this thesis is to reconstruct the events which occurred at the LCRAD site by mapping and analysing the rock avalanche deposits and the surrounding area. A secondary aim is the determination of the triggering mechanism, which becomes important when considering hazard management and assessment. Correlation between dates of the rock avalanches and dated fault ruptures within the region is required for this objective.

More specific objectives of this project are as follows:

1. Detailed mapping of geological and geomorphologic features of both the LCRAD and surrounding area. Mapping methods included aerial photograph interpretation (API), global positioning system (GPS) mapping in conjunction with 1:50,000 topographical maps (K35, NZMS), and detailed fieldwork.

2. Detailed description and statistical analysis of the three rock avalanches which comprise of the LCRAD. This will follow the outline provided by GOVI *et al.* (2002).

3. Identification of fluvial impacts along the lower portion of the Ryton River from the three instantaneous sediment depositions within the riverbed by the rock avalanche events. Infer dam heights and characteristics of dam-break floods from dam outwash terrace deposits. Assigning the rock avalanche event to associated terraces.

4. Excavation of trenches within the three rock avalanche deposits and across Carriage Drive Fault aimed at identifying structure and collecting organic material to date (if suitable).

5. Radiocarbon and if necessary luminescence dating of the three Lake Coleridge rock avalanche deposits, with interpretation and correlation between dated regional fault ruptures, and the LCRAD and other regional rock avalanche deposits. This will test the possible earthquake trigger.

6. Hazard assessment of the site using the LCRAD and associated fluvial impacts on the Ryton River as precedents.

1.3 Geographic Setting

1.3.1 Physiography

The highest point in the immediate field area is Carriage Drive, the source peak, which has an elevation of 1,055 m above sea level. Other significant hills within the area are Cottons Sheep Range (1,369 m), Mt Hennah (1,109 m), Round Hill (898 m), Laings Hill (1,095 m), Kaka Hill (994 m) and Peak Hill (1,240 m) located on the opposite side of Lake Coleridge (see figure 1.1). The lowest elevation within the immediate area is Lake Coleridge within the Lake Coleridge trough, which fluctuates in height at around ~509 m (a.s.l). The Rakaia River flows in the valley next to Lake Coleridge at considerably lower elevations (~ 165 m lower).

The Lake Coleridge trough is enclosed by a series of mountain ranges that are aligned sub perpendicular to Lake Coleridge and the Rakaia River. To the northeast the Craigieburn, Torlesse and Big Ben Ranges trend north-northeast to south-

southwest, while the Black Hill and Mt Hutt Ranges (trending north to south) are to the southwest. An extended area of low subdued topography (covered in this study) is located between the Ryton River and Scamander Stream. This area incorporates geomorphic features including the peninsula extending out into Lake Coleridge, kettle lakes, a paraglacial fluvial fan deposit, and an abandoned riverbed (all discussed in Chapter 2).

1.3.2 Hydrological Features

Lake Coleridge is a glacial lake occupying a 200 m deep trough that was repeatedly excavated and deepened by the Wilberforce Glacier during the Quaternary. During the Acheron 3 Advance of the Late Otiran Glaciation, the lake developed behind a terminal moraine. The lake is a natural reservoir that is utilized for hydro power generation, with New Zealand's first hydro power station (1914) located at its southwestern end.

Originally, few streams flowed into Lake Coleridge with the Ryton River being the largest. The installation of the hydro power station led to diversions of the Harper River in 1922, the Acheron River in 1930 and the Wilberforce in 1977 into Lake Coleridge to augment lake levels (BRITTEN, 2000). The natural outlet for Lake Coleridge is Lake Stream, located at the northern end of the lake. This was also modified to increase lake levels both in 1914 when the stream was partially blocked, and again in 1923 with a new outlet weir constructed to raise the lake level from ~508 m to ~509 m (BRITTEN, 2000). Today, all the water entering the lake is discharged through the Lake Coleridge hydro power station, with the Lake Stream being a controlled outlet (ELVY, 1999).

A number of small lakes are located along the Harper Road (figure 1.1). Kettle lakes are numerous within glacial debris, and relic meltwater channels are also present. Remnant lake beaches (at elevations of 525 and 530 m) and lake sediments are present within the field area, predominantly in the form of rhythmics composed of sand/silt-clay couplets.

1.3.3 Vegetation

Macrofossils of woody plants found in Lake Coleridge lagoonal sediments by BURROWS (1995), dated at (NZ4848) 7,273 ± 104 years before present (B.P.) indicate

that a mixed podocarp-angiosperm forest was present in the middle Rakaia Valley during most of the Aranuian, from 7,500 years to a few hundred years ago and extending up to an altitude of 1,400 m (BURROWS, 1995). A mixed forest is believed to have begun developing by 10,000 years ago (MOAR, 1971; LINTOTT and BURROWS, 1973; BURROWS, 1983). Pollen analysis from sediments in mires with age-confining radiocarbon dates from charcoal horizons and palaeosols at Quagmire Tarn (see figure 4.5) and Prospect Hill in the upper Rakaia Valley provide further evidence for a change in vegetation cover at around 10,000 years ago (BURROWS and RUSSELL, 1990).

Fire has played an important role in shaping the vegetation that is present today around the Lake Coleridge area. There is a belief that natural fires may have been responsible for the change from mixed forest to native tussock and grassland (species including *festuca novae-zelandiae* and *Chionochola*) (MACBETH, 1988). BURROWS and RUSSELL (1990) also believe that the vegetation covering the slopes of the middle Rakaia Valley was decimated by fire in the recent past. The onset of a drier and more variable climate coincided with the first human colonisation (BOWDEN, 1983). Further "burn-off" of the vegetation occurred with the arrival of European settlers (around 1850) to remove tall native tussocks and replaced with exotic short stemmed grasses and tussock to feed stock (CONNOR, 1965).

Present day vegetation surrounding Lake Coleridge includes fescue tussock (*Festuca novae-zelandiae*), matagouri (*discaria toumatou*), mānuka (*Leptospermum scoparium*), small stands of mountain beech (*Nothofagus solandri* var. *cliffortiodes*), and various other native species. Exotic species introduced with European settlement include browntop (*Agrostis tenuis*), sweet vernal (*Anthoxanthum odoratum*), and the highly invasive weed *Hieracium spp.* which is becoming an increasing problem on high country runs. Other introduced species found in close proximity to the LCRAD include broom (*Cytisus scoparius*), gorse (*Ulex europaeus*), briar (*Rosa rubignosa*), *Pinus radiata* and Douglas fir (*Pseudotsuga menziesii*) (BOWDEN, 1983). The introduction of new farming techniques, such as cultivation and aerial topdressing, has increased the fertility of high country soils, although in general the soil has a low fertility for supporting introduced grass species.

1.3.4 Soil

Most of the soils within the catchment of the Rakaia have developed from underlying Torlesse Supergroup greywacke parent material. Aside from being the basement material, "greywacke" occurs as *in situ* rock, alluvium, colluvium, glacial till, loess, combinations of these (BOWDEN, 1983) and rock avalanche deposits. Various vegetation types that have developed in different geomorphic settings have influenced the nature of soil development by adding organic matter (BOWDEN, 1983), along with fluvial systems bringing in new nutrients. Soils within high country areas have two major features associated with them, these being their weakly developed structure and low fertility (BOWDEN, 1983).

1.3.5 Climate

1.3.5.1 Post Glacial Aranuian Paleoclimate

Changes identified in sediments, pollen assemblages, and macrofossils are attributed to changes in climate during the early Aranuian post glacial history of the Lake Coleridge area (BURROWS and RUSSELL, 1990; see figure 4.5). Interpretation from New Zealand's pollen spectra, from BURROWS and RUSSELL (1990) after RODGERS and MCGLONE (1989), for the period 9,500-7,500 years B.P. indicates that westerly winds and southerly airflow onto the country were weaker than present conditions, while northerly airflow was stronger. Due to this, they suggest that winters were warmer and drier on the eastern sides of both the North and South Islands. Summers were noted for high frequencies of easterlies with associated cloud and rain that increased precipitation to levels similar to those of the present day.

1.3.5.2 Present Climatic Conditions

The present day climate of the Lake Coleridge area is dominated by the effect of the Southern Alps on the predominantly westerly winds which pass over the South Island (BOWDEN, 1983). The orographic effect of the Southern Alps results in high precipitation on the West Coast which consequently causes a decline in precipitation to the east. Rainfalls on the Canterbury Plains and foothills are associated with southwesterly airflows and cold fronts (BOWDEN, 1983). Due to the close proximity of the Lake Coleridge area to the Southern Alps, the major source of precipitation is from north-westerly rain spilling over from the Main Divide. Rainfall in the Alps leads to high river flows which can also be accompanied by high temperature and low humidity on the Canterbury Plains (BOWDEN, 1983). The predominant wind blows

from the northwest, and since European settlement in the valley in 1853 it has acclaimed legendary status with the locals. The wind is topographically channelled down the Rakaia Valley and other main valley systems, including the Coleridge trough. A summary of climatic data from a meteorological recording station (elevation 364 m (a.s.l), grid reference K35:908 594) is provided in Table 1.1.

Table 1.1: Summary of Climatic Factors for Lake Coleridge. Data obtained from New Zealand Meteorological Service (1980).

Variable		Value	Period of recording
Mean annual rainfall (mm)		830	1913-1980
Maximum 1-day rainfall		124	1913-1980
Maximum 2-day rainfall		192	1913-1980
Highest recorded temperature (°C)		36.1	1918-1980
Average daily maximum		15.9	1918-1980
Mean temperature		10.4	1918-1980
Average daily range		11.1	1918-1980
Average daily minimum		4.8	1918-1980
Lowest temperature		-12.2	1918-1980
Lowest grass minimum		-15.7	1918-1980
Average grass minimum		1.7	1918-1980
Average days of ground frost		123.8	1917-1980
Average days of:	snow	9.3	1928-1976
	hail	1.3	1930-1976
	thunder	1.8	1955-1976
	gale	3.0	1928-1976
	fog	5.8	1928-1976

1.4 Regional Tectonic Setting and Geology

1.4.1 Present Day Plate Boundary

Geologically New Zealand is positioned where two plates are actively colliding and moving past each other through the centre of the South Island (figure 1.2). Due to the oblique collision of the Pacific Plate on the eastern side of New Zealand with the Australian Plate on the western side, continental deformation is occurring between the two plates (CHAMBERLAIN, 1996). It is this collision that accounts for the extensive

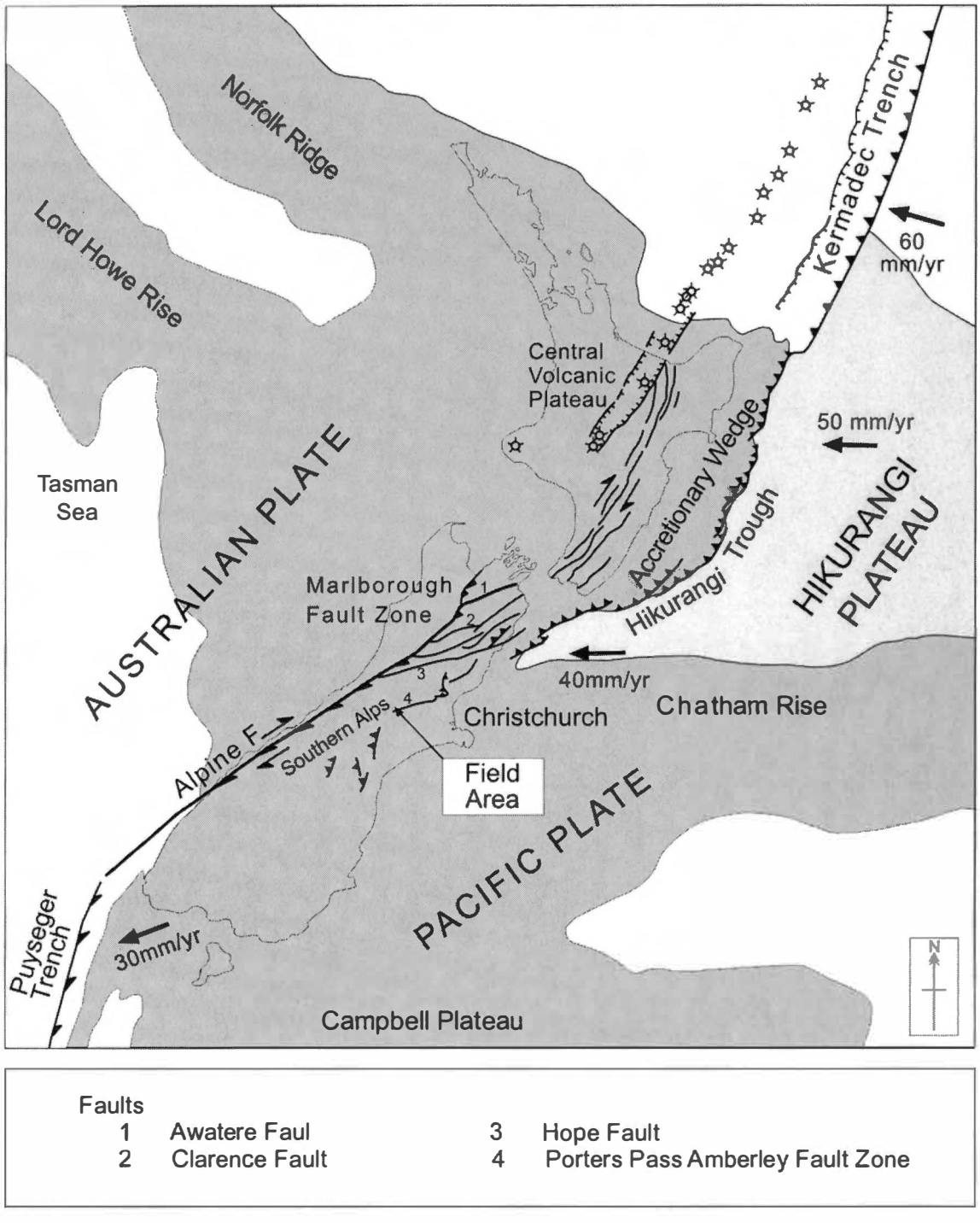

Figure 1.2: Tectonic setting and main structural features of the New Zealand micro-continent located across the Australia-Pacific plate boundary zone. Numbered arrows indicate rates of convergence (from DEMETS *et al.*, 1990). Field area is indicated. Sourced from PETTINGA *et al.* (2001).

mountain ranges of the Southern Alps and the high seismicity the country experiences.

The plate boundary relationship changes dramatically through the country. To the north of New Zealand the Tonga-Kermadec trench is created by nearly pure subduction of the Pacific Plate under the Australian Plate. The obliquity of the Pacific plate meeting the Australian Plate increases southwards, where the Alpine Fault is a zone dominated by right lateral reverse slip motion (ELVY, 1999). In Fiordland, the Alpine Fault transfers the strike slip off shore towards oblique subduction. The near vertical subduction surface of the Australian Plate shallows towards the south where the Puysegur Trench signifies the change to subduction, with the Australian Plate moving beneath the Pacific Plate (REYNERS *et al.*, 2002).

1.4.2 Inland Canterbury Structural Setting

The Lake Coleridge area is located on the eastern side of the Southern Alps in inland Canterbury (figure 1.2). This area is within a zone of continental – continental collision where the South Island lies astride the active boundary of the Australian and Pacific Plates (NORRIS *et al.*, 1990). Structurally, it is located in between the southern limit of the Hikurangi Margin and the Southern Alps (figure 1.2); (CHAMBERLAIN, 1996). To the north, major dextral northeast trending predominantly strike-slip faults of the Marlborough Fault Zone transfer oblique plate motion from the Hikurangi Margin through to the Alpine Fault (CHAMBERLAIN, 1996). These faults include the Awatere, Clarence and Hope Faults; however, many minor faults are incorporated making up the Marlborough Fault Zone (figure 1.2). The Hope Fault marks the approximate southern extent of the Marlborough Fault zone (CHAMBERLAIN, 1996).

Inland Canterbury tectonics are characterized by a transition from subduction to collision. To compensate for the change in plate motion the structure of the upper crust is dominated by thrust faults associated with growing folds (CHAMBERLAIN, 1996). The closest major active fault zone to the Lake Coleridge site is the Porter's Pass-Amberley Fault Zone or PPAFZ (figure 1.3). The southwest termination of the predominantly right-lateral strike-slip fault is located approximately 10 km to the southeast of the LCRAD, striking across the southern tip of Lake Coleridge (HOWARD, 2001). The PPAFZ trends northeast from the Rakaia River Valley in the Southern Alps through to Amberley on the Canterbury Plains.

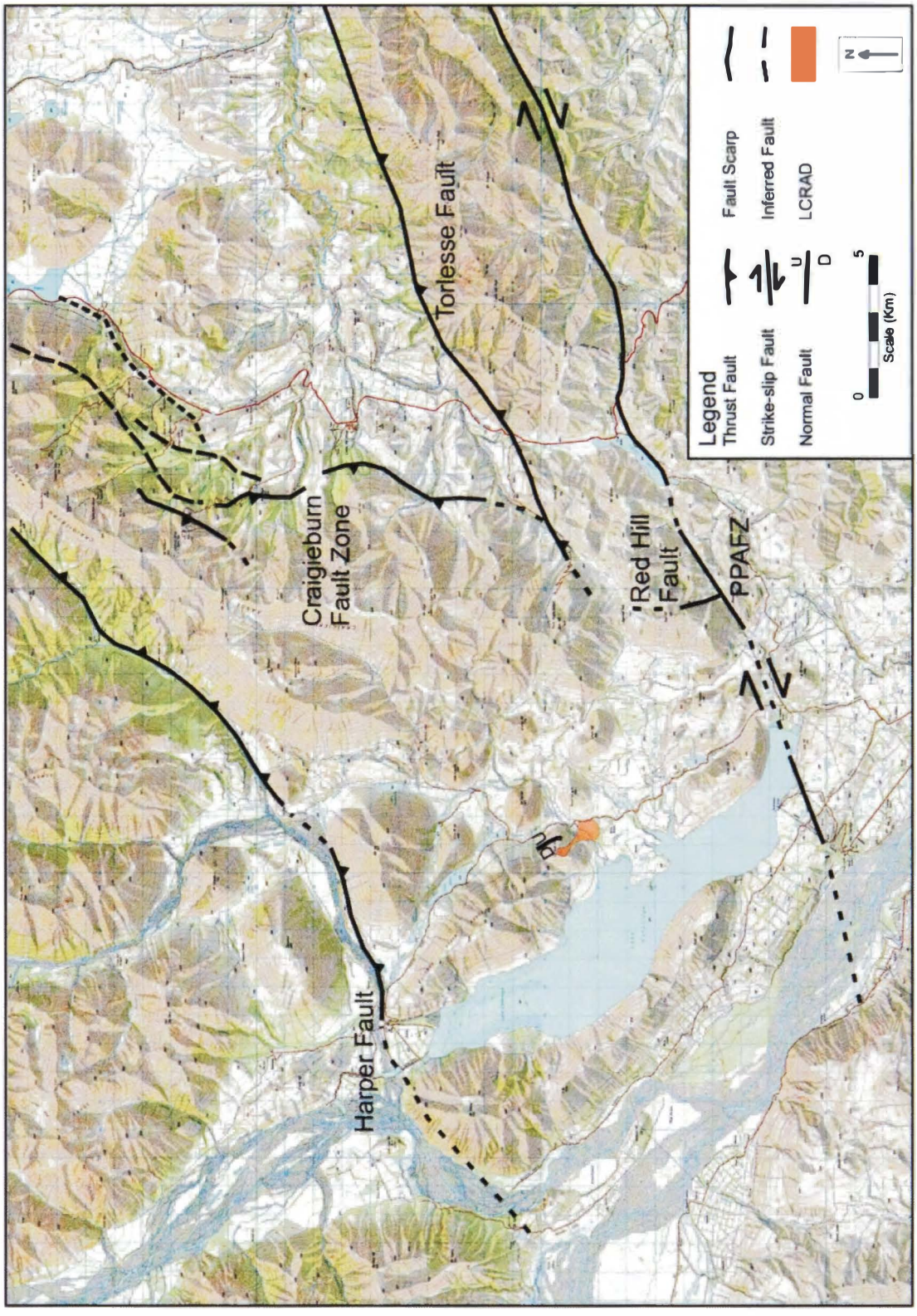

Figure 1.3: Active faults relative to the LCRAD site including: the Harper, Craigieburn, Torlesse, Red Hill and Porters Pass-Amberley Fault Zone. Adapted from HOWARD (2001).

1.4.3 Regional Geology

1.4.3.1 Torlesse Supergroup

The basement rock in Canterbury is the Torlesse Supergroup. As discussed in detail by BRADSHAW *et al.* (1981), the Torlesse Supergroup terrane is the most easterly of Permian and Mesozoic terranes in New Zealand, and is interpreted to have been accreted to the Pacific edge of the Gondwana margin approximately 250 million years ago (COATES, 2002).

Torlesse Supergroup rocks consist of massive volumes of sedimentary basement strata, forming the basement material for over half of the exposed continental crust of New Zealand. The Torlesse Supergroup rocks can be divided into two broad distinct accretionary complexes; or three sub-terranes; the Permian-Triassic Rakaia sub-terrane which increases in metamorphic grade towards a cryptic suture in the Caples terrain within the Haast Schist in Otago, the Late Jurassic to Early Cretaceous Pahau sub-terrane, and the Esk Head sub-terrane separating the two (figure 1.4; see also BISHOP *et al.*, 1985). The Lake Coleridge field area is situated within the Rakaia sub-terrane and consists of the oldest Torlesse Supergroup rocks in New Zealand (BRADSHAW *et al.*, 1981).

The Rakaia sub-terrane rocks have been interpreted as submarine fan type sequences (HOWELL, 1981; MACKINNON, 1983). They are made up of well indurated, weakly metamorphosed bedded sequences of moderately to poorly-sorted coarse to fine sandstone to siltstone. According to ELVY (1999) minor lithologies including conglomerate, intra-formational conglomerates and breccias, volcanogenic chert beds and minor intrusives are present within the Torlesse Supergroup.

1.4.3.2 Cretaceous-Tertiary Cover Rocks

Within the field area no Cretaceous-Tertiary cover rocks exist. The extensive uplift, glacial scouring and mobilization of sediment from the Late Pleistocene glaciations have stripped the middle Rakaia Valley clean of such cover rocks. SMITH (2003) notes that Tertiary outliers within the North Canterbury region are usually confined to fault bounded pockets which are located across the eastern divide of the Southern Alps. The scenic Castle Hill Basin is the largest cover rock deposit in the area and is located ~15 km to the northeast of this study area.

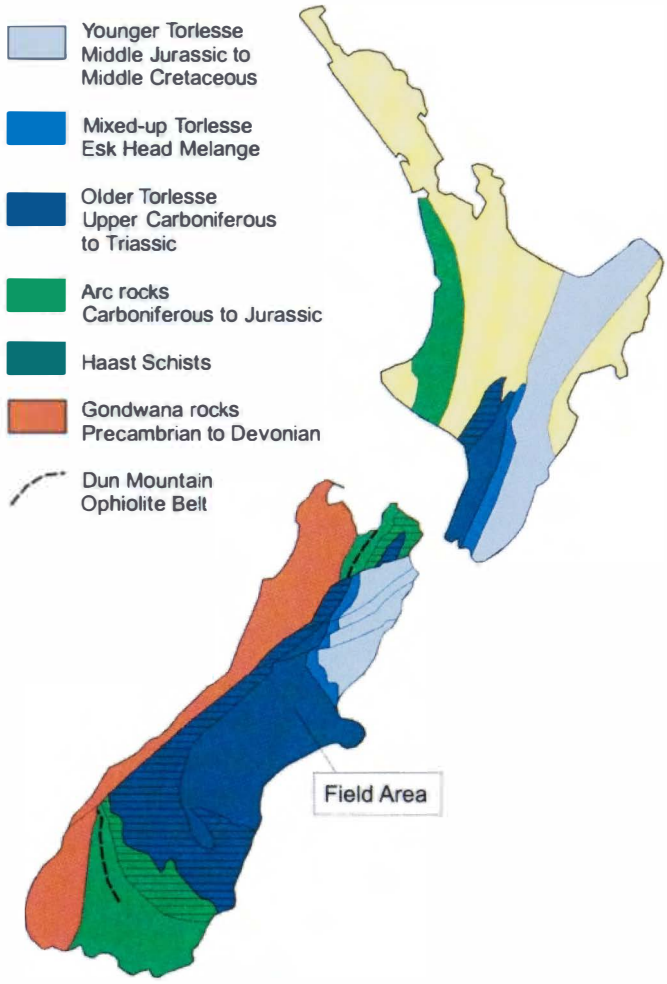

Figure 1.4: The basement rocks of the Eastern Province can be divided into terranes which were added one after the other to the Gondwana continent before break-up. Sourced from COATES (2002).

1.5 Mechanisms and Morphology of Rock Avalanches

This section is a brief overview of rock avalanches and their effects from emplacement into fluvial systems. For a comprehensive discussion of rock avalanches see SMITH (2003), who dedicated a Chapter of his thesis to the mechanisms and morphology of rock avalanches.

1.5.1 Definition of the term Rock Avalanche

A rock avalanche is a large bulk of predominantly dry, massive rock instantaneously detaching from a mountainside and travelling as debris at a very high velocity down slope and depositing out onto the valley floor (HSÜ, 1975). Due to speed of descent downslope (their velocity can be in the order of tens of metres per second) and

volume (volumes normally exceeding 1 x 10^6 m^3) they pose a serious threat to human lives and structures (Table 1.2).

Table 1.2: Terms describing the velocity of a landslide and probable human response. From CRUDEN and VARNES (1996).

Velocity Class	Description	Velocity (mm/sec)	Typical Velocity	Human Response
7	Extremely Rapid	5 x 10^3	5m/sec	Nil
6	Very Rapid	5 x 10^1	3m/sec	Nil
5	Rapid	5 x 10^{-1}	1.8m/hr	Evacuation
4	Moderate	5 x 10^{-3}	13m/month	Evacuation
3	Slow	5 x 10^{-5}	1.6m/year	Maintenance
2	Very slow	5 x 10^{-7}	16mm/year	Maintenance
1	Extremely slow			

The first recorded historical rock avalanche event was the Elm rock avalanche in Switzerland in 1881 (HEIM, 1882; HSÜ, 1975; VOIGHT, 1978) where HEIM (1881) described that "*rock falls did not slide, they crashed, and their debris flowed*". From this statement HEIM translated this term into the German "Sturzstrom", meaning rock fall-stream. The English equivalent of Sturzstrom (rock avalanche) was initially used by MCCONNELL and BROCK (1904) in their study of the Frank Slide in Alberta, Canada.

Classification schemes have been widely applied when describing landslides. Classifications from VARNES (1978), CRUDEN and VARNES (1996) and HUTCHINSON (1988) are the most widely accepted. A summary of CRUDEN and VARNES (1996) landslide classification is presented below (Table 1.3). However, as shown in Table 1.3 there is no clear definition provided for rock avalanches. VARNES (1978) recognised that rock avalanche movement was different from the initial failure process and included the complex type of movement in an attempt to categorise rock avalanche processes. Classification schemes are still fundamentally important, however, the writer believes that they have proven inadequate to explain the unique diagnostic factors of rock avalanches.

Table 1.3: Summary of CRUDEN and VARNES (1996) landslide classification.

TYPE OF MOVEMENT	TYPE OF MATERIAL	ENGINEERING SOILS	
	BEDROCK	PREDOMINANTLY COARSE	PREDOMINANTLY FINE
Fall	Rock fall	Debris fall	Earth fall
Topple	Rock topple	Debris topple	Earth topple
Slides – rotational	Rock slump	Debris slump	Earth slump
–	Rock block slide	Debris block slide	Earth block slide
translational	Rock slide	Debris slide	Earth slide
Lateral spreads	Rock spread	Debris spread	Earth spread
Flow	Rock flow (deep creep)	Debris flow	Earth flow (soil creep)
Complex	**Combination of two or more principal types of movements**		

It is essential that a correct description is provided for a rock avalanche as discussed by DIKAU *et al.* (1996). SMITH (2003) highlighted that a rock avalanche is not derived from remobilizing debris as inferred by VARNES "*rock fall / rock slide-debris avalanche*", but rather from a large (greater than 1×10^6 m^3) and relatively intact rock mass. Initial failure predominantly occurs along pre-existing defects, which is a process described as collapse by DAVIES and MCSAVENEY (2002). A rock avalanche is defined by SMITH (2003) as the process which occurs immediately following the detachment of the semi-coherent rock mass from the mountainside. A transformation from a semi-coherent rock mass to a fragmenting mass starts just after detachment allowing the debris to "flow", and to reach extremely high velocities with long runout distances if unconfined by local topography.

An interesting field of study and debate that has come from studying rock avalanches is the explanation of the phenomenon of long runout distances for the debris. Under normal friction coefficient conditions, rock avalanches should have certain runout lengths, however excessive runout paths occur, transferring the distal debris farther than expected. Numerous authors have attempted to explain the long runouts described from rock avalanche debris identified around the world, but none has yet met with a consensus which can justify all the evidence gathered in the field. Ideas for mechanisms to allow long runout paths include; mud lubrication (HEIM, 1932), air fluidization (KENT, 1966), air cushioning (SHREVE, 1968), mechanical

fluidization (SCHEIDEGGER, 1963; HSÜ, 1975; and others), and most recently rock fragmentation (DAVIES and MCSAVENEY, 2002).

1.5.2 Triggering Mechanisms

Triggering mechanisms for rock avalanches include; earthquakes, oversteepening (including both human excavation and over steepening from glacial and fluvial erosion), dilation of the rock mass (including rock weathering) and storm events. Removal of toe support and human interference are other triggering mechanisms, with a classic example being the 1881 Elm rock avalanche in Switzerland, that is believed to have been caused by a combination of natural causes and the extraction of slate from a quarry located at the foot of the mountain (TURNER and JAYAPRAKASH, 1996).

1.5.2.1 Earthquake

Seismic shaking can induce significant horizontal and vertical dynamic stresses in slopes of any rock type (KRAMER, 1996). Earthquakes are *the* most commonly perceived mechanism for rock avalanche activation. Evidence for this occurrence has come from studies which have found regional and temporal "clustering" of rock avalanche deposits (e.g. KEEFER, 1984; VOIGHT and PARISEAU, 1978). However, SMITH (2003) notes that of the six historic rock avalanches that have occurred in New Zealand only two were triggered by earthquakes. Studies of rock avalanche "clusters" have been used as paleoseismic indicators of regional seismicity (e.g. COWAN *et al.*, 1996; JIBSON, 1996). KEEFER (1984) suggested that local geologic conditions and seismic parameters other than magnitude were also responsible for the number of landslides (including rock avalanches) triggered.

Earthquakes do provided one of the main requirements to initiate a rock avalanche, which is the almost instantaneous failure of rock mass that is emphasised by seismic loading during a fault rupture (HUNGR *et al.*, 2001). A study undertaken by EISBACHER and CLAGUE (1984) revealed that rapid detachment of blocks that initiated rock avalanches were generally formed by earthquakes with an Mw ≥ 6 (within the epicentral area). The effects of seismic shaking on rock masses involve dilation of fractures, joints and defects. This reduces the cohesion or shear strength along the planes of weakness, by largely removing the influence of planar asperities and surface roughness (SMITH, 2003).

A field of research that has emerged from the relationship between ground failure and earthquakes is the study of topographic amplification (e.g. ZASLAVSKY and SHAPIRA, 2000; STEWART, 2004). Studies have shown the effect of topography to be quite significant with seismic shock waves being amplified up to a factor ten at ridge tops (e.g. TRIFUNAC and HUDSON, 1971; BOORE, 1973; GAGNEPAIN-BEYNEIX, 1995).

1.5.2.2 Oversteepening

Characteristically, the slopes in mountainous areas such as are found in the Southern Alps of New Zealand are very steep. Factors contributing to this include; their orogenic origin, normal erosion processes such as fluvial action, and a major influence from the Pleistocene, glacial valley deepening. Inherently, steep sided mountains produce high horizontal stress components relative to vertical components at the ground surface, which increases instability (BRADY and BROWN, 1985). However, WHITEHOUSE and GRIFFITHS (1983) consider that steepness of slope is a necessary precondition only, which does not imply that it is a trigger. They argue that the steepening of slopes is a gradual process, occurring over many years, whereas rock avalanche events are triggered instantaneously.

1.5.2.3 Dilation of the Rock Mass and Weathering

Dilation along joints can also occur as a progressive relaxation process over time where gradual de-stressing processes such as ice wedging and talus production participate in disaggregating the rock mass (SMITH, 2003). This process is promoted by water entering the opening voids and undergoing prolonged episodic freeze-thaw cycles. Recently there has been a new scientific debate arguing that precipitation in the form of ice and snow act as a barrier that protects the mountains from the effects of erosion (MCSAVENEY, 2002). MCSAVENEY (2002) suggests that failure of a mountainside is achieved through bulging of the rock mass along dilated defects which result in the instability of the slope, leaving it vulnerable to the slightest change to the equilibrium.

1.5.2.4 Storm Events

A widely recorded relationship exists between rainfall and precipitation events and landslide occurrence. This relationship is usually associated with soils and superficial failures. Antecedent moisture conditions play a large role in the initiation of landslides. In a rock mass, water pressures along defects may have a significant role in decreasing shear resistance. Uplift pressures may also play a role in tipping the

balance of slope stability (KILBURN and SORENSEN, 1998). VOIGHT and PARISEAU (1978) noted that earthquakes dominate over rainfall storm events as triggers for the larger historical rock avalanches worldwide. MELOSH (1987) also noted that very few historic rock avalanche events were triggered by storm events involving heavy rainfall.

1.5.3 Rock Avalanche Emplacement Characteristics and Effects

A key impact of rock avalanche events is the rapid deposition in the valley floor of large volumes of fragmented rock debris. Due to the close coupling of mountains and valleys containing rivers and streams, the impacts on fluvial systems are usually significant. Rock avalanches not only contribute significant volumes of debris to river channels, but also create temporary or semi-permanent natural barriers impeding the flow of water (KORUP *et al.*, 2004). Therefore the impact of rock avalanches on fluvial systems is also dependent upon whether they; impound water and sediment, lake volume, the dam duration, and how rapidly they breach (dam failure characteristics) (COSTA and SCHUSTER, 1988). The main factors controlling rock avalanche dam stability include; the size and shape of barriers, the composition and natural compaction of the deposits, and the rapid emplacement of material (HEWITT, 1998). The valley geometry also plays a critical role in determining if the barrier is simply going to be bypassed by the river around the perimeter of the deposit, or if the valley is narrow enough to become choked with sediment (figure 1.5).

1.6 The Lake Coleridge Rock Avalanche Deposit

1.6.1 General Setting of the LCRAD

The LCRAD is located approximately 80 km west of Christchurch, within the middle Rakaia Valley near the mouth of the Ryton River (figure 1.1). The distal extent of the LCRAD is ~350 m north of the Ryton Homestead. The present volume of the LCRAD that is present is ~5.5 x 10^6 m^3 (this study) and an estimated 7.5 x 10^6 m^3 (this study) is thought to have been eroded from the Ryton River section since emplacement (Section 3.4 and 3.5).

1.6.2 Previous Studies on the LCRAD

The LCRAD site has previously been studied by WHITEHOUSE (1981) and WHITEHOUSE and GRIFFITHS (1983). These studies were concerned with the size distribution, frequency and hazard of large rock events (exceeding 1 x 10^6 m^3 in volume) within the

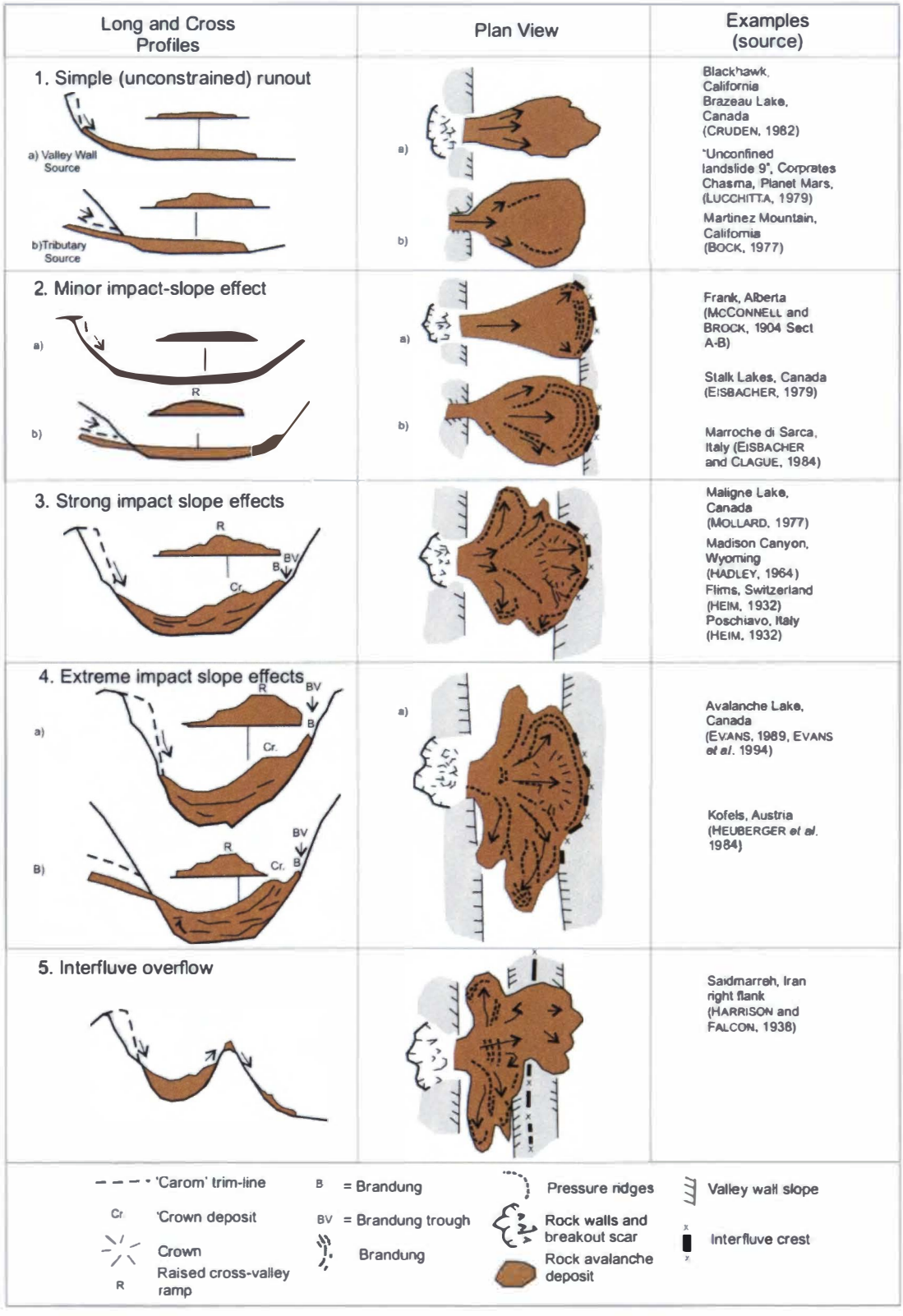

Figure 1.5: Schematic long and cross sections, and plan forms of cross-valley rock avalanche deposits with examples of occurrence around the world. Adapted from HEWITT, 2002.

central Southern Alps (figure 1.6). During the study six rock avalanches were identified in close proximity to the LCRAD site (figure 1.6). Their study outlined the dimensions and ages of rock avalanches which included the LCRAD (Table 1.4). In 1981 WHITEHOUSE conducted a weathering rind study which dated the LCRAD at 120 years (no error margins were provided). WHITEHOUSE and GRIFFITHS (1983) redated the deposit, again using weathering rind dating, at 150 ± 40 years B.P. These surveys were conducted at an undetermined location on the LCRAD.

During the studies by WHITEHOUSE (1981) and WHITEHOUSE and GRIFFITHS (1983) only one rock avalanche deposit was described at the LCRAD site. However the present study has identified three individual rock avalanche events.

1.6.3 General Description of the LCRAD

The LCRAD consists of an old and large rock avalanche deposit overlying glacial till and associated outwash surfaces. Two younger and much smaller rock avalanches are located within the eroded Ryton River section of the older deposit.

The boundary between the oldest Lake Coleridge Rock Avalanche One deposit (LCRA1) and Lake Coleridge Rock Avalanche Two deposit (LCRA2) is easily distinguished by a prominent swash feature described by WHITEHOUSE and GRIFFITHS (1983) (following HEIM, 1932) as a "brandung", with the younger rock avalanche crossing the Ryton River and partially ascending the river-cut eroded face of the LCRA1 deposit by approximately 15 m, leaving a permanent levee.

The Lake Coleridge Rock Avalanche Three deposit (LCRA3) is poorly constrained by geomorphology, being identified by a contact between the LCRA2 deposit and LCRA3 deposit, located in a newly eroded cliff within the Ryton River section.

All three rock avalanches crossed the Ryton River, which flows directly beneath Carriage Drive. The emplacement of rock avalanche debris would have created blockages in flow of the river, for presumably differing periods of time for each rock avalanche event.

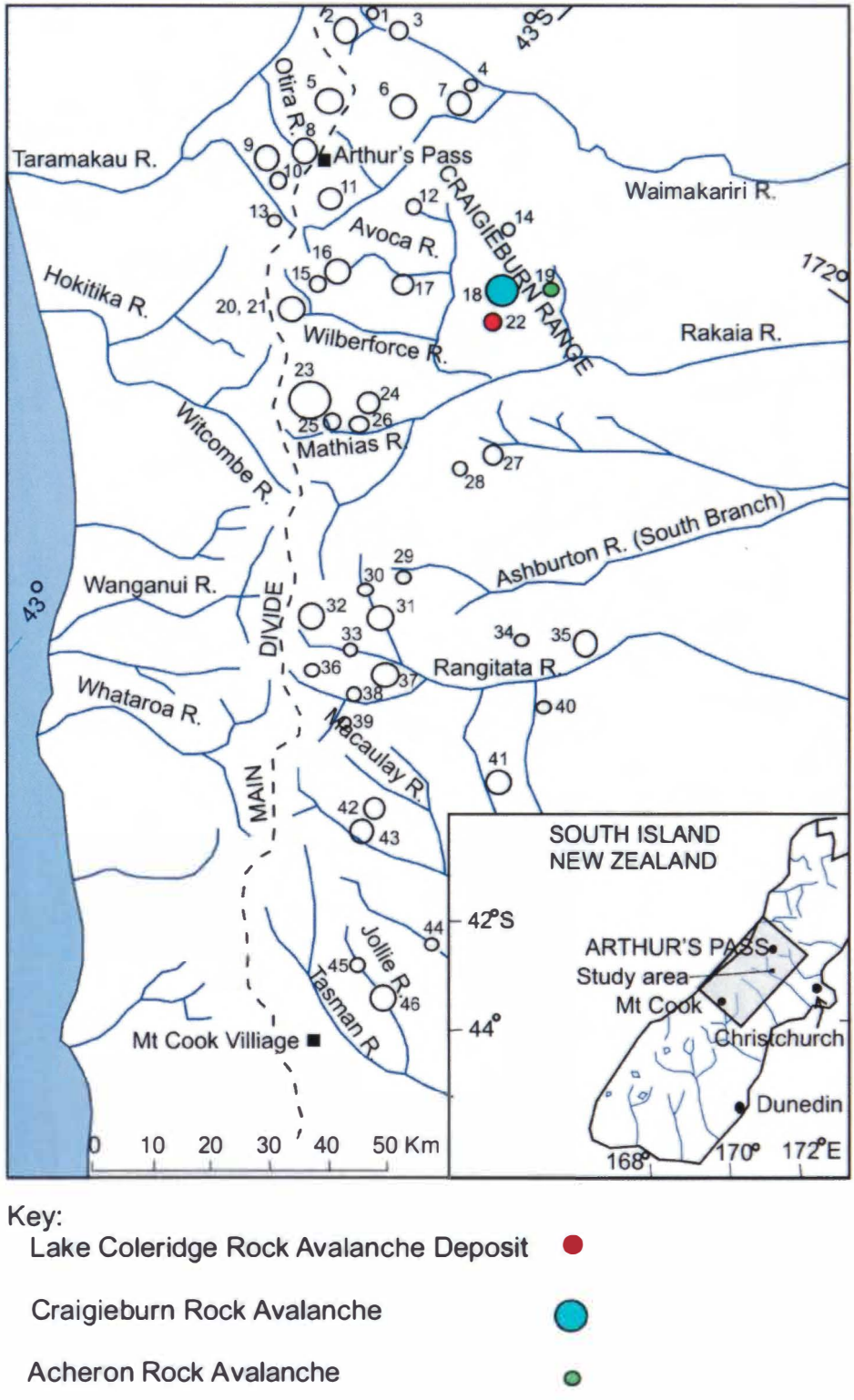

Figure 1.6: Location of rock avalanches included within WHITEHOUSE and GRIFFITHS (1983) study of large rock avalanches (>1 x 10^6 m^3) within the central Southern Alps. Circle size indicates magnitude of deposit volume: small circles = 1 to 10 x 10^6 m^3; intermediate circles = 10 to 100 x 10^6 m^3; large circles = greater than 100 x 10^6 m^3. The LCRAD, Craigieburn and Acheron Rock Avalanches are shaded as indicated. Corresponding numbers beside circles can be identified in Table in Appendix A. Modified from WHITEHOUSE and GRIFFITHS (1983).

Table 1.4: Dimensions and age of the Lake Coleridge rock avalanche from WHITEHOUSE and GRIFFITHS (1983). For complete table see Appendix A.

	Locality*	Deposit† area ($10^4 m^2$)	Thickness‡ (m)	Volume‡ ($10^6 m^3$)	Age (year BP)	Dating Method
22	Lake Coleridge	23	20 ± 2	4.6 ± 0.4	150 ± 40	Weathering rind#

*Number refers to location in figure 1.6.

†Precision error of deposit area is ignored as it is negligible compared with error in thickness.

‡Thickness and volume estimate ± one standard error of the mean.

#Dated from thickness of weathering rinds on surface clasts using method of CHINN (1981). Rinds measured to 0.2 mm. Date ± one standard deviation.

1.7 Thesis Organisation

Chapter One provides an overview of the study area and introduces the reader to the geologic location and geographic setting of the area. The aims and objectives are outlined and a brief introduction to rock avalanches is provided. The LCRAD is introduced to the extent of its current state of knowledge.

Chapter Two provides a detailed description of the geology and geomorphology of the Lake Coleridge area. Particular attention is directed to the basement strata of the Torlesse Supergroup and the internal structures and defects identified within the rock avalanche source area. The Late Pleistocene glacial history of the area is outlined, with the focus on the last Acheron Advances due to their lasting influence on the field area. The postglacial geomorphic and paraglacial evolution of the area is discussed and tied in with changing fluvial systems, specifically those of the Ryton River and Lake Coleridge. Regional active tectonics are discussed with a brief outline of neighbouring significant rock avalanche deposits.

Chapter Three is a description of the LCRAD. The three rock avalanche deposits are discussed and analysed, and a geological model of the source and deposits provided. Evidence for landslide dam-break events comes from fluvial terrace descriptions and interpretations both upstream and downstream of the LCRAD along Ryton River.

Chapter Four is concerned with the age and history of the LCRAD. This chapter describes dating of the three rock avalanche deposits, while providing a general overview of useful dating techniques for rock avalanche deposits. Age constraints on the three rock avalanche deposits are given.

Chapter Five outlines hazards in the immediate area in the event of a further failure from the source area. It highlights the impacts on the; Ryton River, Ryton Bay and camping area, Ryton Homestead and immediate infrastructure including roading (access both to Ryton Bay and further up the valley), the Ryton Bridge, and power lines crossing LCRAD.

Chapter Six provides a summary and conclusions of the main findings of this study and highlights suggestions for further work.

Chapter 2

Geology and Geomorphology of the Lake Coleridge Area

2.1 Introduction

This Chapter describes the geology and geomorphology of the Lake Coleridge area within the Rakaia River catchment. The aim is to inform the reader about the geomorphological evolution of the area surrounding the LCRAD site. As outlined in Chapter 1 the area has a significant glaciation history and this is reflected is the landforms present today. The landscape around the LCRAD site is dynamic and has responded to changes both during the glaciations and after. The deposits discussed in this Chapter reflect this.

The basement strata within the Lake Coleridge area of the Rakaia Valley are solely Torlesse Supergroup "greywacke" which is composed of alternating sandstone and argillite beds. Tertiary "outliers" are located within the region (such as in the neighbouring Red Hill Valley; SMITH (2003)) however none are present within the Lake Coleridge area. Exposed basement strata within the valley floors is uncommon and are mostly buried by glacial or postglacial cover materials to unknown depths, and colluvium and rock avalanche deposits. All of the cover material, regardless of geomorphic origin, is sourced from Torlesse Supergroup bedrock. Characteristically, the Torlesse Supergroup basement, where visible, has undergone severe physical weathering in the form of disaggregation with some near-surface chemical alteration. Because of the fragmented and disaggregated state of the basement material, structural analysis proved difficult. However, some analysis will be presented and discussed in this Chapter.

The Rakaia River Valley is one of the more important drainage systems in Canterbury, flowing from the main divide of the Southern Alps through the Canterbury Plains to the sea. The headwaters are sourced from the now much-diminished Lyell and Ramsay glaciers, and to a lesser extent the Reischek and Mathias glaciers. These glaciers are the northernmost large glaciers in New Zealand (BURROWS and RUSSELL, 1975) and are now just a remnant of their former extent. During glaciations these glaciers combined to form the Rakaia Glacier, and extended various distances down-valley at different times. During these glaciations a major ice tongue from the Wilberforce Glacier also extended down the Wilberforce River and was divided by Mt Oakden into two ice streams; one down the Wilberforce River to the west of Mt Oakden and one between Mt Oakden and Cottons Sheep Range with ice in the Coleridge Trough (present position of Lake Coleridge). Ice from the Wilberforce Glacier is also believed to have flowed around the eastern side of Cottons Sheep Range (figure 2.1).

Within the Lake Coleridge area the effects of glacial activity are very prominent. Identified glacial advances from the Woodlands, Tui Creek, Bayfield and Acheron Advances all reached to or extended beyond the Lake Coleridge area. The geomorphic features that are present today, for example; fluvial fans, fluvial terraces, glacial till, kettle lakes and rock avalanche deposits, nearly all represent geological processes associated with the retreat of ice from the last Acheron 3 Advance, or from postglacial processes (figure 2.1). Features directly relating to glacial ice erosion and processes are also present such as roches moutonnées and striation marks. It is evident within the field area that following ice retreat from the final Acheron 3 Advance the landscape underwent rapid changes and represented a paraglacial environment[1].

Active tectonics have played an essential role not only in their influence on landscape development (predominantly with uplift processes), but also as potential triggers for the large scale mountain failures termed rock avalanches. These active faults will be described and analysed with respect to their potential to trigger rock avalanche events at the LCRAD site, and to consider any controls that they exercised over land form development.

[1] The exposure of landscapes after the retreat of glacier ice commonly causes rapid change due to the susceptibility of erosion. This accelerated geomorphic activity is termed 'paraglacial' (BALLANTYNE, 2002).

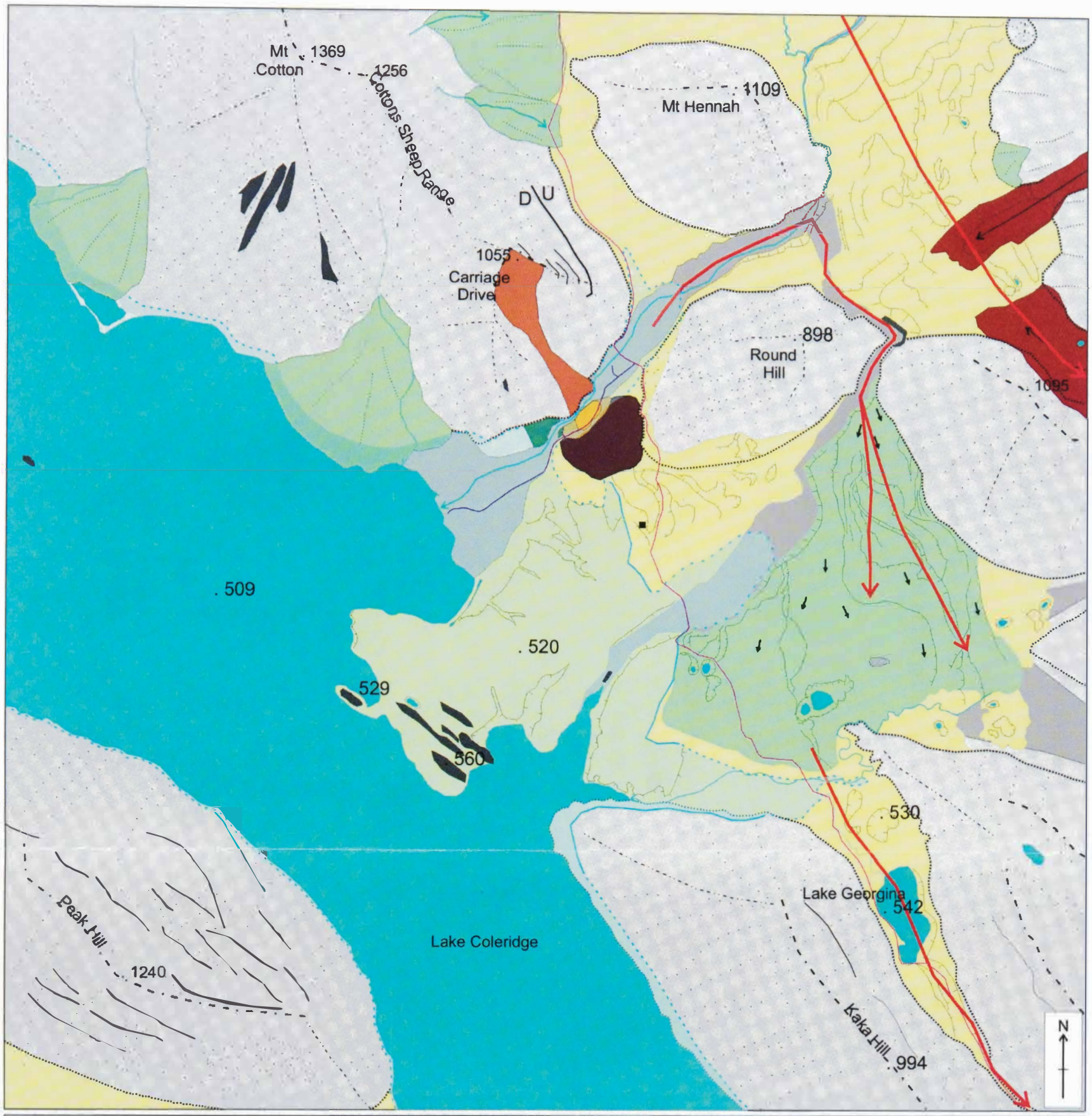

Figure 2.1: Geomorphic map of immediate area surrounding the LCRAD site. The emphasis for this diagram is the deposits and geomorphology located in the valley floors as they provide the most information for geomorphic evolution. Note the Craigieburn Rock Avalanche located in the northwest segment. The fan development to the east of Round Hill will be discussed in full within the text. Carriage Drive is located in the centre with the associated LCRAD's. Map drawn from aerial photograph SN5688 A/6 (New Zealand Mapping, 1980).

Three rock avalanche deposits, the Craigieburn, Acheron and LCRAD, are located within a radius of ~ 5 km from the LCRAD site. This "clustering" of rock avalanche deposits was first recognised by WHITEHOUSE (1981, 1983). WHITEHOUSE and GRIFFITHS (1983), on a much broader scale, provided a model for hazard and frequency of rock avalanches within the central Southern Alps; the three deposits referred to above are summarised briefly, and considered in terms of the geomorphic evolution of the area.

2.2 Basement Strata

2.2.1 Torlesse Supergroup

2.2.1.1 General

Very few outcrops of Torlesse Supergroup basement exist on the valley floor within the Lake Coleridge area (figure 2.1). Thus, exposure is mostly limited to hill slopes and areas that are associated with instability (such as head scarps for ground failure). Field investigation of *in situ* bedrock on Carriage Drive was difficult due to its highly fractured and jointed nature. The process of freeze-thaw, common within mountainous areas where water is present, has also contributed to produce a shattered surface appearance making it difficult to record and analyse rock defect data.

The Torlesse Supergroup bedrock varies in appearance around the source area/headscarp of Carriage Drive. Exposures (where a fresh face could be viewed) were generally dark grey, well-indurated, massive interbeds of sandstone and mudstone. Slight chemical weathering of the basement strata tends to lighten the colour of sandstone beds due to feldspar alteration, while no colour variation is generally seen in mudstone beds (ELVY, 1999). The Torlesse Supergroup rocks are classified as feldsarenite and lithic feldsarenite, mudstone and conglomerate (BRADSHAW, 1989), although no conglomerate was located within the immediate Lake Coleridge area.

2.2.1.2 Bedding

Due to the scarceness of Torlesse Supergroup bedrock within the valley floor, measurements of strike and dip were restricted to the Carriage Drive source area. The measured strikes on Carriage Drive ranged from 252 to 002°. The dip of the beds was

predominantly sub-vertical, but ranged from 42 to 82° with dips mainly to the east (figure 2.2). The variability of the strike and dip of the basement strata is attributed to both superficial gravitational slumping and the inherent nature of deformation, which is common in Torlesse Supergroup.

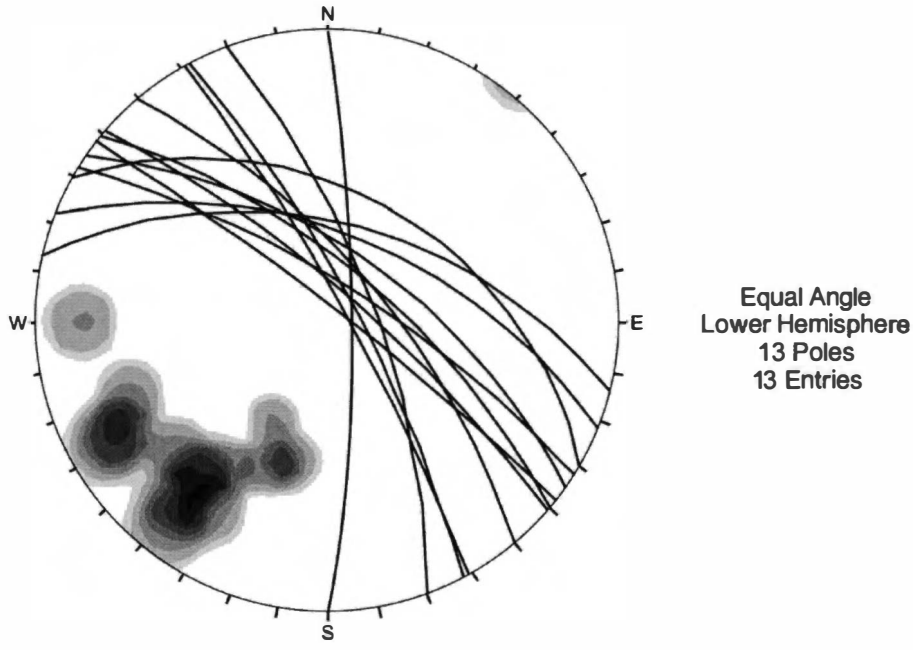

Figure 2.2: Lower Hemisphere stereographic net plot of planes and poles to bedding measured from bedding of basement material on Carriage Drive. Around the source basin bedding varies both in strike and dip. Appendix B1.

Bedding scale varied widely around the source basin (figure 2.3) from thinly bedded alternating sequences of both sandstone and mudstone (millimetres to centimetres) to much higher ratios of thick sandstone beds to thin mudstones. The change in scale of bedding in Torlesse Supergroup greywacke is a common occurrence within the region, and has been noted by various authors (e.g. CHAMBERLAIN, 1996; YOUNG, 1997; ELVY, 1999; SMITH, 2003).

The bedrock within the source area is highly disaggregated. Therefore internal features such as grading, load casts and flute structures (paleocurrent scours) were not identified, although they are commonly found in Torlesse Supergroup strata within the area (e.g. ELVY, 1999). Small fold structures, at metre scales, which are also commonly found outside the area both in this study and in others (e.g. SMITH, 2003; ISSLER, 2004) were present in the basement rock on Carriage Drive. The gross

structure of the Torlesse Supergroup basement within the area has beds striking typically northwest, and dipping sub-vertically to the west and east. Within the Carriage Drive source area toppling failure is occurring along the sub vertical mudstone (argillite) beds, resulting in rock mass dilation.

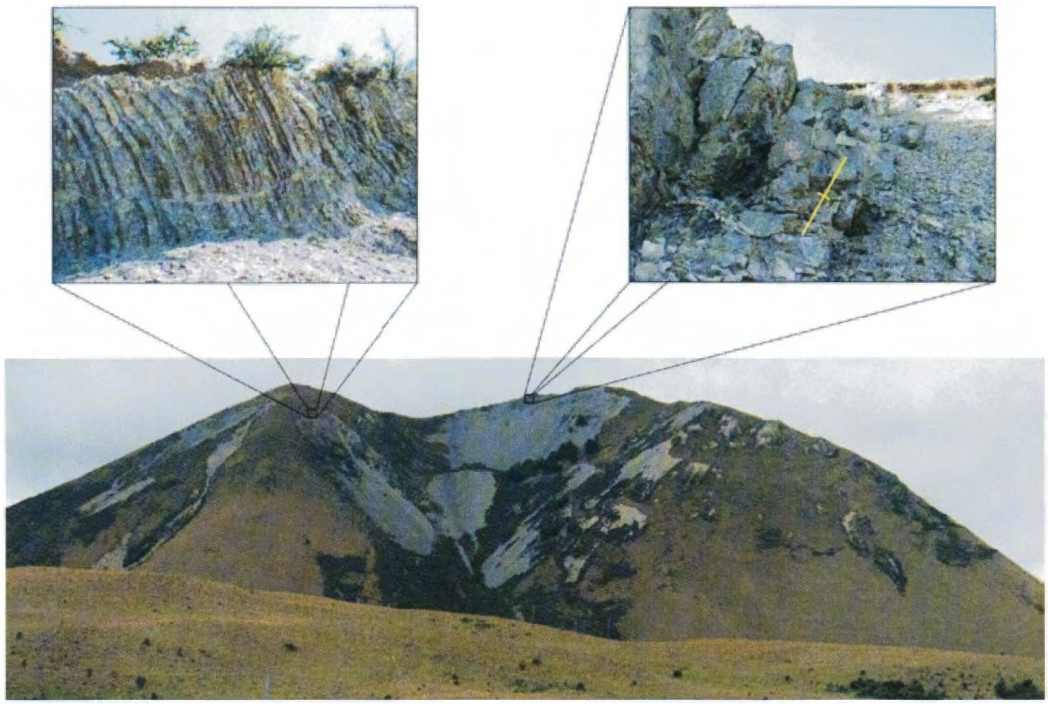

Figure 2.3: Variations in bedding of Torlesse Supergroup greywacke from within the source basin of Carriage Drive. Top right photograph has bedding and strike indicated with a yellow strike and dip symbol. The sandstone beds are tens of centimetres thick while the mudstone beds are only millimetres thick. Alternatively, the rhythmic bedding in the top left photograph is more even between mudstone and sandstone beds. In both photographs the bedding has a very similar strike and dip (~000/80-90 °E), however due to the angle of the photograph they look quite different.

2.2.1.3 Joint Fracture Patterns

The Torlesse Supergroup strata on Carriage Drive are highly fractured. Numerous joint sets intersect the rock mass, which combined with physical freeze-thaw breakdown, creates a complex array of fracture patterns. Damage to the surface of rock masses was explained by GERBER (1980) and SCHEIDEGGER (1963) as being caused by a *combination of exogenous and endogenous forces,* where exogenic forces refer to weathering and erosion, while endogenic forces refer to internal (tectonic) stresses (KINAKIN and STEAD, 2004). It was because of this difficulty that joint set analysis was not undertaken as the level of "background noise" or scatter of randomly

orientated joint surfaces created by both tectonic fractures and freeze-thaw, was thought to have been too great (Appendix B2).

2.2.2 Rock Mass "Relaxation" Features

"Relaxation" or dilation of the Torlesse Supergroup bedrock is evident (figure 2.4) around the exposures on Carriage Drive within the source bowl. Relaxation of the bedrock is also evident along the Cottons Sheep Range where another landslide failure has occurred to the northwest of Carriage Drive. Figure 2.4 is indicative of rock mass dilation where fractures and joints open, thereby creating greater void spaces which then allow more precipitation to enter the rock mass. Greater void space within the rock mass stores more water, and on freezing this results in physical disintegration in the near-surface environment (probably ≤ 3 m depth).

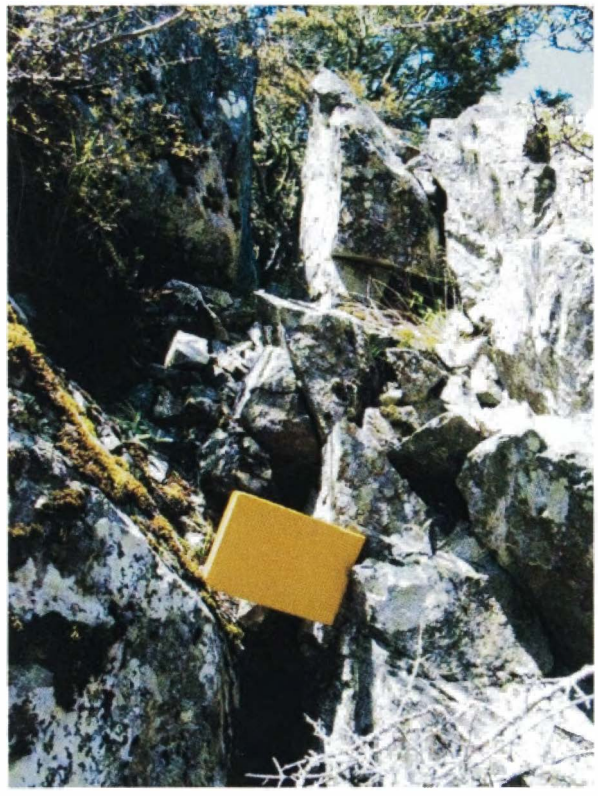

Figure 2.4: "Relaxation" of joint within Torlesse Supergroup greywacke located on the northeastern section of the head scarp of Carriage Drive. The orientation of the joint is (028/76°E). Slope falls away from left to right.

Thus with repetitive cycles of freezing and thawing, the rock mass can progressively disaggregate within the near-surface. The development of fractures not only increases permeability of the rock mass (through greater void space), but also

increases the deformability of the rock mass and reduces the rock mass strength (AUGUSTINUS, 1995a).

2.2.3 Ridge Rent Development

Eight ridge rent or "anti-scarp" structures are located on the northeastern flank of Carriage Drive, adjacent to the source area for the Lake Coleridge Rock Avalanche events. The ridge rents all have uphill facing scarps subparallel to topographic contours. The scarps approximate the strike of the Torlesse Supergroup basement bedding along the northeastern flank, and range in strike from ~330° to 000° (Section 2.2.1.2). The dip of the ridge rents is believed to be controlled by the dip of the Torlesse Supergroup which is typically sub-vertical (42 to 82°, with the dip alternating from east to west on either side of the summit of Carriage Drive). The "anti-scarps" vary between 0.5 metres and 1.5 metres in height from crest to trough. The intersection of two ridge rents along the northeastern ridge and the southwestern ridge, to the north of the summit of Carriage Drive has created a wedge shaped portion of the rock mass. This wedge of material shows ~1.5 m of vertical displacement, and has a horizontal component of movement of ~2 m towards the southeast and is discussed further in Section 3.7.

The ridge rents are spaced irregularly down the ridgeline (the range of spacing varies from 5 m to 40 m in plan view), varying in surface expression and extent. They are only located on the upper portion of the ridge, which is a common characteristic of ridge rents (BECK, 1967). Ridge rents are very common within the Lake Coleridge area, a fact that was highlighted during a regional study by CHAMBERLAIN (1996), and their grouping along steep ridge crests was noted by ELVY (1999).

The development of ridge rents is interpreted to be a response to changing stress fields acting on the rock mass. AUGUSTINUS (1995a) explained that in *hard, slightly fractured, tectonically stressed rock, brittle fractures develop with release of the internal rock stresses*. However, as identified on the flanks of Carriage Drive, the development of ridge rents is controlled by the structure of the Torlesse Supergroup basement strata. On glaciated slopes, either new joints develop or pre-existing joints with suitable orientations enhance rock mass weakening and dilation. AUGUSTINUS (1995a) found that ridge rents were located close to summits within the Mt. Cook

area and that this reflected rock-mass bulging (on a large scale) with downslope movement creating "anti-scarps" (or ridge rents).

CHAMBERLAIN (1996) devoted a Chapter in his MSc thesis to ridge rents, concluding that ridge rent development tends to be associated and best developed in glaciated areas. He suggests that oversteepening of valley walls by glacial erosion increases shear stress in the valley sides to such an extent that release and slip along near vertical dipping structures occurs because of coeval rock mass creep. The development of ridge rents relies heavily on short-term shear stress changes (CHAMBERLAIN, 1996). BOVIS (1982, 1990) studied rock mass deformation on slopes overlooking the Affliction Glacier in southwest British Columbia, where it was occurring in the form of fracture development, antiscarps (termed ridge rents in this project), elongated grabens and collapse pits. BOVIS identified these as being indicators of tension and near-surface movement, in agreement with CHAMBERLAIN'S (1996) findings.

BALLANTYNE (2002) explains that rock mass creep or rock mass deformation is equivalent to 'deep-seated creep' in bedrock and to the German term *Sackung,* which actually describes the process of 'rock mass sagging'. CHIGIRA (1992) suggested that slow rock mass movement landforms such as ridge rents could be a major factor in reducing rock slopes to a conditional stability state, highlighting that these features often occurred before catastrophic failure. The ridge rents along the ridge crests of Carriage Drive are interpreted to be indicators of rock mass dilation occurring within the source area. Outward toppling of the sub-vertically dipping Torlesse Supergroup strata with planar failure along argillite beds is believed to have occurred. This is thought to be a near surface feature, with the persistence of the ridge rents extending for tens of metres into the rock mass.

2.3 Late Quaternary Glaciations within the Rakaia Valley

2.3.1 Overview

Late Quaternary deposits within the Lake Coleridge area are mostly associated with glacial ice advances. However, due to ice advancing down the valley past the field area, many glacial features such as terminal moraines are not present within the study site and are located southeast of the LCRAD site. The terminal moraine of the

Acheron 3 Advance is particularly important to the Lake Coleridge area because of its influence on the lake height during various stages of ice retreat. Because of the extensive record of glaciations, the Rakaia Valley has been the subject of numerous studies; a brief outline of these is given below.

2.3.2 Previous Glacial Studies within the Rakaia Valley

Throughout the history of European settlement, numerous scientists and mountaineers have visited the Rakaia Valley. HAAST (1866) published the results of topographical and geological exploration undertaken in the headwaters of Upper Rakaia Valley. COX (1926) was the first to recognise that there had been multiple phases of glacial advance, finding evidence for two advances at the Rakaia Gorge. SPEIGHT (1926) studied and described the glacial lake silts that are a common feature throughout the entire valley. SPEIGHT suggested that the valley was once the location of a lake from the Rakaia – Wilberforce confluence to the Rakaia Gorge, an idea that has been discarded by all succeeding studies of the area (figure 2.5). SPEIGHT (1933) revisited the area and discussed the evidence for seasonal advances, however did not trace the limits of the multiple ice advances. ROSS (1954) undertook a geomorphological study of the High Peak Valley, extending the research of SPEIGHT.

Studies failed to reconstruct a complete glacial sequence for the Rakaia Valley until SOONS (1963) identified four major ice advances. All of the advances in the valley are Late Pleistocene in age (ELVY, 1999). SOONS divided the younger Otira Glaciation into three major ice advances and recognised a much older Waimaunga (now Waimea) Glaciation separated by a significant interglacial. Throughout succeeding studies of the area, nomenclature used by SOONS (1963) has continued to be used (Table 2.1). CARRYER (1967) recognised a further advance, the Blackford Advance, which preceded the Bayfield 1 Advance; however, it has been grouped with the Bayfield Advance by all later workers (e.g. SOONS and GULLENTOPS, 1973).

2.3.3 Glacial Deposits and Distribution

The Rakaia Valley glacial sequence has been well documented so detailed descriptions of glacial features and deposits are not repeated in this study. Comprehensive descriptions are given by SPEIGHT (1926, 1933), GAGE (1951), SOONS (1963), CARRYER (1967), RAINS (1967), SOONS and GULLENTOPS (1973), BURROWS and RUSSELL, (1975), BURROWS and MAUNDER (1975), SOONS and BURROWS (1978),

BURROWS (1995, 1996), with more recent publications providing summaries of earlier works such as SUGGATE (1990), FITZSIMONS (1997) and ELVY (1999). It is relevant, however, to summarise the last major glaciation that affected the middle Rakaia Valley where the project site is located – the Acheron Advances (Table 2.1).

2.3.4 Late Quaternary Event Chronology

2.3.4.1 General

The Lake Coleridge geomorphology has been strongly influenced by each of the Woodlands, Tui Creek, Bayfield and Acheron Advances. Tectonic activity (Section 2.5) is largely responsible for the relief of the Southern Alps, while a large portion of the mountain range has been carved by ice during glaciations. Due to the nature of succeeding larger glacial advances removing and reworking material left by smaller preceding advances (which destroys any evidence for these), the Acheron 3 Advance is potentially important in the Lake Coleridge area. The Acheron 3 Advance was the last major ice advance through the upper and middle Rakaia Valley, and its effects are clearly evident. Because of its importance, the Acheron 3 Advance discussion will be the focus of Section 2.4, while an overview of the earlier Acheron 1 and 2 Advances is provided first.

2.3.4.2 The Acheron Advance Deposits

The Acheron Advance, identified by SOONS (1963), included all advances in the middle Rakaia Valley that post-date the Bayfield Advances. Identification of moraine deposits allowed recognition of three ice advances in the Acheron sequence. SOONS believed that only relatively minor fluctuations of the ice front were responsible for the different advances, and that there were no major time intervals between them. The Acheron Advances have been dated from before 14,000 years B.P. for Acheron 1 to 11,650 ± 200 years B.P. for the Acheron 3 Advance by BURROWS (1975, 1979, and 1983) and BURROWS and RUSSELL (1975), which indicates a significant but not major time lapse between advances. SOONS (1963) also believed that ice remained at low elevations down the valley during the Acheron Advances.

The two main ice streams affecting the Middle Rakaia Valley were the Rakaia Glacier and the Wilberforce Glacier (figure 2.5). The Rakaia Glacier, sourced predominantly from the Lyell and Ramsay glaciers in the headwaters of the Rakaia River, advanced down the Rakaia River depression. The Wilberforce Glacier occupied

Table 2.1: Summary of Late Quaternary glacial stratigraphy of the Rakaia Valley.

Climatic Event and Stages		Oxygen Isotope Stage**	Advance/ Retreates	Age & Dating Evidence	Reference
Historical times		1	Lyell and Ramsay Glaciers retreat	Terminal moraine mounds mapped from site visits during 1866 – 1950.	HAAST, 1866; SPEIGHT, 1910; BOOT, 1933; GAGE, 1951
Aranui Interglacial ice fluctuations	HOLOCENE		Reischek	Not dated but estimated to have occurred after **4,540±105 year B.P.**	BURROWS and RUSSELL, 1975; FITZSIMONS, 1997
			Meins Knob	Radiocarbon date of **4540 yr BP** (NZ 1287). Fossilised wood.	BURROWS and RUSSELL, 1975
			Jagged Stream	Radiocarbon date of **>9520±95 yr BP** (NZ 688).	BURROWS, 1975
			Lake Stream	Radiocarbon date of organic sediments in Quagmire Tam of **11,900±200 yr BP** (NZ1652) and an earlier age of **10,000±150 yr BP** (NZ1653).	BURROWS and RUSSELL, 1975
		Major Recession of ice from the valley			
Otira Glaciation	LATE PLEISTOCENE	2	Acheron 3	Organic material in lake silts overlain by Acheron 3 moraine provided a radiocarbon date of **11,650±200 yr BP** (NZ1290)*. Luminescence date of loess overlying till at the LCRAD site yielded an age of **9,720±750 yr BP** (WLL389). This date indicates that the project site was ice-free by 9,750±750. †	BURROWS, 1979 *This date is somewhat questionable as BURROWS and RUSSELL (1975) have placed the Lake Stream advance at this time. †Date sourced from this project.
			Acheron 2	**14,000 yr BP to 11,650±200 yr BP**	
			Acheron 1	Acheron 1 Advance **>14,000 yrs BP** with the retreat of the Rakaia Glacier inferred to have begun around **14,000 yr BP**	BURROWS, 1983
		Minor Recession			
		2.2	Bayfield 3	Plant remains in lake silts provided a radiocarbon date of **19,750±600 yr BP** (NZ4298)	SOONS and BURROWS, 1978
			Bayfield 2	A plant rich bed within silts provided a radiocarbon date of **22,800±800 yr BP** (NZ3140)	SOONS and BURROWS, 1978
		3?	Bayfield 1	Outwash dated at **35,170 ± 580 yr BP** within the Lyndon Stream area.	SOONS and BURROWS, 1978
		Major Recession of ice from the valley/Interglacial			
		4	Tui Creek 3	Undated but inferred from ocean oxygen isotope (stage 4) for the Tui Creek advance of **~56,000 yr BP**	RICKER *et al*, 1993 after IMBRIE, *et al*, 1984.
			Tui Creek 2	Undated but inferred through ocean oxygen isotope dating **>56,000 <70,000 yr BP**	RICKER *et al*, 1993 after IMBRIE, *et al*, 1984.
			Tui Creek 1	Ocean oxygen isotope (stage 4) has been inferred for the Tui Creek advance of **70,000 yr BP**	RICKER *et al*, 1993 after IMBRIE, *et al*, 1984.
		5	*Kaihinu Interglacial*		
Waimea Glaciation		6	Woodlands	?	?
		7	*Karoro Interglacial*		
Waimaunga Glaciation		8	Hororata	?	SUGGATE, 1990

** Appendix C for Oxygen Isotope Stages from ELVY (1999).

the Coleridge Trough (position of Lake Coleridge at the present day) and was sourced predominantly from the Wilberforce valley and possibly the Harper valley. During earlier glaciations (i.e. the Bayfield and perhaps the Acheron 1 and 2 Advances) ice would have occupied the adjacent smaller valleys to the east of Cottons Sheep Range. However during the Acheron 3 Advance it is thought that ice was predominantly contained within the two main ice streams from the Rakaia Glacier and the Coleridge Glacier (figure 2.5). During ice retreat, the smaller valleys would have acted as meltwater channels, draining the water away from the glaciers until or unless blocked by fan or landslide debris.

2.3.4.3 Acheron 1 Advance

A terminal moraine loop situated on the west bank of the Rakaia River downstream of Cleardale homestead (grid reference K35: 956 497) marks the maximum extent of the Acheron 1 ice. Lateral moraines located on the south-western edge of Lake Coleridge between Lake Coleridge and the Lake Coleridge Power Station provide evidence for two distinct ice streams; one ice stream down the Rakaia Valley from the Rakaia Glacier and the other ice stream down the Coleridge Trough from the Wilberforce Glacier. Kettle holes are prevalent within and around the Dry Acheron Valley (figure 2.5), which indicates that the glacier wasted *in situ* from its terminal position (SOONS, 1963).

2.3.4.4 Acheron 2 Advance

The Acheron 2 Advance has been defined from lateral moraines, as terminal moraines have not been located (SOONS, 1963). It is believed that during the Acheron 2 Advance the Wilberforce Glacier was much smaller than the Rakaia Glacier, based on evidence from moraines located between Lake Hill and Mount Barker and a moraine between the southern edge of Mount Georgina and Mount Barker toward Red Hill (SOONS, 1963). At a locality just downstream of the Acheron Bridge (grid reference K35: 958 555) an exposure on the right bank (described by SPEIGHT, 1926) reveals a till deposit consisting of unsorted gravels and angular clasts within a blue clay matrix (SOONS, 1963). Rhythmic or glaciolacustrine deposits lie directly above the till, and the silts coarsen upward into sands and gravels. These sediments represent the damming of the Acheron River by glacial ice, and LAUDER (1962) titled the lake the "Rakaia Lake".

Ice from within the Coleridge Trough is believed to have moved eastwards during the Acheron 2 Advance into the low-lying topography between Carriage Drive, Laings Hill and Kaka Hill; with tongues extending towards Mt Barker between Kaka Hill and Mt Georgina (SOONS, 1963; Appendix D; figure 2.5).

2.4 Lake Coleridge Trough and Surrounding Area

2.4.1 Background

The landscape within the Rakaia Valley has undergone extensive changes and reworking both during and between glacial episodes. Sediment reworking continues, for example; fluvial and aeolian erosion, slope instability, alluvial fan development, and lake sedimentation. However, closely following the retreat of glacier ice, the newly exposed landscape underwent rapid change. Accelerated erosion of this nature is highlighted by BALLANTYNE (2002) as "paraglacial"; and debuttressing of glacially steepened valley sides may result in slope failure or enhance rockfall activity. Unvegetated slopes become vulnerable to reworking by debris flows, snow avalanches and slopewash. Aeolian erosion and transportation, frost action and rivers also entrain and redistribute large volumes of unconsolidated glacigenic sediment (BALLANTYNE, 2002). Fluvial system changes between glaciations and inter-glaciations have perhaps been the most significant changes within the area. Meltwater channels around Lake Coleridge have also been abandoned.

The Lake Coleridge Trough is directly adjacent to the LCRAD site. During the Acheron 3 Advance, ice from within the Coleridge Trough is believed to have moved eastwards into the low-lying area between Carriage Drive, Laings Hill and Kaka Hill, with possibly a small tongue of ice extending between Kaka Hill and Mt Georgina. The influence of glacial ice within the area surrounding the LCRAD site during the Acheron 3 Advance was significant (figure 2.5). Similar to the damming of the Acheron River, there is a strong possibility that the plug of ice within the trough blocked the path of the ancestral Ryton River for a significant period (figure 2.5). Section 2.4 attempts to reconstruct the history of the immediate area surrounding the LCRAD site, starting with the Acheron 3 glacial maximum then progressing through to the present day.

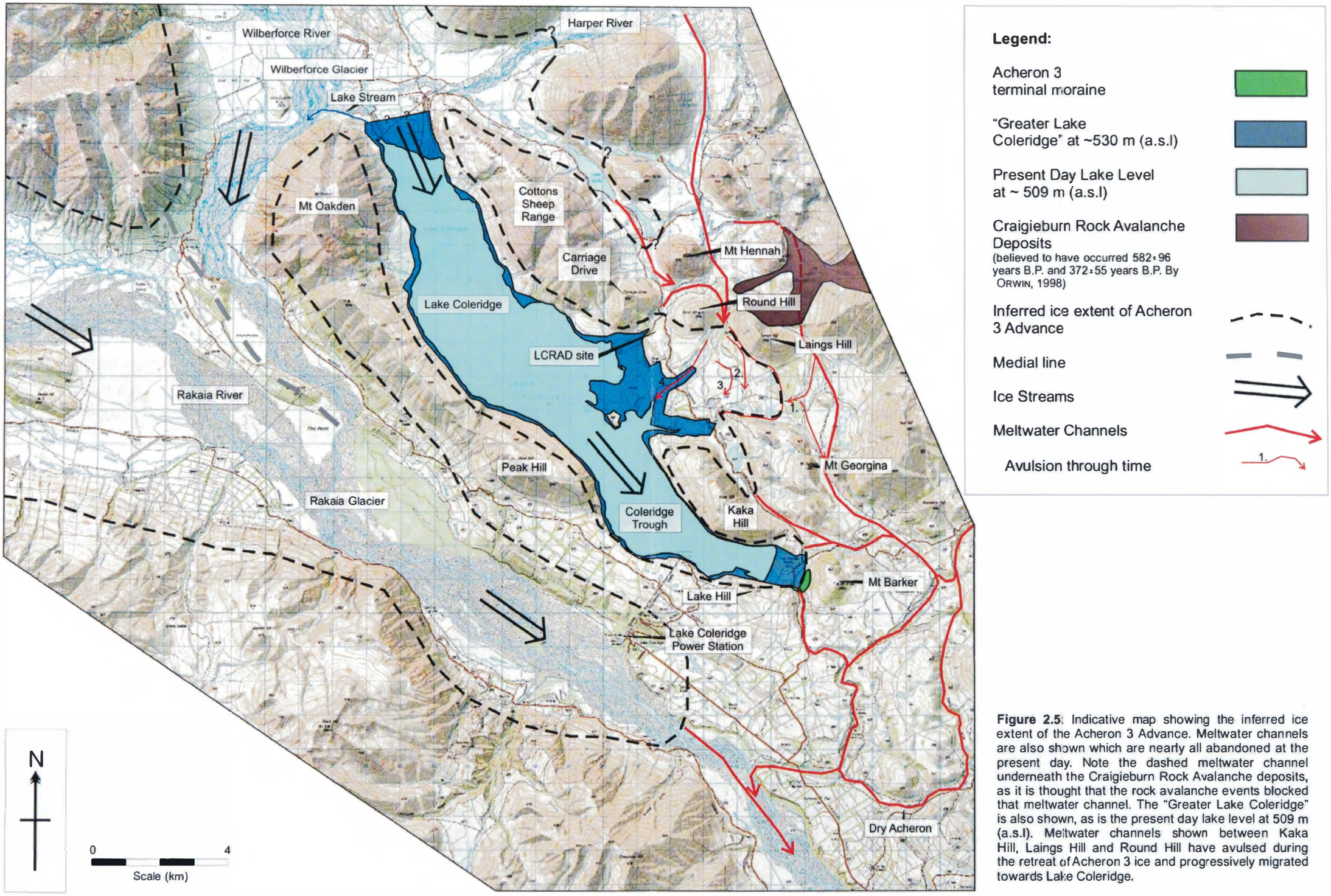

Figure 2.5: Indicative map showing the inferred ice extent of the Acheron 3 Advance. Meltwater channels are also shown which are nearly all abandoned at the present day. Note the dashed meltwater channel underneath the Craigieburn Rock Avalanche deposits, as it is thought that the rock avalanche events blocked that meltwater channel. The "Greater Lake Coleridge" is also shown, as is the present day lake level at 509 m (a.s.l). Meltwater channels shown between Kaka Hill, Laings Hill and Round Hill have avulsed during the retreat of Acheron 3 ice and progressively migrated towards Lake Coleridge.

2.4.2 Acheron 3 Advance

2.4.2.1 Ice Extent and "Greater Lake Coleridge" Development

The Acheron 3 advance was relatively limited, with the associated terminal moraines being very small in extent (SOONS, 1963). Moraines are located near the Lake Coleridge Power Station (specifically Trig Y, grid reference K35: 114 353), and these continue around beneath the Lake Coleridge road to the base of a steep slope located near the Peak Hill Road (SOONS, 1963; figure 2.5). The terminal moraine loop located near the Lake Coleridge homestead represents the readvance of ice from the Wilberforce Glacier within the Coleridge Trough to form the Acheron 3 terminus. A meltwater channel cuts through the moraine, and this is followed by Homestead Road for about 1 km (figures 2.5 and 2.6).

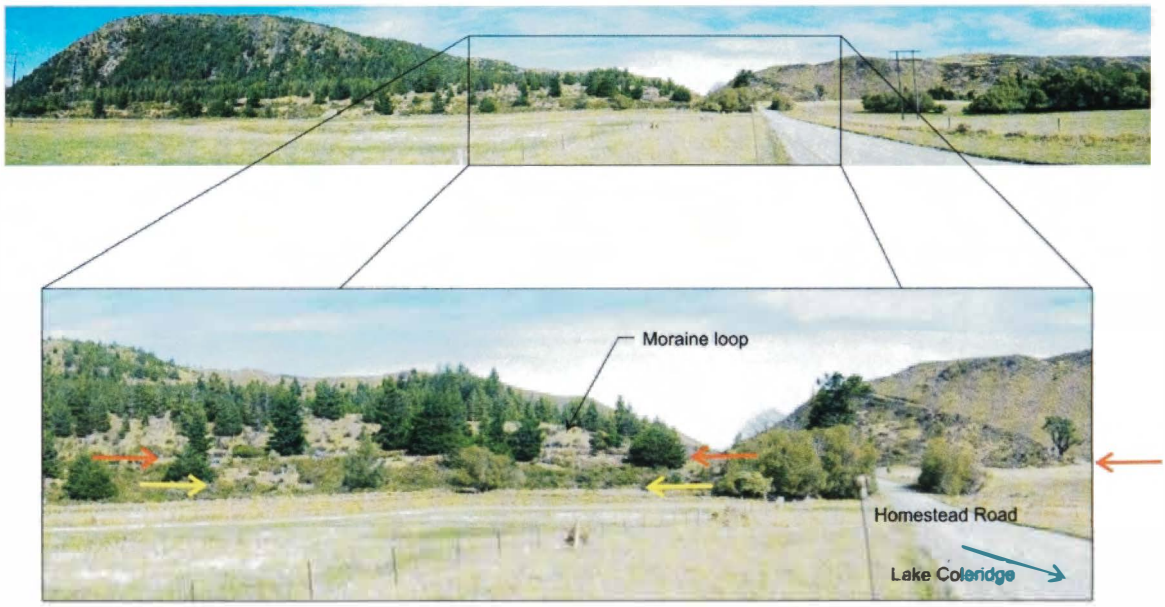

Figure 2.6: Two prominent lake beaches are located within the terminal moraine loop of Acheron 3 near the Lake Coleridge Homestead, at the southeastern end of Lake Coleridge. The orange and yellow arrows pointing along the horizontal beaches indicate the two different heights. The beach indicated by the orange arrows is 530 (± 1.5) m above sea level, while the yellow arrows indicate the beach at an elevation of 525 (± 1.5) m above sea level. The pine trees in the background in the bottom photograph are growing on Acheron 3 terminal moraine. The road (Homestead Road) passes through moraine and is aligned along the meltwater channel (discussed in text). North is directly behind photographer. Note the roche moutonnée hill in the top left of the photograph (Mt Barker).

The maximum extent of the Acheron 3 ice is clearly preserved within the terminal moraine at the foot of Mt Barker (figure 2.6). SOONS (1963) mapped the Acheron 3 ice extent but did not extend into the study area for this project. Acheron 3 ice is believed

to have extended into the low-lying area between Kaka Hill, Laings Hill and Round Hill, but it was not as extensive as during the Acheron 2 Advance and it did not reach Mt Barker.

Figure 2.5 shows the avulsion of meltwater channels progressively moving towards the southeast within a fan deposit between Kaka Hill, Laings Hill and Round Hill. Within this fan, kettle lakes are present within the gravel sequence (figure 2.1) indicating that ice was present during the deposition of the fan gravels. Kettle lakes develop in hollows that are created by the melting of buried ice (LOWE and WALKER, 1997) and it is believed that due to ice blockage (within the present day Ryton River section) meltwaters were diverted around the northern flank of Round Hill. During this time, the diverted sediment-rich waters are thought to have flowed over or around lagging ice within the low-lying area. This ice is believed to have been stagnant and possibly wasted away *in situ,* thus creating the kettle lakes that are present within the fluvial fan. As the ice front either receded or diminished, meltwater that was flowing around the margin of the ice front followed the ice and progressively moved towards the southwest, finally taking a direct route into "Greater Lake Coleridge" (figure 2.5).

The meltwater channel that cut through the terminal moraine near Mt Barker is interpreted to have carried meltwaters from the Acheron 3 Advance, and to have been the drainage channel for "Greater Lake Coleridge", which developed between the snout of the retreating ice front and the terminal moraine. It is also believed that the channel continued to act as an outlet for the enlarged lake for a period after initiation of the ice retreat (SPEIGHT, 1933) until the lake level dropped to an elevation below that of the base of the channel at 530 m (a.s.l). "Greater Lake Coleridge" is believed to have existed until the removal of the ice front from the Coleridge Trough, and then the Lake Stream is believed to have become the outlet for Lake Coleridge (figure 2.5). "Greater Lake Coleridge" progressively lowered with two relatively stable positions at 530 m and the other at 525 m before ultimately lowering to the present day elevation of ~509 m (a.s.l), which is artificially controlled for hydro power generation.

Another beach stand was identified around the northern tip of Kaka Hill (figures 2.1 and 2.5) from a "nick point" in the Torlesse Supergroup bedrock. Topographic

contours between 520 and 540 m (a.s.l) show that this beach was at approximately the same elevation as the beaches at the southern end of Lake Coleridge within the Acheron 3 terminal moraine, although a precise elevation has not been obtained.

2.4.2.2 Glacial Till Deposits

The glacial till deposits located around the LCRAD site are well compacted, and contain well-rounded clasts (some with striation marks) that are poorly sorted and matrix-supported within fine-grained silty sands. The till that is present within the field area is interpreted to be supraglacial till and probably melt-out till due to its internal appearance (e.g. fluvial seepage has occurred through the till that is inferred to be syndepositional). Professor J. SHULMEISTER, University of Canterbury, *pers. comm.*, 2004, confirmed this. During excavation of Trenches 1 and 4 (Sections 3.4.4 and 3.4.5), glacial till was exposed underlying the LCRA1 deposit. Internally the till was an unweathered, moist, compact, light greyish brown, massive, matrix-supported, silt to sand with some well-rounded to sub-rounded coarse to fine Torlesse Supergroup greywacke gravels.

2.4.2.3 Lake Sediments or Glaciolacustrine Deposits

Coarse lake sediments (granule to coarse sands and silts) were located along the banks of the Ryton River (grid reference K35: 923 694) where approximately 1 m of the section is exposed (figure 2.7). Within the section there are laminar beds (millimetres to centimetres thick) with alternating grain sizes from silts in the finer-grained beds to sands and granules in the coarser-grained beds. Colluvial gravels believed to be from glacial tills deposited upslope during earlier glacial activity overlie the lake sediments, creating soft sediment deformation within the top 15 cm of the deposit.

The lake sediments are thought to represent ephemeral ponding of an ancestral Ryton River and quite possibly meltwater channels during glacial activity (as discussed in Section 2.4.1). A GPS survey revealed that the elevation for these sediments of 557 m (a.s.l) did not correlate with a maximum height of "Greater Lake Coleridge", being well above the maximum lake level of ~530 m (Section 2.4.2.1). The lake sediments are thought to be coeval or older than the Acheron 3 Advance, however their actual age is unknown.

Figure 2.7: Glaciolacustrine deposits exposed by a small superficial landslip, located on the true left bank of Ryton River ~200 m upstream from the Ryton Bridge. Soft sediment deformation (highlighted by arrow) has occurred at the top of the section by overlying colluvial gravels.

Fine sediments of sand and granule size, located further upstream within the Ryton River (grid reference K35: 927697), also on the true left, are contorted and deformed (figure 2.8). GPS surveying showed that the sediments were at an elevation of 557 ± 1 m, and are therefore not associated with the "Greater Lake Coleridge". Glacial tills overlie the small 'pocket' of fine sediment. SOONS (1963) highlights the tendency for lake silts in the Rakaia Valley to be contorted in character, suggesting that their depositional environments were in a number of ice-marginal lakes relating to different ice advances, particularly in retreat stages, and not in one continuous lake. The deformed sediments identified within the Ryton River are thought to be ice-contact deposits that have been deformed, due to excess pore pressure and water escape, caused by overburden pressures and/or effects of readvancing ice and till.

Figure 2.8: Deformed lake sediments exposed on the true left bank of Ryton River ~1 km upstream from the Ryton Bridge. Yellow arrows indicate foreset beds in overlying gravels, while orange arrows indicate planed surface directly above soft sediments. Note the backpack for scale.

2.4.3 Drainage Changes

2.4.3.1 Fluvial Drainage Changes within the Valley

Fluvial drainage within the Lake Coleridge area has changed markedly between glaciations and interglacial periods. During glaciations, the glaciers within New Zealand had characteristically large volumes of water associated with them, and because of this during glaciations large volumes of water are flushed through the glacial system, out through meltwater channels and away from the ice front. During interglacial periods, precipitation is the main source for fluvial systems, which is normally less than during glaciations. Because of this, the geomorphology of the area displays relict fluvial systems such as alluvial fans and meltwater channels. The following discussion refers to figures 2.1 and 2.5 for locations.

2.4.3.2 Meltwater Channels

During SOONS' (1963) study of the glacial sequence of the area, meltwater channels were identified (Appendix D), two of which are located towards the southeastern edge of the present field area (figure 2.5). The first is located on the northeastern side of Kaka Hill (figures 2.5 and 2.9), where waters flowed to the northeast of Mt Barker, before draining down towards the south and joining water within the Rakaia riverbed (figure 2.5). The second is a meltwater channel that has eroded the Acheron 3 terminal moraine at the south-eastern end of Lake Coleridge, between Mt Barker and Lake Hill. The meltwater channels during the Acheron Advances are believed to follow drainage established during earlier advances, with minor exceptions such as the channel through Acheron 3 terminal moraine (SOONS, 1963). The two meltwater channels that have been mentioned both lack stream flow at the present day.

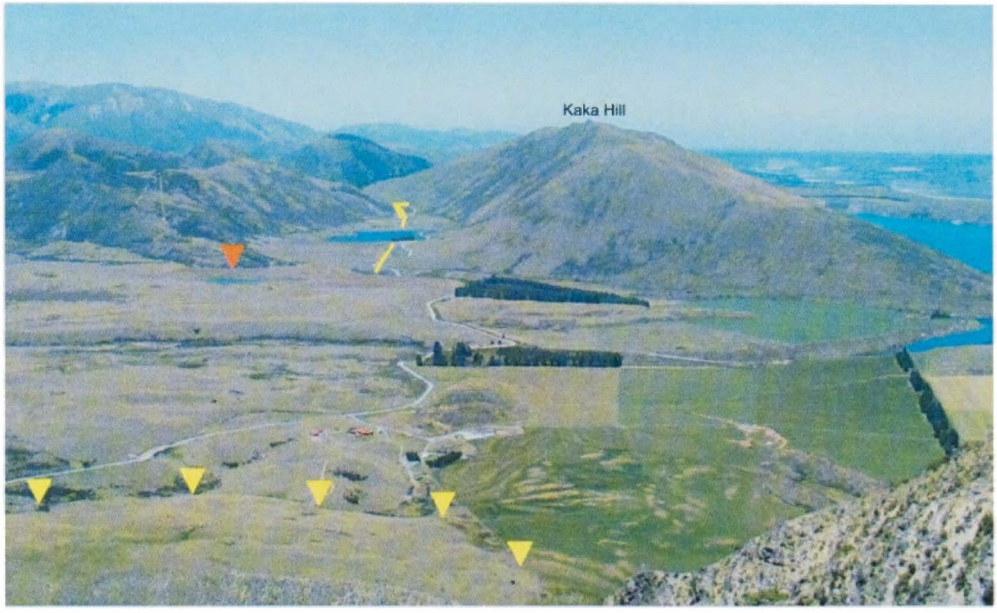

Figure 2.9: View to the south looking at the Kaka Hill meltwater channel (highlighted by yellow arrow in background) which transferred Acheron 3 glacial meltwater out of the valley. Lake Georgina (located within broken section of arrow) is located within this meltwater channel. A kettle lake is visible (highlighted by the orange arrowhead). The outline for the LCRA1 is shown with the yellow arrowheads. Photograph taken from top of Carriage Drive. Lake Coleridge is just visible to the right of the photograph.

As briefly discussed in Section 2.4.2.1, drainage into Lake Coleridge has also been altered during the course of the last glaciations. Drainage from Lake Coleridge has changed from the Mt Barker end (through the meltwater channel discussed above) to the head of the lake (figure 2.5). During the retreat of Wilberforce ice from the Coleridge Trough it is thought that the "Greater Lake Coleridge" lowered in elevation to a level that is similar to the present day. Lake Stream, situated at the head of the lake, would have then regulated the lake height. Since withdrawal of Acheron 3 ice the main watercourses have been confined to two Rakaia tributaries out of the upper valley, the Harper and the Wilberforce Rivers, which flow into the Rakaia just north of Lake Coleridge (figure 2.5). Historical alterations to the lake level occurred during the construction of the Lake Coleridge Power Station (1911 - 1914) raising the height by just a few metres (BRITTAN, 2000).

2.4.4 Ryton Delta – Present Day Activity

The Ryton River flows down the most direct, low-lying path to Lake Coleridge. There is clear evidence that at some stage an ancestral Ryton River was diverted around the northeastern flank of Round Hill (figures 2.1 and 2.5). Acheron 3 ice is believed to have dammed the flow of water near the LCRAD site, and this blockage within the

riverbed would have also redirected meltwater flowing down adjacent valleys (figure 2.5). As discussed above, the waters flowed around Round Hill and then created a fan deposit overriding wasting Acheron 3 ice. The withdrawal or wastage of ice from the area between Round Hill, Laings Hill and Kaka Hill is recorded by the fan terraces cut by avulsing meltwaters (Section 2.4.2.1). When the ice retreated from the LCRAD site, the meltwaters and ancestral Ryton River waters were reinstated within the lower portions of the Ryton riverbed which cut off the outlet to the aggrading fan (discussed above).

The Ryton River as it exists today began to erode into the Ryton riverbed depression, carrying sediment into "Greater Lake Coleridge", and depositing it as a delta. The "Greater Lake Coleridge" height continued to lower with the withdrawal of the Wilberforce Glacier from the Coleridge Trough until the height was similar to that of the present day. Sediment input into the river has been aided by the three rock avalanche events (the LCRA1, LCRA2 and LCRA3). These events temporarily dammed the river for different periods of time (as discussed in Section 3.8). However after each event, the Ryton River overtopped the "dam" and was reinstated within the riverbed. The influx of sediment from the rock avalanche deposits into the Ryton River, combined with the natural bedload, has contributed to the development of a gravel delta at the mouth of the river into Lake Coleridge. With the continued deposition of material, the delta will continue to prograde into the lake.

2.5 Active Tectonics

2.5.1 Introduction

Lake Coleridge is situated in a high seismicity zone and is surrounded by numerous large scale thrust and combination thrust/ strike-slip faults (figure 2.10). The Lake Coleridge area is located ~ 140 km to the east of the Alpine Fault, which is the surface expression for the plate boundary between the Australian and Pacific plates. The plate motion vector is trending approximately 30° to the Alpine Fault, with an estimated 37 mm/year of right lateral and 11 mm/year of reverse slip (NORRIS and COOPER, 1995). This implies that seismicity is a key factor in the development of the Lake Coleridge area and modern uplift rates are as high as 8 – 10 mm/year (SIMPSON *et al.*, 1994).

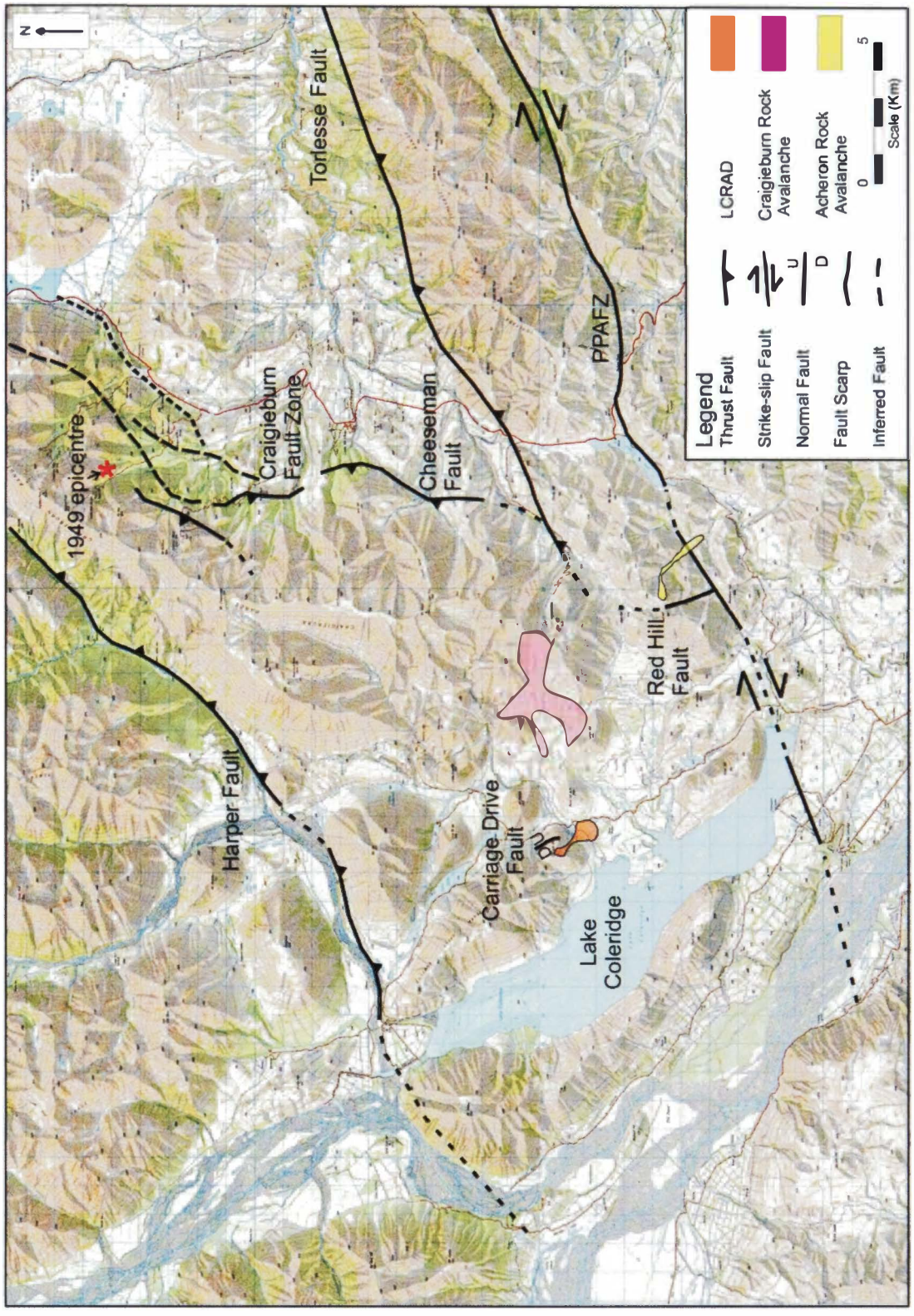

Figure 2.10: Topographic map of major fault systems located around the LCRAD site. The LCRAD, Craigieburn and Acheron Rock Avalanche deposits are also shown. The 1949 earthquake epicentre discussed by EIBY (1990) is also shown.

The studies of major faults within the Lake Coleridge and surrounding areas by COYLE (1988), COWAN (1992), CHAMBERLAIN (1996), ELVY (1999) and HOWARD (2001), combined with studies of seismic hazard analysis by HANCOX *et al.* (2002) and STIRLING *et al.* (2002), have provided a substantial database for the seismic history of the region. The major faults identified within the region (figure 2.10) are the Harper Fault (thrust), Craigieburn Fault Zone (predominantly thrust), Torlesse Fault Zone (thrust), and Porters Pass-Amberley Fault Zone (predominantly strike-slip). Although the Alpine Fault is located outside the immediate study area, due to its ability to generate large scale earthquakes it is also a significant hazard to the region. Lastly, Carriage Drive Fault, located on the northeastern flank of Carriage Drive is discussed in relation to rupture, timing and origin.

These faults have all contributed to the development of the landscape around Lake Coleridge. The structural control placed on Lake Coleridge and surrounding area by large faults is important. The current alignment of the northwest to southeast drainage systems of both the Rakaia and Wilberforce and the Coleridge Trough have been attributed to a regional structural trend, however no fault traces are evident. SPEIGHT (1933) thought that the Rakaia owed its alignment to a major fault which was not exposed within the valley due to the highly dynamic environment and coverage by river gravels. SOONS (1963) also believed that there were hidden faults that were controlling the structure of the landscape. Active faults control some drainage within the area, for example the Harper Fault alignment along the Harper River. The major thrust systems shown in figure 2.10 are also clearly controlling topography. Other internal structures (e.g. bedding or joints) may influence valley orientation and glacier erosion. This subject is not discussed further as the main focus for this project is faulting as potential triggering mechanisms for the LCRA1, LCRA2 and LCRA3.

As outlined in Section 1.5.2.1 an earthquake magnitude of M>6 is needed for the initiation of landslides, and for rock avalanche triggering this is believed to require ≥ M6.5 (HANCOX *et al.*, 2002). The Modified Mercalli Intensity (MMI), which is the intensity felt within an area, correlates with earthquake magnitudes (M) and needs to be ≥MM6 for landslides to occur. The faults discussed briefly below are all capable of producing a M6 or greater earthquake (STIRLING *et al.*, 2002), and therefore of triggering both landslides and rock avalanches. Ruptures outside the Lake Coleridge

area are not discussed (with the exception of the Alpine Fault), but it is acknowledged that their influence on seismic shaking should not be underestimated as illustrated from the historic earthquake cases below.

2.5.2 Historic Earthquakes within the Region

Active tectonics plays a very important role within the Lake Coleridge area. During historic times, four large earthquakes with magnitudes M>6 have affected the area. Two earthquakes in 1929 were felt strongly within the Lake Coleridge valley, from centres near Arthur's Pass on the 9th March and near Murchison on the 17th June. These earthquakes caused no structural damage to any buildings, but the Murchison earthquake created a seiche ~ 30 cm in height in Lake Coleridge, which remained cloudy from suspended sediment for some weeks after the event (BRITTEN, 2000).

In 1946 (approximately midnight on 27th June), a M6.2 earthquake event with an epicentre very close to Lake Coleridge (figure 2.10) awoke residents and damaged all cob buildings in the valley (EIBY, 1990). The Lake Coleridge Power Station suffered broken windows, cracking of joints and pipelines; a crack developed between the original foundation of the powerhouse and an extension (1924-1930); and the concrete weir constructed at Lake Stream needed repair (BRITTEN, 2000). Extensive landslides occurred throughout the area, which at the time were thought to be reactivations of old pre-existing slides, but probably new landslides were activated also (ANDERSON, 1963).

In 1994 on the 18th June, an earthquake centred near the Avoca River was strongly felt in the Rakaia Valley. The Lake Coleridge Power Station suffered damage with broken windows and cracking of perimeter walls. The earthquake was higher in intensity up-valley towards the Harper River end of Lake Coleridge, where slumping of the canal banks occurred. The MMI is estimated for this event at ~ MM6, and once again the lake became clouded with disturbed suspended sediment, remaining so for several months (BRITTEN, 2000).

2.5.3 Harper Fault

The Harper Fault, as described by CHAMBERLAIN (1996), is a major thrust fault which is associated with a wide crushed zone in the Torlesse Supergroup basement (figure 2.10). The strike of the fault is ~070° with a dip of 35° towards the south. The Harper

Fault cuts across Mt Oakden, which is situated on the northeastern shores of Lake Coleridge (figures 2.5 and 2.10). The fault controls the course of the Harper River and can be traced along the banks of the Harper River and further northeastwards. STIRLING *et al.* (2001) interpret the Harper Fault to be capable of producing a M7.1 earthquake rupture. With its proximity to the LCRAD site, a rupture along the Harper Fault could therefore potentially trigger a rock avalanche within the area. Using relative chronology only, PETTINGA *et al.* (2001) believe that the last rupture along the Harper Fault was >10,000 years ago, with a recurrence interval of >10,000 years.

2.5.4 Porters Pass-Amberley Fault Zone (PPAFZ)

The PPAFZ extends over 100 km from the Rakaia River, near the southern end of Lake Coleridge, to north of Waipara and Amberley (COWAN *et al.*, 1996; figure 2.10). The strike of the PPAFZ varies from 058° to 098° (HOWARD, 2001), however the general direction of strike is 077° which corresponds with the relative plate motion vector (DEMETS *et al.*, 1994 in HOWARD, 2001). The PPAFZ is a right lateral strike-slip fault with a component of normal displacement that is evident at high elevations where the fault crosses ridges and hillcrests (SMITH, 2003). Well-developed fault scarps are located irregularly along the PPAFZ, with some scarps being up to 1.2 km in length (HOWARD, 2001).

The slip rate along the fault is believed to range from 0.5-5.0 mm/year (PETTINGA *et al.*, 2001). Paleoseismic evidence highlighted by COWAN *et al.* (1996) shows that two large (M>7) earthquake ruptures has occurred along the PPAFZ within the last ~2,500 years. This was suggested by STIRLING *et al.* (2002) who indicated that the PPAFZ is capable of rupturing with a magnitude of 7.2. SMITH (2003) showed that the PPAFZ represents the likely source of seismicity that triggered the Acheron Rock Avalanche at an age of (Wk 12094) 1,152 ± 51 years B.P. With the limited data from COWAN *et al.* (1996), PETTINGA *et al.* (2001) placed a tentative rupture return period of 1,300-2,000 years between large earthquakes on the PPAFZ.

The PPAFZ is believed to have developed a segmentation fault rupture style where different segments or portions of the fault have ruptured at different times (HOWARD, 2001). Numerous studies focussing on various aspects of the PPAFZ have been conducted (e.g. COYLE, 1988; COWAN, 1992; COWAN *et al.*, 1996; HOWARD, 2001;

SMITH, 2003). From this combined work, a rupture along the western PPAFZ is considered highly likely to have occurred between 500 to 700 years B.P., and SMITH (2003) noted that nine rock avalanche deposits extending to 100 km in distance from the PPAFZ correlated in age with the Acheron Rock Avalanches around 1,000 ± 200 years B.P. This may indicate an episode of seismicity at this time along the PPAFZ, although these rock avalanches could have been triggered by movement on the Alpine Fault.

2.5.5 Alpine Fault

The Alpine Fault is the plate boundary. It is an east-dipping oblique dextral shear structure, which forms a linear feature that extends onshore for ~420 km along the West Coast of the South Island (BERRYMAN *et al.*, 1992; figure 1.2). The fault dips east underneath the Canterbury region (PETTINGA *et al.*, 2001), and therefore has potential epicentres that are beneath west and inland Canterbury including the Lake Coleridge area. The surface rupture is located ~140 kilometres northwest of the LCRAD site (figure 1.2).

The Alpine Fault is briefly considered here within the active tectonics discussion, even though it is located outside the immediate Lake Coleridge area, due to its capability of generating a large earthquake (M>8) that is believed likely to affect the entire Canterbury region (PETTINGA *et al.*, 2001). STIRLING *et al.* (2002) concur with previous findings that the Alpine Fault is capable of producing an M≥8.1 earthquake, which would still produce an intensity of approximately MM9 within the region (HANCOX *et al.*, 2002).

There has been no historical surface rupture on the Alpine Fault, but the last rupture is believed to have been around 290 years ago with a recurrence interval of approximately 250 years (PETTINGA *et al.*, 2001). An earthquake along the Alpine Fault would cause major seismic shaking across the region (PETTINGA *et al.*, 2001), and it is therefore considered a likely source to initiate rock avalanches.

2.5.6 Carriage Drive Fault

The Carriage Drive Fault is located on the northeastern flank of Carriage Drive (figure 2.10). CHAMBERLAIN (1996) mapped Carriage Drive as a normal fault during his study of seismic hazards from cross-faulting within the area. The fault's surface expression

is a scarp ~10 m wide, with the hill-slope side (the southwest) dropping down relative to the valley side (the northeast) as shown in figure 2.11.

A trench (T_5) was excavated across the scarp (figure 2.11) with the primary aims of establishing the nature of faulting and the history of movement on the Carriage Drive Fault (Appendix E). Excavation of T_5 exposed a graben structure containing ~2 m thickness of loess and topsoil which show a maximum vertical displacement of ~1.8 m and a horizontal displacement of ~1.2 m (figure 2.12). The dip of the main fault plane is ~57° to the southwest, with the strike ~140°. Two smaller normal faults were located within the hanging wall of the graben structure in T_5 showing small displacements (30 cm and 10 cm) along both of them (figure 2.11).

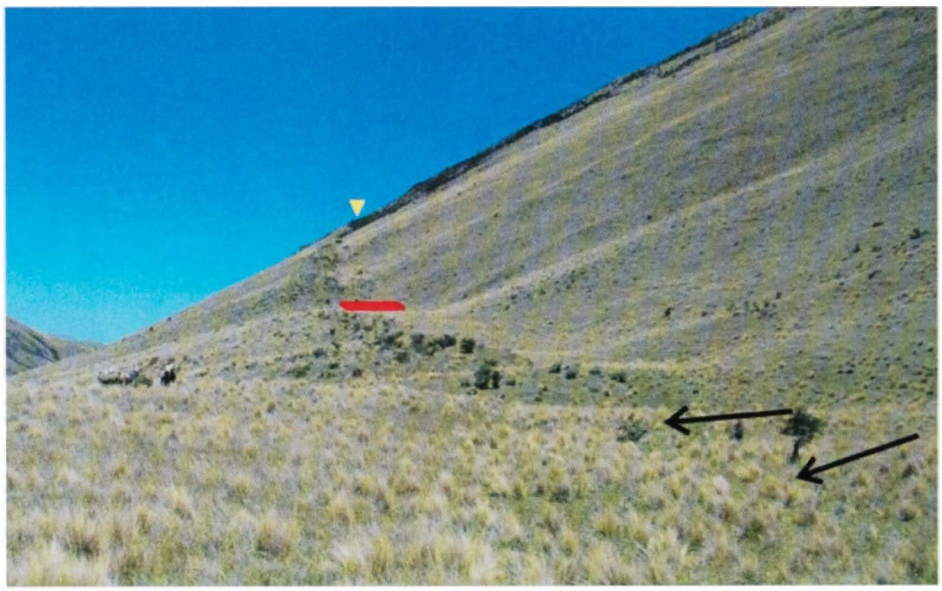

Figure 2.11: Carriage Drive Fault scarp (highlighted by yellow arrowhead). Trench (T_5) location is shown as a red rectangle (figure 2.12). Black arrows show alluvial fan development that has buried the fault scarp. Photograph is taken looking south. Note sheep for scale.

Within the loess one continuous charcoal horizon (~5 mm thick) is present, and a zone rich in charcoal flecks is also present below this (figure 2.12). The two charcoal horizons were dated at (WK15118) 755 ± 46 years B.P. for the upper horizon and (Wk15119) 4,428 ± 35 years B.P. for the lower fleck horizon. Both horizons show drag into the fault, suggesting the rupture post-dates 755 years B.P. It is not possible to determine whether the dates bracket a rupture event.

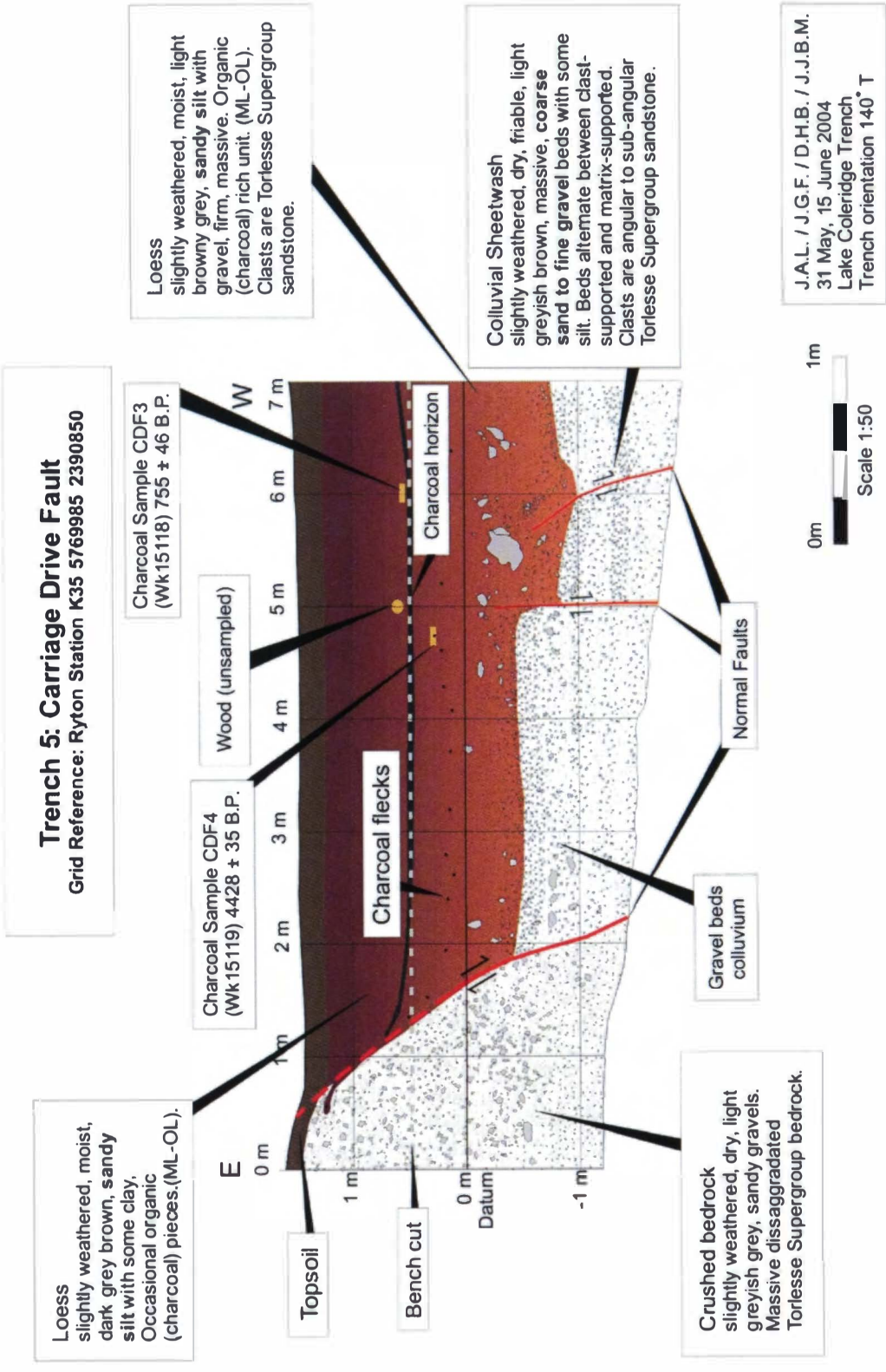

Figure 2.12: T_5 across Carriage Drive displaying small offsets along normal faults. Disturbed charcoal horizons were radiocarbon dated to provide dates of 4,428 ± 35 years B.P. and 755 ± 46 years B.P., which are discussed further in Chapter 4.

The development of the Carriage Drive Fault may be a possible source for a seismic trigger for the Lake Coleridge Rock Avalanche event(s) given its potential size and proximity to the source area. The nature of faulting of Carriage Drive is further discussed in Appendix E.

2.5.7 Other Major Regional Faults

2.5.7.1 Cheeseman Fault

The Cheesman Fault strikes ~190° with a dip of 45° to the southeast (STIRLING *et al.*, 2002). The southwestern segment of the fault is located ~12 km to the northwest of the Lake Coleridge (figure 2.10). The Cheeseman Fault is a reverse fault and extends for approximately 23 km in length (PETTINGA *et al.*, 2001). The estimated slip rate on the Cheeseman Fault is 0.25 to 1.0 mm per year. The calculated maximum magnitude of a rupture along the Cheeseman Fault is believed to be M7.0 by both PETTINGA *et al.* (2001) and STIRLING *et al.* (2002). The last rupture along the Cheeseman Fault is not known, although a recurrence interval is estimated at between 2,000 to 5,000 years by PETTINGA *et al.* (2001). The Cheeseman Fault and the Torlesse Fault (discussed below) both bound the Castle Hill Basin.

2.5.7.2 Torlesse Fault

The Torlesse fault strikes along the northern flank of the Torlesse Range, ~12 km to the east of the LCRAD site. Like most of the faults within the region, the Torlesse Fault is a reverse fault with an interpreted dip angle of the fault plane from 20 – 70° to the east (PETTINGA *et al.*, 2001). The last rupture along the fault has not been constrained, however from slip rates measured within inland Canterbury a recurrence interval for the Torlesse Fault is believed to be from between 2,000 to 4,000 years (PETTINGA *et al.*, 2001). STIRLING *et al.* (2002) have calculated a recurrence interval for the fault of 3,000 years, and both PETTINGA *et al.* (2001) and STIRLING *et al.* (2002) infer the maximum magnitude of a rupture event on the Torlesse Fault to be M6.7.

2.5.8 Discussion of Fault Triggering Potential

From the faults reviewed in Section 2.5 it is clear that there are numerous active structures situated around the LCRAD site which are capable of producing earthquake ruptures with magnitudes greater than M6. A problem exists, however, as ruptures along the major thrust faults such as the Harper, Cheeseman and Torlesse

are poorly constrained. Recurrence intervals have been calculated from net slip rates but often have error margins of 1,000 years, which for this project is not useful. Ruptures along the PPAFZ and the Alpine Fault are constrained with some certainty. The last two ruptures believed to have occurred on the PPAFZ are at 1,100 ± 100 years B.P. and 600 ± 100 years B.P., while the last four Alpine Fault ruptures are considered to have occurred 1100 AD (850 years B.P.), 1450 AD (500 years B.P.), 1620 AD (330 years B.P.) and 1717 AD (253 years B.P.); (YETTON *et al.*, 1998). From radiocarbon dates obtained within the Carriage Drive Fault scarp (T_5) at least one rupture is bracketed within 4,428 ± 35 years B.P. and 755 ± 46 years B.P., and this also needs to be considered as a potential trigger.

2.6 Regional Rock Avalanches

2.6.1 Background

Within inland Canterbury there are a number of large rock avalanche deposits. Pioneering studies by WHITEHOUSE (1981, 1983), and WHITEHOUSE and GRIFFITHS (1983), highlighted the widespread and relatively common occurrence of rock avalanches within the Torlesse Supergroup greywacke of the Southern Alps (figure 1.6). During WHITEHOUSE'S (1981) study, 42 large (>1 Mm^3) rock avalanche deposits were identified within the central Southern Alps. Of these within the Lake Coleridge region, the Craigieburn, Acheron and now Lake Coleridge Rock Avalanches have had detailed studies undertaken on them, with the majority of the others simply being identified as rock avalanche deposits and dated where possible. The Craigieburn Rock Avalanche deposit was studied by WHITEHOUSE (1981) and again by ORWIN (1998). The most recent work undertaken on the Acheron Rock Avalanche deposit was by SMITH (2003). Both the Craigieburn and Acheron Rock Avalanches are discussed briefly below.

2.6.2 Craigieburn Rock Avalanches

The Craigieburn Rock Avalanche Deposit is located on the western flanks of the Craigieburn Range near Porter Heights ski field (figure 2.10). It is a large deposit with an estimated volume of 0.5 km^3 (WHITEHOUSE, 1981), the debris covers ~4 km^2, and is up to 300 m thick in some places. Constrained by topography, the debris "flowed" down the source mountain (Blue Hill) and was divided by a bedrock topographic high (figure 2.13). Material moved into a meltwater channel (figure 2.5) from possibly the

Bayfield or Acheron 1 or 2 Advances, and travelled northwest up the channel, west over a bedrock high creating a narrow "tongue" of debris in the next valley, and southwest towards Laings Hill (figure 2.13). The debris constrained by Laings Hill was diverted towards the northwest and created a prominent swash feature or brandung along the lower slopes of that hill (figure 2.13).

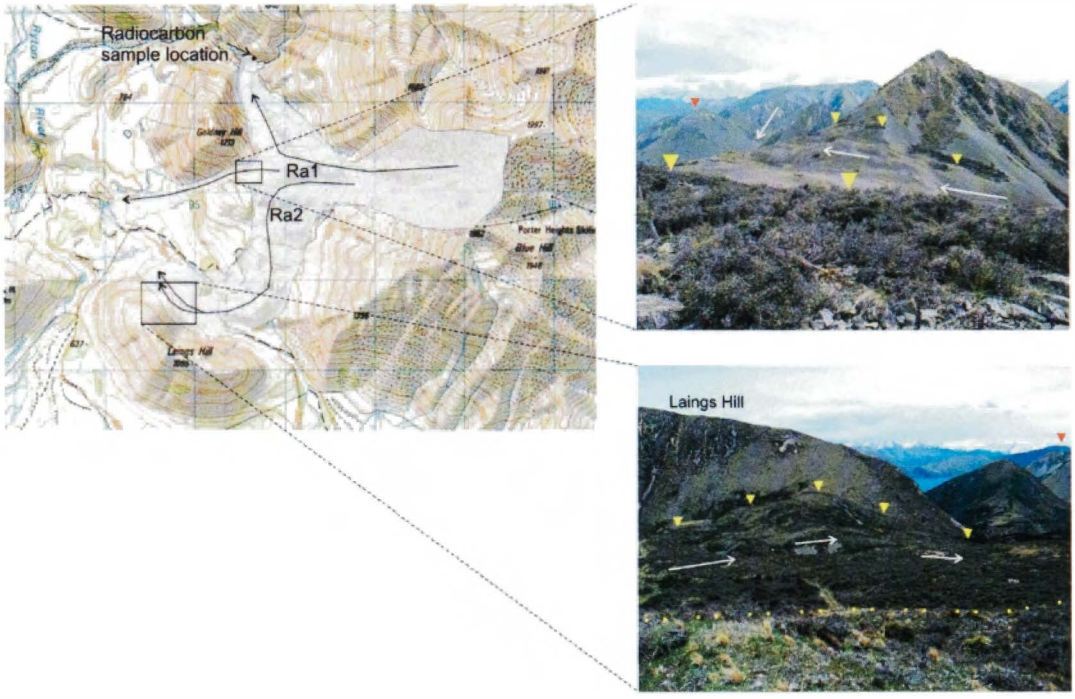

Figure 2.13: Photographs of the Craigieburn Rock Avalanche deposit with corresponding topographic map. The radiocarbon sample site from WHITEHOUSE (1981) is also shown. Top photograph shows debris that "flowed" over a bedrock high and traversed down the slope. Bottom photograph displays the swash mark (or brandung) of the rock avalanche debris as it "flowed" downhill and was affected by the topography of Laings Hill. In both photographs yellow arrowheads indicate the edge of the deposit, with white arrows showing direction of movement. Note the orange arrowhead in both photographs, which indicates the location of Carriage Drive.

WHITEHOUSE (1981) dated the Craigieburn Rock Avalanche event by radiocarbon dating a piece of wood (*Nothofagus* sp.) and conducting a weathering rind survey on 247 surface boulders. The radiocarbon date was (NZ4885C) 952 ± 36 years B.P., while the weathering rind date gave an age of 300 years using CHINN'S (1981) empirical function of age (years) = 1030 $R^{1.24}$ where R = rind thickness (mm). The difference between the two dates was explained by a time lag between death of the tree (sample NZ4885C) at ~650 years B.P. to when it became incorporated into the 300-year rock avalanche event (WHITEHOUSE, 1981).

ORWIN (1998) conducted a weathering rind study of the Craigieburn Rock Avalanche, which indicated two distinct frequency distributions and hence two rock avalanche events. Indicated on figure 2.13, the northern segment of the deposit (Ra1) was dated at A.D. 1,422 ± 96 years (528 ± 96 years B.P.), while the southern portion of the rock avalanche deposit was dated at A.D. 1,632 ± 55 years (318 ± 55 years B.P.) (indicated on figure 2.13 as Ra2). The younger age and event recognised by ORWIN (1998) appears to coincide with the weathering rind age obtained by WHITEHOUSE (1981). There is however a still significant difference between the radiocarbon age obtained by WHITEHOUSE (1981) and the weathering rind age for the earlier event determined by ORWIN (1998).

2.6.3 Acheron Rock Avalanche Deposit

The Acheron Rock Avalanche deposit is located in a small northwest to southeast trending valley called the Red Hill Valley (figures 2.10 and 2.14). It has been studied by BURROWS (1975); WHITEHOUSE and GRIFFITHS (1983); BULL (1996); BULL and BRANDON (1998); and HOWARD (2001), but none of these were as detailed as the recent investigation by SMITH (2003). The debris extends 3.4 km from the top of the source scar to the distal edge, with an estimated source volume of 8.9×10^6 m^3 (SMITH, 2003). The run-out path of the debris was controlled by the narrow valleys, and the rock avalanche deposit overrides the PPAFZ in the lower valley. Thi s is significant if the rock avalanche is assumed to be coseismic, and the Acheron Rock Avalanche deposit has been subjected to numerous dating studies.

Dates obtained from these studies include a radiocarbon age of (NZ547) 500 ± 69 years B.P. (BURROWS, 1975); a lichen age of 460 ± 10 years B.P. (BULL , 1996; BULL and BRANDON, 1998); and weathering rind surveys (which were recalibrated numerous times by WHITEHOUSE and GRIFFITH (1983), MCSAVENEY (1992) and HOWARD (2001)) providing an age of 490 ± 55 years B.P. (HOWARD, 2001). HOWARD (2001) averaged the combined ages from all of the dating techniques and came up with an average deposit age of 464 ± 79 years B.P. However, SMITH'S (2003) study of the Acheron Rock Avalanche provided four radiocarbon dates, which placed the event at the much earlier age of 1152 ± 51 years B.P., which SMITH believes to represent the age of the deposit and to date the likely paleoseismic triggering event along, either the

PPAFZ or the Alpine Fault. Trench excavations in SMITH'S (2003) study showed a further movement on the PPAFZ between 500-700 years B.P. which may have "reset" the weathering rind and lichen dates obtained by earlier workers.

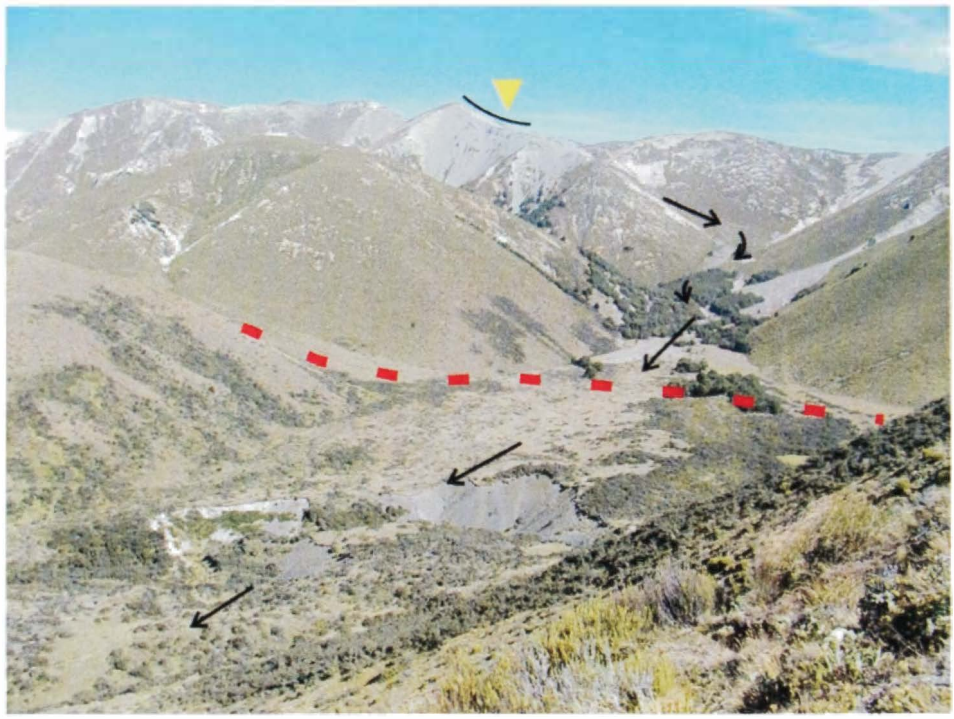

Figure 2.14: Photograph of the Acheron Rock Avalanche deposit. Source area is a bowl-shaped feature located behind the ridge indicated by yellow arrowhead and curved black line. The deposit ramps up on either side of the narrow valley, before continuing down valley (indicated by black arrows). The Porters Pass Fault is indicated by the dashed red line. Deposit continues down valley for another ~500 m. Photograph taken by Dr T. DAVIES, University of Canterbury, 2003.

2.6.4 Lake Coleridge Rock Avalanche Deposits

The LCRAD is the focus of this study. The deposit is located on Ryton Station, near the mouth of the Ryton River where it flows into Lake Coleridge (figure 2.15). The deposit was originally identified in the regional rock avalanche study by WHITEHOUSE (1981), who called it the Lake Coleridge rock avalanche deposit. WHITEHOUSE'S (1981) study found that the deposit covered an area of 23×10^4 m^2, had a thickness of 20 m, and a volume of 4×10^6 m^3. A weathering rind survey, using the method outlined by CHINN (1981), was conducted at an undefined location on the surface of the deposit and gave an age of 120 years B.P. (WHITEHOUSE, 1981).

The Lake Coleridge rock avalanche was further reviewed by WHITEHOUSE (1983), and WHITEHOUSE and GRIFFITHS (1983), as part of a regional study of rock avalanches

within the Southern Alps (figure 1.6 and Appendix A). The original calculations of WHITEHOUSE (1981) were used for both of the 1983 studies, however WHITEHOUSE and GRIFFITHS (1983) included error margins for the calculations. The only other change between the 1981 study and the two 1983 studies was an alteration to the weathering rind age, making it 150 ± 40 years B.P. No further studies of the rock avalanche deposit have been reported.

The present study has identified three individual rock avalanche deposits within the Lake Coleridge rock avalanche. They have been assigned numbers in chronologic order and have been named the LCRA1, LCRA2 and LCRA3 deposits (figure 2.15). A cirque-like head scarp on the southern face of Carriage Drive is the source for the three rock avalanche deposits that are located at the foot of Carriage Drive. A description of the three rock avalanche deposits is given in Chapter 3. The LCRAD material is sourced from Torlesse Supergroup "greywacke" and therefore, in composition, is the same as the valley floor tills and gravels. The highly fragmented, fractured angular clasts of the rock avalanche deposit, however, differentiate readily from the sub-angular to sub-rounded glacial tills and river gravels located on the valley floor.

The Ryton River has incised through the Lake Coleridge Rock Avalanche deposits, and reinstated its flow into Lake Coleridge after being temporarily dammed by each of the rock avalanche events. The LCRAD is the only rock avalanche deposit within the immediate Lake Coleridge area. A tongue of the Craigieburn Rock Avalanche deposit (Section 2.6.2) is located ~ 3 km to the northeast of the LCRAD (figures 2.1, 2.5 and 2.10). The rock avalanche deposit complex which makes up the LCRAD is the subject of this thesis. Volume calculations and other statistics for the deposits have been revised from those initially calculated by WHITEHOUSE (1981). The failure mechanisms and triggering mechanisms are discussed, as are the damming events within the Ryton River associated with the rapid emplacement of rock avalanche debris.

Legend:

Deposit

Braided Riverbed Gravels

Rock Avalanche 3 Deposit

Rock Avalanche 2 Deposit

Rock Avalanche 2 Dam Outwash Terrace

Rock Avalanche 1 Deposit

Till

Other

Roads

Geomorphology

Scree slopes (Open arrows indicate movement direction)

Change in slope

Levees & Steep Banks

Ryton River

Flood Plain

Pinus Radiata Trees

Beech Trees

Hill Slopes

Lakes and Ponded Water

Figure 2.15: Opposite Page: A) Features seen from top of source area, which include LCRA1, LCRA2 and LCRA3 deposits (see legend above). B) Corresponding photograph taken looking down the valley (towards the southeast).

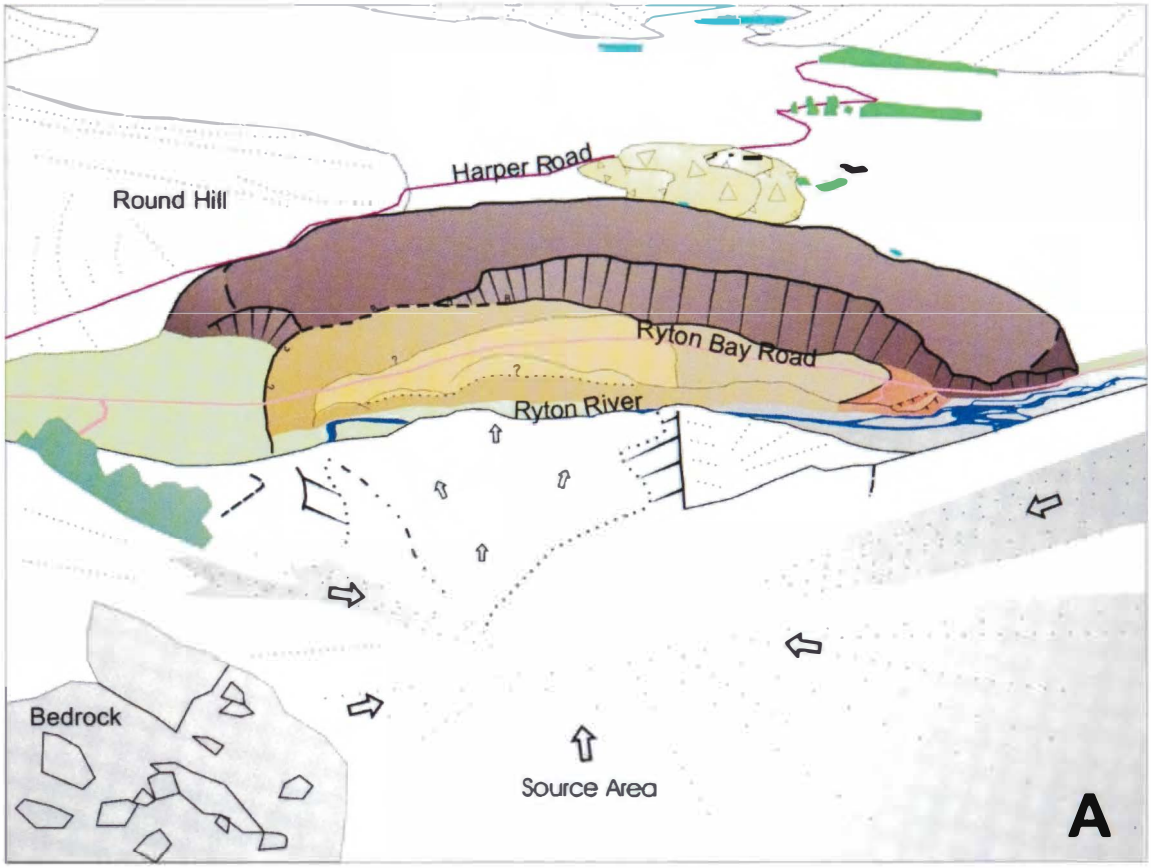
Harper Road
Round Hill
Ryton Bay Road
Ryton River
Bedrock
Source Area
A


B

2.7 Summary

The basement material and all overriding cover material within the Lake Coleridge area (including the LCRAD and source area) is derived from Torlesse Supergroup. Within the basement strata, variations in bedding thicknesses between the alternating sandstone and mudstone are evident around the LCRAD site. Strike of the Torlesse Supergroup is predominantly to the northeast, however the dip of the beds ranged from 42° to 82° dipping mainly to the east. However the dip changed on the eastern ridge of Carriage Drive to dip towards the west. Weathering of the Torlesse Supergroup is predominantly near-surface physical disaggregation by local dilation and the repetitive cycles of freeze-thaw, with a slight lightening in colour of the sandstones through chemical alteration.

Ridge rents are present on the northeastern ridge and flank of Carriage Drive, and are believed to be indicative of gravitational collapse after the retreat of glacial ice within the valley. The intersection of the topmost ridge rent on the eastern ridge with a bedding controlled ridge rent dipping eastward on the southwestern ridge at the back of the source scarp has produced a "wedge" which may provide the failure mechanism for the earlier rock avalanche events.

The influence of the Pleistocene Glacial Advances within the area is significant. Within the valley four major advances during the Late Pleistocene are recorded; the Woodlands, Tui Creek, Bayfield and Acheron Advances. The last glacial advance to affect the area is the Acheron Advance, dated from <~14,000 years B.P. to >~10,000 years B.P. The last ice advance (Acheron 3) directly influenced geomorphological features that are present today however most features have been inherited from the earlier Woodlands, Tui Creek, Bayfield and Acheron (1 and 2) advances.

Since the recession of the Acheron 3 ice, the Lake Coleridge area has undergone geomorphological changes. Such changes include; "Greater Lake Coleridge" some 20 m higher than present-day lake elevations, relict meltwater channels, fluvial fan developments, and emplacement of rock avalanche debris.

Tectonic activity is believed to have had a significant effect on the area. The LCRAD site is surrounded by large fault systems, which have been shown to be

capable of producing a M6 or greater earthquake. These fault systems include the; Porters Pass Amberley Fault Zone (PPAFZ), Harper Fault, Cheeseman Fault, Torlesse Fault, Carriage Drive Fault and the Alpine Fault. Historical earthquakes have affected the region, however no rupture along the faults discussed have occurred during European settlement. A MMI of 6 is also believed to be the lower threshold for rock falls, landslides and rock avalanches.

The LCRAD is one of many rock avalanches located within the Southern Alps. The neighbouring deposits of the Craigieburn and Acheron Rock Avalanches are discussed briefly for completeness.

Chapter 3

Description of the Lake Coleridge Rock Avalanche Deposits

3.1 Introduction

The Lake Coleridge Rock Avalanche Deposit (LCRAD) displays typical rock avalanche characteristics. The debris is highly fragmented, compacted and chaotic; there are internal flow structures visible in eroded cliff sections within the Ryton Riverbed; and the failed material has interacted with the local topography by "flowing" over it. Rock avalanche deposits generally have a sheet-like character that can be either rough or hummocky, and some have lobe-shaped fronts. Internally, rock avalanche deposits can be chaotic and/or inversely stratified (CRUDEN and VARNES, 1996), and there is some field evidence for both of these happening at the LCRAD site.

The LCRAD, identified and used in correlative studies of rock avalanches within the Southern Alps by WHITEHOUSE (1981) and WHITEHOUSE and GRIFFITHS (1983), was originally categorised as a single rock avalanche deposit. Previously the rock avalanche deposit has been dated at 120 years by weathering rind studies (WHITEHOUSE, 1981), and again by WHITEHOUSE (1983) with an age of 150 years ± 40 years. The understanding before commencing *this* study was that two separate rock avalanche deposits were present at the site (Dr T. DAVIES, Lincoln University, *pers. comm.*, 2003). A clear contact between two rock avalanche deposits exists within the small cliffs lining the Ryton Riverbed, but this study has revealed that the LCRAD in fact consists of three individual rock avalanche deposits superimposed on each other within the Ryton Riverbed section. The source material for all three deposits is derived from the summit of Carriage Drive, located directly upslope of the deposits.

Progressively, the deposits decrease in volume from the first rock avalanche (10 x 10^6 m^3; this study), to the youngest which has a volume of about 0.1 x 10^6 m^3 and is of very limited extent. The geomorphic expression of the LCRA1 deposit is clearly visible on aerial photographs, being mostly devoid of shrubby vegetation such as matagouri, and the geometry is lobate in appearance. The younger two deposits (LCRA2 and LCRA3) are not clearly defined from aerial photograph interpretation, which is perhaps an explanation for the lack of identification in earlier studies by WHITEHOUSE (1981; 1983), as both are densely covered in matagouri.

This Chapter will describe the LCRA1, LCRA2 and LCRA3 deposits, and discuss in detail the dimensions and morphology of the deposits, comparing them with the nearby Acheron rock avalanche studied by SMITH (2003), and with other rock avalanche deposits around the world. The Carriage Drive source area is studied in terms of defect analysis, failure mechanisms and triggering mechanisms. The impacts of the LCRA1, LCRA2 and LCRA3 events on the Ryton River and riverbed are also discussed.

3.2 Mapped Geology

3.2.1 Fieldwork and Mapping Techniques

Fieldwork was conducted during the 2003-2004 summer. Due to the lack of surface detail from the available 20 m contour topographic maps (NZMS 260 K35 1:50,000), air photo interpretation was essential for mapping the rock avalanche complex and surrounding area. A series of NZ Aerial Mapping Limited photographs taken between 1959 to 1986 was utilized; the 1959 photo was used as the base map for the aerial photograph interpretation due to the lack of vegetation cover exposing more geological and geomorphological detail. The photograph was enlarged to a scale of 1:5,000, which enabled detailed mapping to be carried out. Digital Elevation Modelling (DEM) was also utilized to obtain three-dimensional views of the Carriage Drive slope and the deposits in relation to the surrounding land (figure 3.1). Again, due to the lack of information obtained from the standard 20 m contour maps, Global Positioning System (GPS) surveys allowed delineation of the relatively low-lying rock avalanche deposits and river terraces on the valley floor. This enabled clearer definition of the deposit from the surrounding ground. The GPS data were combined with DEM elevation data to produce a DEM image of the area (figure 3.1).

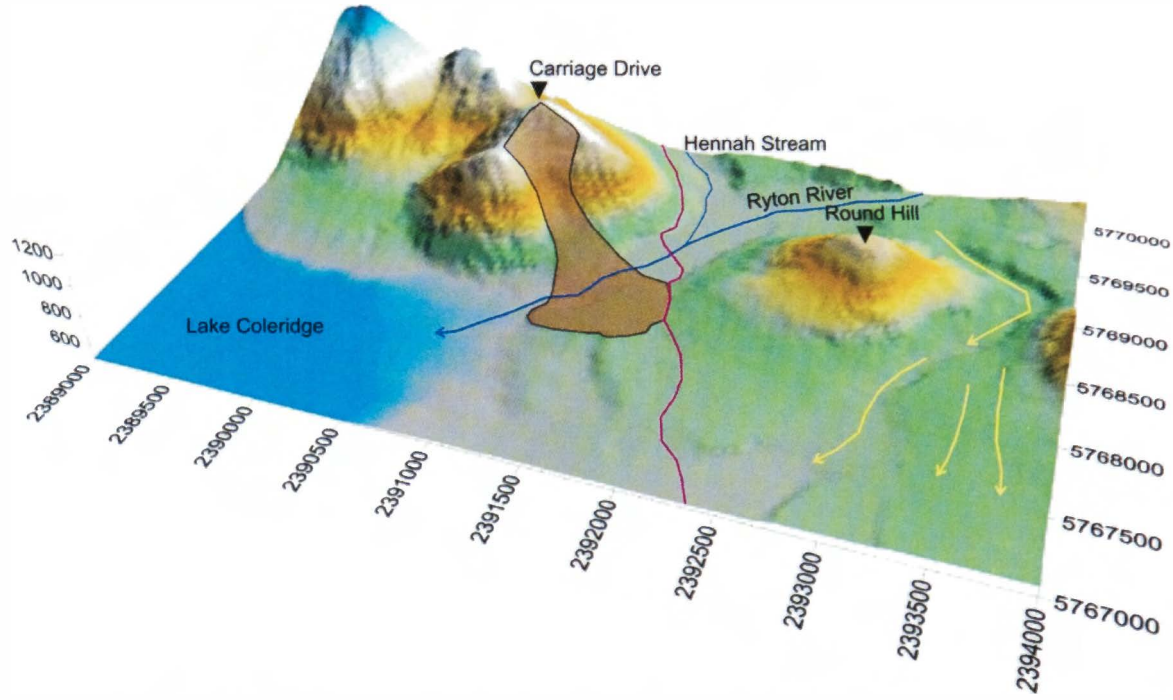

Figure 3.1: Digital Elevation Model (DEM) of the LCRAD and surrounding area. The LCRAD is delineated by brown shading with the deposits all sourced from the head scarp at the summit of Carriage Drive. The Ryton River and small tributary Hennah Stream are shown. Harper Road is the magenta line. An old relict riverbed channel is identified (located to the south of Round Hill) by the yellow arrows indicate its flow paths (Section 2.4.2.1).

3.2.2 Plan View

Initial field mapping combined with aerial photograph interpretation enabled a geomorphological map to be developed for the immediate LCRAD site (figure 3.2). This map shows the different deposits on the valley floor and the geomorphic features within the source area. Cultural features are also shown on the map. Key features to note from this map are:

- The ridge rents or "antiscarps" along the northeastern ridge of Carriage Drive above the Carriage Drive Fault.
- The Carriage Drive Fault along the northeastern flank of Carriage Drive, and the absence of surface expression away from this immediate area.
- The glacial till ridges and gullies in the valley floor. The gullies are believed to have developed in response to concentrations of surface water runoff into the elevated Lake Coleridge ("Greater Lake Coleridge"; this study).
- The lack of beaches for the "Greater Lake Coleridge" at its maximum height of 530 m (a.s.l) within the immediate area of the LCRAD site (Section 2.4.2.1). This is most like due to the dynamic environment failing to preserve the beaches.

- The extent of the LCRA1 deposit out over the valley floor relative to the later failures of LCRA2 and LCRA3. The geometry of the LCRA1 deposit closely resembles experiments where small volumes of sand flowed down a slope and onto a horizontal surface (DAVIES and MCSAVENEY, 1999).
- The absence of dam-break outwash terraces for the LCRA1 deposit. This absence is again believed to be due to the dynamic fluvial environment, with extensive erosion of the central portion of the LCRA1 deposit and transport by the Ryton River, as part the delta formation at the mouth of the river.
- The brandung swash feature created by the runup of the LCRA2 debris onto LCRA1 material.
- The dam-break outwash terraces from the LCRA2 damming event of the Ryton River. The northern terrace is greater in extent than the two smaller terraces on the southern side of the river, which have been eroded by the Ryton River. On the southern side of the river the dam-break outwash terraces have two different elevations, with the higher terrace correlating in elevation to the larger northern terrace while the lower terrace signifies a later and waning stage of dam-break flooding.
- The complexity of the Carriage Drive source area with multiple failures occurring from it. Scree slopes dominate the source bowl now, indicating continued fretting of the exposed Torlesse Supergroup basement. The present day scarp is interpreted to include the three ridge lines around the bowl. The two flat surfaces (referred to in this study as the "lip"), located within the middle of the source bowl, are interpreted to be the breakout surface for the rock avalanche events. Although as discussed further later, this "lip" may be from slumped material from the headscarp.

3.2.3 Section View

A cross-section of the source area and rock avalanche deposits is shown in figure 3.3. Inferred topography is included for the pre-failure ground surface to give an indication of Carriage Drive section before the rock avalanche events. The key features to note from this are:

- The interpreted height of the Torlesse Supergroup basement within the valley floor, which is estimated at a height of 525 m, due to erosion by glaciers and the ancestral Ryton River.

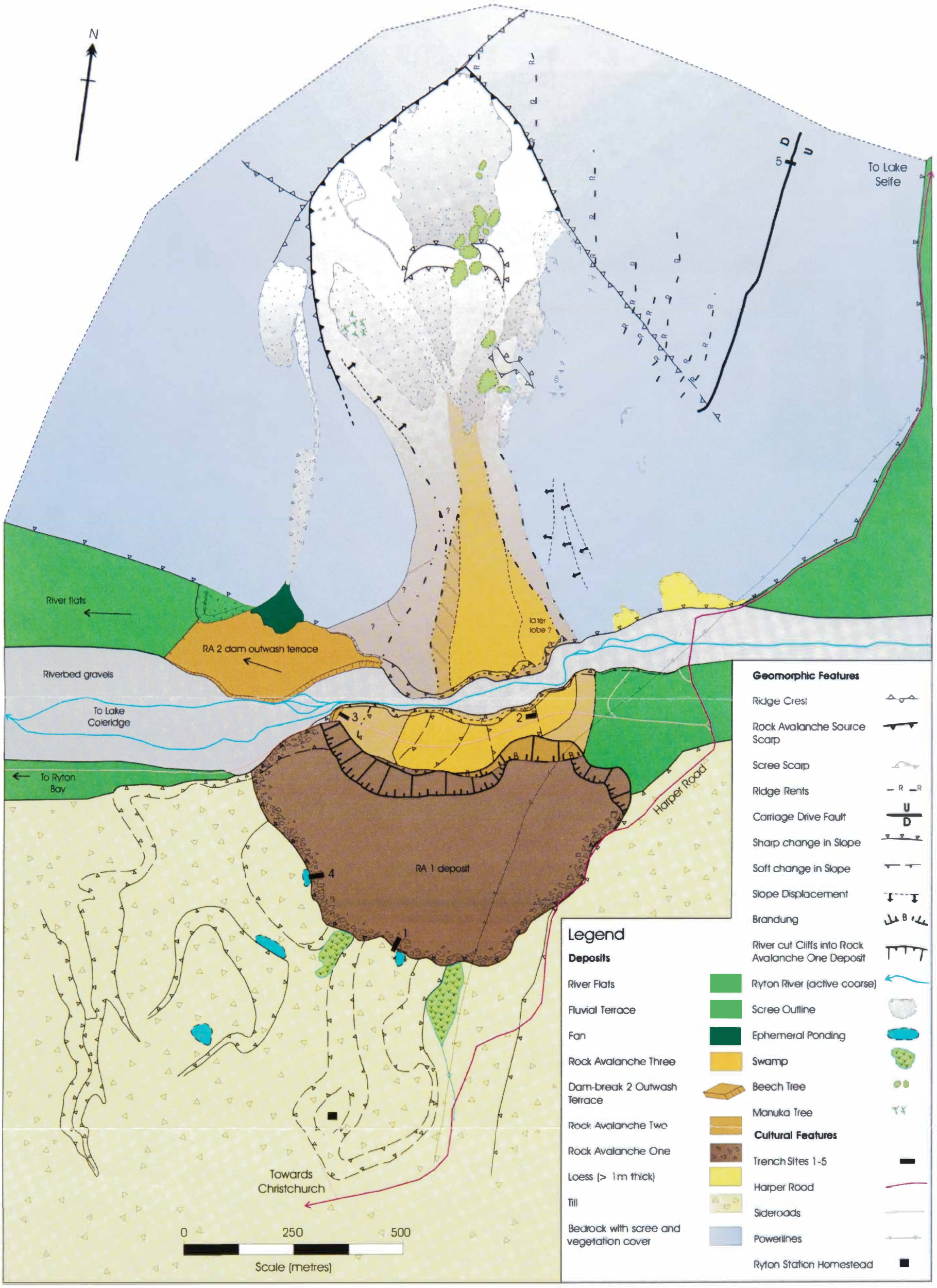

Figure 3.2: Plan view of the geomorphology within the Carriage Drive source area, the Lake Coleridge Rock Avalanche Deposits, and the surrounding area.

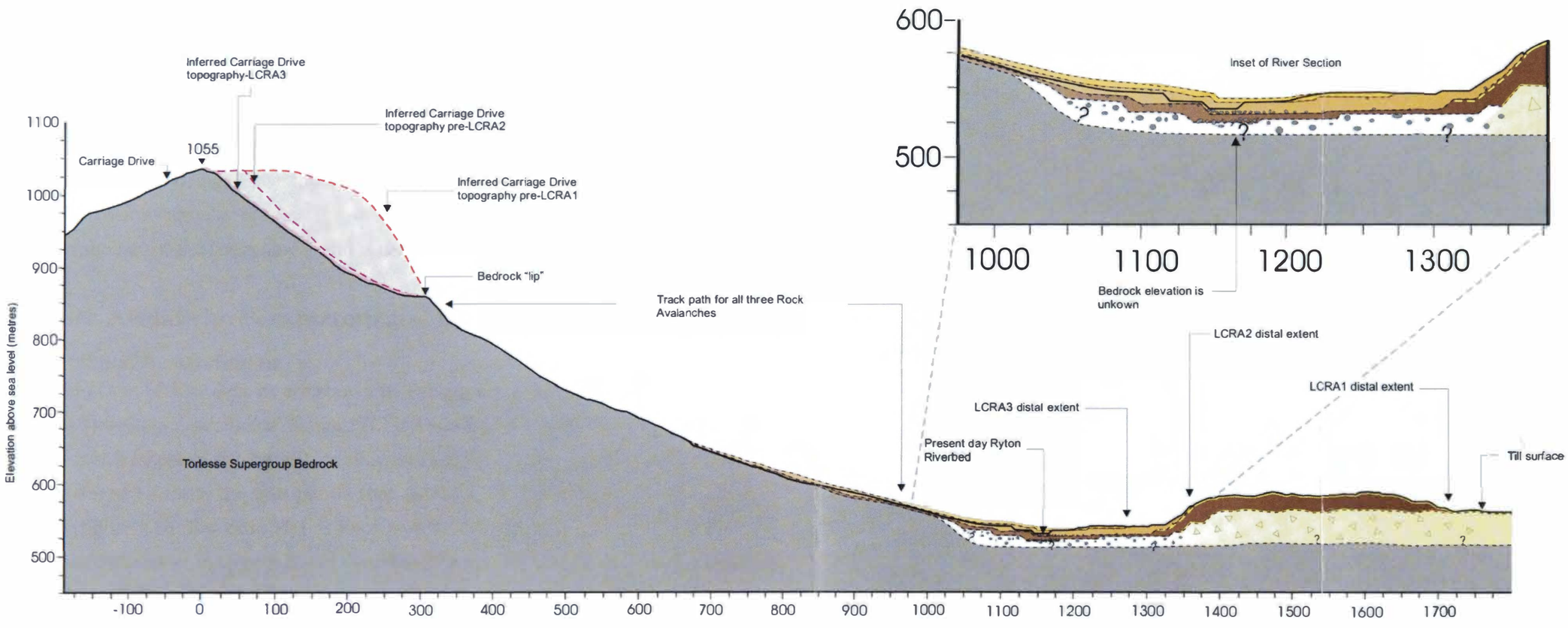

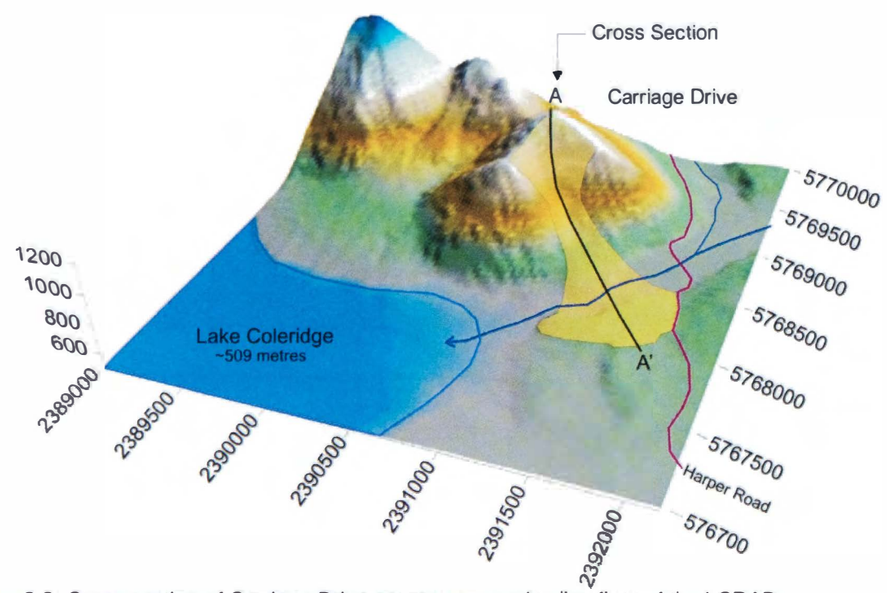

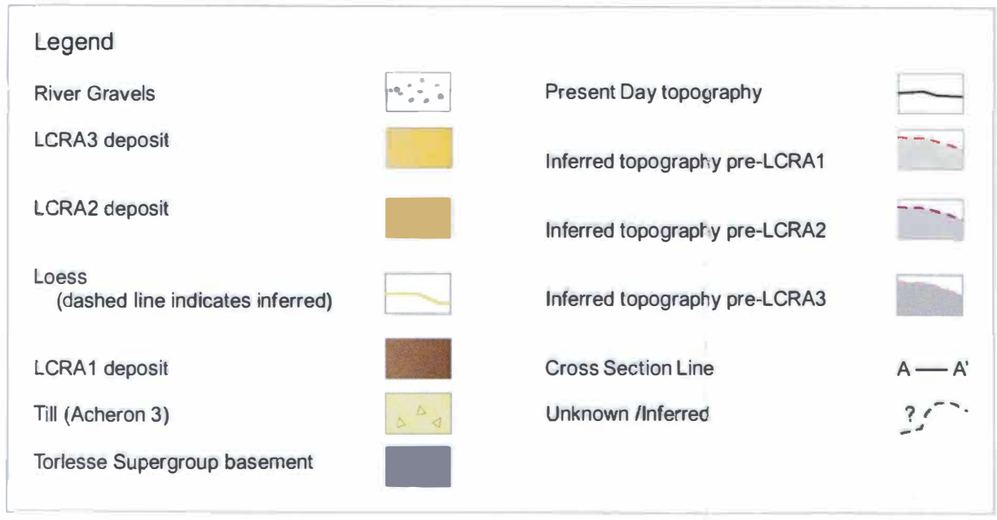

Figure 3.3: Cross section of Carriage Drive source area and valley floor of the LCRAD.

- The erosion of glacial till by the Ryton River before the emplacement of the LCRA1 deposit. The geometry is uncertain, however the writer believes it is realistic to infer the existence of the Ryton River before the LCRA1 event. Therefore, erosion of the glacial till into river cut terraces is believed to be highly likely.
- The inferred Carriage Drive topography and relative sizes of source area for the three rock avalanche events. The interpretation is based on the present day morphology of the source area, and is believed to be a realistic approximation.

3.3 Rock Avalanche Parameters and DAN Modelling

3.3.1 Specific Attributes

Parameters of the LCRA1 deposit are shown in Table 3.1, the terminology of which is as follows: The maximum runout distance (L) is measured from the top of the source scar to the distal extent of the deposit, as shown in figure 3.4. The elevation difference (H) is measured between the two points that define *L*. *D* is the length of the rock avalanche (figure 3.6). The ratio H/L is known as the Fahrböschung (HEIM, 1932). It has been used to detect excessive travel distance (HSÜ, 1975). This logic has recently been questioned (DAVIES and MCSAVENEY, 1999), who showed that the relationship between H/L and internal friction was complex. However, excessive travel distance

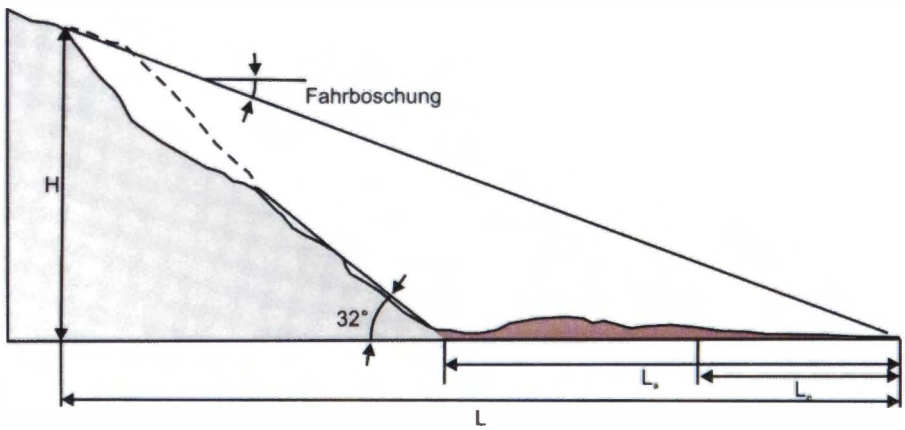

Figure 3.4: A typical cross-section of a rock avalanche with schematic definitions of geometrical terms (after LI, 1983; modified from HUNGR, 1990).

(L_e) of rock avalanche deposits is a widely acknowledged process, and the Fahrböschung is an empirical measure of this occurrence (figure 3.4). The LCRA1 Fahrböschung is 0.28 (or 15.5°), consistent with other documented rock avalanche

values measured around the world (Appendix F1). Mobility is defined as H/L, and the LCRA1 and LCRA2 debris both display high mobility relative to their volume, as shown in figure 3.5. Conventionally high mobility was assigned to rock avalanche deposits with lower "internal friction coefficient" or H/L of ~0.6, which is the internal friction coefficient for granular material.

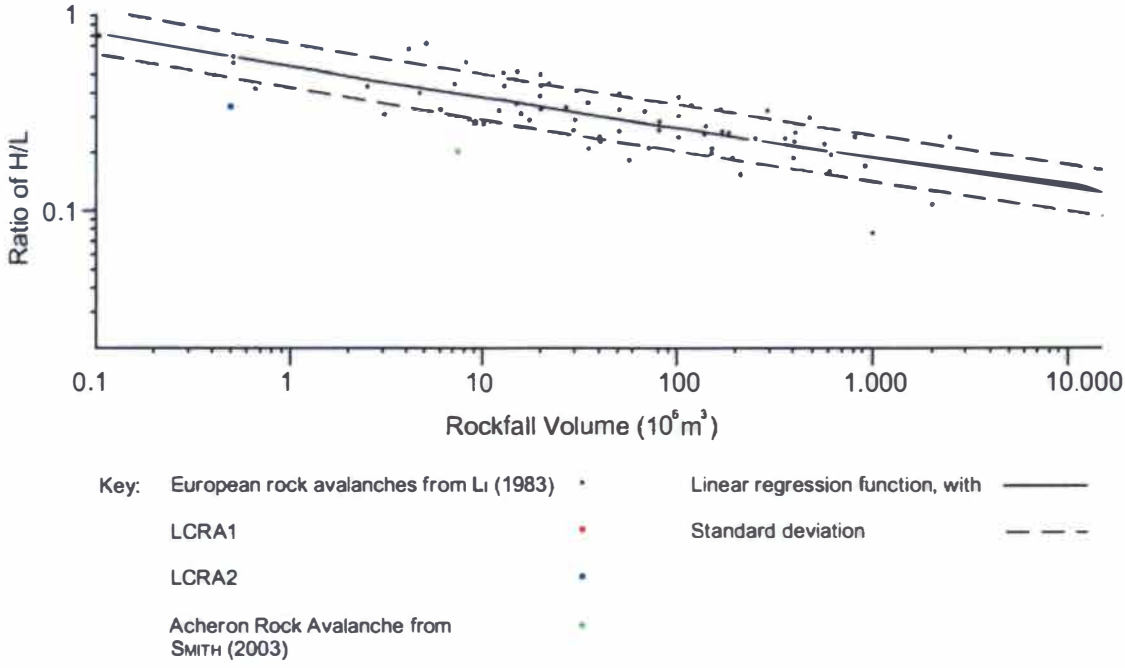

Figure 3.5: Correlation between the H/L ratio and rock avalanche volume using 76 European cases from Li (1983), the LCRA1 and LCRA2, and the neighbouring Acheron Rock Avalanche studied by Smith (2003). Modified from Hungr (1990).

Mobility parameters that are used to define the rock avalanche deposit geometry include:

- W_a is the horizontal component of the maximum width of the rock avalanche deposit.
- W_m is the horizontal component of the width of the rock avalanche measured at D/2.
- *L* as defined above is the horizontal component of the overall runout and *D* is the length of the rock avalanche which is also measured horizontally.

Various combinations of these parameters are used to characterise rock avalanche deposits for example, W_m/W_a, W_m/L, W_m/D, W_a/L and W_a. These values are shown for LCRA1 LCRA2 and are shown in Tables 3.1 and 3.2 and figures 3.4 and 3.6 respectively.

Another indicator of mobility as discussed by NICOLETTI and SORRISO-VALVO (1991) is the shape of the deposit in association with geomorphic control. They found that the overall shape of the rock avalanche deposit could be easily classified into one of three types (figure 3.6):

1) Channeling of the debris mass creates an elongated hourglass shape (figure 3.6A).

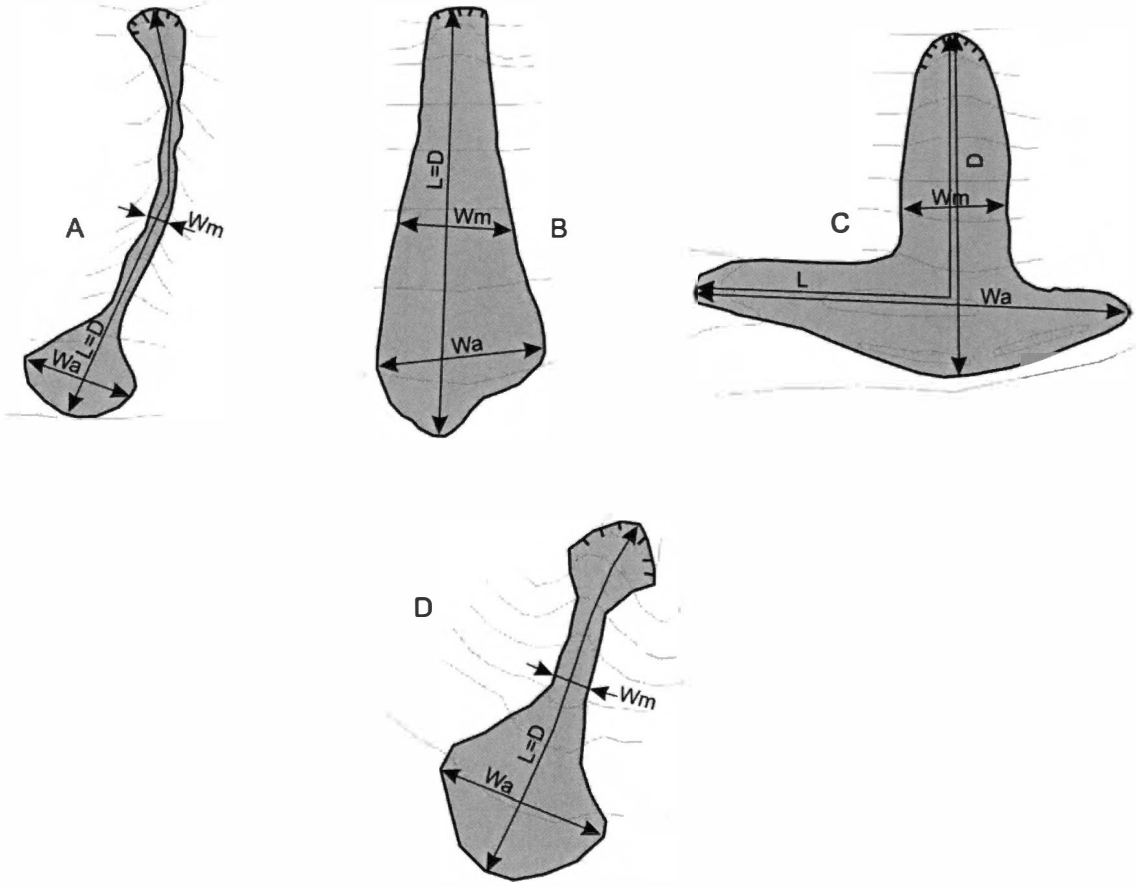

Figure 3.6: The three configurations (A, B, and C) that a rock avalanche can assume as a result of geomorphic control (refer to text), from NICOLETTI and SORRISO-VALVO, 1991. The LCRA1 deposit is shown as a comparison (D) and closely resembles (A) – an hourglass shape.

2) Unobstructed spreading of the debris mass creates nearly an oval, lengthened trapezium or tongue shape (figure 3.6B).

3) Right angle or almost right-angle impact of the debris mass against the opposite slope creates a deformed T shape (figure 3.6C; NICOLETTI and SORRISO-VALVO, 1991).

Mobility decreases from situation 1 to 3. The LCRA1, LCRA2 and LCRA3 deposits all closely resemble an hourglass shape (figure 3.6D), which is another indication of high mobility. Mobility parameters of the rock avalanche shown in Table 3.1 (V_d (volume of deposit), L_e/L, H/L W_m/W_a, W_m/D, W_a/D, and D/L) also correlate well with the findings of NICOLETTI and SORRISO-VALVO (1991); (Appendix F1).

3.3.2 DAN Modelling

The LCRA1 event (discussed in Section 3.4.6) was modelled using the dynamic analysis model DAN (HUNGR, 1995) and a friction rheological model. DAN was developed to provide a model which incorporated the ability for rock avalanche debris to travel further than is expected under normal coefficient frictional pressures. This was termed "excessive travel distance" earlier in this section (Le). DAVIES and MCSAVENEY (2002) have explained the result of long runouts or excess travel distances within deposits as due to fragmentation of the rock mass during the runout processes. DAN modelling was used to simulate the Falling Mountain (1929) rock avalanche deposit in the west branch of the Otehake River and again by SMITH (2003) for the Acheron rock avalanche. As discussed in Section 3.4.6 the DAN simulation for the LCRA1 event was attempted with limited success.

3.4 Lake Coleridge Rock Avalanche 1 Deposit

3.4.1 Background

The LCRA1 deposit is located at the southeastern base of Carriage Drive and immediately north of the Ryton Station Homestead (figure 3.2). The rock avalanche deposit displays a classic lobate structure (e.g. MITCHELL *et al.*, 2001), which is common in rock avalanche deposits, and has a runout of 1,780 m (Table 3.1). The deposit is about 300 m from the Ryton Station Homestead and local infrastructure; including the Harper Road, the Ryton Bridge (the only land access up-valley), the Ryton Bay Road to the popular summer holiday camping ground and boat access into Lake Coleridge, and the power lines which cross the deposit.

3.4.2 Dimensions and Statistics

Morphometric data for the LCRA1 are presented in Table 3.1. Using SMITH'S (2003) example, the format to describe the morphology of the rock avalanche deposit follows the outline provided by GOVI *et al.* (2002), which is a systematic approach to describing the deposit. Values for distances have been rounded to the nearest five

metres, while parameters including the runout and debris spreading statistics have been rounded to the second decimal place. Volume calculations have also been rounded to 0.1 x 10^6 m^3. These values are believed to be realistic representations of the morphometric data from the LCRA1 event, and the method was repeated for the analysis of the LCRA2 deposit.

Estimates for the original *in situ* rock mass volume, pre-failure, have been difficult. The problem of interpreting prehistoric pre-failure topography, although not unique to this site, is compounded due to multiple rock avalanche events falling from the source bowl and large volumes of deposited material being removed by the Ryton River, and also by scree accumulation. Initial calculations, using geometric shapes to approximate the topography of the source bowl, provided a rock mass volume of 6.81 x 10^6 m^3. As discussed below, this volume is considered conservative because a flat upper surface was used, whereas a "bulging" or convex topographic surface is more likely to have existed at the ridge crest. This volume was also considered conservative because another source volume calculation was taken from the actual LCRA1 deposit. Dilation of the deposit was taken into consideration, and this is normally estimated to average 20% of the deposit (MCSAVENEY, 1978; EVANS *et al.*, 2001) and is often referred to as "bulking". By using this method, an in situ volume of 9,997,200 m^3 or 10 x 10^6 m^3 was calculated. Due to the uncertainty associated with the source volume calculation, the volume obtained by back calculating from the deposit is considered more realistic and has been used in this study.

The volume calculated for the LCRA1 deposit from this study is 12.5 x 10^6 m^3 (computed volume 12,496,500 m^3). An initial volume calculation of the deposit by WHITEHOUSE (1981) gave a figure of 4 x 10^6 m^3, which is approximately 70% smaller than this estimate (Appendix A). A possible explanation for this large difference in volume calculations is the interpretation of eroded rock avalanche material within the Ryton River section. From this study an estimated 7.4 x 10^6 m^3 (computed volume 7,395,000 m^3) of material is calculated to have been removed by incision and erosion of rock avalanche debris by the Ryton River, whereas in WHITEHOUSE (1981) only 0.7 x 10^6 m^3 was interpreted to have been eroded (Appendix A). From the geometry of the erosion channel of Ryton River through the LCRA1 deposit, the value from

Table 3.1: Lake Coleridge Rock Avalanche 1 – Morphometric Data

Dimensions of Original Rock Mass in Source Area	
Planimetric surface of original rock mass (S_r)	0.108 km²
Probable volume of original rock mass (V_r)	10 x 10^6m³
Minimum estimate of *in situ* rock 6.8 x 10^6m³	
Maximum thickness of original rock mass	110 m
Dimensions of Debris	
Planimetric surface of debris accumulation of remaining debris (S_r)	0.261 km²
Estimated planimetric surface of eroded debris (S_e)	0.2905 km²
Planimetric surface of original deposit (S_d) ($S_d = S_e + S_r$)	0.5515 km²
Volume after erosion of debris	5.1 x 10^6m³
Estimate of volume eroded by Ryton River	7.4 x 10^6m³
Total Volume of debris (V_d)	12.5 x 10^6m³
Runout Statistics	
Total planimetric surface (S)	0.701 km²
Runout (L)	1780 m
Length (D)	1725 m
Elevation difference (H)	495 m
Excessive travel distance ($L_e = L - H/H\tan 32°$)	1,030 m
H/L; Fahrböschung = arc tangent (H/L)	0.28 (15.5°)
L_e/L	0.58
Length of accumulation	450 m
Length of accumulation (L_a)	750 m
Planimetric width at D/2 (W_m)	320 m
Maximum planimetric width of accumulation (W_a)	880 m
Mobility Statistics	
W_m/W_a	0.36
W_m/L	0.2
W_m/D	0.19
W_a/L	0.49
W_a/D	0.51
Debris Spreading Statistics	
Maximum thickness of accumulation	40 m
Average thickness of accumulation (V_d/S_d)	~23 m
Relative thickness of accumulation [$(V_d/(S_d\sqrt{S_d})$]	0.03
Spreading (S_d/S_r)	2.11
Debris Run-up Statistics	
Relative hollow	0.1
Height of descent slope (h_1)	460 m
Height of runup (h_2)	60 m
h_2/h_1	0.13

WHITEHOUSE (1981) appears extremely small and is considered to be somewhat inaccurate.

As shown in Table 3.1, the average thickness of the *present day* accumulation zone is calculated to be 23 ± 1 m. Due to the large volumes of eroded rock avalanche material, it is unrealistic to attempt to calculate an average thickness for pre-erosion conditions. WHITEHOUSE (1981) estimated an average thickness of 20 m for the deposit, which correlates well with this study. A true cross section of the deposit is not present anywhere at the site. The large cliffs eroded by the Ryton River within the deposit are the likely place for a true thickness estimate, but subsurface till terraces are inferred to underlie the rock avalanche debris, thus creating an exaggerated thickness to the deposit (figure 3.3). The basal contact of the rock avalanche was only visible in two trenches excavated into the perimeter of the deposit (discussed below in Sections 3.4.4 and 3.4.5).

3.4.3 Composition and Internal Structure

Exposure of the internal rock avalanche was limited to two test pits (trenches) dug around the periphery of the deposit and cliff sections formed by recent lateral erosion of the Ryton River, where vegetation was sparse (figure 3.7). Due to the lack of exposure, two trenches were excavated into the deposit, with the primary aim of obtaining organic material for radiocarbon dating (as discussed in Section 4.3.1). The secondary aim of trenching was to examine the internal structure of the debris, and to view the basal contact of the deposit with the underlying till. Post emplacement slumping and surface slopewash has produced a colluvial deposit which was identified within the test pits, and also occurs on the south-eastern limit of the deposit (figure 3.7). The perimeter of the rock avalanche deposit is marked by an obvious change in topography, and where visible a difference in clast angularity with the rock avalanche material being highly fractured and angular, compared to rounded clasts for tills and river gravels.

Depending on distance away from the base of Carriage Drive, a difference in internal structure is identifiable. Within the medial zone of the deposit identified within the cliffs (figure 3.7) highly compacted, shattered, granular to small gravel sandstone clasts have their a-axis (i.e. their longest axis) aligned perpendicular to

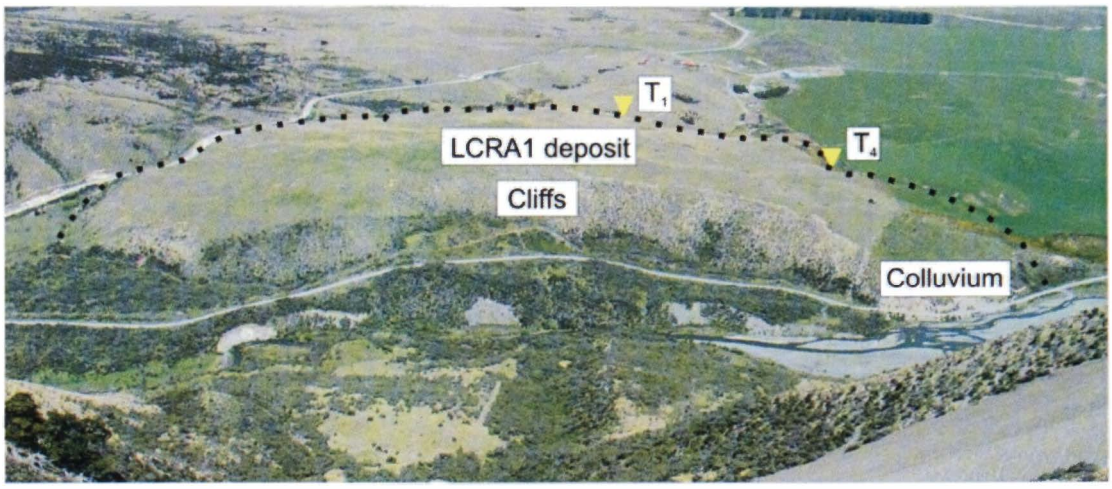

Figure 3.7: Oblique view from source area of the LCRA1 deposit. The deposit is outlined by aqua dots and yellow arrowheads indicate the two trench sites. Trench 1 (T_1) is located to the left while Trench 4 (T_4) to the right. The cliffs of the deposit are labelled, as is the colluvium. Photograph taken looking southeast.

flow direction of the rock avalanche debris. These are surrounded by highly fractured, and in some places sheared argillite (mudstone) units. This appears almost as an emplacement bedding structure (figure 3.8), with alternating beds of sandstones and mudstones similar to intact rock mass characteristics of Torlesse Supergroup greywacke observed within the Carriage Drive source area (Section 1.4.3.1). Such preservation of source structure is commonly reported in rock avalanche deposits. The internal structure of the rock avalanche debris around the perimeter is quite different from this, displaying a larger clast size and a chaotic fabric with no apparent bedding (figure 3.9). The rock avalanche material within Trenches T_1 and T_4 was matrix-supported, with angular cobble to granular sized sandstone clasts. Although the debris displayed characteristic features of a rock avalanche deposit, including angular clasts and poor-sorting, features that are commonly described within rock avalanche debris such as a surface layer of large rocks and isolated boulders supported within a matrix of powder (MITCHELL *et al.*, 2001) were not found. This is possibly due to the trench sites located at the distal edge of the deposit, because as energy within the deposit dissipates the clasts come to rest without further fragmentation.

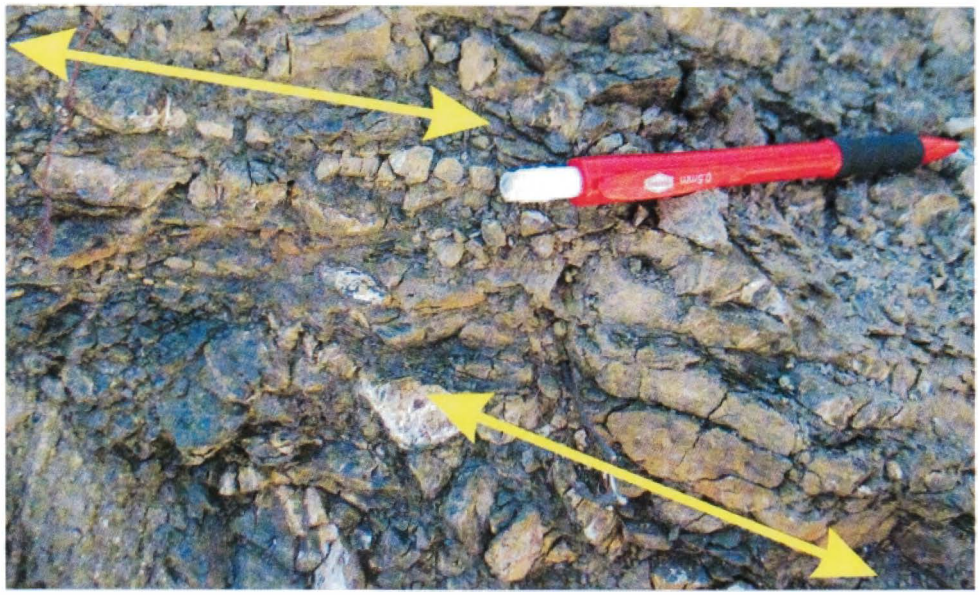

Figure 3.8: Photograph of small pseudo bedding of alternating sandstones and mudstones within the LCRA1 deposit. A-axis of sandstone clasts (the larger, lighter clasts) are perpendicular to flow direction of the rock avalanche. Pencil ~10 cm for scale. Yellow arrows highlight the bedding structure.

3.4.4 Trench 1 (T_1) Interpretation and Discussion

T_1 was located at the crest of a till ridge (grid reference K35: 150 700), with excavations cutting into the distal extent of the LCRA1 deposit (figure 3.10). The trench face was logged by sectioning the face into a 1-metre grid pattern, which enabled a 1:50 scale log to be drawn of the face (figure 3.11). Guyon SMITH (MSc Student) and Dr Philip TONKIN (Research Associate, Department of Geological Sciences) assisted with logging. Three sodium fluoride field tests were conducted by Dr Philip TONKIN to confirm the age and development of the soil profile on the LCRA1 deposit. The stratigraphic sequence exposed in T_1 was as follows (figure 3.11):

- At the base of the profile glacial till is present, and this is described as a silty to sandy gravel. The Torlesse Supergroup clasts are well rounded to sub-rounded, and the clasts are matrix-supported.
- Sandy "loess" is present over the glacial till. This soil was ~150 mm thick. Grain size analysis conducted on the fine sediment found it to consist predominantly of fine sands and silts (Appendix G).
- The LCRA1 deposit unconformably overlies the glacial till and sandy "loess". The angular Torlesse clasts were matrix-supported in a chaotic unit with no apparent structure.

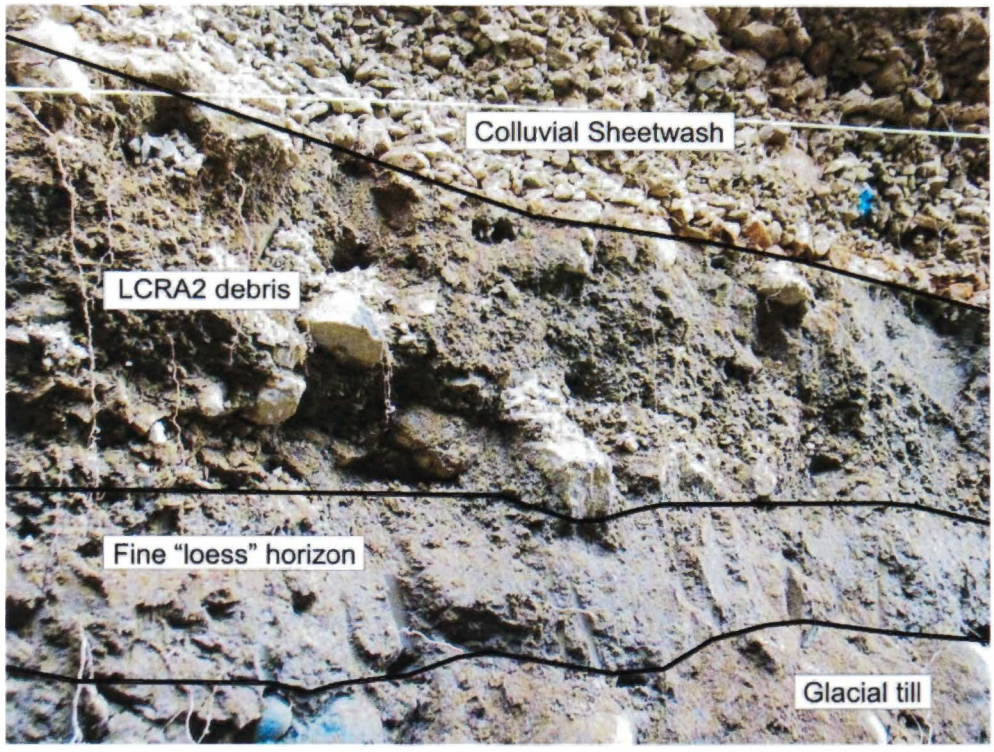

Figure 3.9: Photograph of Trench face within T_4. Colluvium interpreted to be caused from slopewash overlies the LCRA1 deposit. A small grey fine sediment horizon underlies the rock avalanche debris and overlies till. A clear distinction between the rock avalanche debris and till can be made, mainly from the clast angularity (rock avalanche material has angular clasts while till has rounded to subrounded) and colour (the rock avalanche is grey to brown while the till is bluey-grey). A capping loess unit is located at the top of the sequence out of shot. Photograph displays ~1.5 m (horizontal) of exposure.

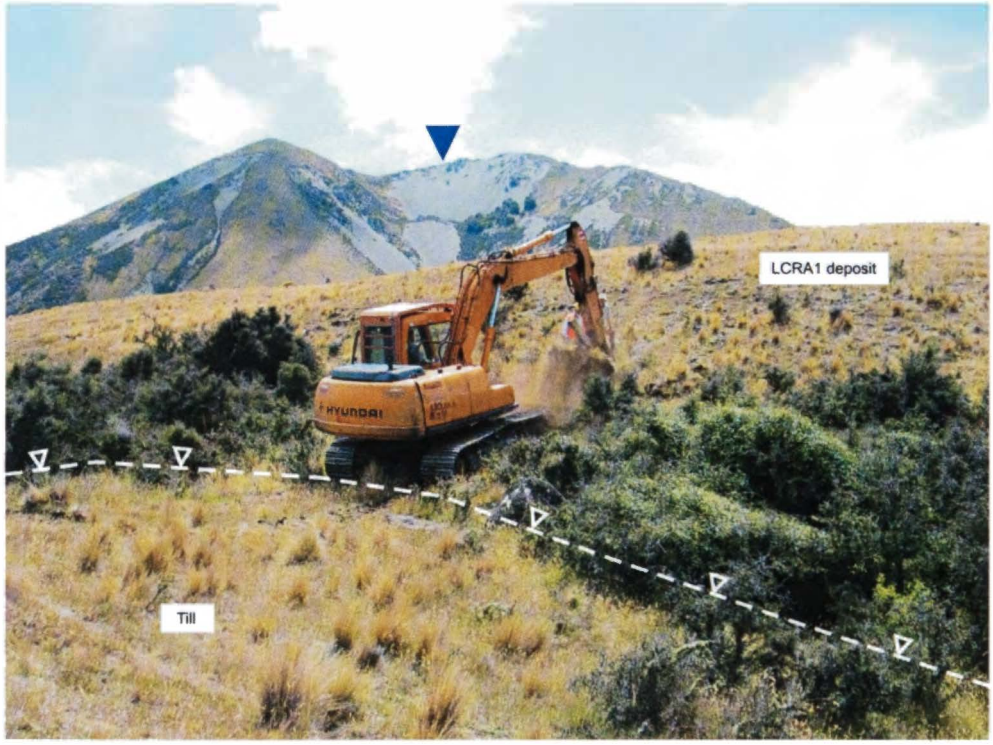

Figure 3.10: Excavation of T_1 into LCRA1 deposit. The white dashed line indicates the change in slope at the rock avalanche edge onto glacial til. Carriage Drive, the source area, is indicated with a blue arrowhead. Photograph taken looking north.

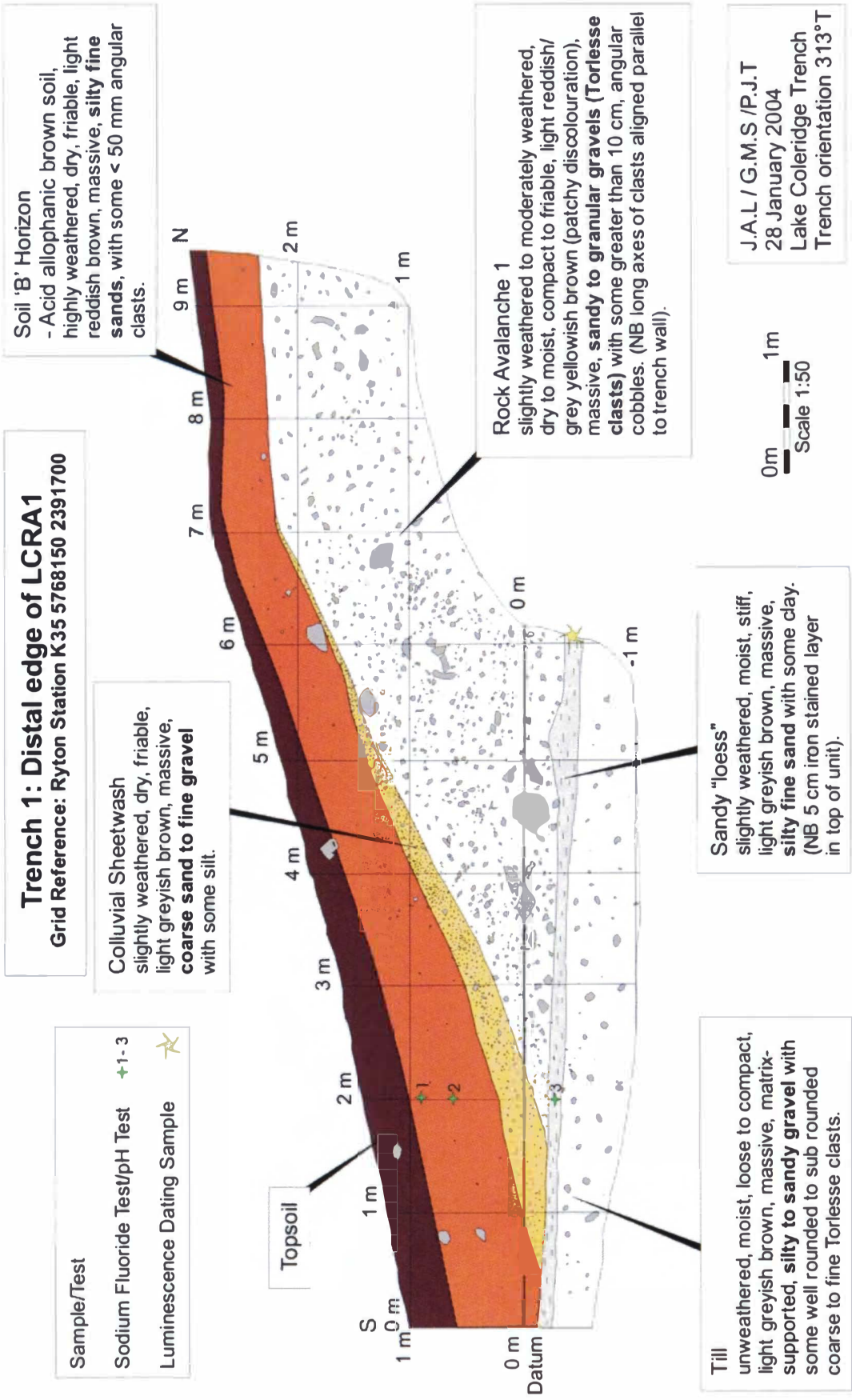

Figure 3.11: T_1 log displaying the units both above and below the LCRA1 deposit. Three sodium fluoride tests were conducted within the "loess" horizons within the trench face. An OSL sample was also taken from the sandy "loess" horizon.

- Colluvial sheetwash or slopewash forms a wedge shaped unit overlying the outer slopes of the LCRA1 deposit, which is associated with water runoff erosion of finer particles on the surface of the rock avalanche deposit. The colluvium is clast-supported, with very little matrix material, and is well sorted.
- A ~600 mm covering of acid allophanic brown soil (informally described as "loess") overlies the rock avalanche sequence. Topsoil has developed within the top ~30 cm of the "loess", indicating a stabilisation of erosion and initiation of vegetation growth at the site.

An indirect age of the "loess" profile overlying the LCRA1 deposit was obtained by the sodium fluoride pH test carried out by Dr P. TONKIN, University of Canterbury, 2004. The rapid colour change from all three samples (refer to figure 3.11 for locations), provide a semi quantitative indication that the soils are at least 4 to 6,000 years old assuming an annual rainfall of ~1 to 1.5 m (Dr P. TONKIN, University of Canterbury, *pers. comm.*, 2004). An optically stimulated luminescence (OSL) sample was collected from the sandy "loess" horizon located directly below the basal contact of the LCRA1 deposit (Section 4.3.2), but was not dated as the sample from T_4 was analysed instead.

3.4.5 Trench 4 (T_4) Interpretation and Discussion

T_4 was located on the edge of the southwest flank of the rock avalanche deposit near an ephemeral pond at grid reference K35: 295 955 (figure 3.12). Excavation of T_4 was carried out because no organic material was found within T_1 to enable radiocarbon dating to place an age on the rock avalanche event, and to provide a further cross-sectional view of the distal limits of LCRA1 The methodology for logging T_4 was the same as T_1, with a 1 m grid pattern placed on the face allowing a log to be drawn (figure 3.13). The stratigraphic sequence was very similar to that logged in T_1, as follows:

- At the base of the profile glacial till is exposed, and is described as a gravely sand to sandy gravel. The till is matrix-supported, with the Torlesse Supergroup clasts being well rounded.

- Sandy "loess" with a thickness of ~150 mm overlays the glacial till. Grain size analysis conducted on the fine sediment found it to consist mostly of fine sands and silts (Appendix G).
- The LCRA1 deposit overlies the till and sandy "loess". The chaotic rock avalanche deposit has angular Torlesse clasts that are supported within a matrix of finer sand grains.
- Colluvial sheetwash overlies the LCRA1 deposit. This unit pinches out towards the south where a change in gradient and flattening of the LCRA1 underneath is probably responsible for this. The sheetwash is clast supported.
- Capping off the sequence is a ~600 mm covering of acid allophanic brown soil (loess) overlies the LCRA1 sequence. Like the T_1, topsoil has developed within the top 30 cm of the loess.

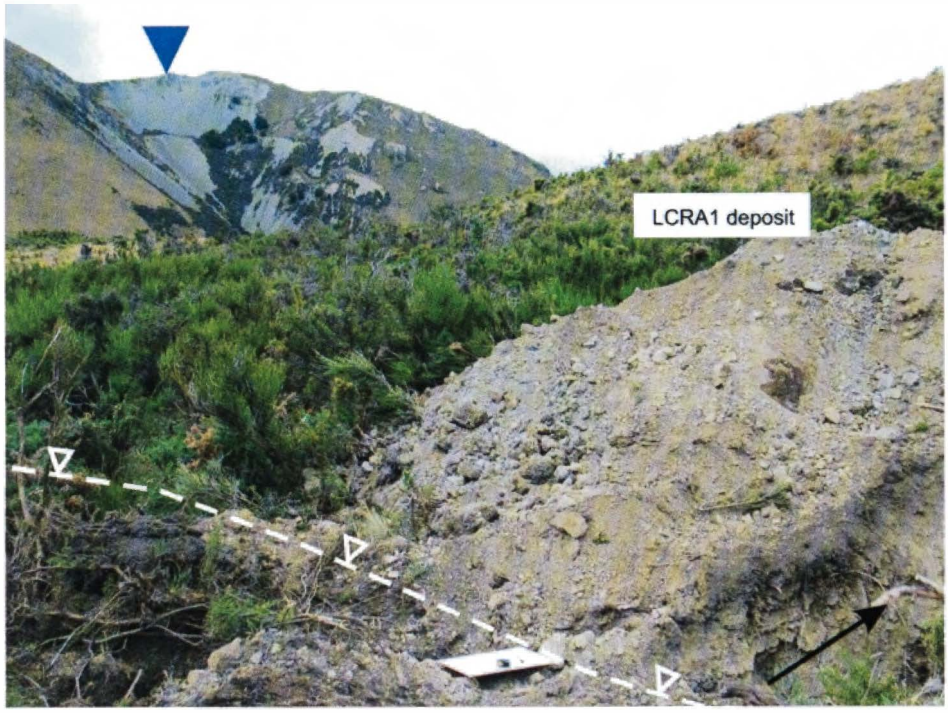

Figure 3.12: Photograph of T_4 site. The white dashed line indicates the change in slope at the rock avalanche contact with glacial till. The Carriage Drive source area is indicated with a blue arrowhead. The black arrow indicates the trench location and its orientation. Photograph taken looking north-northeast.

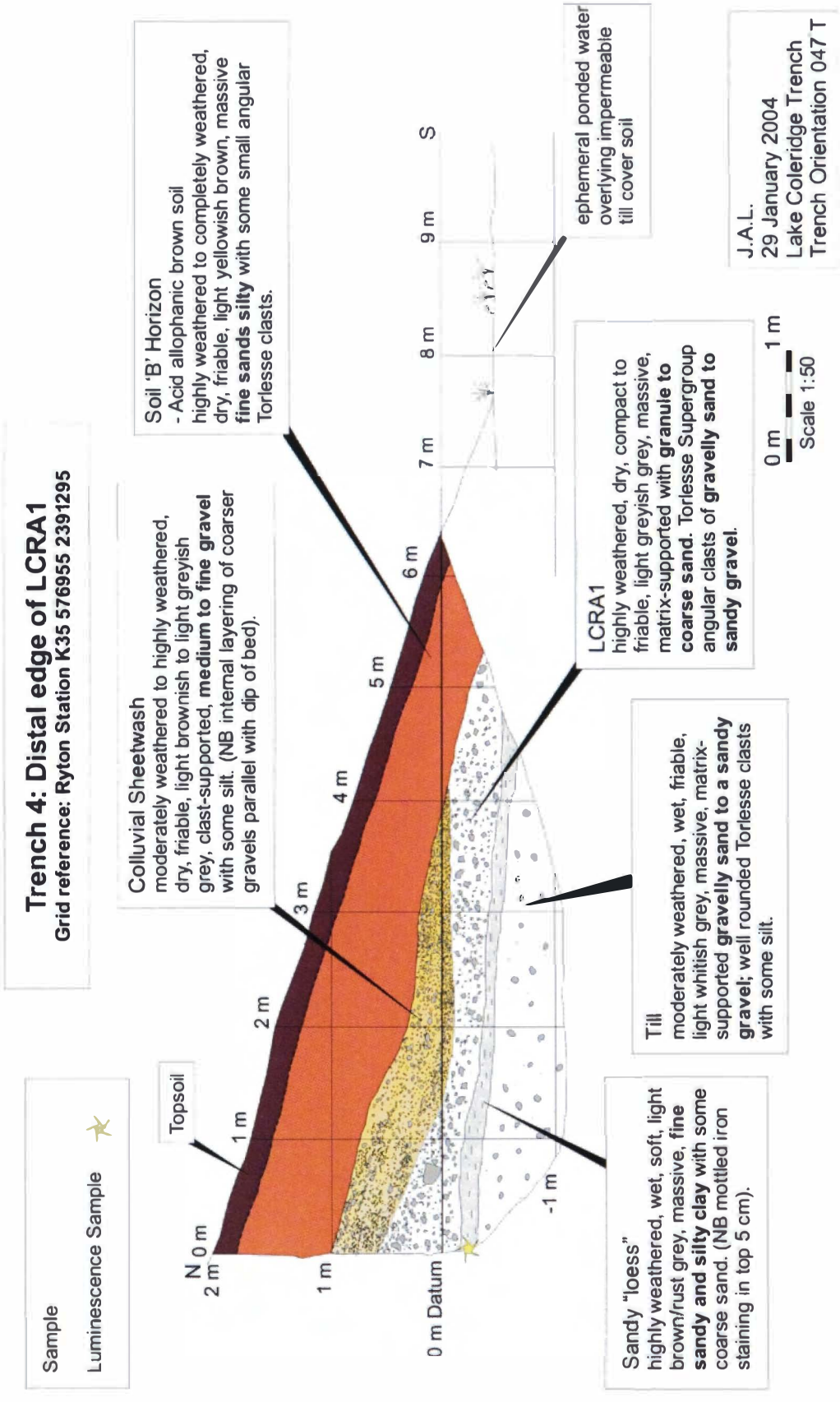

Figure 3.13: T_4 log displaying the units both above and below the LCRA1 deposit. An OSL sample was taken from the sandy "loess" horizon and was sent away for dating.

An optically stimulated luminescence sample (OSL) was collected from the loess horizon located below the basal contact of the rock avalanche deposit. This sample was sent to the Luminescence Dating Laboratory at Victoria University of Wellington (Appendix H4). The sandy "loess" horizon was dated at 9,720 ± 750 years B.P., and this is further discussed in Section 4.3.2 in relation to possible triggering of the LCRA1 event.

3.4.6 DAN Simulation

A DAN simulation was modelled to the LCRA1 event. Although the simulation reached the same approximate runout length as the LCRA1 deposit the geometry of the simulated deposit did not correlate well. The programme also struggled with the steepness of the slope on Carriage Drive and the narrowing of the runout through the lower portions of Carriage Drive (figure 3.2). However, as at Falling Mountain and the Acheron rock avalanche, the simulation of the LCRA1 deposit displays the need for *something else* other than the internal friction to explain long runouts within rock avalanche deposits (i.e. fragmentation). During failure simulation the front of the debris reached a maximum velocity of 102 ms^{-1} or ~370 km/hr, with the distal debris reaching the extent of the runout within approximately 30 seconds. Although the model was too inaccurate to adequately simulate the LCRA1 event, the velocity of the failure is believed to adequately represent the approximate velocity of failure for the LCRA1 event at ~100 ms^{-1}. The speed of emplacement of the LCRA1 and also the subsequent LCRA2 and LCRA3 events is believed to have been very rapid, and the DAN model simulates this.

3.5 Lake Coleridge Rock Avalanche 2 Deposit

3.5.1 Background

Like the LCRA1 deposit, the LCRA2 deposit is located at the foot of Carriage Drive, and is clearly derived from the same source area. The LCRA2 deposit is much smaller in areal extent, volume and geomorphic expression than the first. It is unclear at this stage whether this rock avalanche deposit was incorporated into the WHITEHOUSE (1981) and WHITEHOUSE and GRIFFITH (1983) studies as part of the LCRA1 deposit (numbers assigned to the rock avalanches in this study), as only one rock avalanche deposit was described from their work. It is also possible that it was ignored by them as it failed to meet their threshold minimum volume of 1×10^6 m^3.

3.5.2 Dimensions and Statistics

The LCRA2 event is a relatively small deposit having an estimated loose volume of ~523,000 m^3. Morphometric data for the LCRA2 is displayed in Table 3.2, following the format outlined by GOVI *et al.* (2002). Estimates for the original *in situ* rock mass volume pre failure are difficult, and this is compounded by a) the LCRA1 having already failed, removing ~10 x 10^6 m^3 of material from the source area, and b) back calculating from the deposit is made difficult due to the unknown amount of the eroded material of the LCRA2 deposit by the Ryton River.

The most *realistic* approach to calculating the initial rock mass volume for the second rock avalanche was to assume a base level for the Ryton River at the time of emplacement of the rock avalanche debris at a reference datum of 530 m (a.s.l), compute the deposit volume, and then correct for the increased void space or "bulking". The reference elevation of 530 m was assumed because the basal contact of the LCRA2 deposit was not visible, but was estimated by a combination of a GPS survey of the present day riverbed and field investigations that revealed the inclusion of rounded to subrounded clasts within the lower metre of an exposure within the rock avalanche deposit (figure 3.14). This was interpreted to signify the basal mixing zone, which is present in some rock avalanches studied around the world such as the Elm sturzstrom in Switzerland (HEIM, 1932) and in New Zealand at Falling Mountain rock avalanche (DAVIES *et al.*, 1999).

The volume calculated for the LCRA2 deposit from this study is 654,300 m^3, which gives an *in situ* rock mass volume of 0.5 x 10^6 m^3 assuming a bulking factor of 20%. The average thickness of the deposit is calculated to ~be 5.9 m, and it thins to ~ 2 m (Table 3.2) as it climbs the northeastern face of the LCRA1 deposit creating a distinctive brandung feature (figure 3.15).

Table 3.2 provides the measured and calculated parameters of the LCRA2 deposit. In summary, these are as follows:

- Runout (L) was measured at 1,350 m from the source scar to the distal edge of the deposit (the top of the brandung).
- The drop in elevation (H) between the two points that define L was measured as 470 m.

- From this the Fahrböschung (figure 3.4) developed by HEIM (1932) was measured to be 19° or 0.38. The ratio for the Fahrböschung is also the "equivalent coefficient of friction" of SHREVE (1968). The LCRA2 event has a Fahrböschung or equivalent coefficient which is relatively consistent with results from Europe and America (Appendix F2).
- Excessive travel distance (L_e) of the rock avalanche deposit was calculated as ~640 m however it is arguable as to how relevant this figure is. HSÜ (1975) found that excessive travel distance is commonly minor or negligible for rock avalanche deposits with volumes less than 5×10^6 m^3, making the LCRA2 deposit a marginal case with a source volume of 0.5×10^6 m^3.
- The LCRA2 deposit displays high mobility parameters as shown in figure 3.3. The mobility parameters (shown in Table 3.2) V_d, L_e/L, H/L W_m/W_a, W_m/D, W_a/D, and D/L also correlate with NICOLETTI and SORRISO-VALVO (1991) findings, indicating a highly mobile rock avalanche deposit (Appendix F1).

  Although much smaller, the second rock avalanche closely resembles the hourglass shape of the LCRA1 deposit. The material was released from the scarp of Carriage Drive, transferred downslope into the Ryton riverbed and partially up the opposing slope. However, topographic constriction by the first rock avalanche prevented further transportation of the second rock avalanche debris, and this is clearly represented by the brandung feature shown in figure 3.15.

3.5.3 Composition and Internal Structure

Recent clean exposure is present for the LCRA2 deposit due to erosion and undercutting of the central section by the Ryton River. The cliff section (grid reference K35 440575) displays an almost complete cross-section of the LCRA2 deposit, except for the lower 1 metre below the present-day ground surface which allows the internal structures of the deposit to be assessed (figure 3.16). A ~400 mm piece of wood (figure 4.8 and 4.9) was found embedded within the lower 1 m of the deposit. This was later identified as a piece of *Leptospermum scoparium* (mānuka) and sent away for ^{14}C dating (Section 4.4.1).

- **Table 3.2:** Lake Coleridge Rock Avalanche 2 – Morphometric Data

Computed Dimensions of Original Rock Mass	
Planimetric surface of original rock mass (S_r)	Not known
Volume of original rock mass (V_r)	0.5 x 10^6m³
Source volume estimates taken from back calculation of 20% bulking of deposit	
Average maximum thickness of original rock mass	?
Dimensions of Debris	
Planimetric surface of debris accumulation of remaining debris (S_r)	50,700 m²
Estimated planimetric surface of eroded debris (S_e)	59,600 m²
Planimetric surface of original deposit (S_d) ($S_d = S_e + S_r$)	110,300 m²
Volume of debris accumulation (Present day)	0.40 x 10^6m³
Volume of **eroded** debris	0.26 x 10^6 m³
Total Volume of debris (V_d)	0.66 x 10^6m³
Runout Statistics	
Total planimetric surface (S)	80,700 m²
Runout (L)	1410 m
Length (D)	1400 m
Elevation difference (H)	480 m
Excessive travel distance (L_e = L - H/Htan 32°) negligible if under 1 x 10^6m³ Hsü (1975)	639 m
H/L; Fahrböschung = arc tangent (H/L)	0.35 (19°)
L_e/L	0.47
Length of accumulation (Present day)	140 m
Length of accumulation (L_a)	240 m
Planimetric width at D/2 (W_m)	230 m
Maximum planimetric width of accumulation (W_a)	510 m
Mobility Statistics	
W_m/W_a	0.45
W_m/L	0.17
W_m/D	0.17
W_a/L	0.38
W_a/D	0.38
Debris Spreading Statistics	
Maximum thickness of accumulation	7 m
Average thickness of accumulation (V_d/S_d)	5.9 m
Relative thickness of accumulation [$(V_d/(S_d\sqrt{S_d})$]	0.018
Spreading (S_d/S_r)	0.42
Debris Run-up Statistics	
Relative hollow	0.13
Height of descent slope (h_1)	490 m
Height of runup (h_2)	30 m
h_2/h_1	0.06

Figure 3.14: Rounded clasts (highlighted by black circles) within the probable lowest 1 m of the LCRA2 deposit. The majority of the clasts display angular corners signifying break-up and fragmentation (fracturing) during transportation of the rock avalanche. Photograph taken by Dr T. DAVIES, University of Canterbury, 2003.

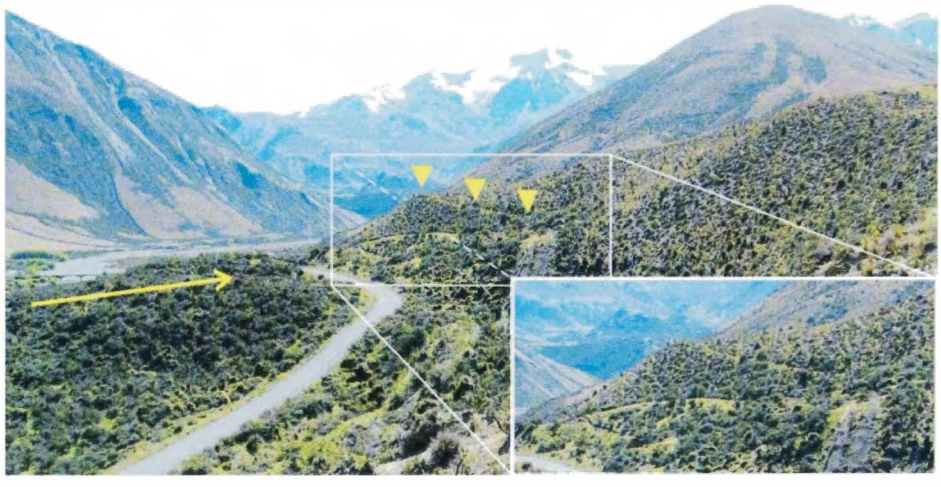

Figure 3.15: Brandung feature (with inset) of the LCRA2 deposit. The rock avalanche debris has partially "climbed" the LCRA1 deposit, essentially wrapping around the pre-existing topography. The brandung is highlighted by the yellow arrowheads, while the yellow arrow indicates flow direction of the rock avalanche debris from the LCRA2 event.

As shown in figure 3.16, internally the rock avalanche deposit is chaotic, which is a common feature (MITCHELL *et al.*, 2001). It is matrix-supported with a large percentage of fines (pebbles to fine sands), while larger angular sandstone clasts are spaced randomly throughout. Very little structure is visible within the lower portion of the section, but towards the top faint alternating pseudo bedding or lenses of sandstones and mudstones are present (figure 3.17). This type of layering is a characteristic of rock avalanche deposits and is often titled "inverse stratification". Examples include the famous Blackhawk landslide of SHREVE (1968), and the Acheron Rock Avalanche located in the neighbouring valley (SMITH, 2003). SHREVE (1968) noted that the detailed stratigraphy within distal portions of the Blackhawk landslide indicated almost laminar flow of the deposit during transportation. The pseudo-bedding or laminations identified within the cliff section of the LCRA2 deposit were also identified within Trench 3 (T_3) excavated into the deposit (Section 3.4.3.1).

Figure 3.16: Cliff exposure of LCRA2 deposit. Photograph taken looking southeast with source area directly behind. The contact between LCRA2 and LCRA3 is visible near the top of the cliff (shown with yellow arrows). Note people for scale. Photograph taken by Dr T. DAVIES, University of Canterbury, 2004.

3.5.4 Trench 3 (T_3) Interpretation and Discussion

Trench T_3 was located on the southwest (downstream) edge of the LCRA2 deposit (figure 3.18). This trench differed from T_1 and T_4 because it was also excavated into a terrace on the downstream side of the deposit (figure 3.18) to identify the relationship between the two units. Organic material was also sought for radiocarbon dating, although the mānuka sample had already been recovered from the cliff face within LCRA2.

Before logging of the trench face commenced, a 1 m grid pattern was placed over the face. This differed slightly from T_1 and T_4 because both sides of the face were

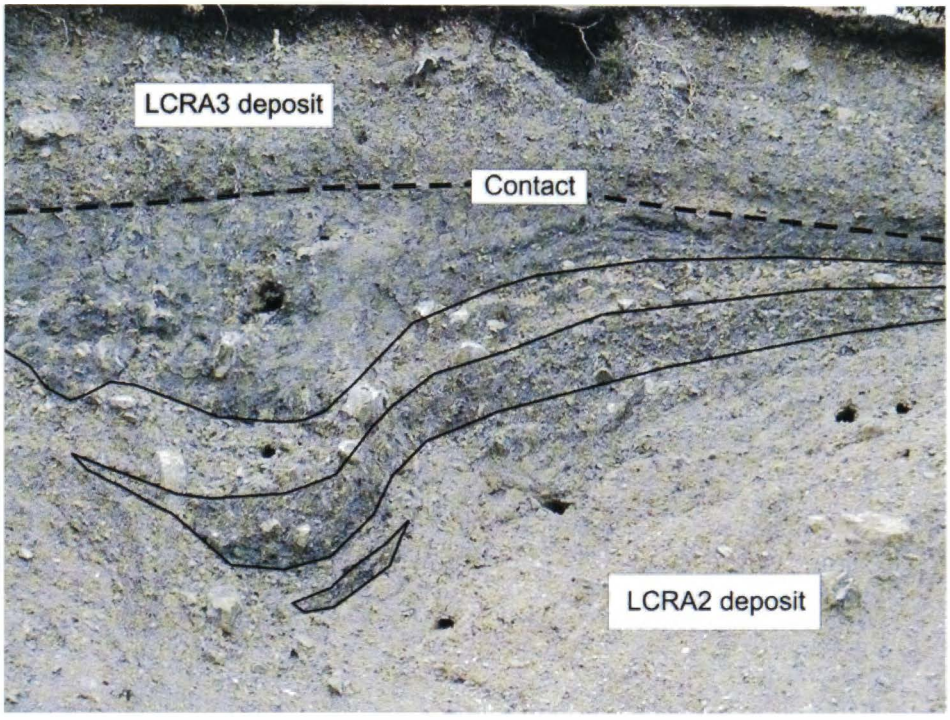

Figure 3.17: Pseudo bedding (or lenses) within the LCRA2 deposit of alternating sandstone (light grey) and mudstone (dark grey) beds. Deformation of these lenses is clearly evident and may be the result of interaction with a boulder, with the material "wrapping" around it during emplacement. Photograph taken by Dr T. DAVIES, University of Canterbury, 2004.

Figure 3.18: Photograph of T_3 site. The white dashed line indicates the change in slope between the LCRA2 deposit and the dam-break outwash terrace surface in the foreground. The trench is highlighted with a yellow arrow, while the source area direction is indicated with the aqua arrow. Photograph taken looking southeast.

logged to determine if the recognised units continued over the width of the trench, which was also approximately 1 m (figure 3.19). This was significant because unlike the chaotic nature of the rock avalanche deposits seen in T_1 and T_4, the rock avalanche deposit within T_3 was stratified or layered into distinct brown and grey lenses which are described as separate units on the trench log (figure 3.19) and are the "inverse stratification" discussed above. The grey units have a matrix rich in mudstone fines, giving the unit the grey appearance, while the brown units have more of a sandstone matrix producing a lighter colour. Within the grey units, small pockets of dark grey to black fine-grained material were present, which were was sampled because of the possibility of its origin being organic, such as charcoal. The sample was then dried and examined under the microscope to determine if organics were present. No organic material was found and the dark grey appearance was due to fine (silt-size) mudstone or argillite grains covering the coarser clasts (Dr N. NEWMAN, CRL, *pers. comm.*, 2004).

The stratigraphic sequence identified within T_3, which was excavated into the LCRA2 debris and the dam-break outwash terrace, was as follows (figure 3.19):

- At the base of the profile LCRA2 debris is exposed, and this is described as two distinct units due to inverse stratification of the deposit, causing two distinct colour changes within lenses. The units are similar except for the matrix content, which alternates between the lenses from Torlesse sandstone (brown unit) and argillite or mudstone (grey unit).
- Overlying the stratified debris is a fine grained unit which, although its origin is uncertain, is still believed to be part of the LCRA2 deposit. The unit is described as being fine sand to coarse silt which coarsens upwards.
- Unconformably lying over the LCRA2 deposit is the Rock Avalanche 2 dam-break outwash terrace. Erosion of the LCRA2 deposit by the dam-break flood waters has produced an outwash terrace which is stratified and clearly displays fluvial sorting of the clasts. The Torlesse clasts are angular, which suggests that the source material is from the adjacent LCRA2 deposit.
- A thin (~25 cm thick) topsoil has developed over both the LCRA2 deposit and the dam-break outwash terrace surface.

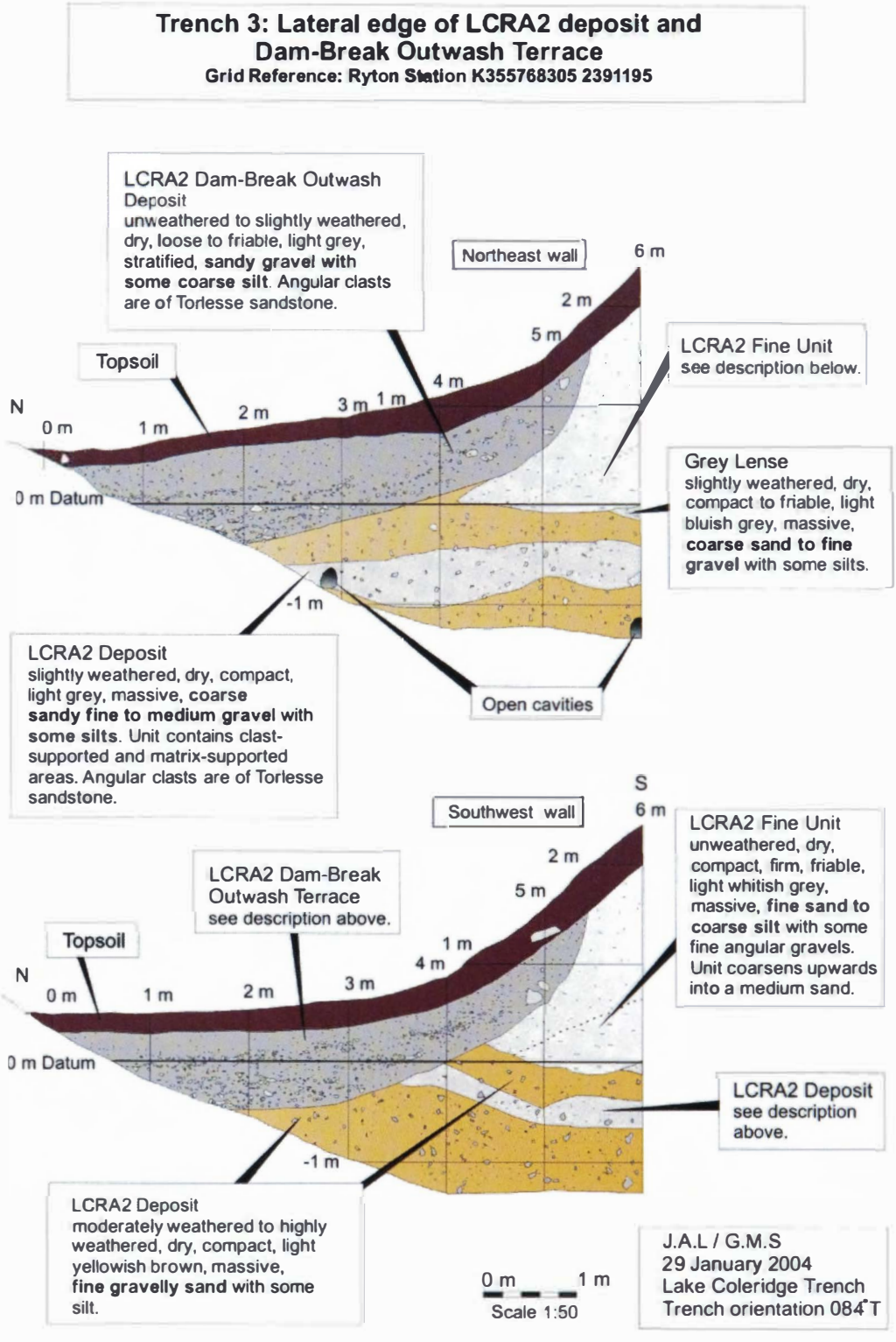

Figure 3.19: T_3 log displaying both the left and right walls of the trench. Stratification of the rock avalanche debris is evident, as is the dam-break outwash terrace related to the second rock avalanche event.

Interpretation of the sequence of events that are represented within T_3 can be divided into three different phases, as follows:

- Firstly, failure of *in situ* rock material within Carriage Drive occurred, creating the LCRA2 event which was deposited within the eroded river section of the LCRA1 deposit. The LCRA2 deposit displays a "colour banding" or pseudo-bedding which is not unique to this rock avalanche deposit. The origin of the fine material situated within the upper portions of the rock avalanche deposit is unclear.
- Secondly, the rock avalanche dam, created by the instantaneous deposition of rock avalanche debris emplacement into the Ryton River, was overtopped by the impounded lake (Section 3.8.4). During the breach of the dam, water flowing over the top of the deposit would have begun incising and eroding the deposit, which is a common occurrence during dam-breach (e.g. COSTA (1988); COSTA and SCHUSTER (1988); BROOKS and HICKIN (1991)). The Rock Avalanche 2 dam-break outwash terrace represents this period of incision and erosion of the rock avalanche deposit by the Ryton River, until the breach level dropped below that of the terrace. The stratification within the terrace deposits displays grain size sorting, which is associated with fluvial action, and the angularity of the clasts indicates that the material is sourced locally from the LCRA2 deposit.
- Lastly, stabilisation of the surface of the deposit and terrace, combined with further incision of the Ryton River below the terrace surface enabled a topsoil to develop. Compared to the LCRA1 deposit there is a lack of loess accumulation on top of LCRA2.

3.6 Lake Coleridge Rock Avalanche 3 Deposit

3.6.1 Background

The LCRA3 deposit is located at the foot of Carriage Drive on the south-eastern side of Ryton River. The source for the deposit is from Carriage Drive, as for the LCRA1 and LCRA2 events. The deposit is very small, being far smaller in extent, volume and geomorphic expression than the LCRA2 deposit. The existence of this rock avalanche deposit was not known before this study.

The deposit directly overlies the LCRA2 deposit and is visible in an eroded cliff section within the Ryton riverbed (figure 3.14). The thickness of the deposit, estimated from the visible cross-sectional view from the cliff exposure, is ~2 m. The geomorphology of the deposit is poorly constrained and the boundary between the larger and underlying LCRA2 deposit is unclear. Therefore, little is known about the morphology and geometry of the deposit, and no statistical analysis was undertaken due to its smallness in size, making statistical analysis impractical. Trench 2 (T_2) was excavated into the deposit (figure 3.20) and displayed chaotic swirling patterns around a large (~ 1 m diameter) Torlesse sandstone boulder (figure 3.21).

3.6.2 Trench 2 (T_2) Interpretation and Discussion

Trench T_2 was located within the LCRA3 deposit, and was positioned adjacent to the Ryton Bay Road (figure 3.2). The trench was excavated into rock avalanche debris at a change in slope (figure 3.20). The primary aim of this trench was to locate the contact between the LCRA2 and LCRA3 deposits, as it was believed that the change in slope represented this boundary. Organic matter was also sought during the excavation and logging exercise for radiocarbon dating.

Figure 3.20: Photograph of T_2 site. The white dashed line indicates the change in slope believed to be the contact between the LCRA2 and LCRA3 deposit. However after logging the face this was found to be not the case (figure 3.21). Ryton Bay Road is located to the left of the photograph approximately 3 m out of the view. Photograph taken looking southwest.

Logging was undertaken with the same methodology, as the earlier trenches, discussed in previous sections. A 1 m grid pattern was established which enabled a 1:50 scale log to be drawn, and figure 3.21 shows that the deposit at this locality is chaotic. Lenses of differing matrix material (similar to T_3) appear to have distorted around the large fractured boulder of Torlesse sandstone positioned just below the ground surface. A slight increase in clast size and a change in colour of matrix material (from grey to brown) occur within the lower metre of the trench. This is possibly a simple alternating bed and part of the inverse stratification discussed earlier, although this is not the preferred interpretation. The colour change is in-fact interpreted to represent the contact between the LCRA2 and LCRA3 deposits for the following reasons:

- Firstly, the change in clast size appears to indicate a different deposit. Although this is recognised as an insufficient determining characteristic by itself, combined with the evidence below it is thought to be important.
- Secondly, the elevations of the visible contact within the Ryton River cliffs between the LCRA2 and LCRA3 deposits (figure 3.16 and 3.17) and the proposed contact between the two deposits within the T_2 face, are within 0.5 m of each other, as surveyed by GPS to an accuracy of ± 0.2 m. This strongly suggests a correlation, since the two sites are less than 40 m apart.
- Thirdly, the probable contact between the two rock avalanche deposits within T_2 approximates the present day ground surface, which indicates that the LCRA3 debris flowed over the LCRA2 deposit following the underlying topography, which is a consistent characteristic with rock avalanche deposits.

The interpreted, stratigraphic sequence within the exposed profile of T_2 is described as follows:

- The contact between the LCRA2 and LCRA3 deposits is exposed within the bottom metre of the T_2 (figure 3.21). The LCRA2 deposit has a larger clast size than the LCRA3 deposit located directly above it. There is a lack of a soil profile on the LCRA2 deposit, which probably provides evidence for LCRA3 emplacement very soon after the LCRA2 event.

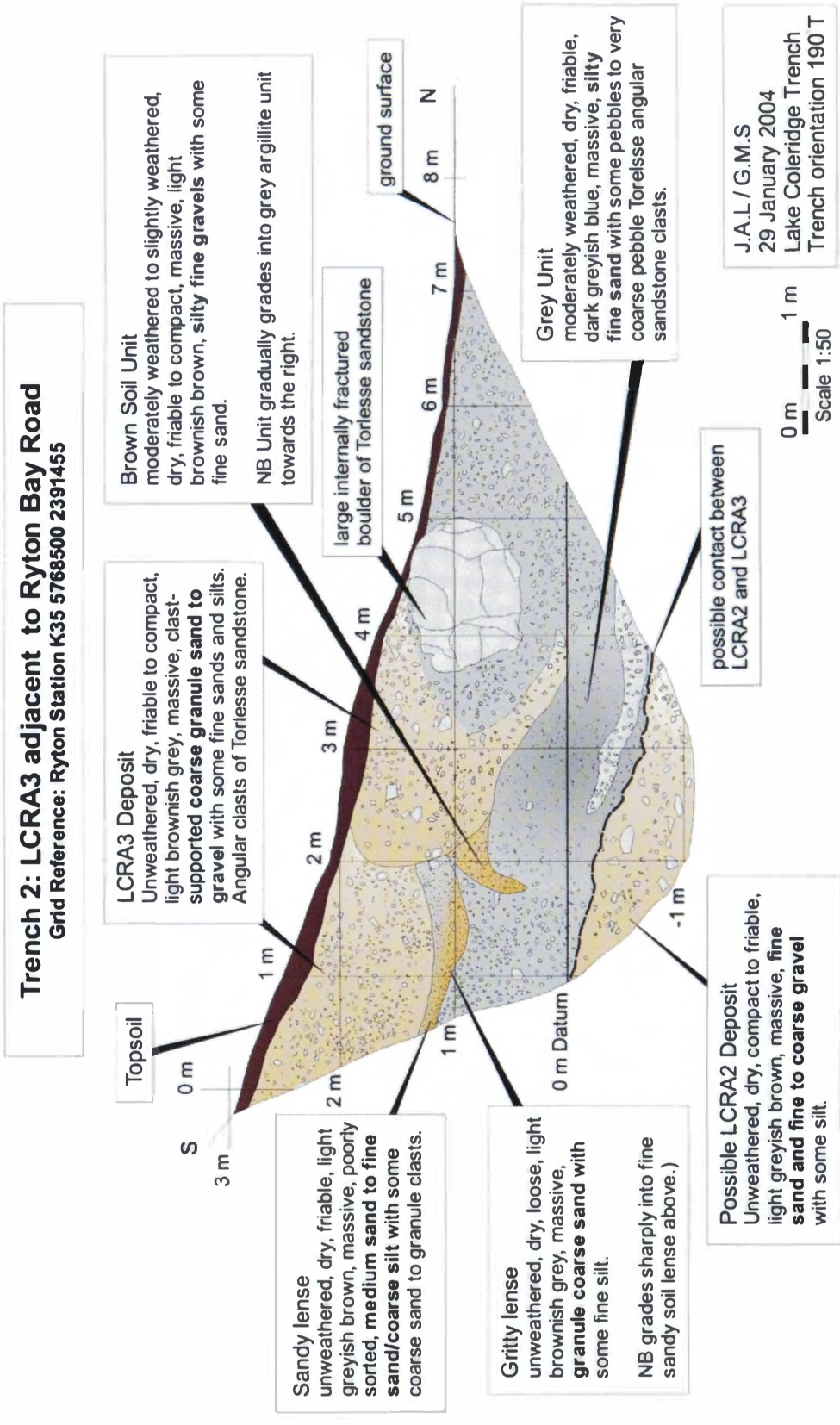

Figure 3.21: T_2 log displaying western face of the trench which was excavated into the middle of LCRA3 deposit. A chaotic structure is present within T_2. During transit downslope the material has "flowed" and the influence of the large boulder appears to have locally influenced the stratigraphy of the LCRA3 deposit.

- The LCRA3 deposit directly overlies the LCRA2 deposit. Although it is very small for a rock avalanche, with only ~2 m thickness both at the cliff exposure (figure 3.16) and at the T_2 site, it shows a very chaotic structure. This in part is assigned to the presence of a large Torlesse sandstone boulder ~1 m in diameter, which is believed to have distorted the inverse stratification of the lenses of sandstone and mudstone-rich matricies.
- Topsoil (ranging from 5 cm to 20 cm) has established a cover over the LCRA3 deposit.

3.6.3 Interpretation of the Third Rock Avalanche deposit

The LCRA3 deposit is very small in extent, which leads to the question of why did it fail and when did it fail? It is interpreted, to represent a lag deposit from the LCRA2 event, in which a small portion of loosened material remained within the source area of Carriage Drive until it failed either seismically or by gravity. It is also believed that the LCRA3 event occurred closely after the LCRA2 event for the following reasons:

- Within T_2, no soil horizon has developed on the pre-LCRA3 surface of the interpreted LCRA2 deposit. The lack of soil development indicates a very limited time between the events.
- Although the volume of the deposit has not been calculated, the LCRA3 is clearly a small deposit (with an estimated surface area of <20,000m^2). The average thickness of the LCRA3 is ~2 m, based on the exposed cliff (figure 3.20) and the trench log from T_2 (figure 3.21). As Chapter 5 demonstrates, a deposit with this thickness would not have the volume and momentum to reach up and onto the opposing cliff surface, given the present-day hollow or depression within the riverbed, which has been created by the incision into rock avalanche debris by the Ryton River. Therefore, the LCRA3 event must have occurred, before any significant incision of the LCRA2 deposit occurred for it to have reached the elevation of the top of the LCRA2 deposit on the opposite side of the Ryton River.
- The contact between the LCRA2 and LCRA3 deposits (figures 3.16 and 3.17), shows evidence for water sorting and this is almost certainly fluvial in origin. Due to this, it is believed that the LCRA2 deposit dam was overtopped by the Ryton River and before any significant dam failure, erosion or incision into the LCRA2 deposit occurred, the LCRA3 event was initiated. This suggests that

perhaps the significant portion of the LCRA3 was deposited onto, or adjacent to the LCRA2 "dam".

- Therefore, the lack of geomorphic expression of the LCRA3 deposit may be explained by the subsequent flooding, erosion and down-cutting of the LCRA2 dam, which carried most of the LCRA3 debris away downstream. Protection of the LCRA3 deposit occurred due to incision of the Ryton River at the cliff exposure (figure 3.16).

3.7 Carriage Drive Source Area

3.7.1 Mapped Geology

The Carriage Drive source area is located at the south-eastern end of the Cottons Sheep Range front, facing outwards towards the southeast (figure 1.1). The Carriage Drive peak is elevated to 1055 m above sea level, with the surrounding valley floors at approximately 520 m above sea level. The southeast facing hill slope has been heavily glaciated, and as a result has a slope angle of ~34°. The upper source basin for the LCRAD is roughly a horseshoe-shaped bowl (figure 3.2), and is largely covered by loose scree with slope angles of about 40°. Basement exposure is generally restricted to the uppermost headscarp region due to large volumes of loose scree, and measurements of the source area age given in Tables 3.1 and 3.2.

A distinctive topographic "lip" is present at an elevation of 860 m in the source bowl (figures 3.3 and 3.22). It is relatively flat on the southwestern side, however steps up to a chaotic hummocky surface on the northeastern side, where a stand of beech trees are present (figure 3.2). The uneven topography is believed to be due to numerous slumping and scree movements from the upper slopes post evacuation of the Lake Coleridge Rock Avalanche events. The interpretation of the "lip" is either one of two things. Firstly the "lip" represents the lowest breakout level for the removal of the source material. Alternatively, the "lip" is slumped material from the headscarp which has become wedged within the bottleneck runout path. The preferred interpretation is that the "lip" represents the basal breakout of the failure surface for the rock avalanche events, although the latter alternative cannot be completely discounted. Below the "lip", scree slopes predominate with increased development of matagouri growth. The nature of the scree allows the source material to be traced downslope, because of colour variations between the Torlesse

Supergroup sandstone and mudstone (argillite) beds. This is apparent on the south-eastern side of the "lip", where dark argillite staining is evident downslope.

Along the northeastern ridge bedrock exposure is limited and therefore measurement and analysis was difficult. CHAMBERLAIN (1996) mapped a single dip and strike displaying the beds as overturned (figure 3.22), although in the present study no such bedding was recognised.

The key features of the source area geology are as follows:

- The existence of ridge rents along the eastern ridge, clearly shows extensive dilation of the rock mass around the Carriage Drive source bowl (figures 3.22 and 3.23). The ridge rents are believed to be orientated parallel to the strike of the Torlesse Supergroup basement strata.
- The initial geometry of the Carriage Drive source area is interpreted to have been hollowed (figure 3.22) by superficial retrogressive failure, similar to that occurring on the western side of Carriage Drive at the present day.
- The Torlesse Supergroup basement strata, where exposed, show significant dilation of the rock mass, both along bedding planes and along numerous joint sets (figure 2.4).
- From the geometry of the present day source scarp, there appear to be three principal releasing surfaces, which are represented by the three ridge lines around the main source bowl (figures 3.22, 3.23 and 3.24).

3.7.2 Defect Analysis

Defect analysis proved difficult, due to the disaggregated state of much of the Torlesse Supergroup basement rock mass as discussed in Section 2.2. However, field observations revealed a number of defect sets around the source bowl of Carriage Drive. Bedding within the basement strata varied in strike and dip (figure 2.2), but the dominant strike direction was north-northwest to south-southeast, with a steep dip of 70-80° towards the northeast. This geometry is within the toppling envelope for rock mass failure (figure 2.34). On the southwestern ridge of Carriage Drive, thinly bedded (5 to 30 cm) sandstone and mudstone (argillite) beds predominate (figure 2.3). EISBACHER and CLAGUE (1984) identified that the mudstone or argillite beds were weak layers within a rock mass, and failure along the mudstone beds was

identified within the source bowl of Carriage Drive in the present study. The development of ridge rents along the eastern ridge is interpreted to be due to rock mass dilation and outward toppling-style failure of the rock mass along the strike of the basement strata (figures 3.22 and 3.23).

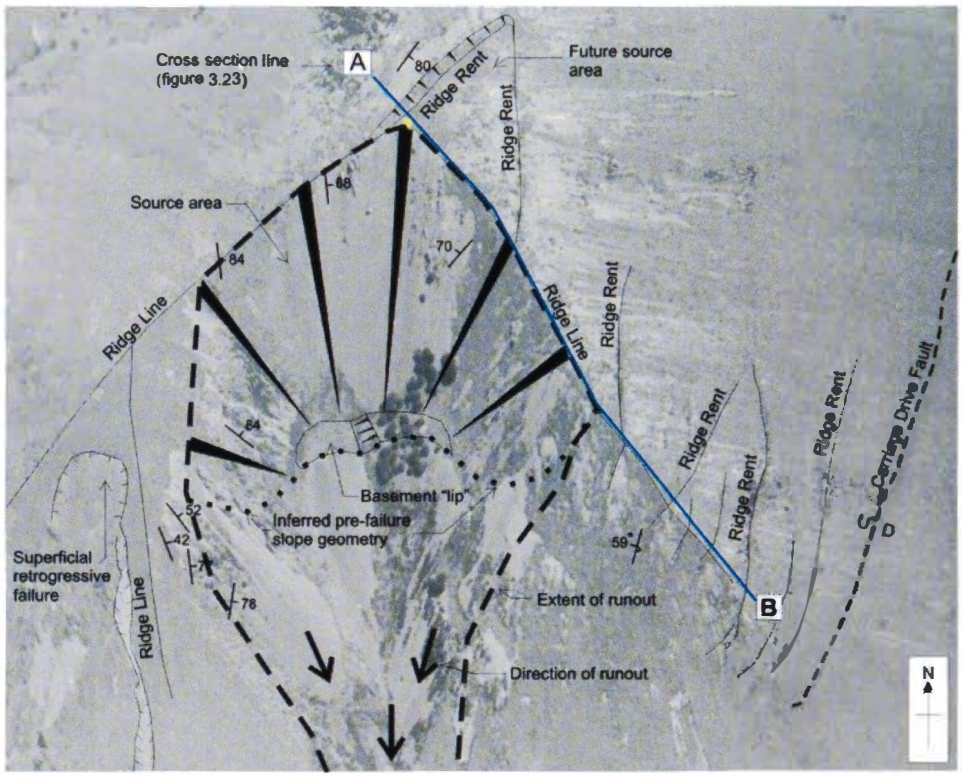

Figure 3.22: Aerial photograph of the source scar around the crest of Carriage Drive for the Lake Coleridge Rock Avalanche deposits. Bedding strike and dip measurements are shown along with the ridge rent structures. The summit is indicated by the yellow triangle. Carriage Drive Fault is also highlighted on the eastern side of the photograph. The scarp behind the summit is indicated. The heavy dashed line indicates the inferred outline for previous rock avalanche failures. Note the * indicates a strike and dip measurement taken by CHAMBERLAIN (1996).

The ridge rents display the following characteristics and are believed to be significant to the dilation and toppling interpretation of the rock mass (figure 3.23):

- Eight ridge rents dissect the eastern ridge line on the upper slopes of Carriage Drive within the topmost 400 m of the slope.
- They all display backwards facing scarps (dipping to the west) of no more than 1.5 m in height and have varying lengths in tens of metres. One ridge rent on the western side of Carriage Drive dips east, but still displays the backwards-facing scarp (figure 3.23).

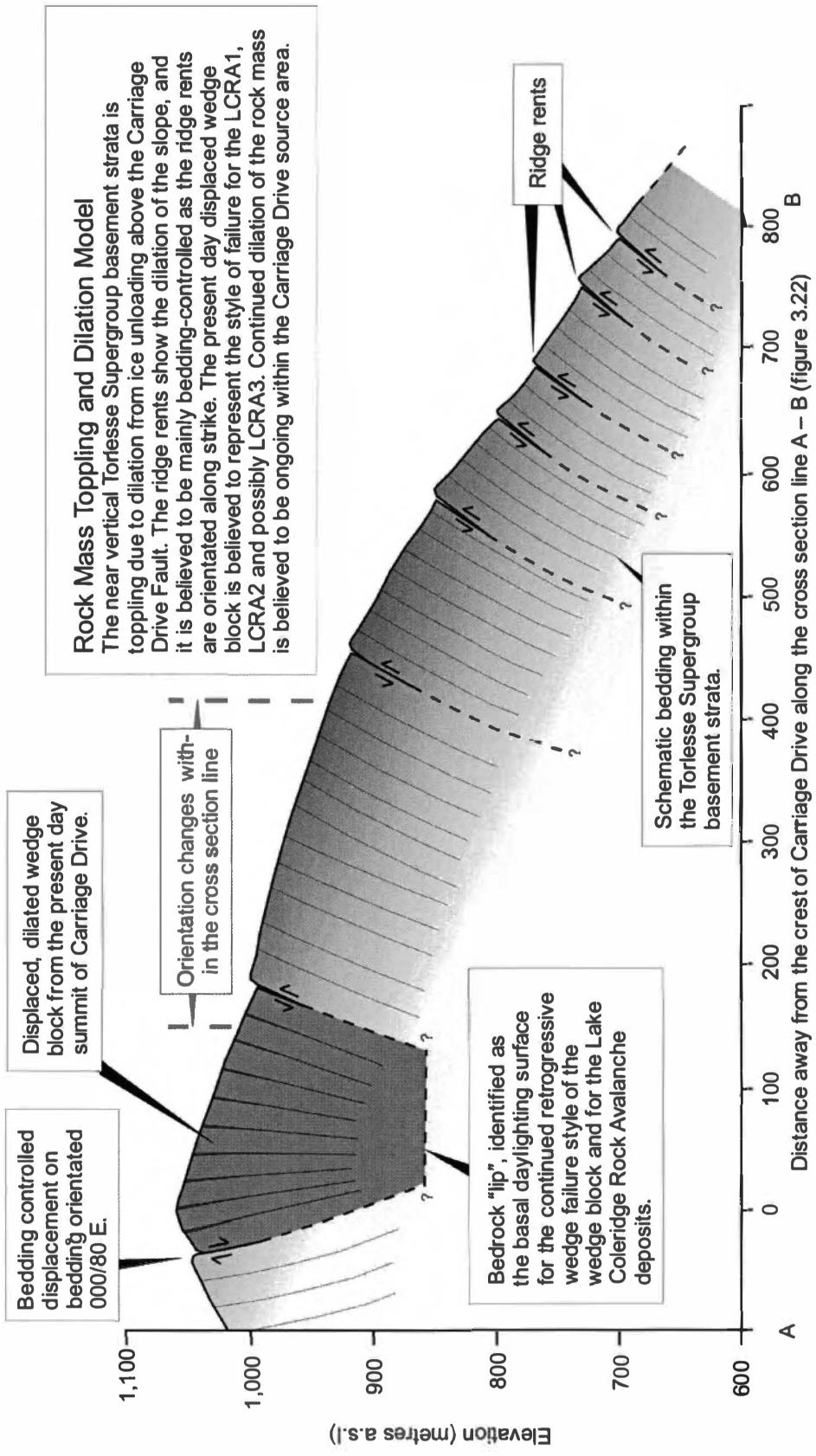

Figure 3.23: Schematic cross section along the eastern ridge of Carriage Drive (refer to figure 3.22) showing the interpreted wedge failure and the ridge rents developing due to outward toppling of the dilating rock mass.

- The persistence of the ridge rents downwards into the rock mass is not known, but is inferred to extend downwards for many tens of metres. This is thought to be indicative of rock mass dilation that has occurred after ice retreat and unloading.

Dilation of the rock mass is believed to be a critical part of the failure mechanism for the Lake Coleridge Rock Avalanche events. The present day wedge block (figure 2.23) that is located at the summit of Carriage Drive is not *in situ* and has been displaced approximately 1.5 m downwards and outwards towards the southeast. This wedge block was shown to be kinematically feasible when the major defect sets were plotted within a stereographic net with the intersection of the defect planes within the daylight envelope (figure 3.24).

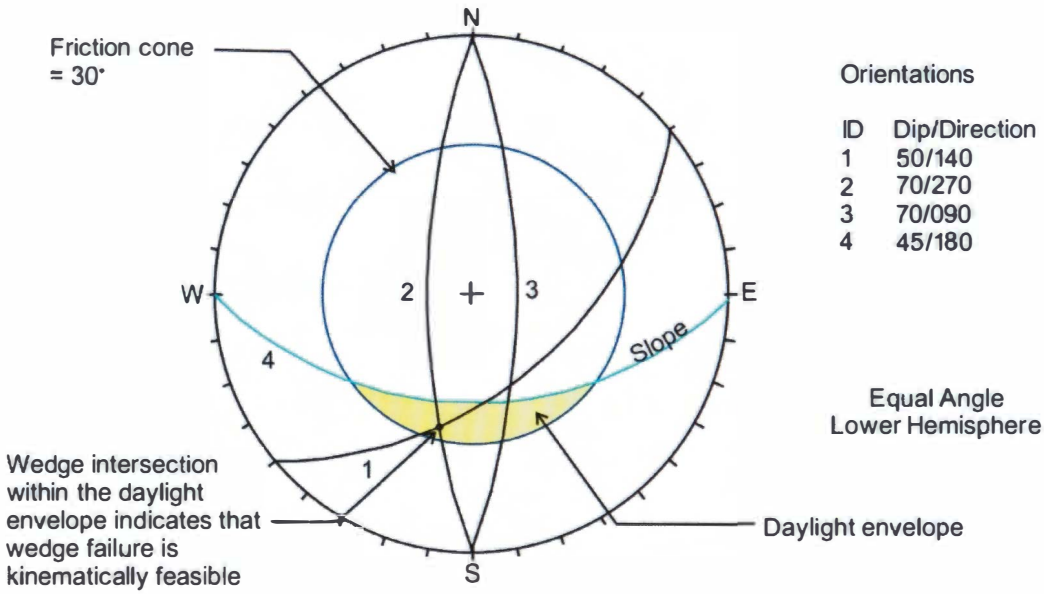

Figure 3.24: Stereographic net of an equal angle lower hemisphere projection of the major defect sets intersecting with Carriage Drive which indicates that wedge failure along these defect planes is kinematically feasible.

3.7.3 Pre-Failure Rock Mass Conditions

In order to attempt to interpret a failure sequence (including mechanisms and triggers of rock mass failure), the antecedent conditions of the source area and surrounding slopes are required. The slopes of Carriage Drive are understood to have been buried by ice from repeated glaciations within the Late Pleistocene, as discussed in Chapter 2. As a consequence of repeated glaciations, wide "U" shaped valleys exist

on both sides of Carriage Drive and the Cottons Sheep Range. Glacial processes reducing the rock mass strength of mountains are a widely acknowledged phenomenon (e.g. AUGUSTINUS, 1992, 1995a). AUGUSTINUS (1995a) noted that *"rock slopes of glaciated valleys undergo continual modification during both glacial and interglacial periods, with the rock slope failure and form modification being most active following glacier retreat when the removal of the glacier buttress promotes rock slope failure through the redistribution of internal rock stresses."*

Therefore, pre-failure rock mass conditions of the Torlesse Supergroup basement strata post ice retreat are thought to have been as follows:

- Due to erosion by the glaciers, Carriage Drive slopes were oversteepened with slope gradients probably ~35°.
- Rock mass strength of the Torlesse Supergroup strata had reduced due to changes in internal rock stresses.
- The reduction in rock mass strength coincides with the development of joint defect sets, and/or the growth in persistence of pre-existing defects. Throughout the source area, joints are prolific within the Torlesse Supergroup strata, with defects cutting across both sandstone and mudstone beds. Their persistence cannot be realistically determined, but like SMITH (2003) some joints are assumed to be persistent for tens of metres and representative of pre-failure rock mass conditions.
- Increase in joint defect frequency and/or persistence allows slope relaxation and dilation of the rock mass by gravitational forces downslope.
- The dilation of the slope increases the amount of water within the rock mass which causes higher pore water pressures. A positive feedback system develops between rock mass dilation and pore water pressure, where freeze-thaw is also occurring in the near-surface.
- Vertical dipping beds within the Torlesse Supergroup strata begin to undergo toppling failure down the eastern slopes, and regional earthquakes possibly enhance ridge rent development.
- Shallow or superficial erosion is interpreted to have been occurring within the Carriage Drive slope at the present day location of the source bowl and runout path prior to the rock avalanche events. Therefore a hollow or depression within the slope exists before the LCRA1 event.

3.7.4 Failure Conditions for the Lake Coleridge Rock Avalanche 1 Event

The LCRA1 event is believed to have been caused by a combination of; a) steepening of the rock slope by glacier erosion; b) rock mass dilation due to rebounding of the rock mass; and/or c) a seismic event within the region. Cleft water pressures[2] may have played a key role in increasing destabilization of the slope. Therefore, both freeze-thaw processes and pore pressures may have played vital roles in destabilisation of the slope. As the pre-failure slope of Carriage Drive is interpreted to have been hollowed out by erosion and the presence of a spring halfway up the runout slope at the present day (figure 3.2), it is feasible to consider that the erosion and the spring developed together. Therefore, ice plugging of drainage may have also encouraged failure. Although the Ryton River flows directly beneath the Carriage Drive source area it is not believed to have created any loss of slope support through scouring and erosion of the hillside immediately following ice retreat. Seismicity also may have been a leading trigger for the rock avalanche event.

Dilation of the rock mass (dominated by a toppling-style of failure of the near vertical beds) predominantly along mudstone or argillite beds, and persistent joint sets (orientations shown in figure 3.24), are believed to have been the critical failure mechanism for the LCRA1 event (figure 3.23). The present day wedge of displaced bedrock at the summit of Carriage Drive is thought to represent the releasing mechanisms that occurred for the LCRA1 event. The triggering of this rock avalanche event, which occurred c. 10,000 years B.P. is further discussed in Chapter 4.

The antecedent conditions of the rock mass within the Carriage Drive source area are believed to have been highly dilated and therefore, with a reduced rock mass strength. Continual slope relaxation by gravitational forces may alone have resulted in a gradual decrease in the factor of safety for the slope.

3.7.5 Failure Conditions for the Lake Coleridge Rock Avalanche 2 Event

The antecedent conditions in the Carriage Drive source area before the LCRA2 event can be summarised as follows. Removal of lateral support of the Carriage Drive

[2] When water enters the ground within a slope an increase in pore water pressure and a decrease in the shearing resistance of the rock mass also occurs (TERZAGHI, 1950).

source area slope by the LCRA1 event, which led to continued dilation of the rock mass, as was identified by the present study within the source. Failure either involved simple retrogression of the LCRA1 headscarp, or a specific wedge-type failure on master defects within the source area. However, the assumption is that releasing mechanisms of the three major defect sets (discussed in Section 3.6.4) that controlled the failure for the LCRA1 event, were also controlling the failure for the LCRA2 event. This probably indicates a similar style of failure as the first one, but on a smaller scale, with the headscarp retrogressing to allow further large scale block failures.

The LCRA2 event is believed to have been caused by a combination of; a) steepening of the rock slope by the removal of lateral support due to the LCRA1 event (~9,000 years earlier), b) continued gravitational-induced defect-controlled dilation of the rock mass; and c) the strong probability of a seismic rupture along the western segment of the Porters Pass-Amberley Fault Zone. Dating the LCRA2 deposit at an age of (Wk14221) 668 ± 36 years B.P. (as discussed in Section 4.4), enabled a good correlation between an interpreted rupture along the western segment of the Porters Pass-Amberley Fault Zone between 500 to 700 years B.P. (Section 2.5.4), and possibly the Alpine Fault.

3.7.6 Failure Conditions for the Lake Coleridge Rock Avalanche 3 Event

The failure mechanism for the LCRA3 event, like the LCRA1 and LCRA2 events, is considered to be continued rock mass weakening from gravitational dilation along bedding planes and joints. The three major defect sets controlling failure, are believed to have been the same as for the LCRA1 and LCRA2 events, as discussed in Section 3.6.2 and shown in figure 3.24. Continued slope unloading from the earlier two rock avalanches, and thus loss of lateral support, is also deemed important for repeated failures within the Carriage Drive source area.

The LCRA3 event in interpreted to have failed closely after the LCRA2 event, and due to its smallness in size it is possibly a lag deposit from the LCRA2 source volume which came down as a secondary event. Instability of the source scarp and runout path after rock avalanche events, is a documented occurrence where rock falls and small failures continue for days. This was witnessed after the Mt Adams Rock Avalanche in 1999, where later collapses were thought to have been caused by stress

releases from the rapidly unloaded rock mass around the source scarp (HANCOX *et al.*, 2002).

Although the third event is very small in volume for a rock avalanche event, the chaotic nature and "flow-like" appearance of the deposit imply that it was indeed a rock avalanche. The deposit was not dated during this study, and therefore no coseismic trigger could be established. Gravitationally-forced dilation from the removal of material after the LCRA2 event is considered a likely failure trigger without an earthquake, although even a large aftershock from the PPAFZ event triggering LCRA2 may have been sufficient.

3.8 Impacts on the Ryton River

3.8.1 Background

Each failure and subsequent runout of the three rock avalanche events making up the LCRAD, temporarily dammed the Ryton River for varying periods of time. Damming of waterways by rock avalanche debris emplacement is a common natural process and COSTA and SCHUSTER (1988) found rock and debris avalanches to be the most common form of mass movement to cause landslide dams. It is therefore reasonable to assess evidence for river, lake and dam-break "outwash" terraces having developed as a result of changing base levels for the Ryton River before, during and after the LCRA1, LCRA2 and LCRA3 events. Dam-break outwash terraces are considered here, to be the terraces deposited downstream after the overtopping of the rock avalanche dam and the subsequent dam-break depositional sequence.

Fluvial terraces both upstream and downstream of the LCRAD were studied during this project, in an attempt to determine whether they could provide information about the stream response to the rock avalanche events (figure 3.25). Initial investigations focused on distinguishing the type of terrace from surface gradients, geology and relative elevations and positions taken from a GPS survey of the river bed and adjacent terraces. Subsequent investigations then focused on impounded lake heights behind the temporary dams and successive dam breach by overtopping and downcutting through the rock avalanche deposits in the channel or via a "natural" spillway.

The distinctive determining features to separate out the type of terraces (i.e. river, lake or dam-break "outwash") were their gradients and elevations relative to other features (figure 3.25). The composition of the deposits, including the angularity of the clasts, was also a useful tool to distinguish the type of terrace. It was assumed that:

- River terraces would typically have gradients which corresponded to the present-day gradient of the Ryton River. It was realised that throughout time, the base level of the Ryton River has fluctuated, however there would still be a common gradient associated with the downward flow and transport of the sediment load.
- Lakeshore terraces would have near horizontal surfaces, and relate to still stands reflected in beach levels.
- Dam-break outwash terraces formed as a result of dam overtopping and rapid failure are obviously going to be located downstream of the rock avalanche deposit. Due to their hyper-concentrated/debris flow nature (KORUP, 2002) these were identified by their steepness of gradient and the angularity of the clasts within the deposit.

3.8.2 Pre-Lake Coleridge Rock Avalanche 1 Event

The Ryton River is interpreted to have developed or re-established itself after the retreat of Acheron 3 glacial ice from the valley to an initial base level of R.L 530 m ("Greater Lake Coleridge"). Ryton River has a present day catchment area of 76 km² and therefore using the method of MCKERCHAR and PEARSON (1989) a mean annual flow for the Ryton River can be calculated as ~2 cumecs (Table 3.3). Incision of the Ryton River through glacial outwash terraces and the development of fluvial terraces within the glacial till is considered likely. This has occurred at the southwestern foot of Mt Hennah and the northern foot of Round Hill (figure 2.5). However, the development of fluvial terraces within the glacial till has not been identified within the lower portions of the Ryton River, and it is inferred that these terraces do exist, but the emplacement of rock avalanche material of the LCRA1 event has buried them (figure 3.3).

The presence of "Greater Lake Coleridge" during the early stages of Acheron 3 ice retreat to an inferred maximum height of 530 m (Section 2.4.2.1), would have inundated the present day Ryton riverbed up to and including the area where the

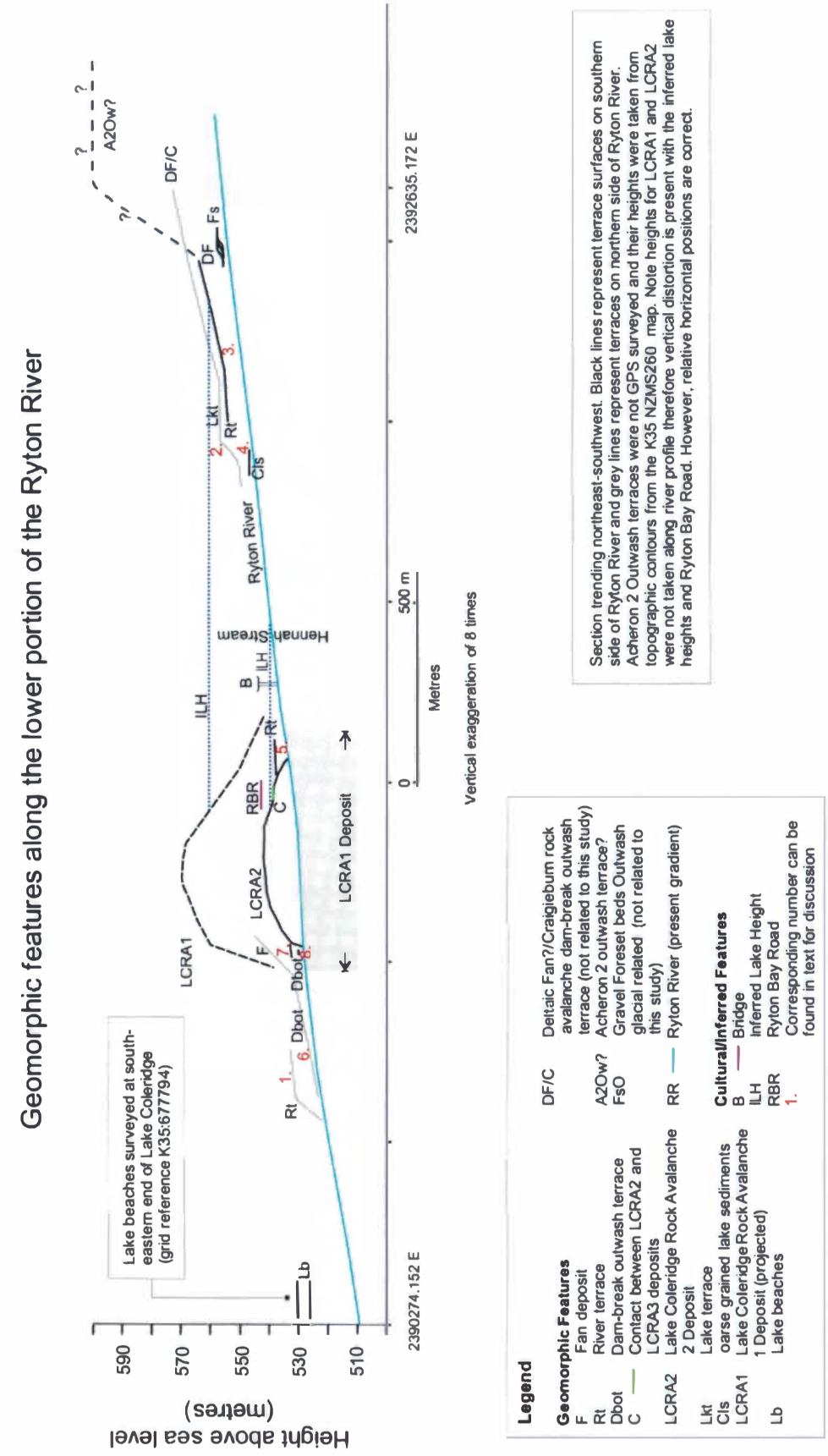

Figure 3.25: Geomorphic features along the lower portion of the Ryton River as surveyed by GPS methods.

present day LCRAD is located. One river terrace possibly relating to "Greater Lake Coleridge" is located on the true right bank of the riverbed and directly abuts against the flanks of Carriage Drive (labelled 1 in figure 3.25). There is no other evidence within the riverbed for terraces that have developed before the LCRA1 event.

Table 3.3: Ryton River Flow Calculations from the Method of MCKERCHAR and PEARSON (1989).

Calculation	Value
Mean annual rainfall (Mar) Lake Coleridge Meteorological Station (records from 1913-1980; refer to Table 1.1) Note that the mean annual rainfall is assumed to be the same as the present day	0.83 m
Planimetric Catchment Area (A)	76,000,000 m^2
Mean annual flow of Ryton River = Mar x A / (365 x 86400)	2.00 cumecs (2dp)
Mean annual flood of Ryton River $Q_1 = A^{0.8} \times 0.5$*	15.98 cumecs (2dp)
Mean 100 year flood of Ryton River Q_1 x 2.5**	39.88 cumecs (2dp)

*Value read off South Island contour map of $Q_1 / A^{0.8}$ (refer to figure 5.6).

**Value read of South Island contour map of q_{100} (refer to figure 5.6).

3.8.3 Emplacement of the Lake Coleridge Rock Avalanche 1 Deposit

The LCRA1 event caused significant disruption and alteration to the Ryton River and these are summarised as follows:

- After initial rock avalanche emplacement, the flow of Ryton River to Lake Coleridge would have ceased due to rock avalanche damming, although seepage possibly created a very small flow through the LCRA1 dam.
- Ponding of Ryton River waters would start flooding upstream of the LCRA1 site to the maximum height of any natural spillway that was formed.

  The interpreted dam height for the LCRA1 event is ~30 m above the present day riverbed within the central portion of deposit. From the inferred emplacement height of the dam calculations about the development, volume and time to overtop the rock avalanche deposit can be made (Table 3.4). The volume calculations have been made using the present day topography which was repeated when calculating volumes for the LCRA2 dam.

- The calculations involving the length of time for overtopping by the Ryton River have ignored seepage through the dam and are considered the "worst case scenario", providing the shortest time span to dam breach and the maximum dam height. If a natural spillway were to develop through a low section of the dam these calculations would vary, and this applies to the LCRA2 damming event discussed below in the next section as well.

Table 3.4: Lake Coleridge Rock Avalanche 1 Lake Statistics. Rainfall, catchment area and mean flow data as for Table 3.3

LCRA1 Lake Statistics (R.L. of 560 m (a.s.l))	**Dimensions**
Planimetric surface (S)	1.0975 km²
Volume (V)	16,802,500 m³
Length of time for lake to develop under mean annual flow conditions (V/Mar)/86400	97.2 days
Length of time to develop under mean annual flooding conditions (V/Q_1)/86400	12.2 days

Very little evidence exists from the LCRA1 damming episode within the Ryton River. No dam-break outwash terraces are located downstream from the LCRA1 deposit, and from the size of the deposit this could be considered as quite unusual. However, given the interpreted age of the deposit (~9,720 ± 750 years B.P.; refer to Section 4.3.4), the length of time for erosion by the Ryton River to remove any terraces that had formed in response to the damming is sufficient to explain the lack of terrace preservation. However, there are three features upstream of the LCRA1 deposit which are interpreted to correlate with the development of a lake dammed behind the rock avalanche dam. These are described as follows, and are shown on figure 3.25:

- A lake terrace located on the true right bank of the Ryton River just upstream of the Hennah Stream confluence (labelled 2 in figure 3.25) is almost certainly related to an enlarged lake from the LCRA1 damming event. It has a horizontal surface approximately 100 m long and ~6 m thick, and is at an elevation of 557 m (a.s.l). The presence of the terrace probably implies that the lake lasted a much greater period than the 97 days calculated in Table 3.4, and may have existed for years with the Ryton River flowing over the rock avalanche debris.

- A river terrace is located on the true left bank of the Ryton River (labelled 3 in figure 3.25) ~8 m above the present grade of the riverbed. This may also be associated with an increase in the base height of the river during the LCRA1 damming event, but relating to progressive outlet lowering.
- Coarse lake sediments located within the Ryton riverbed (grid reference K35: 923694) discussed in Section 2.4.2.3 may relate to an early stage of lake filling from the LCRA1 dam (labelled 4 in figure 3.25). The sediments range from silts to granules, therefore making them very coarse for lacustrine sediments. However, thin beds (millimetre to centimetre scale) of alternating grain sizes have been deposited in a laminar sequence (figure 2.7), which implies that the energy within the depositional environment was minimal.

Subsequent to dam overtopping by the ponded Ryton River, it is interpreted that the dam did not fail catastrophically with a dam-break flood but self armoured an natural spillway within the deposit at or just above 557 m (a.s.l). This coincides with the lake terrace identified upstream of the dam which was discussed above. Continued re-establishment of the Ryton River over a period of almost 10,000 years has removed any further evidence of a temporary lake developed in response to the LCRA1 event. Over the period of time between the LCRA1 and LCRA2 events, the Ryton River eroded considerable volumes of rock avalanche debris from the LCRA1 deposit (Table 3.1). The river is interpreted to have graded to the Lake Coleridge elevation of ~507-8 m (pre-Lake Coleridge Power Station height). However, some armouring of the riverbed is likely to have existed through the LCRA1 deposit, which may have caused a slight change in gradient of the riverbed through the rock avalanche deposit as is present today (figure 3.25).

3.8.4 Emplacement of the Lake Coleridge Rock Avalanche 2 Deposit

The LCRA2 event created an almost instantaneous dam within the narrow Ryton riverbed which had the following effects:

- After initial rock avalanche debris emplacement from the LCRA2 into the Ryton riverbed, water would begin to pond behind the natural dam. Seepage of some water through the barrier may have occurred.
- As flood waters increased in height upstream of the barrier, more low-lying land became inundated.

- The interpreted dam height for the LCRA2 event (R.L. 540 m) is approximately 10 m above the present day central portion of the LCRAD. As for the LCRA1 "dam" discussed above, calculations were made for the lake that is believed to have developed behind the LCRA2 dam (Table 3.5).

Very little evidence for a temporary dam from the emplacement of the LCRA2 deposit exists upstream of the site. A river terrace is located above the present day riverbed, which may be associated with a higher base level caused from the temporary dam (labelled 5 in figure 3.25). The lack of evidence for upstream flooding and aggrading terrace development is most likely attributed to the very limited period that the dam existed and the fact that it was a relatively small lake which developed. Figures from Table 3.5 show that to reach a maximum dam height of 540 m (a.s.l), which is 10 m above the central portion of the LCRAD at the present day, would only take ~14 days under the normal estimated flow of Ryton River, therefore the barrier structure was too temporary to have fluvial features develop in response to its brief presence within the riverbed.

Table 3.5: Lake Coleridge Rock Avalanche 2 Lake Statistics. Rainfall, catchment area and mean flow data as for Table 3.3

LCRA2 Lake Statistics (R.L. of 540 m (a.s.l))	**Dimensions**
Planimetric surface (S)	0.46 km²
Volume (V)	2,326,250 m³
Length of time for lake to develop under mean annual flow conditions (V/Mar)/86400	13.5 days
Length of time to develop under mean annual flooding conditions (V/Q_1)/86400	1.7 days

Directly downstream from the LCRA2 deposit significant dam-break "outwash" terraces (figure 3.3) have formed during the dam-break flood which appears to have resulted from overtopping of the dam by the Ryton River (labelled 6, 7 and 8 in figure 3.25). The three dam-break outwash terraces are described as follows:

- A large terrace (with a volume of ~95,000 m³ estimated on the present day river as the base of the terrace) is present on the true right of the Ryton River (labelled 6 in figure 3.25). It has an elevation of ~533 m (a.s.l) at its upstream extent.

- A terrace (on the true left of the river) at a corresponding height to the terrace on the opposite bank is present (labelled 7 in figure 3.25). This terrace has been mostly eroded away by the Ryton River, with an estimated volume of ~6,000 m^3 remaining down to the bed of the Ryton River. The excavation of T_3 was partially into this trench, as discussed in Section 3.5.4.
- Another terrace on the true left bank is present (labelled 8 in figure 3.25), but ~3 m lower in elevation than the higher terrace it abuts against (terrace labelled 6). This terrace has also been heavily eroded into by the Ryton River, with a volume of only 600 m^3 remaining.
- The three dam-break outwash terraces have a considerably steeper surface gradient of 0.019 (taken from the largest terrace located on the northern bank of the Ryton River (labelled 6 in figure 3.25)), compared to the river gradient/profile of 0.014.
- The terraces are composed of angular clasts from the LCRA2 deposit, and could be described as the product of a hyper-concentrated flow which typically contain clast sizes ranging from coarse sands through to large boulders of up to 1 m in diameter.
- All three terraces display moderately sorted stratified sequences of alternating coarser (gravel) and finer (pebble to granule) beds of angular Torlesse Supergroup clasts, which are predominantly sandstone.

The dam-break outwash terraces indicate that subsequent to dam overtopping by the ponded Ryton River, dam failure occurred with material being eroded rapidly from the LCRA2 deposit. The presence of the dam-break outwash terraces indicate that after overtopping, the LCRA2 was actively incised and eroded by the Ryton River, and that material from the dam was transported downstream. Erosion into these terraces by the Ryton River is continuing presently, almost 700 years after the event (as discussed in Section 4.4.3). The riverbed is still affected by the rock avalanche debris armouring the bed and therefore there is a change in gradient of the riverbed through the LCRAD.

3.8.5 Emplacement of the Lake Coleridge Rock Avalanche 3 Deposit

The LCRA3 event is interpreted to have occurred closely after the failure of the LCRA2 event, before any significant erosion and incision of the Ryton River took

place into the LCRA2 deposit (Section 3.6.3). Therefore it is highly likely that the dam-break "outwash" terraces discussed for the LCRA2 event also incorporated the LCRA3 deposit. If this is the case then the Ryton River, already dammed by the LCRA2 event, would not have been altered by any significance from the LCRA3 emplacement. No other terraces were identified which relate to the LCRA3 event.

3.8.6 Present Day Ryton Riverbed Profile

A surveyed profile along the Ryton River gave an average gradient of 0.014 (figure 3.25). HEWITT (1998) noted that river channel sections flowing through rock avalanche deposits within the streambed are usually steeper in gradient, and this is evident at the initial upstream section of the deposit in the Ryton riverbed. The steepness in gradient through the top half of the rock avalanche (0.017) deposits such as is seen at the LCRAD, was a notable feature that WHITEHOUSE (1983) discussed during a study of numerous rock avalanches in the Southern Alps of New Zealand. It is a common feature among rivers that have been blocked by rock avalanches, because many failure deposits contain coarse interlocking material that locally armours the streambed (COSTA and SCHUSTER, 1988). The composition and dense compaction of the deposits also promote resistance to erosion (HEIM, 1932). A change in gradient just below the Ryton Bridge from 0.014 to 0.017 is followed by a subsequent decrease in the river gradient of 0.0060 through the lower half of the LCRAD. This indicates that the river has not yet fully returned to an original base level, and a delta is continuing to prograde into Lake Coleridge at the mouth of the river.

3.9 Summary

The LCRAD consists of three rock avalanche deposits. Various mapping, surveying and dating techniques (discussed in Chapter 4) have enabled a thorough description of particularly the LCRA1 and LCRA2 deposits. Due to the poor geomorphic expression of the LCRA3 deposit and its small size, little is known about the event and the deposit statistics.

The LCRA1 deposit had an original volume of 10×10^6 m^3, with the deposit covering an area 0.261 km^2. The Fahrböschung for the LCRA1 is 0.28, with the equivalent angle of 15.5°. The LCRA1 event displayed a high mobility which was

shown through comparisons with European examples of rock avalanche runouts and with the work of NICOLETTI AND SORRISO-VALVO (1991). Trench excavations (T_1 and T_4) exposed the internal chaotic structure of the LCRA1 deposit, however no organic material was found to radiocarbon date. This was because of its probable occurrence very soon after retreat of Acheron 3 ice.

The LCRA2 deposit has an original volume of 0.5×10^6 m^3, which is considered to be quite small for a rock avalanche event. Like the LCRA1 deposit, the LCRA2 event displayed high mobility, and has also been compared to other rock avalanches from around the world (figures 3.5 and 3.6). A mixing zone was identified within the lower portion of the deposit, and the LCRA2 deposit has a distinctive brandung swash feature at its distal extent where rock avalanche debris has run up onto the LCRA1 deposit. Although trenching (T_3) revealed no organic material to radiocarbon date, a piece of mānuka was found embedded within the LCRA2 deposits in cliffs that line the Ryton River, which was sampled to date the rock avalanche event.

The LCRA3 deposit, although identified during this study, still remains poorly defined. A lack of geomorphic expression away from the cliff exposure is the main reason for this. This deposit was excavated into with T_2, but the deposit could not be dated and it is inferred to have failed closely after the LCRA2 event.

The Carriage Drive source area was mapped and described. Limited defect analysis was carried out within the source bowl, which was made difficult by the disaggregated and weathered nature of the Torlesse Supergroup bedrock. However, the series of eight ridge rents located down the eastern ridge line are believed to be a crucial diagnostic feature of the rock mass dilation and outward failure via a toppling mechanism along steeply dipping argillite beds, which are the dominant planes of weakness within the rock mass. Continued dilation of the rock mass along the near-vertical bedding planes, combined with intersecting joint defects which have also dilated, is interpreted to be the precursory condition before each of the rock avalanche events (LCRA1, LCRA2), except for the LCRA3 event, which may be part of the LCRA2 failure. A wedge of displaced bedrock is present at the summit of Carriage Drive.

Triggering mechanisms for the LCRA1 event is considered to be from a combination of; a) oversteepening of the rock slope by glacier erosion, b) rock mass dilation, and/or c) a seismic event. A seismic triggering mechanism was not identified for the LCRA1 although it is likely for it to have been triggered coseismically. The triggering mechanism for the LCRA2 event is considered to be coseismic, which is discussed further in Chapter 4.

The impacts on the Ryton River during the LCRA1, LCRA2 and LCRA3 events, vary in significance and effect. The LCRA1 damming event is believed to have created a lake for several years before the river completely incised into the deposit and returned to a relatively normal base level. The LCRA2 event is thought to have created a temporary dam which lasted only days, and the dam-break flood was probably quite significant with downstream dam-break "outwash" terraces recording its occurrence. The LCRA3 event is thought to have had little effect, on the already dammed Ryton River by the LCRA2 event, and may in fact have added to the LCRA2 dam before lake filling was complete. Presently the Ryton River is continuing to erode rock avalanche material from the LCRA2 and LCRA3 deposits and transport it down into the aggrading delta at the mouth of the river. The Ryton River average gradient is 0.014 however steepens through the first half of the LCRAD to 0.017, and then shallows for the second half of the LCRAD to 0.0060 before returning to 0.014 and flowing into Lake Coleridge.

Chapter 4

Age and History of Lake Coleridge Rock Avalanche Deposits

4.1 Introduction

Much geomorphological interpretation, and indeed this study, relies heavily on placing time controls on the landscape (BURBANK and ANDERSON, 2001). One of the foci of this project is to estimate the timing of three individual rock avalanche events situated in the Ryton River area. By dating the three rock avalanches it is possible to reconstruct the sequence of events which took place at the site and shaped the landscape as it appears today. By dating the rock avalanche events, it may also be possible to infer triggering mechanisms for the failures. For example, previous studies have obtained ages for rock avalanches and used them to date earthquakes (e.g. SCHUSTER *et al.*, 1992). Temporal clustering of rock avalanches can also be attributed to regional seismic activity (CROZIER, 1991). However, heavy rainfall events and specific climatic conditions can also lead to rock avalanche failure. Failures, unrelated to earthquakes or rainfall should not be disregarded as was shown by; the Randa rockfall (NOVERRAZ and BONNARD, 1991), the 1991 Mount Cook rock avalanche (HANCOX *et al.*, 1991) and the Mount Adams rock avalanche in 1999 (KORUP *et al.*, 2004) all of which were aseismic. Dating the rock avalanches not only allows the reconstruction of temporal events within the area and the regional seismic history, but also may provide useful information for future hazard management.

Until the development of radiocarbon dating in the late 1940's, the principal method of establishing timing in the field was through the use of relative dating techniques (BURBANK and ANDERSON, 2001). Relative dating was achieved by methods such as identifying cross-cutting relationships or marker beds displaying

offset along fault planes. Basic geomorphologic mapping is still an essential procedure when estimating relative surface ages, however the development of absolute dating (as briefly outlined in the following) has greatly reduced the uncertainty and allowed actual dates of the surfaces to be calculated (BURBANK and ANDERSON, 2001). However, absolute dating techniques need to be applied with caution due to the potential errors inherent in each of the methods, (BURBANK and ANDERSON, 2001) and it is here that geomorphic mapping complements dating as a fieldwork procedure.

This Chapter summarises dating methods that can be applied to rock avalanches. Further information on the various techniques are referred to within the text. This Chapter concentrates on the dating techniques used to date the three Lake Coleridge Rock Avalanche deposits. Placing temporal constraints on the three rock avalanche events enables a number of things. Firstly, inaccuracies in dates in broad studies of rock avalanches within the Southern Alps undertaken in the past (e.g. WHITEHOUSE, 1981, 1983; WHITEHOUSE and GRIFFITHS, 1983) can be identified. Secondly, by obtaining a temporal constraint on the rock avalanche events, triggering mechanisms may be hypothesised. Thirdly, dating the three rock avalanche deposits allows a geomorphic history of the immediate and surrounding area to be interpreted.

4.2 Review of Dating Methods with Applications to Rock Avalanche Deposits

4.2.1 Introduction

Dating rock avalanche deposits is essential for most studies concerned with describing prehistoric rock avalanche events (e.g. WHITEHOUSE, 1981; WHITEHOUSE and GRIFFITHS, 1983; BULL, 1996; BULL and BRANDON, 1998; ORWIN, 1998). Outlined below is a summary of dating techniques applicable to rock avalanches in general, and their limitations as dating methods. Early dating studies undertaken on rock avalanche deposits consisted of radiocarbon methods. Other methods utilized for aging rock avalanches include; lichenometry, dendrochronology (although not as commonly used in New Zealand), weathering rinds, optically stimulated luminescence, and cosmogenic radionuclide dating. Table 4.1 provides a summary of different dating techniques applied to rock avalanche deposits. Within Table 4.1 the

relationship between the dated material and the failure event is highlighted and for further discussion and explanation of this refer to Section 4.2.3.

4.2.2 Available Dating Techniques

4.2.2.1 Radiocarbon Dating

Radiocarbon dating measures the half-life of carbon 14 (^{14}C) that is found within all organic material. ^{14}C is the unstable isotope of carbon, and it decays exponentially over time through a series of atomic reactions to ^{14}N (nitrogen) atoms, in the process emitting beta particles that can be measured (BOWMAN, 1990). The constant and known rate of decay of ^{14}C is 5730 ± 40 years, which is based on the radioactive decay equation. The actual standard half-life decay rate used when dating organic samples is 5568 ± 30 years, which is called the Libby half-life (HOGG, 1982).

Carbon (^{14}C and ^{13}C) is formed through interactions between cosmic radiations and atmospheric nitrogen. Most of the carbon oxidises forming CO_2 in the atmosphere and is therefore well mixed and relatively uniformly distributed around the Earth over short periods of time. Atmospheric carbon is fixed through the process of photosynthesis in plants. The theory of radiocarbon dating is based on carbon levels and isotopic percentages in plants mimicking levels found in the atmosphere (BURBANK and ANDERSON, 2001). Once a plant dies, the intake of carbon ceases and radioactive decay of ^{14}C begins. The decay rate of ^{14}C is known and the date when that sample died can be back-calculated from the amount of ^{14}C that remains in the organic material. Therefore, by finding organic material within landslide or rock avalanche deposits that is relevant to the emplacement episode, the events can be dated using the radiocarbon method. Radiocarbon dating is used throughout the scientific community for various applications. However this discussion is focused on using the method for dating rock avalanche deposits.

Accelerator mass spectrometric (AMS) dating is a variant method of the traditional ^{14}C radiocarbon technique. Instead of measuring the rate of decay (as is done for ^{14}C dating), the isotopic weight is measured (BURBANK and ANDERSON, 2001). By using AMS dating, the sample size is vastly reduced and the possible age range for dating material has been extended to ~50,000 years B.P.

Table 4.1: Summary of Dating Methods applied to Rock Avalanche Deposits.

Technique	Material Dated	Time Range of Applicability	Relationship of dated material to failure event	Used in this study
Radiocarbon Dating (^{14}C)	Organic material e.g. shell carbonate, bone, plant matter	200 – 35,000 years B.P.[†]	Direct. Vegetation buried by deposit located at basal contact.[F]	Yes
Radiocarbon Dating - Accelerator mass spectrometer (AMS)	Organic material i.e. shell carbonate, bone, plant matter	0 – 50,000 years B.P.	Direct. Vegetation buried by deposit located at basal contact	Yes
Lichenometry	Lichen species	250 – 1000 years B.P.[‡]	Direct. Lichen growing on *stabilized* exposed bedrock including bedrock clasts or boulders on avalanche deposit surface.	No
Dendrochronology	Wood	10,000 years B.P.[†]	Direct. There are various relationships from tilting of trees due to physical disturbance and termination of tree growth (death of tree) from burial of debris.[†]	No
Weathering Rind	Boulders	130 – 8,000 years B.P.[†]	Direct Boulders displaced by failure now exposed at the surface with initiation of weathering.	No
Optically Stimulated Luminescence (OSL)	Quartz silts (including loess)	0 – 300,000 years B.P.[†]	Indirect. Sediment sampled in accumulated loess overlying rock avalanche deposit. Relative. Sample sediment on geomorphic surfaces underlying the rock avalanche deposit.[†]	Yes
Cosmogenic Radionuclide (^{10}Be, ^{26}Al)	Quartz grains and quartz veins	10 – 20 ka to 3 – 4 Ma	Direct Sample bare bedrock at the headscarp, which was exposed directly after the rock avalanche material detached from the rock mass.	No

Table 4.1 Continued: References and Comments for the summary of dating techniques.

References	Comments
†HOGG, 1982	
‡MCFADGEN, 1982; SMITH, 2003	It is critical to find organic samples directly relevant to the rock avalanche event. Finding material at the basal layer is paramount. The time lapse between the death of samples and rock avalanche events and contamination of organics after deposition are sources for error.
†BURBANK and ANDERSON, 2001	Due to the technique measuring the isotopic weight and not the rate of decay, smaller and older samples can be accurately dated.
‡BULL, 2000	Age range applicable to New Zealand. However, age ranges vary due to growth rate curves and biological and physical effects on lichen growth. Range of applicability can extend beyond 9,000 years (LOCKE *et al.*, 1979).
†BURBANK and ANDERSON, 2001	This is dependent upon the existence of a local master chronology record.
†WHITEHOUSE, pers. comm., 1979 in CHINN, 1981	
†CHINN, 1981	Weathering rinds in New Zealand develop over a very short length of time compared to countries such as America where their weathering rinds can be measured up to 200,000 years B.P. (BURBANK and ANDERSON, 2001).
†JACOBY, 2000	
†AITKEN, 1998	
†LANG *et al.*, 1999	

4.2.2.2 Lichenometry

Lichenometry is a biological dating method based on the measurement of lichen sizes to determine age estimations for rock surfaces (NOLLER *et al.*, 2000). Practical benefits in using lichenometry include the relatively low expense to undertake a survey, and due to the broad environmental tolerance of lichens, lichenometry is globally applicable provided a 'local' growth curve has been established.

The fundamental assumption of lichenometry is that the size of the largest individual lichen (or thalli) on a rock surface is a function of the age of the substrate. NOLLER *et al.* (2000) explain that more specifically, the largest individual thalli on a surface reflect early colonisation and an optimal microenvironment that allows age assignment to be both possible and accurate. Lichens grow on rock substrates at relatively uniform rates, which is another advantage for using them for dating. The lichen most commonly used in such surveys is *rhizocarpon* or other species from the subgenus (BURBANK and ANDERSON, 2001). In numerous studies (e.g. BULL *et al.*, 1994; BULL and BRANDON, 1998; BULL, 2000) lichenometry has been applied to New Zealand situations, particularly in the Southern Alps of the South Island. Refer to BURBANK and ANDERSON (2001) and LOWE and WALKER (1997) for further discussion on lichenometry dating techniques and applications.

4.2.2.3 Dendrochronology

Tree ring analysis is believed to be the most precise and accurate method for dating landslides due to the capability of using calendar years to back date when the event occurred (LANG *et al.*, 1999). Dendrochronology dating is based on variations in annual growth of tree rings (JACOBY, 2000). Tree ring development responds to climatic variations and by cross-dating tree-rings between trees within an area, a comprehensive chronology of the climate can be established. Physical disturbance such as seismic shaking and ground failure are known causes for tree ring disturbance and therefore allow the dating of these events to an actual calendar year (providing a chronology has been established for that area). Indicators for direct disturbance to tree ring development due to rock avalanches include rock avalanche debris transecting a forested area, which physically damages trees and/or roots, burial, and scarring of trees by avalanche debris. Emplacement of rock avalanche deposits is related to age of trees growing on its surface. Indirect effects to tree ring growth from rock avalanche events include trees inundated from flooded areas in upstream sections of dammed rivers, and tilting from ground disturbance (JACOBY, 2000).

4.2.2.4 Weathering Rind

Weathering rind dating was initially applied to dating subsurface basalt and andesite boulders in America by PORTER (1969, 1975) and COLMAN (1977). The method is based upon measuring the weathering rind thicknesses of ~50 boulders on a surface to be dated (CHINN, 1981). The development of the rind thickness is time dependent and the length of time the clast has been exposed at the surface is calculated from age (years) = 1030 $R^{1.24}$ where R (mm) represents the modal rind thickness of a representative sample of approximately 50 boulders (CHINN, 1981). There is now a more modern and complex weathering rind calibration available for use of on surface-exposed grey sandstones of the Torlesse Supergroup in New Zealand (Dr. M. MCSAVENEY, IGNS, *pers comm.*, 2004).

Weathering rind dating is a useful tool to date surfaces in the absence of other dating techniques, as difficulties in dating Quaternary surfaces can arise such as lack of organic material for radiocarbon dating (Section 4.3.3).

4.2.2.5 Luminescence Dating (Optically Stimulated Luminescence)

Luminescence dating was developed in the late 1960's primarily to date sediments (ATIKEN, 1994). Two types of luminescence dating exist: a) thermoluminescence (TL) which is concerned with dating heating events, and b) optically stimulated luminescence (OSL) which is used to date sediments. This discussion, focuses on OSL dating due to its ability to date rock avalanche deposits.

The theory behind luminescence dating is somewhat complicated and a detailed description of sample testing is not necessary for this project, however the basic theory is outlined. OSL dating is based on the principle that minerals, particularly quartz and feldspar, contain impurities and structural defects (LIAN and SHANE, 2000). Some of these defects act as traps or dosimeters for free electrons which include alpha, beta, gamma and cosmic rays (MURRAY-WALLACE *et al.*, 2002). The aim of luminescence dating methods is to determine the timing of events, which have reset the stored luminescence signal in defects within minerals. Resetting events include: a) crystallisation events, b) heating the sample to 400°C or above (for thermoluminescence), c) exposing the sample to sunlight (OSL). After burial, the sample is exposed to natural radiation from the environment that creates free electrons which are subsequently trapped within the defects in minerals (MURRAY-WALLACE *et al*, 2002). The rate at which the electron traps are filled by electrons is proportional to the rate that free electrons are produced, which is in turn proportional to the environmental dose rate. The dose rate is from the decay of radioactive elements both within the minerals and in the surrounding sediment (LIAN and SHANE, 2000). Once excavated, if the sample is protected from light and analysed, the time elapsed since the sediment was exposed to sunlight can be determined.

The process in obtaining luminescence dates relies completely on a resetting event to occur to the sediment before subsequent burial. For OSL dating, exposure to sunlight for a few seconds empties electrons from traps within the mineral defects. Loess and dune sands have been found to be particularly good for OSL dating due to their wind-transported nature, with the grains spending considerable time in transit (PRESCOTT and ROBERTSON, 1997). When samples are excavated, if the minerals are optically stimulated, an associated emission of light is defined as an optically stimulated luminescence (OSL). The procedure to obtain the luminescence emission

is somewhat complicated and varied throughout the luminescence community and to discuss the various methods used is outside of this projects' scope. However, as OSL dating was employed for the dating of a sandy "loess" sample from below the LCRAD, the procedure undertaken at the Victoria University Luminescence Laboratory is presented in Appendix H2.

4.2.2.6 Cosmogenic Radionuclide Dating (CRN)

Cosmogenic Radionuclide Dating (CRN) allows dating of bare bedrock surfaces and alluvial deposits, which have been continuously exposed to cosmic radiation (BURBANK and ANDERSON, 2001). This has the important implication it is now possible to date the exposure to the atmosphere of bedrock head scarps, and rock avalanche debris (figure 4.1). The *simplified* theory behind CRN is that cosmic rays isotropically bombard the solar system, coming into the Earth's atmosphere from every angle (BURBANK and ANDERSON, 2001). The incoming particles have a charge associated with them and therefore are "steered" by the Earth's magnetic field. Because of this, a funnelling effect concentrates particles at high geomagnetic latitudes (BURBANK and ANDERSON, 2001). Interaction of the particles with atmospheric atoms creates species such as ^{14}C. These interactions reduce the number of energetic particles that reach lower altitudes (creating an atmospheric attenuation). The particles that reach bedrock interact with mineral atoms, which are susceptible to nuclear reactions, thus generating CRNs within the top few tens of centimetres of the surface (BURBANK and ANDERSON, 2001). Quartz is one such mineral which reacts with the energetic particles to produce ^{10}Be and ^{26}Al that would not otherwise occur during development.

Sample preparation is crucial and is a lengthy process. The costs of obtaining CRN dates are also high. However, application of CRN to date exposed rock avalanche head scarps within the Southern Alps is viable due to the common occurrence of quartz veins and mineral grains within the sandstone component. Detailed reviews of CRN can be found in LAL (1991), MORRIS (1991), BIERMAN (1994), CERLING and CRAIG (1994), and BURBANK and ANDERSON (2001).

4.2.3 Direct, Indirect and Relative Dating

The importance of obtaining temporal distributions of rock avalanche events has been an essential element in determining triggering mechanisms, and for geomorphic

reconstructions. For this project, dating the three Lake Coleridge rock avalanches has been paramount. In obtaining dates for rock avalanches by various dating methods a clear understanding of what the date actually represents is vital. A brief discussion follows regarding direct, indirect and relative dating in relation to determining the age of rock avalanche deposits and landslide deposits. Further discussion can be found in LANG *et al.* (1999).

Depending on the relationship between the rock avalanche event and the material dated, direct, indirect and relative dates can be obtained. The dating methods discussed above in Section 4.2.2 do not all necessarily allow dating of the actual rock avalanche event, but of the processes that are related to the event. Dating methods are necessary for prehistoric rock avalanche events, as there is no other way of establishing the absolute timing of the events.

4.2.3.1 Types of Dates

Direct dating refers to dating processes which are directly related to the mass movement event (LANG *et al.*, 1999). Typical examples of direct dating include dendrochronology where disturbance to ring growth patterns is a direct result of the landslide (providing this can be proved to be the case). Lichenometry and cosmogenic dating can also be used to directly date the mass movement as their response is directly related to the rock avalanche event (LANG *et al.*, 1999). **Indirect dating** is referred to when the date obtained provides a minimum or maximum age for the mass movement. This is sometimes referred to as **relative dating**. The latter two can be distinguished by the precision of the method. LANG *et al.* (1999) explain that if the failure event probably occurred within the error margin of the date it is said to be an indirect date, but if not the date is relative. For example, by OSL dating of the sediments in a terrace that has been overridden by landslide debris a relative age is achieved. Thus, if sediments directly overlying or underlying the landslide debris are OSL dated, an indirect age is obtained.

The type of dating (direct, indirect or relative) and the purpose of dating should be carefully considered before any dating techniques are used on landslide deposits. Due to its nature, direct dating is the obvious choice to use when dating a deposit, but this is not always possible due to the nature of the site or the purpose for dating. In some situations, it is only possible to determine a relative date, which is obviously better

than obtaining no date for the event. Another important issue to consider is the dated object's stratigraphic position with respect to the landslide (figure 4.1); (LANG *et al.*, 1999). SCHOENEICH (1991) identified three different types of sampling locations as: a) above, b) below and c) mixed within the landslide debris. The position of the dated sample determines what type of date is obtained (see figure 4.1) and in turn defines the error range for the dated deposit.

4.2.4 Dating Techniques used in this Project

A number of factors contributed to the choice of dating techniques utilised in this project. Initial site investigations highlighted the lack of woody vegetation in the immediate vicinity, eliminating dendrochronology as a possible dating method. Agricultural practices including cultivation and ploughing combined with a general lack of surface clasts proved unfavourable for both lichenometry and weathering rind surveys, although a weathering rind survey by WHITEHOUSE (1981) was conducted at the site on the most recent rock avalanche deposit. Cosmogenic radionuclide dating was not utilized due to significant costs to date samples, the long time needed to 'date' the samples being impractical for a Masters thesis (Professor J. SCHULMEISTER, University of Canterbury, *pers. comm.*, 2004). Due to this thesis being a non-funded project cost restrictions had to be kept in consideration also.

As Table 4.1 illustrated, three techniques were utilized to date the LCRAD. Initially a ^{14}C radiocarbon date on an organic sample gave a date for the LCRA2 deposit. Material suitable for ^{14}C radiocarbon dating was scarce, and after considerable investigation an optically stimulated luminescence (OSL) sample was taken for the LCRA1 deposit during excavation of a trench across the basal contact of the rock avalanche deposit with underlying loess and glacial till. Finally, accelerator mass spectrometric (AMS) and ^{14}C dating was used on two charcoal samples located in a graben structure on Carriage Drive Fault. AMS was used due to the smallness of sample provided, and it was believed that ^{14}C radiocarbon dating would yield an unsatisfactory high standard error of ~ ± 200 years at 5,000 years whereas AMS dating could reduce the standard error to ± 60 years at 5,000 years B.P. (Dr F. PETCHEY, University of Waikato, *written comm.*, 2004).

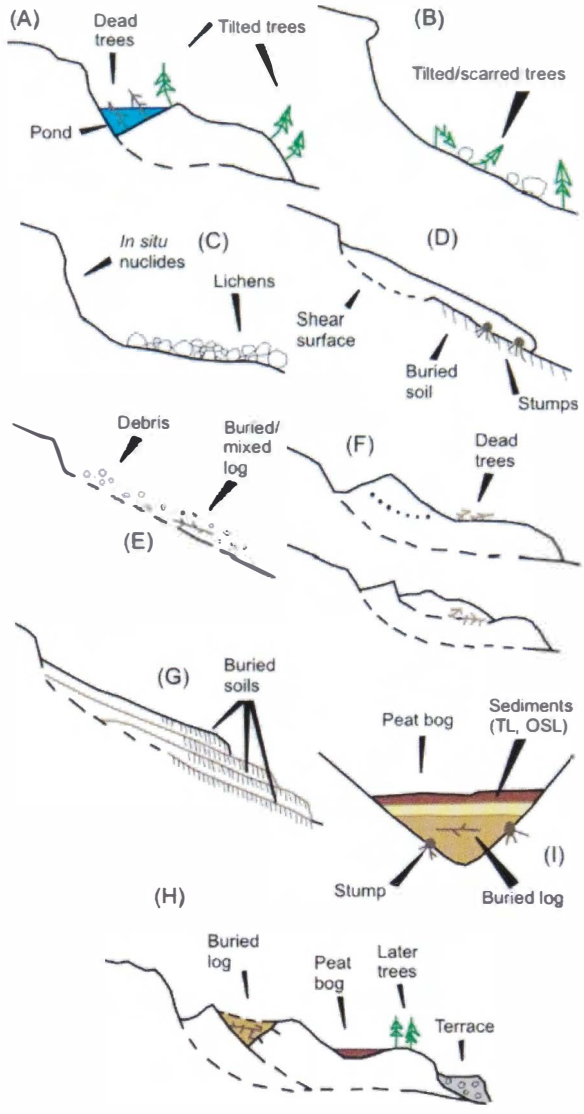

Figure	Description
	Direct dating
A	Tilting of trees (dendrochronology) allow dating of movement with an accuracy of one calendar year.
B	Tilting, destruction and disturbance of trees allow dendrochronology dating.
C	Exposed rock surfaces (i.e. scarps) can be dated by cosmogenic nuclides or lichenometry.
D	Trees buried *in situ* by debris allow radiocarbon dating and dendrochronology (if chronology has been established within the region).
E	Organic matter incorporated into debris during failure.
F - G	Organic material within superimposed deposits can be radiocarbon dated. Soil developments between deposits may be dated providing a maximum age for the overlying debris.
	Indirect dating
H	Water ponding and accumulation of organic sediments allow ^{14}C and AMS radiocarbon dating. Dating lichens, trees and sediments (OSL) that have established on the surface of the deposit will also give minimum age.
	Relative dating
I	Development of lakes and lake sediments behind natural dams can be dated by OSL and radiocarbon techniques. *In situ* vegetation becomes buried and can be radiocarbon dated.

Figure 4.1: Location of dateable sampling locations relative to rock avalanche and landslide deposits with the type of dating obtainable (i.e. direct, indirect or relative). Modified from LANG *et al.* (1999).

4.3 Age of Lake Coleridge Rock Avalanche 1 Deposit

4.3.1 Approach to Dating

The LCRA1 deposit is the largest of the three, extending out over the valley floor. Clearly defined by morphology, the deposit has buried the topography of the valley floor covering glacial till and a thin loess cover, presumably from the last Acheron Advance (Acheron 3). Dating the LCRA1 event was an essential part of this project and the following methods were used.

The intention was to date organic material within the basal zone of the LCRA1 deposit, which would give a constraining age for the event. This was based on the premise that postglacial soil and vegetation development had occurred. This approach was taken because of the success in SMITH'S (2003) study of the Acheron Rock Avalanche, where four wood samples (*Nothofagus solandri var. cliffortiodes*) were located within the basal contact between pre-failure topography and rock avalanche debris. From the Acheron Rock Avalanche investigations, it is clear that the rock avalanche debris inundated a forested area, thus providing large quantities of organic material, which provided direct dates for the rock avalanche event. Therefore, with the assumption that the LCRA1 deposit buried vegetation on the surface of the glacial till, the same approach was adopted for the LCRAD.

Two trenches were excavated at the perimeter of the deposit (figure 4.2) to locate organic matter (Sections 3.4.4 and 3.4.5). Both trenches were similar in profile, a sequence of basal glacial till with a thin sandy "loess" horizon, rock avalanche debris and a capping loess unit with a thin veneer of topsoil (figure 4.3; figures 3.11 and 3.13). Relevant organic material was sought at the basal contact of the rock avalanche debris and glacial till capping soil. Organic matter found within the basal contact would provide a direct date of rock avalanche emplacement, as the death of plants, such as trees in SMITH'S (2003) study, due to burial by rock avalanche debris would directly relate to the rock avalanche event. Similarly, but not as conclusively, organic matter found *within* the rock avalanche deposit could provide a direct date from plants becoming entrained within the rock avalanche debris, during failure. The origin of organic matter dated within deposits is not always clear and as noted by ORWIN (1998) dead plant matter such as deceased trees can be incorporated and mobilized downslope into rock avalanche deposits. No organic matter was located within either trench. Therefore, no direct date for the LCRA1 event was obtained, and alternative methods were needed.

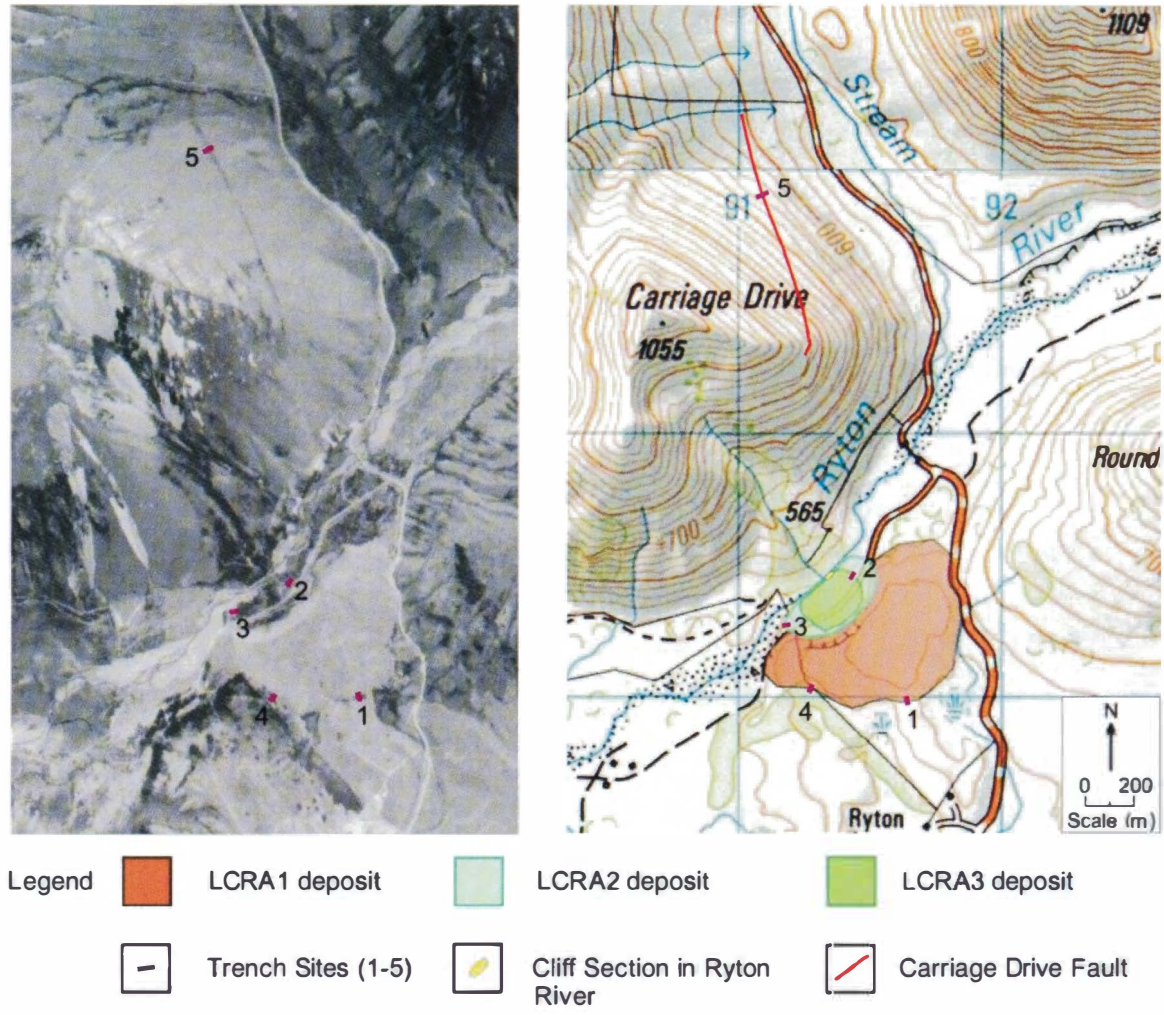

Figure 4.2: Aerial photograph of immediate LCRAD area and corresponding topographic map (NZMS K35, 1:50,000 [260]) of trench sites and cliff section (refer to text).

4.3.2 Optically Stimulated Luminescence (OSL) Dating

During excavation of T_1 and T_4 (located at the edge of the LCRA1 deposit; Sections 3.4.4 and 3.4.5), glacial till was identified on the pre-rock avalanche surface. Directly overlaying the glacial till is a shallow (~150 mm) sandy "loess" horizon, (figure 4.3). The LCRA1 debris directly overlays this horizon, therefore has its basal contact with the sandy "loess" capping glacial till. OSL dating was undertaken on the sandy "loess" horizon because fine-grained aeolian transported sediment is favourable for OSL dating due to complete exposure to sunlight during transportation (Section 4.2.2.5). The sandy "loess" horizon is very thin (~150 mm) and therefore, burial by further sedimentation is unrealistic and the possibility that the date provided from the OSL technique actually dated a transportation episode where the grains were in transit is considered unlikely.

The OSL date was interpreted to represent the earliest time the LCRA1 could have occurred. This interpretation was based on the assumption that sandy "loess" horizon was last exposed to sunlight shortly before the rapid emplacement of LCRA1.

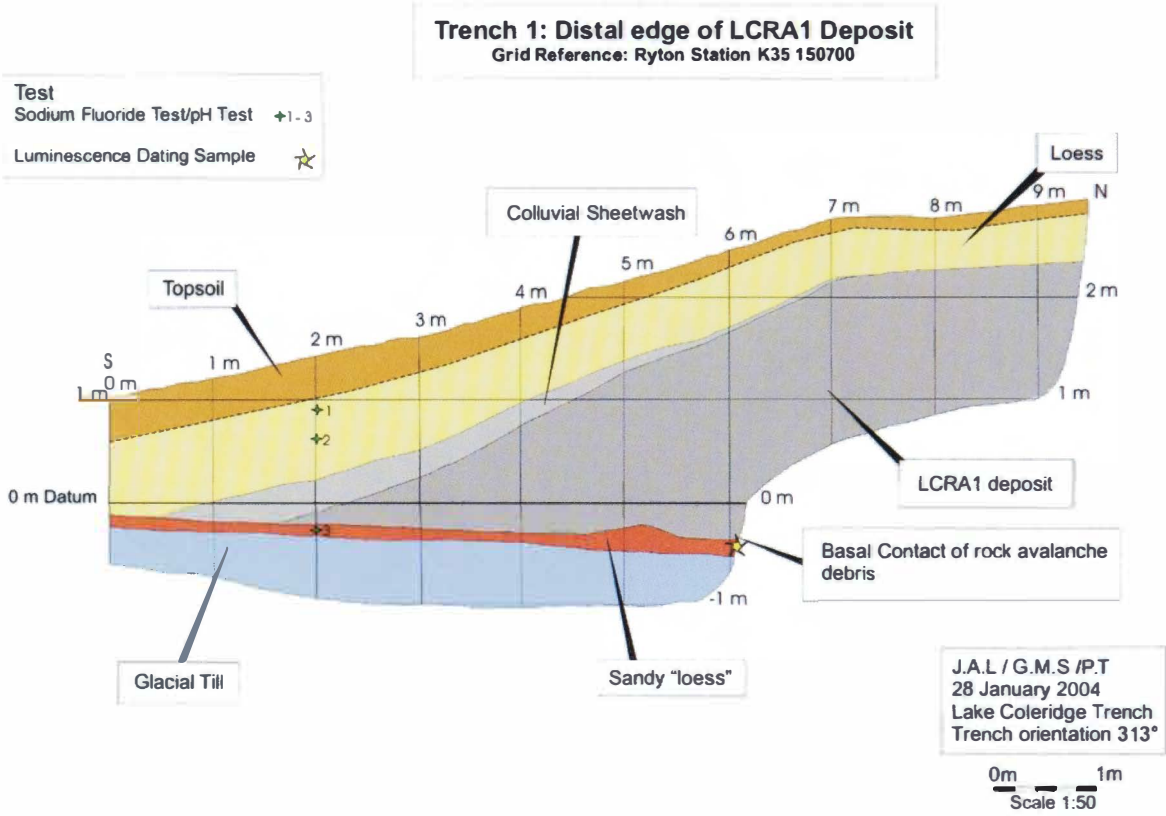

Figure 4.3: Schematic representation of T_1 log. The test locations (Sodium Fluoride Tests and Luminescence Dating Sample) are shown (refer to text for explanation).

4.3.2.1 Methodology of Sampling and Age

Two OSL samples were taken from T_1 and T_4 before they were infilled (Sections 3.4.4 and 3.4.5). The appropriate sampling methodology was followed, with a 45 mm diameter tube hammered into the trench face to collect the sample (figure 4.4). The full length of the sampling tube was driven into the trench face and the surrounding sediment extracted to reveal the tube. The tube containing the sediment sample was then extracted with both ends of the sample tube being immediately covered to prevent luminescence resetting within the electron traps in the minerals of the sample. After extraction, the tubes were wrapped in foil and sealed to prevent sunlight resetting the grains. Sampling in both trenches was undertaken in the

middle of the thin (~150 mm) sandy "loess" palaeosol[3] horizon which, as discussed above, is stratigraphically located between the glacial till and overlying rock avalanche deposit

Figure 4.4: Luminescence sampling in trench face (T_4). Sample tube has been hammered into soft sandy "loess", and is about to be extracted, with the sampled soil coming away within the tube.

Due to the cost of OSL dating, only one sample (out of the two) was dated, from T_4 (figure 4.2). This sample was coded "LCRA1 Trench 4" (laboratory code WLL389) and sent to the Luminescence Dating Laboratory at Victoria University of Wellington. The dating and sample preparation report on OSL sample WLL389 is reproduced in Appendix H2. The OSL sample of the sandy "loess" was dated at 9,720 ± 750 years B.P. (Appendix H4). If this was the maximum age of the deposit the OSL date it places the LCRA1 event much earlier than the 120 years of WHITEHOUSE (1981) and the 150 ± 40 years B.P. of WHITEHOUSE (1983) and WHITEHOUSE and GRIFFITHS (1983).

[3] The term 'palaeosol' was initially defined by RUHE (1965) as any soil that has developed on a land surface of the past. They frequently form under different environmental conditions than at the present day.

Three sodium fluoride tests were carried out on the soil profile within T_1 by Dr P. Tonkin, University of Canterbury, 2004 (figures 4.3 and 3.11). These field tests measured the pH of the soil by providing an indication of the increase in alkalinity as the solution displaced hydroxyls (the indicator was phenolphthalein). The rapid change in colour of the samples was consistent with other sites within the high country where ^{14}C have dated the soils at ~9,500 years (Dr P. TONKIN, University of Canterbury, *pers. comm.*, 2004; TONKIN and BASHER, 1990). This provides an indirect date for the LCRA1 deposit to be greater than 5,000 years (Chapter 3, Section 3.3.4).

4.3.3 Quagmire Tarn Evidence

The apparent lack of organic material within the faces of the two trenches that were excavated into the LCRA1 deposit indicates one of three things. Either, the lack of plant matter within the deposit indicates that there was no vegetation on the source area of Carriage Drive or on the valley floor at the localities of the two trench sites, or environmental conditions were unfavourable for preservation of organic matter. Alternatively, in the attempt to locate organic material within the deposit, vegetation absence was coincidental. If the lack of vegetation matter within and underneath the LCRA1 deposit indicates an unvegetated environment at the time of emplacement of the rock avalanche debris this would give weight to the OSL date for the failure event that placed its maximum age at ~9,750 years B.P.

It can be suggested that the actual *lack* of organic matter found within the deposit indicates that debris emplacement occurred shortly after the last Acheron glacial ice retreat. A widely acknowledged process following glacial ice recession is of gradual re-colonisation with small grasses and herbs leading to woodier larger plant varieties (e.g. BURROWS and RUSSELL, 1990; TURNEY *et al.*, 2003). An appropriate example of this occurring comes from the Quagmire Tarn, from a pollen core analysis (BURROWS and RUSSELL, 1990), (figure 4.5) in the upper Rakaia Valley, which is located ~ 30 km from Lake Coleridge at grid reference J35: 780 300.

Pollen analysis was not conducted during this study, due to possible contamination of the samples during collection and the lack of resolution required for this study (Mrs J. GUISE, University of Canterbury, *pers. comm.*, 2004).

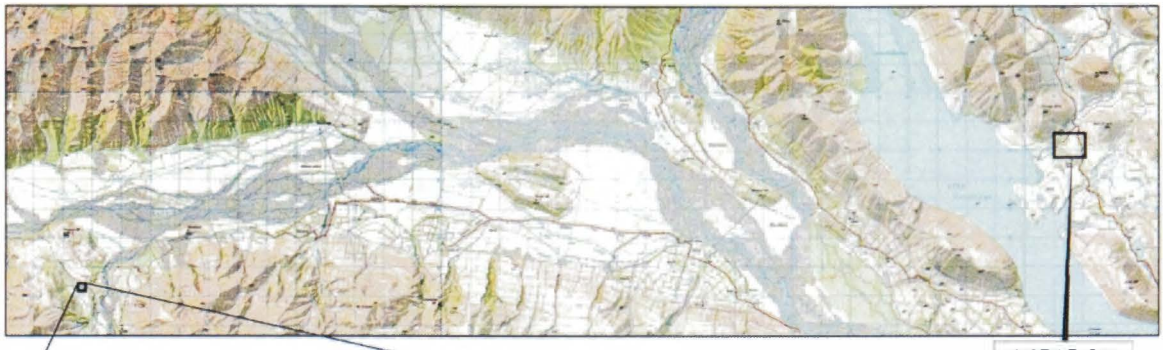

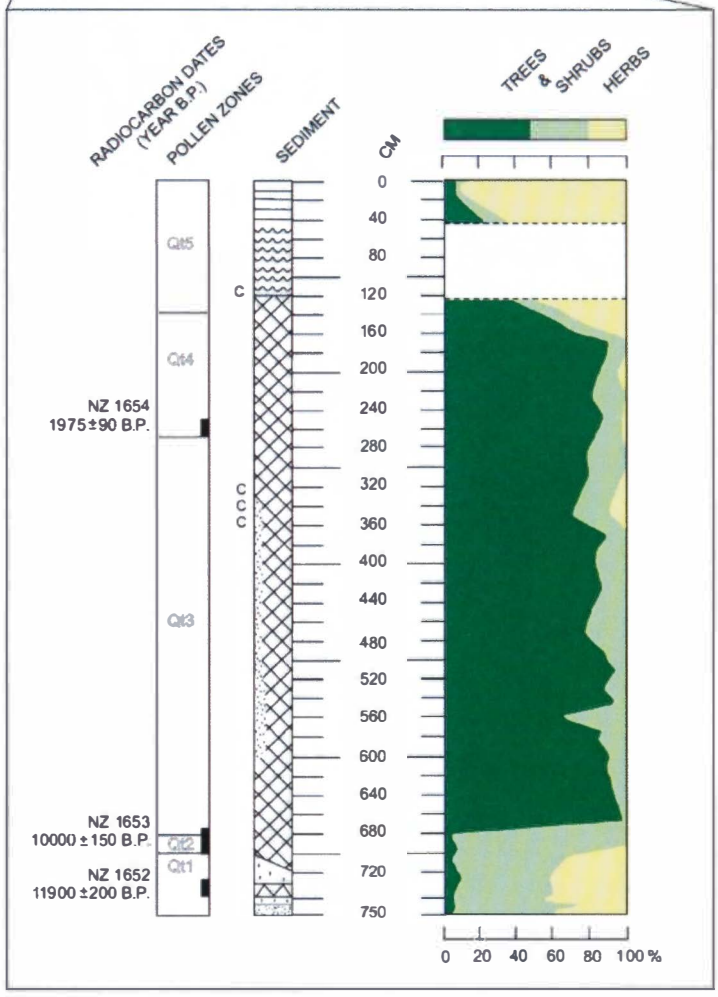

Pollen Zonation Summary

Zone Q.T.5: Due to water replacing sediment in the sampled core a break in pollen information is observed. From sediments overlying the water pollen from species: Poaceae, Cyperaceae, Asteraceae and Apiaceae were identified. To a much lesser extent tree pollen was also found. Interpretation of this period pinpoints **human influences from forest fires to expansions of grasslands** with herbaceous species.

Zone Q.T.4: Abundance of *Nothofagus menziesii* pollen. There is a steady increase in *Nothofagus fusca*-type while *Phyllocladus* and "*Podocarpus*" continue to be important. The interpretation indicates that during this period there was a continuous or near-continuous mountain beech forest on both sides of the Rakaia valley downstream of the Lake Stream Confluence and also in the Mathias River. Interpreted decline in *Libocedrus* and *Halocarpus* being possibly due to a **decrease in precipitation.**

Zone Q.T.3: A lengthy period from **9,500 to 2,000 years B.P.** with *Phyllocladus alpinus* dominating and a strong prescence of "*Podocarpus*". During this period, pollen of trees and tall shrubs are predominant however, *Coprosma* species and Poaceae were still significant. This period was interpreted to represent a **milder and wetter climate than today** by the evidence of abundant *Phyllocladus alpinus* which requires more than 125 cm per annum to regenerate effectively.

Zone Q.T.2: A brief period of *Halocarpus*-type pollen dominated which indicates a **cool climate** (WARDLE and CAMPBELL, 1976). This period was dated at approximately **10,000 years B.P.**, which was suggested to coincide with the Jagged Stream-Reischek Drift glacial events that ended before 9,500 years B.P.

Zone Q.T.1: Dominant *Coprosma*-Poaceae and abundance of Asteraceae, Cyperaceae and monolete fern spores indicate a **period of gradual warming** post Otiran glaciation apporximately **14,000 years B.P.**

Figure 4.5: Summarised pollen diagram for the Quagmire Tarn site in the Upper Rakaia Valley highlighting the change from grass and herb lands through to shrubs and trees after the retreat of glacial ice within the valley. Note the sudden change from shrubs and herbs just after 10,000 ± 150 years (between Zones Q.T.2 and 3). Modified from BURROWS and RUSSELL (1990).

4.3.4 Age Interpretation

The *interpretation* of the OSL age of a glacial till capping loess from within T_4 of (WLL389) 9,720 ± 750 years B.P. is essential for understanding when the LCRA1 event occurred. Importantly the age does not directly date the avalanche event, however it does provide an indirect maximum age constraint on when the rock avalanche occurred. Further evidence of the LCRA1 event occurring post-ice retreat, around 9,720 ± 750 years B.P., is derived from the lack of organic material within the basal layer of the rock avalanche debris and within the debris. Pollen core analysis from BURROWS and RUSSELL (1990) at Quagmire Tarn (figure 4.5) indicate that there was a significant shift from herbs and shrubs to trees just after 10,000 years B.P.

The OSL date is based on the assumption that the dated loess was "reset" by sunlight prior to burial by the LCRA1 deposit, thus essentially dating when the rock avalanche occurred. This date suggests that shortly after the withdrawal of Acheron 3 glacial ice (Acheron 3 Advance is dated 11,650 ± 200 years B.P. by BURROWS (1975) and this study indicates that the valley was ice-free at 9,720 ± 750 years B.P.) a significant portion of Carriage Drive failed catastrophically in the LCRA1 event. Such events following deglaciation have been widely documented, such as AUGUSTINUS (1995b) who concluded that glacially steepened rock slopes often fail during or very soon after ice downwastage. In paraglacial environments such as the Lake Coleridge area, debuttressing of oversteepened glaciated valley slopes, combined with high cleft-water pressures and favourably orientated defects/bedding may be all that is required to initiate a rock avalanche.

The lack of matagouri growth on the LCRA1 deposit provides a relative indication for the age of the deposit. Matagouri is a pioneering shrubby species and is commonly located around areas of instability where fresh bedrock is exposed to yield relatively high levels of phosphorus. The ~600 mm covering of loess on the LCRA1 deposit represents a more degraded environment where the competitive advantage for matagouri rapidly decreases with soil fertility (Dr P. TONKIN, University of Canterbury, *pers. comm.*, 2004). This is perhaps less of an indication for the age of the first rock avalanche than the last two, due to their dense coverage of matagouri.

4.3.5 Triggering Mechanisms

One of the aims of this project was to determine (if possible) the triggering mechanisms for all three-rock avalanche events. Many rock avalanches around the world have been triggered by earthquakes. Therefore, major fault systems within the region were analysed to assess whether a correlation between known fault rupture dates and dated rock avalanche deposits could be found (Sections 2.5 and 2.6). In addition to this, a trench (T_5, figure 4.2) (figure 4.6) was excavated perpendicularly across the Carriage Drive fault-trace (figure 4.2 and further discussion on this can be found in Section 2.5.6 and Appendix E).

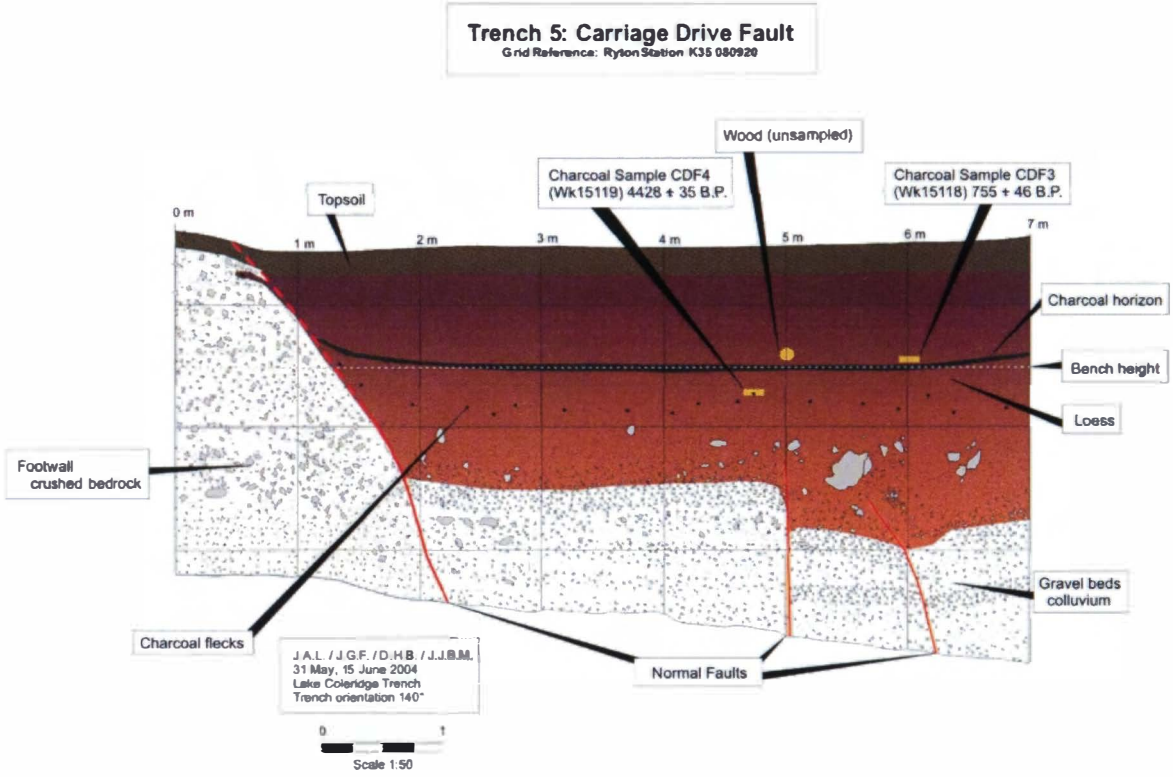

Figure 4.6: T_5 log across Carriage Drive Fault. Graben structure infilled with charcoal and loess. Prominent gravel is located at the base of the trench. Two radiocarbon dates were analysed by Professor A. HOGG, University of Waikato, 2003.

Organic material in the form of charcoal was present within the trench face. A small piece of wood was also located, however the relationship between fault rupture(s) and the sample was not clear. Two discrete charcoal samples were found (labelled CDF3 and CDF4) within horizons that were visibly offset by normal faulting (figure 4.6), and were sent to the Radiocarbon Dating Laboratory at Waikato

University. CDF3 was dated at (Wk15118) 755 ± 46 years B.P. (Appendix H2) while CDF4 was dated at (Wk15119) 4,428 ± 35 years B.P. (Appendix H3).

If a datable interrupted horizon within the trench face correlated with the OSL date obtained from fine sediments below the LCRA1 deposit, a correlation could be established between tectonic movement on the Carriage Drive Fault and initiation of the rock avalanche. The two dated samples should "bracket" the last movement on the Carriage Drive Fault. However, there is no evidence to "fix" the age of rupture along the fault. The two dates (Wk15118 and Wk15119) do not correlate with the OSL date providing a maximum age for the LCRA1 event of (WLL389) 9,720 ± 750 years B.P.

No evidence could be found to establish when initial movement along the Carriage Drive Fault occurred. However the scarp is obviously a post-glacial feature, placing its surface signature development after ice retreat. The OSL date indicates that the Lake Coleridge area was "ice-free" by (WLL389) 9,720 ± 750 years B.P. (this study) to allow sediment deposition directly overlying glacial till. BURROWS (1979) dated Acheron 3 moraine approximately (WNZ1290) 11,650 ± 200 years B.P. However, this date is somewhat questionable, as BURROWS and RUSSELL (1975) have dated the Lake Stream Advance at this time. Minimum temporal constraint on initial failure from this study shows that a scarp had already developed by 4,428 ± 35 years B.P. However, this only constrains the initial rupture date to between (WLL389) 9,720 ± 750 years B.P. and 4,428 ± 35 years B.P. which leaves a significant period of approximately 5,300 years in which little information can be obtained. Therefore, a rupture along the Carriage Drive Fault may have triggered the LCRA1 event however, this study found no evidence to support or contradict this. Similarly, ruptures along any number of faults within the area such as the PPAFZ or the Alpine Fault may have triggered the rock avalanche event.

4.4 Age of Lake Coleridge Rock Avalanche 2 Deposit

4.4.1 Approach to Dating

The LCRA2 deposit is the second rock avalanche of the three, with a much smaller extent than the first. The deposit is confined to the low topography of the eroded Ryton River section of the LCRA1 deposit, with a small run-up (or brandung) feature

partially climbing up the cliffs of the LCRA1 deposit (figure 4.7). The LCRA2 deposit is densely covered with matagouri. The surface of the deposit is undulating. Dating the LCRA2 event was an important part of this project.

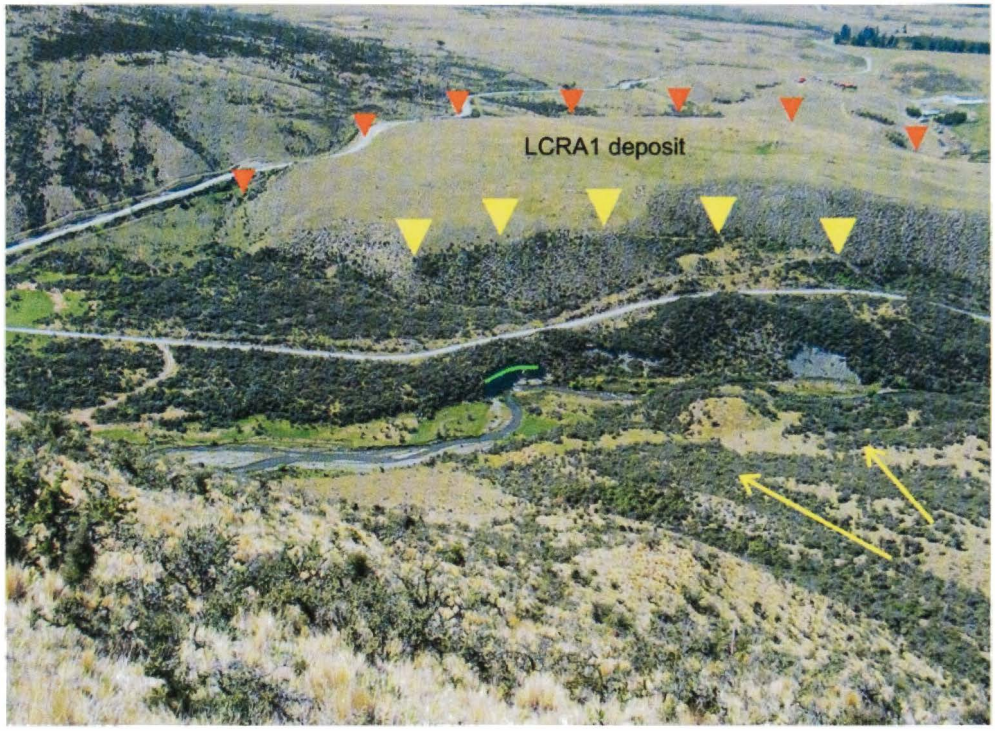

Figure 4.7: Brandung feature of the LCRA2 deposit (outlined by yellow arrowheads). The Second Rock Avalanche Deposit partially flowed up the side of the LCRA1 deposit. Yellow arrows indicate flow paths from source area on Carriage Drive. Orange arrowheads mark the limits of the LCRA1 deposit. Green line within small cliffs adjacent to riverbed indicates the only visible contact between the LCRA2 and LCRA3 deposits. Photograph taken looking south-southeast.

The hypothesis was again to date organic material immediately underlying the LCRA2 deposit, which would give a constraining age of the event. One trench (T_3, figure 4.2) was excavated at the edge of the deposit, and cut into both the side of the rock avalanche deposit and the dam-break "outwash" terrace associated with the second rock avalanche (Section 3.8.4). No organic matter was found within the trench face. Interestingly, the basal contact for the LCRA2 deposit was not located during this study. Rounded clasts however, incorporated into rock avalanche debris towards the lower portion of the outcrop exposure adjacent to the Ryton River were thought to indicate a mixing zone towards the bottom of the deposit (Section 3.5.3).

Investigation of the small cliff (see figures 4.2 and 4.8) along the Ryton River that cuts through the LCRA2 and LCRA3 deposits located organic matter. Prior to this

study, this cliff section was ambiguously believed to represent the contact between LCRA1 and LCRA2 (labelled in this study), with the third rock avalanche unidentified. Through dating the deposit, a third (and much smaller) rock avalanche event was identified. Four organic lenses were identified within the LCRA2 deposit;

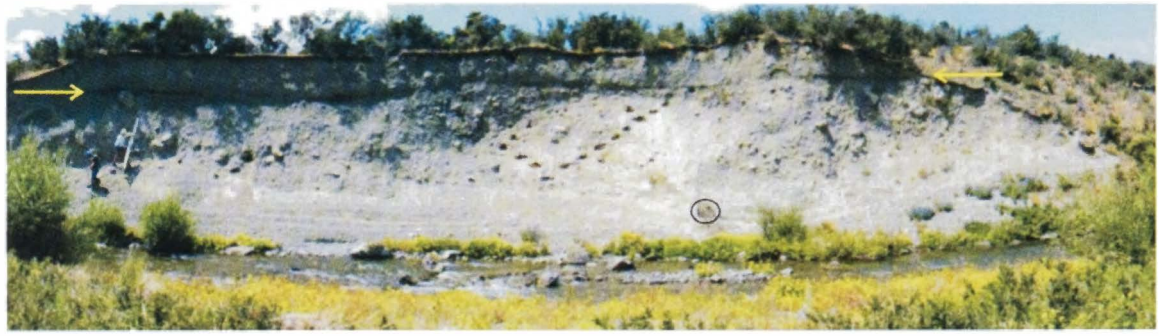

Figure 4.8: Exposure of rock avalanche debris within Ryton River cliff section (figure 4.2 and 4.7 for site location). Contact between LCRA2 and LCRA3 is located near the top of cliff and is highlighted by the two yellow arrows. Wood sample location indicated by black circle. Note people on far left for scale. Ryton River flows from left to right.

however, these were not tested as a ~400 mm piece of wood (figure 4.9) was found embedded within the deposit. This was later identified as a piece of *Leptospermum scoparium* (mānuka) by using an electron microscope at the University of Canterbury (Professor B. BUTTERFIELD, University of Canterbury, *pers. comm.*, 2004).

Figure 4.9: Mānuka sample found in LCRA2 debris within a cliff face eroded by the Ryton River. Refer to figure 4.8 for location. Geological hammer for scale.

4.4.2 Radiocarbon Dating (^{14}C)

The mānuka sample found *within* the LCRA2 deposit was interpreted to represent a direct date of the rock avalanche event due to the absence of a basal contact (as discussed above). It is inferred that a mānuka tree was incorporated into the debris as it travelled downslope and therefore died as a direct result of the activation and emplacement of the LCRA2 event.

4.4.2.1 Methodology of Sampling and Age

The mānuka sample from the cliff-face was removed is such a way as to prevent contamination of the sample. Clean stainless steel tools were used to prise the wood out of the compacted rock avalanche sediments, and the sample was immediately wrapped in plastic. The sample was then dried in a 40°C oven to remove any residual water. A small piece of the sample was sawn off for identification by electron microscopy, and another piece of approximately 70 mm in length was cut and sent to the Radiocarbon Dating Laboratory at the University of Waikato. The mānuka sample (reference Wk14221) was dated at 668 ± 36 years B.P. (figure 4.10 and Appendix H1).

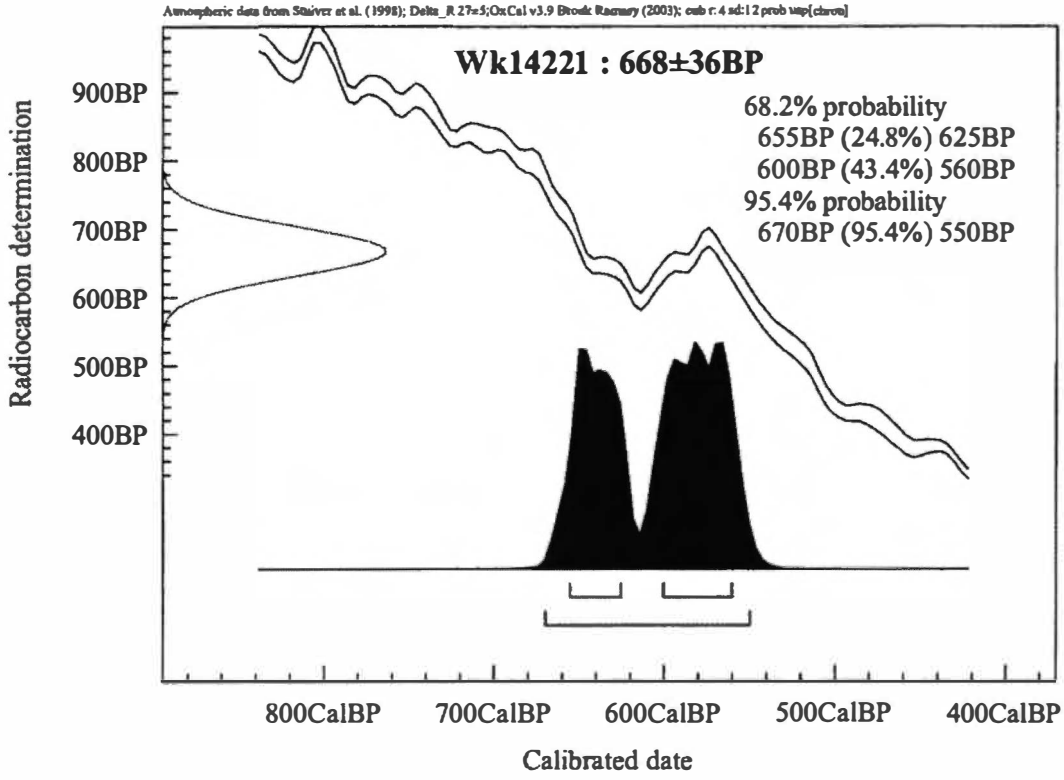

Figure 4.10: Radiocarbon sample Wk14221 obtained from a mānuka sample located within the LCRA2 debris. Sample dated at 668 ± 36 years B.P (Appendix H1). Sample analysed by Professor A. HOGG, University of Waikato, 2004.

4.4.3 Age Interpretation

The interpretation of the radiocarbon age is that it directly dates the LCRA2 event at (Wk14221) 668 ± 36 years B.P.

4.4.4 Triggering Mechanisms

A triggering mechanism was sought for the LCRA2 event. Comprehensive paleoseismic studies of landslides (e.g. COWAN *et al.*, 1996), rock avalanche deposits (e.g. WHITEHOUSE and GRIFFITHS, 1983; BURROWS, 1975; BULL and BRANDON, 1998; SMITH, 2003) and fault scarps (e.g. HOWARD, 2001) within the region have enabled a regional seismicity history to be formulated (SMITH, 2003). COWAN *et al.* (1996) and HOWARD (2001) found indications that the western end of the PPAFZ ruptured between 700-500 years B.P. There is also known activity along the Alpine Fault during this period also.

During subsurface investigations T_5 (figure 4.2) was excavated across the Carriage Drive Fault (Section 4.3.5). Within the trench, two charcoal horizons, dissected by normal fault rupture, were radiocarbon dated and as discussed earlier the ages for these samples were (Wk15118) 755 ± 46 years B.P. and (Wk15119) 4,428 ± 35 years B.P. The AMS charcoal horizon dated at (Wk15118) 755 ± 46 years B.P. suggests that the last seismic event along Carriage Drive Fault may have triggered the LCRA2 event during the period of high seismicity within the region.

4.5 Age of Lake Coleridge Rock Avalanche 3 Deposit

4.5.1 Approach to Dating

The LCRA3 deposit is the third and final rock avalanche. It is a very small deposit, which is poorly geomorphologicaly constrained, and as discussed above, was only identified by dating the LCRA2 deposit. The only exposure of the deposit is within the cliff section adjacent to the Ryton River (discussed above and illustrated in figure 4.8). Similar ly to the second rock avalanche, the LCRA3 deposit is covered with matagouri and has an undulating surface.

The approach to dating the LCRA3 event differed from that of the first two. Firstly, due to its poorly defined geomorphic outline, initial fieldwork failed to

recognise its existence. After identification however, a trench was excavated into the avalanche deposit (T_2, figure 4.2) in an attempt to locate some organic matter for a radiocarbon date. No organic matter was found.

The exposure of the LCRA3 deposit within the Ryton River cliff (figure 4.8) was investigated. Proper access to the face was difficult due to the location of the deposit at the upper most height of the cliffs, and the substantial coverage of matagouri over the surface. After initial investigations of the thin deposit, concern arose over the amount of present-day vegetation that was growing down into the deposit. If organic material was found *within* the deposit, there was a high possibility of contamination with recent vegetation. Therefore no further investigation to find organic material to radiocarbon date occurred.

OSL dating may have been appropriate for dating the thin palaeosol contact between the LCRA2 and LCRA3 deposits, however budget constraints prevented its use for this study. Therefore, no date was obtained from this study for the LCRA3 event. However conclusions can still be reached as to the interpreted age of third rock avalanche from field evidence, including the stratigraphic location of the deposit.

4.5.2 Evidence for Age Interpretation

The possibility of assigning an accurate and precise age for the LCRA3 event when an absolute dating technique has not been applied is not high. However a maximum relative age range can be assigned to the deposit due to its stratigraphic location. The LCRA3 deposit directly overlies the LCRA2 deposit, which as discussed in the above Section (Section 4.4), has been confidently dated at 668 ± 36 years B.P. Therefore the LCRA3 deposit must be younger than the LCRA2 deposit.

The LCRA3 event was a small rock avalanche. The debris was contained within the low topography of the small valley within the eroded section of the LCRA1 deposit, like the second rock avalanche. However, unlike the LCRA2 event, there are no run-up or brandung features associated with debris flowing up the corresponding valley wall and then slumping back downslope. As discussed in Section 3.6.1, the contact between the LCRA2 and LCRA3 deposits is depositional. Presumably, it represents the height of the Ryton River when the emplacement of the LCRA3 occurred. Along the entirety of the contact and within T_2, no soil horizon was present.

This fact, along with the *relatively* low energy emplacement of the debris, indicates that the LCRA3 event occurred closely after the Second Rock Avalanche and before the Ryton River had deeply incised into the LCRAD 2 debris. The flatness of the contact between the LCRA2 and LCRA3 deposits also suggest it may have been water-eroded before the LCRA3 deposit as emplaced.

4.5.3 Age Interpretation

The suggested age for the LCRA3 deposit inferred to be slightly younger than the LCRA2 deposit, which has an age of 668 ± 36 years B.P.

4.5.3 Triggering Mechanisms

The LCRA3 event is believed to have closely followed the LCRA2 event. The deposit is very small for a rock avalanche, and there is a possibility that disrupted debris, which did not fail and move downslope during the LCRA2 remobilized at a brief period later, which has resulted in the LCRA3 event. If this is the case, a local earthquake such as an aftershock from the main rupture which is thought to have triggered the LCRA2 event may not have been necessary for activation with gravitational pressures creating instability. A rainstorm may also have been responsible for triggering the material, reducing the factor of safety of the slope from increased pore pressure. There is no evidence to suggest what triggered the LCRA3 event. However, if the interpretation of *what* the rock avalanche debris *represents* is correct, a major triggering mechanism may not have been needed to initiate the small failure.

4.6 Summary

- Geomorphology relies heavily on placing timing controls on landscapes. Before the development of absolute dating techniques such as radiocarbon, and optically stimulated luminescence dating, there was no way to date with any accuracy landforms such as rock avalanche deposits.
- Absolute dating techniques discussed in this study include radiocarbon (both ^{14}C and Accelerator Mass Spectrometer), lichenometry, and dendrochronology, weathering rind, OSL and cosmogenic radionuclide dating.
- An important understanding of what the absolute date obtained in dating studies mean is an essential part of interpreting the age of dated landforms.

- The LCRA1 event indirectly dated by an OSL date sampled from sandy "loess" material underlying the rock avalanche deposit it is interpreted to have occurred just after Acheron 3 ice retreat at (WLL389) 9,720 ± 750 years B.P. Evidence from soil analysis within T_1 and from Quagmire Tarn support this hypothesis of post-ice retreat failure.
- The LCRA2 event was directly dated using radiocarbon dating technique on a mānuka sample found within the deposit. This provided an age of (Wk14221) 668 ± 36 years B.P.
- An absolute date was not possible for the LCRA3 event. Lack of organic matter and the possibility of present-day root contamination eliminated the possibility of radiocarbon dating. OSL dating may have been possible on the contact between the LCRA2 LCRA3 deposits, however due to budget constraints was not undertaken.
- Triggering mechanisms for the three rock avalanches situated at the LCRAD site were generally poorly constrained and unidentifiable.
- A rupture along the western end of the Porters Pass-Amberley Fault Zone (PPAFZ), between 500-700 years B.P., located within a few kilometres of the LCRAD is considered a likely source for triggering the LCRA2 event. However, the Alpine Fault is known to have ruptured during this period also.
- A rupture along the PPAFZ between 500-700 years B.P. is believed capable of initiating rupture of the small Carriage Drive Fault (an indirect AMS radiocarbon date of a rupture event occurring after (Wk15118) 755 ± 46 years B.P.), which is also considered a likely source for triggering the LCRA2 event at 668 ± 36 years B.P.
- An aftershock following the main rupture of the PPAFZ may have initiated the LCRA3 event.
- Therefore seismicity is a possible trigger for the LCRA1. However, so is ice retreat in which destressing of the valley side resulted in a gravity collapse of the slope.

Chapter 5

Future Rock Avalanche Hazard

5.1 Introduction

A future rock avalanche event at the LCRAD site is a potential hazard to the immediate area, both upstream and downstream. Three rock avalanches have occurred at the LCRAD site over the last ~10,000 years, with an average frequency of about ~3,300 years, although dating the deposits during this study has helped refine this estimate. A scarp is present behind the summit of Carriage Drive, which is controlled by failure along sub-vertical argillite beds, and dilation of the rock mass is occurring in the form of ridge rent development along the eastern ridge (Section 3.7). The dilation observed within the source area provides evidence for continued relaxation of the rock mass, and of the potential for continuing future slope instability. Therefore, a further significant rock avalanche from the source bowl of Carriage Drive is quite possible, and the most likely trigger for this event is a large-magnitude earthquake within the region.

A rock avalanche is a geomorphological event which may be hazardous; however the effects or hazard associated with the event depend on its scale and location. This Chapter considers the hazards associated with three rock avalanche scenarios; differing in orders of magnitude from, 10,000 to 100,000 to 1,000,000 m^3, from the source bowl of Carriage Drive. These different volume analyses are intended to straddle the likely magnitude of a future rock avalanche failure from the failed wedge block at the summit of Carriage Drive (Section 3.7). This approach provides a useful picture of the effects on the valley floor from events of different magnitudes, and their impacts on the Ryton River will also be assessed. However the focus will be the potential future failure event with a geomorphological hazard interpretation. A

geomorphological hazard is defined as *a natural event or process which has a negative impact upon human and cultural activities* (MURCK *et al.*, 1997).

The human and cultural features which are at risk from a rock avalanche event sourced from Carriage Drive are: 1) the water supply for the Ryton Homestead (sourced from a spring within the LCRAD runout track), 2) the Ryton Bay Road, 3) the Harper Road, and 4) the holiday camping ground located near the mouth of the Ryton River, on the shore of Lake Coleridge (figure 5.1). The Ryton Bridge and powerlines (figure 3.2), which cross the LCRA1 deposit, are not considered likely to be impacted directly by a future rock avalanche event. However, the major risk from any rock avalanche event is the loss of life, and the level of activity within the immediate runout zone will depend on the time of year and time of day the event occurs.

This Chapter outlines three scenarios of different magnitudes, that highlight the hazards involved in a future rock avalanche from Carriage Drive. An emergency response plan for such events and a long-term plan is also outlined.

5.2 Scenarios

5.2.1 Introduction

Three rock avalanches have failed from the source area on Carriage Drive; the LCRA1, LCRA2 and LCRA3. The LCRA1 and LCRA2 events have been dated, and their volumes (both original and present day) and their spreading and runout statistics have been analysed (Tables 3.1, 3.2 and 5.1). The volumes decrease by approximately an order of magnitude for each failure, but this trend cannot be expected to continue in the future. This is a consequence of the majority of source rock material failing during the LCRA1 event, meaning that the subsequent failures have limited volumes of source material available.

5.2.2 Source Model

The failure model introduced in Sections 3.7.1 and 3.7.2 showed that a scarp is present around the rear of the *current* Carriage Drive summit in which some displacement has already taken place. Outward toppling by near-vertical Torlesse Supergroup strata along argillite beds, associated with rock mass dilation along the eastern ridge line to form ridge rents, is considered to be the crucial failure

mechanism within the source area (figure 3.23). The identified wedge block of displaced material is interpreted to not only reflect the style of failure for the earlier rock avalanches, but also to constrain the source material for a future rock avalanche event. The volume of dilated displaced material at the crest of Carriage Drive is estimated to be ~35,000 ± 5,000 m^3, which would have a failed volume of ~40,000 m^3 incorporating further bulking (Section 3.4.2). This volume is much smaller than the LCRA2 deposit (*in situ* rock mass of 0.5 x 10^6 m^3), and therefore with a smaller volume of debris, the effects on the Ryton River and cultural factors will reduce significantly.

Table 5.1: Summary of LCRAD statistics from this study

Rock Avalanche	Age (years B.P.)	Deposit Volume (m^3 x 10^6)		Runout Distance (m from source)
		Present Day	Original	
LCRA1	Maximum of 9,720 ± 750 (WLL389)	5.1	12.5	1,780
LCRA2	668 ± 36 years (Wk14221)	0.37	0.65	1,350
LCRA3	Undated, interpreted to be close to 668 ± 36 years	<0.1?	~0.1?	<1,340?

However, in the event of a large magnitude seismic event (M≥6) affecting the area there is the possibility of a greater volume of material failing from the source area. EISBACHER and CLAGUE (1984) noted that the distortion of massive *in situ* rock faces by seismic shaking causes, *widening of existing fractures and thus sets in motion a complex process involving loss of cohesion, slippage, internal toppling, crushing, and eventual failure along a composite detachment surface.* The rock mass within the Carriage Drive is heavily fractured, and therefore the volume of failed material may increase substantially during a large earthquake. The defects within the Carriage Drive source basement strata are dilated and suggest continued "relaxation" of the slope and deterioration of the rock mass. Therefore, an earthquake within the region is likely to trigger a further rock avalanche event from Carriage Drive.

5.2.3 Runout Considerations

Three scenarios of different magnitude events have been modelled. Scenario 1 has an *in situ* source volume of 10,000 m^3, Scenario 2 has a volume of 100,000 m^3, and Scenario 3 has a volume of 1,000,000 m^3. The rationale behind the three different volumes for the scenarios is that a future rock avalanche event will most probably lie between the minimum and maximum volume limits chosen. The three scenarios are shown in figure 5.1 with the largest two existing rock avalanche deposits (the LCRA1 and LCRA2) shown for reference. All areas discussed in this Chapter are also shown on figure 5.1.

The calculated runout for the three scenarios is based on the area of the Ryton Riverbed footprint where the debris would initially deposit. This footprint area was estimated solely from; 1) the confinement produced by the present day levees that exist within the lower runout zone on the lower slopes of Carriage Drive, and 2) comparisons with where the LCRA2 and LCRA3 deposits initially entered the Ryton riverbed. The footprint area (shown in white on figure 5.1) is approximately 16,000 m^2 (200 m long x 80 m wide), with a gap volume space of ~160,000 m^3 to a height of 10 m. The footprint area is the hollow within the Ryton River section which has been created by incision of the Ryton River into the LCRA2 and LCRA3 deposits (figure 5.1). Analogous to a catch ditch for rock falls along a road (HOEK, 2000), the incision of the Ryton River into the LCRA2 and LCRA3 deposits will prevent rock avalanche debris from very small to small events (<100,000 m^3) moving out of the riverbed (figure 5.1). By confining the runout of the rock avalanches to the Ryton Riverbed this reduces the hazard and the effects of a rock avalanche event substantially.

5.2.4 Event Triggering

The triggering mechanism for a future rock avalanche from Carriage Drive is most likely to be seismic shaking accompanying local fault rupture, or an earthquake of large magnitude outside the immediate area which affects the Lake Coleridge region. A less likely triggering mechanism could be from a rainstorm where antecedent moisture conditions are high, creating instability from high cleft and pore-water pressures within the rock mass. Simple deterioration of the rock mass and continued dilation of the defect sets within the basement strata around the present day source scarp may also initiate an aseismic failure. In any event the rock avalanche will occur without significant warning.

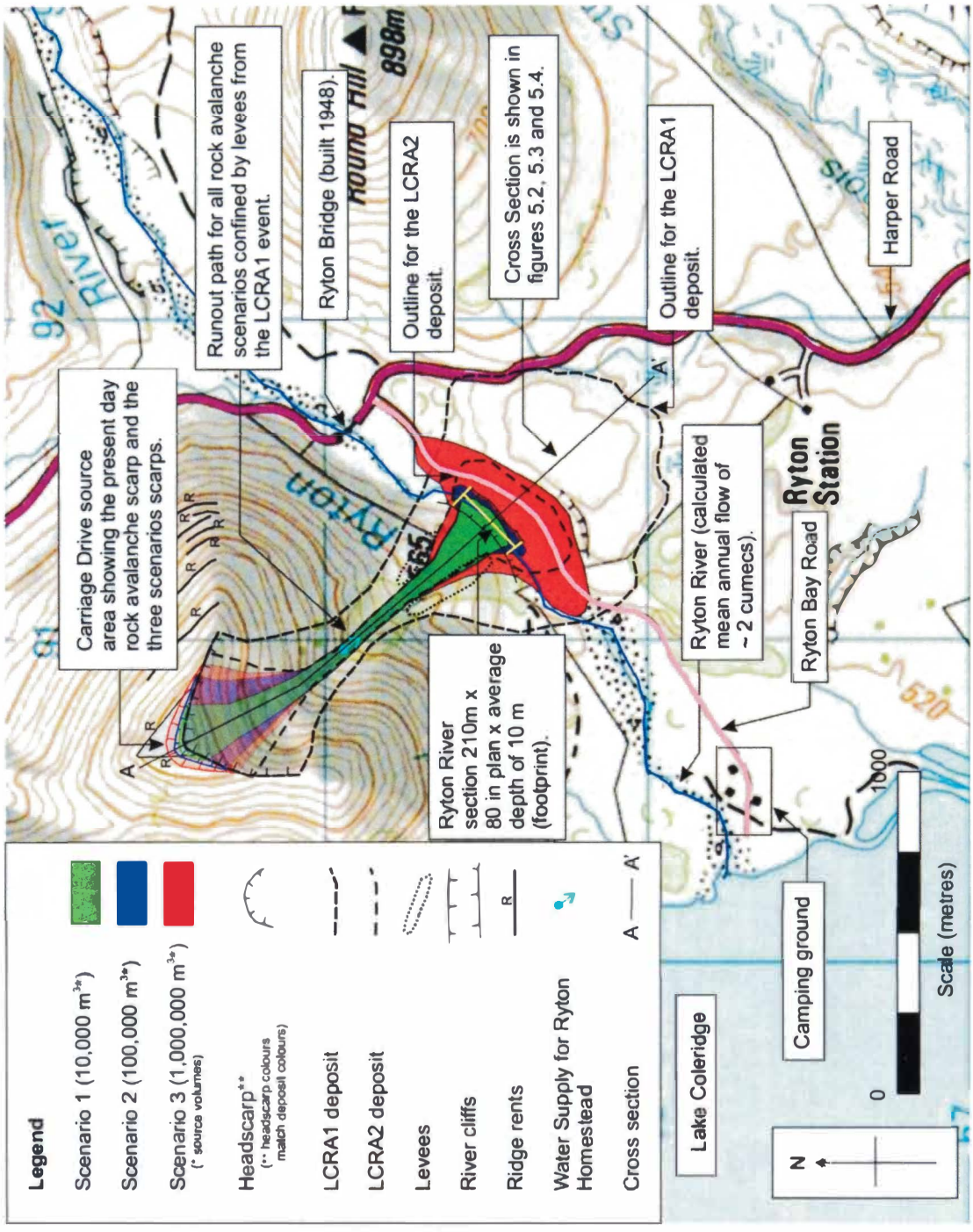

Figure 5.1: Predictive hazard map showing the three scenarios for a future rock avalanche event from the source bowl of Carriage Drive. The LCRA1 and LCRA2 deposit extents are indicated and were used as a scale of magnitude to help develop the extent of runout associated with various volumes of debris. The grey shaded area at the summit of Carriage Drive is the interpreted future source area. Cultural features at risk are identified within the map area.

Another risk which will not be discussed in depth because it is outside the scope of this project, but important to note, is the occurrence of a landslide or rock avalanche occurring on one of the other ranges that surround Lake Coleridge (figure 1.1). The consequent wave of displaced water poses a great threat to the camping ground which is located only metres from the shore, and possibly to other facilities including the intake to the power station.

5.2.5 Emergency Response (EM Response)

The rock avalanche event will take only seconds during failure and transportation down the slope of Carriage Drive. Due to the velocity of the moving debris, human response is considered nil (Table 1.2), and therefore an event of any size will be hazardous to people within; the source area, the runout zone, or the riverbed during the rock avalanche. The event will be very noisy and there will be a dust cloud associated with the fine material becoming airborne. If the event occurs at night "sparks" may also be visible. The EM response for a rock avalanche event within the Ryton riverbed will be the same for any size of event; however the steps and decision points (→ d) shown in figures 5.2 and 5.3 will depend greatly on the size and nature of the event. Figure 5.2 indicates evacuation from the downstream of the rock avalanche deposit, including the camping ground, should occur, and it is believed that people should evacuate and move towards or meet at the Ryton Homestead located to the east of the camping ground.

5.2.6 Long-Term Management

The longer term management of the Ryton Riverbed after a rock avalanche event is clearly dependent on both the size (volume of debris) and height of the "dam" and the floor in the riverbed. Figure 5.3 shows a long-term management plan which could be implemented after the immediate threat from a rock avalanche event with the Ryton riverbed has been dealt with.

The influx of sediment from the rock avalanche event is thought likely to create significant long-term changes to the behaviour of the lower portion of the Ryton River, especially downstream from the rock avalanche deposit. KORUP (2004) found that excessive lateral sediment input (such as occurs when a rock avalanche is deposited) becomes a critical control on fluvial transport capacity and also

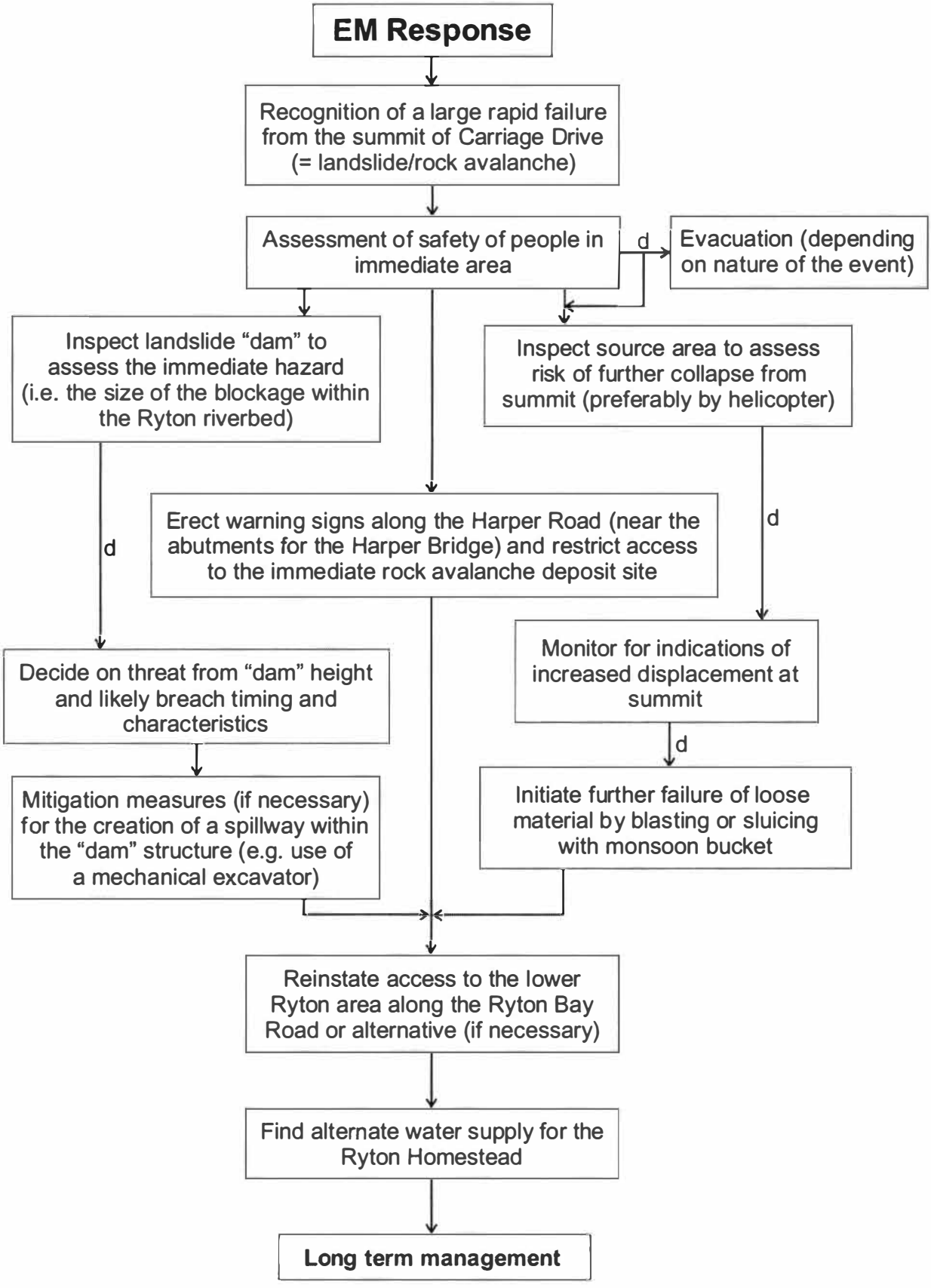

Figure 5.2: Emergency Response Plan for a rock avalanche event within the Ryton riverbed. Note that "d" = decision point, which is required by the EM manager.

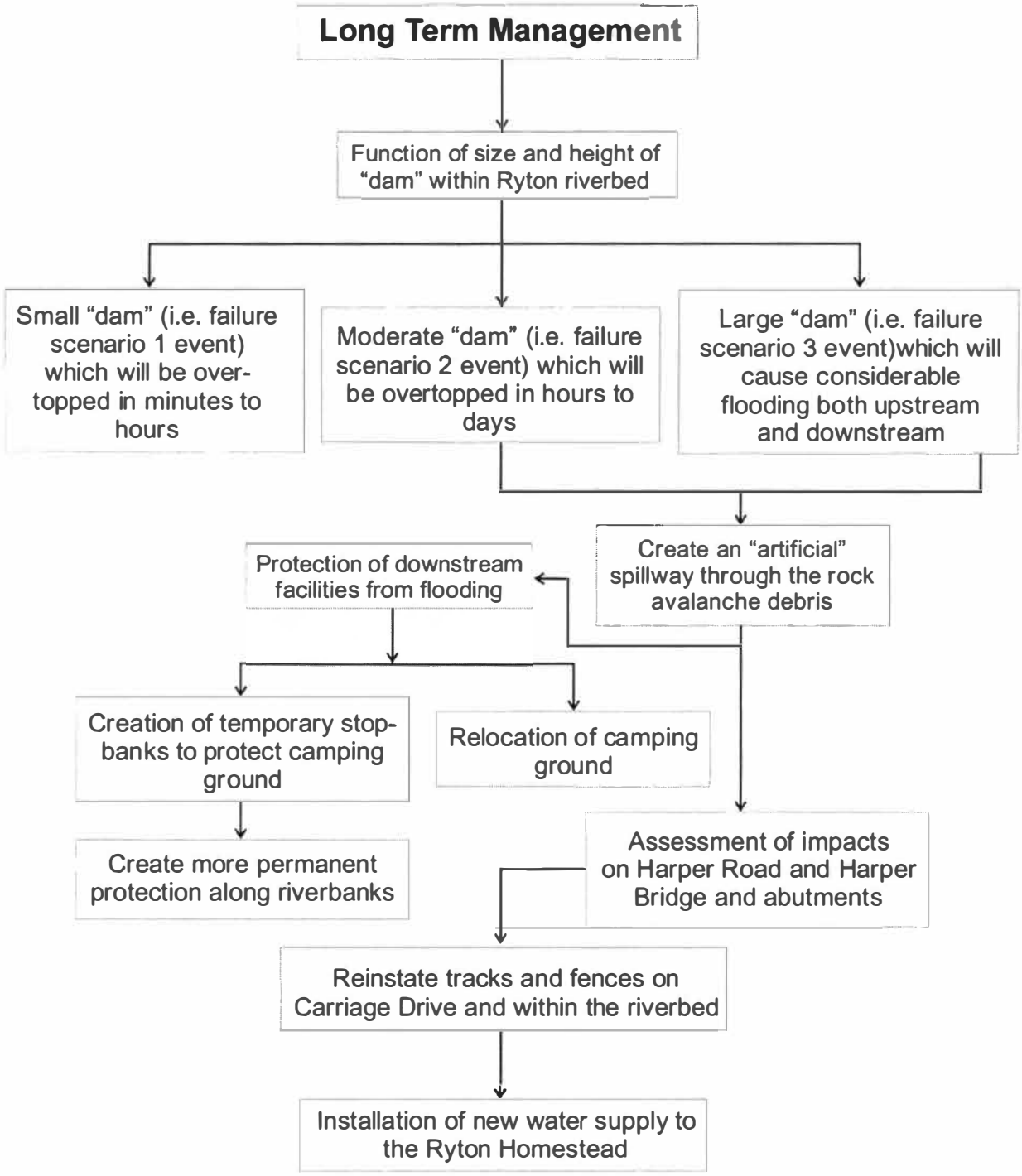

Figure 5.3: Long-term management for a rock avalanche event with the Ryton riverbed.

morphology. He also highlighted the long-term changes to riverbeds in which sediment overloading creates:

- aggradation of the riverbed,
- reduction of the channel cross-sectional area, and

- lateral instability and channel avulsion.

Channel avulsion is described as the *rapid lateral relocation of a river course across parts of its floodplain due to changes in local valley slopes* (JONES and SCHUMM, 1999). Sediment aggradation was recently identified after the Mt Adams rock avalanche occurred in 1999 and dammed the Poerua River in Westland (HANCOX *et al.*, 2002); it was also found to be a significant problem on the downstream river-flats (KORUP, 2004).

Within the Ryton riverbed, adjustments to a rock avalanche emplacement will cause a decrease in cross-section, which would increase flood frequency and therefore overbank deposition of gravel and finer sediments. Therefore the camping ground which is located at the mouth of the river, on the shores of Lake Coleridge, will have a greater flood risk than at the present-day because aggradation promotes channel avulsion and the camping ground will continue to be threatened by flooding with an increased frequency (note that it is already at risk from flooding at present).

5.3 Scenarios 1 and 2

5.3.1 Introduction

Scenarios 1 and 2 are discussed together due to their similar runout paths, effects on the valley floor, and the hazards that they pose. As shown in figure 5.1 scenario 1 (10,000 m^3) has a small head scarp (~200 m wide) with a limited and narrow runout path. The present-day levees that exist through the lower portion of the runout path on Carriage Drive effectively channelise the rock avalanche debris and limit the width of runout. The debris impacts into the Ryton riverbed within the footprint area, and is forced to stop due to the topographic constraints of the opposing ~10 m high cliffs created by incision of the Ryton River into the LCRA2 and LCRA3 deposits. The reference level for the footprint area floor is 530 m (a.s.l).

Scenario 2 (100,000 m^3) has a moderate headscarp (~300 m wide) and a runout path that is simular to the scenario 1 runout. Towards the lower portion of the runout zone the debris may spread wider than in scenario 1, although the levees will still help to contain the rock avalanche material. The rock avalanche material is interpreted to also be contained within the Ryton riverbed, but it will create a much more substantial "dam" than scenario 1.

5.3.2 Scenario 1

The effects of a rock avalanche emplacement into the Ryton River section with a source volume of 10,000 m^3 would be limited. During the rock avalanche event, the Ryton Homestead house water supply which is sourced from a spring in the runout path of the LCRAD will be cut off, and fences that cross the runout path will be destroyed and buried under debris. If stock or people are within the source area or runout zone, there will be losses.

Rock avalanche material will enter the Ryton riverbed and within the identified footprint have an average thickness of only ~0.7 m (figure 5.4), based on an increase in deposit volume due to bulking as discussed in Section 3.4.2. Locally, debris will be thicker (2 to 3 m), however the best estimate of "dam" height is considered to be ~1 m high over the footprint area. The Ryton River was estimated under normal flow conditions to have a flow of 2 cumecs per second, using the method by MCKERCHAR and PEARSON (1989) as summarised in Table 3.3. Assuming there was no seepage through the barrier, the Ryton River would pond for only minutes before overtopping the rock avalanche debris. This would produce a minimal flood downstream, and is unlikely to pose any threat or hazard to the camping ground near the mouth of the Ryton River on the true left bank (figure 5.1) where banks are presently ~1 m high.

The ~12,000 m^3 (bulked volume) of debris in the fluvial system will be eroded relatively rapidly from the rock avalanche site, and transported downstream towards the delta which is prograding into Lake Coleridge. The immediate impact from a dam-break flood is therefore considered to be minimal with this volume of material, as the Ryton River will overtop the barrier in minutes. Long-term impacts to the riverbed are also considered to be minor. Due to the smallness in volume of the scenario 1 event, aggradation and subsequent avulsion of the lower section of Ryton River is not believed to be a major concern for the camping ground. Presently the camping ground is ~1 m above the river, and the scenario 1 event is likely to have a similar impact on the riverbed as a flood from a major rainstorm.

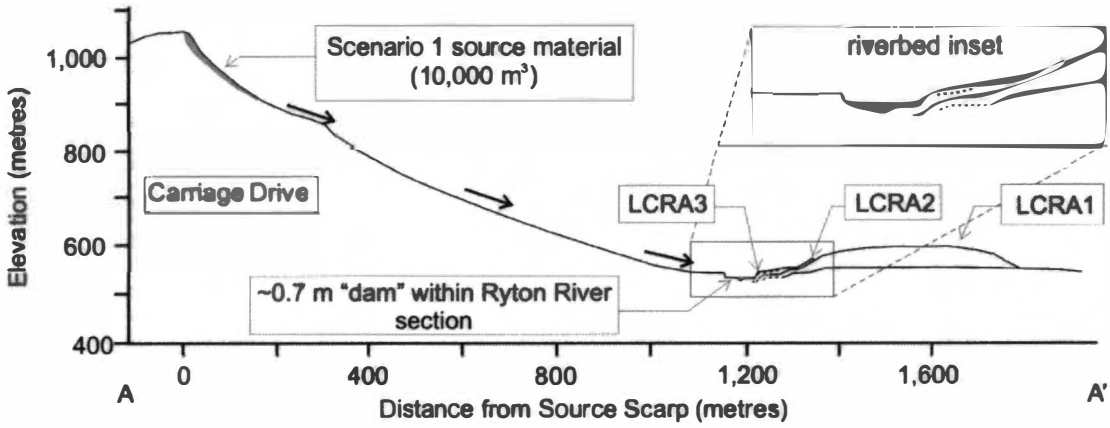

Figure 5.4: Schematic cross section for the scenario 1 rock avalanche event with a source volume of 10,000 m^3. The debris is trapped within the Ryton River section, creating a 0.7 m high "dam" within the riverbed which will have minimal effect on the flow regime.

5.3.3 Scenario 2

5.3.3.1 Footprint Blockage

Scenario 2 has a source volume of 100,000 m^3 (deposit volume of approximately 120,000 m^3), an order of magnitude greater than scenario 1. Apart from the increases in volume, the effect within the runout zone is very similar to scenario 1 due to the confinement of the rock avalanche debris by levees on either side of the path. Immediate impacts from the rock avalanche event will be; the destruction of fences within the runout zone, possible stock losses and the loss of human life, the disconnection of the Ryton Homestead water supply, and the emplacement of ~120,000 m^3 within the Ryton River. With this volume of material, the debris is predicted to also be contained within the Ryton River section (figure 5.5), and Ryton Bay Road is not therefore considered to be in serious danger of burial by debris. The immediate blockage of Ryton River, is probably the most important impact from the rock avalanche event due to the flooding hazard both upstream and downstream.

5.3.3.2 Upstream Inundation

Inundation of land upstream will be the initial concern, and the significance of the upstream flooding will be entirely dependent on the height of the barrier created within the Ryton River section. The footprint dimensions are similar to scenario 1 due to the channelised effect by the levees during runout, and if this is the case a "dam" height of ~7 m is estimated (figure 5.5). Upstream flooding by ponding water from a ~7 m "dam" is not likely to inundate the Harper Road abutments to the Harper

Bridge and the turnoff to Ryton Bay, which have a lowest elevation of 546 m (a.s.l) compared to the footprint reference level of 530 m. However, it is uncertain how much the deposit will "spread" once it reaches the Ryton River section, but if spreading is minimal the likely height for the emplacement "dam" will average between 5 and 7 m. Localised thickening of the deposit is likely, which may reach right across the river and if this happens it will increase the "dam" height and also increase the area upstream which is inundated.

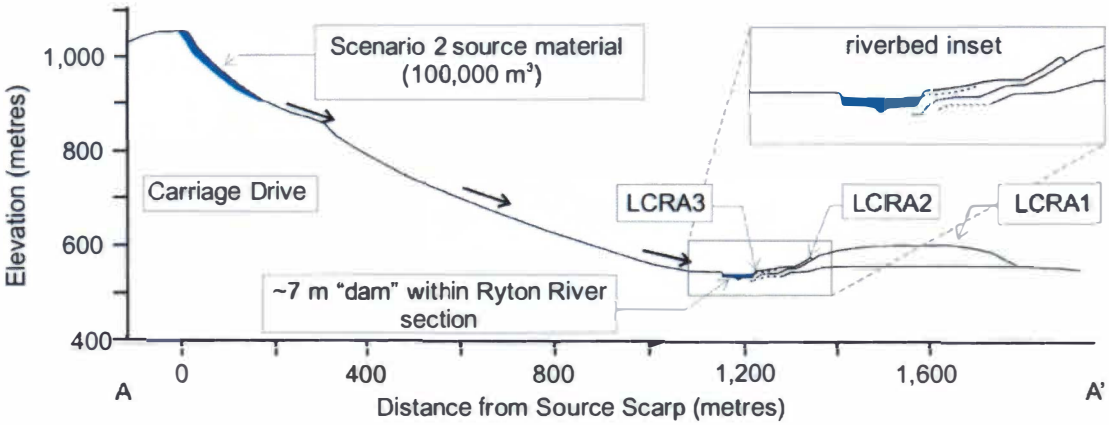

Figure 5.5: Schematic cross section for the scenario 2 rock avalanche event with a source volume of 100,000 m^3. The debris is trapped within the Ryton River section, creating a 7 m "dam" within the riverbed.

The development of a temporary lake behind the rock avalanche deposit will occur over a short period of time, as shown in Table 5.2. Calculations have been made using the present day topography and a reference level of 537 m (a.s.l) for the maximum height of the water body behind the "dam". Calculations for the temporary lake behind the scenario 2 rock avalanche "dam" use:

- The mean annual rainfall taken from the Lake Coleridge Meteorological Station (Section 1.3.5.2); and
- The catchment area (Table 3.3) for the Ryton River (taken from NZMS K35).

This allows an estimate of 2 cumecs for the Ryton River mean annual flow (Mar) based on the mean annual rainfall and catchment area. Flood estimates were calculated for both the annual flood (Q_1) and the 100 year flood (q_{100}), using the methods of MCKERCHAR and PEARSON (1989), and results are shown in figure 5.6. The assumptions to undertake these calculations were:

- There is localised thickening of the rock avalanche "dam", which reaches across the entire riverbed.

- The "dam" height averages ~7 m and this is maintained during the filling of the lake upstream with no natural spillway development at a lower elevation.
- There is no significant seepage of water through the "dam", which could cause premature piping failure.
- Mean annual flow is assumed to represent normal flow conditions, and therefore to be a realistic basis for the time to overtopping estimates.
- The 100 year flood was assumed to be the worst case scenario for the flow of the Ryton River, with anything above this considered unlikely.

Table 5.2: Lake Statistics for the Scenario 2 event

Lake Statistics for the Temporary Lake development for Scenario 2	
(R.L. of 537 m)	
Dam height (H)	7 m
Planimetric surface of water body (S)	0.1 km^2
Water Volume (V)	350,000 m^3
Mean annual rainfall Lake Coleridge Meteorological Station records from 1913-1980 (Mar) (Table 1.1)	0.83 m
Planimetric Catchment Area (A) (Table 3.3)	76,000,000 m^2
Mean annual flow of Ryton River = Mar x A / (365 x 86400)	2.00 cumecs
Mean annual flood of Ryton River $Q_1 = A^{0.8} \times 0.5$*	15.98 cumecs
~ 100 year flood Q_1 x 2.5** (q_{100})	39.88 cumecs
Length of time for lake to fill under mean annual flow	2.0 days
Length of time for lake to fill under mean annual flood	6.1 hours
Length of time for lake to fill under ~100 year flood	2.4 hours
Landslide dam-break flood $Q_{max} = 181(HV)^{0.43}$ (DAVIES and SCOTT, 1997)	266 m^3s^{-1}

*Value read off South Island contour map of $Q_1/ A^{0.8}$ (refer to figure 5.6).
**Value read of South Island contour map of q_{100} (refer to figure 5.6).

Taking the assumptions mentioned above into consideration, a 7 m "dam" under normal flow conditions is believed to take approximately 2 days to overtop, but under Q_1 and q_{100} flooding conditions this period is dramatically reduced to hours as shown in Table 5.2.

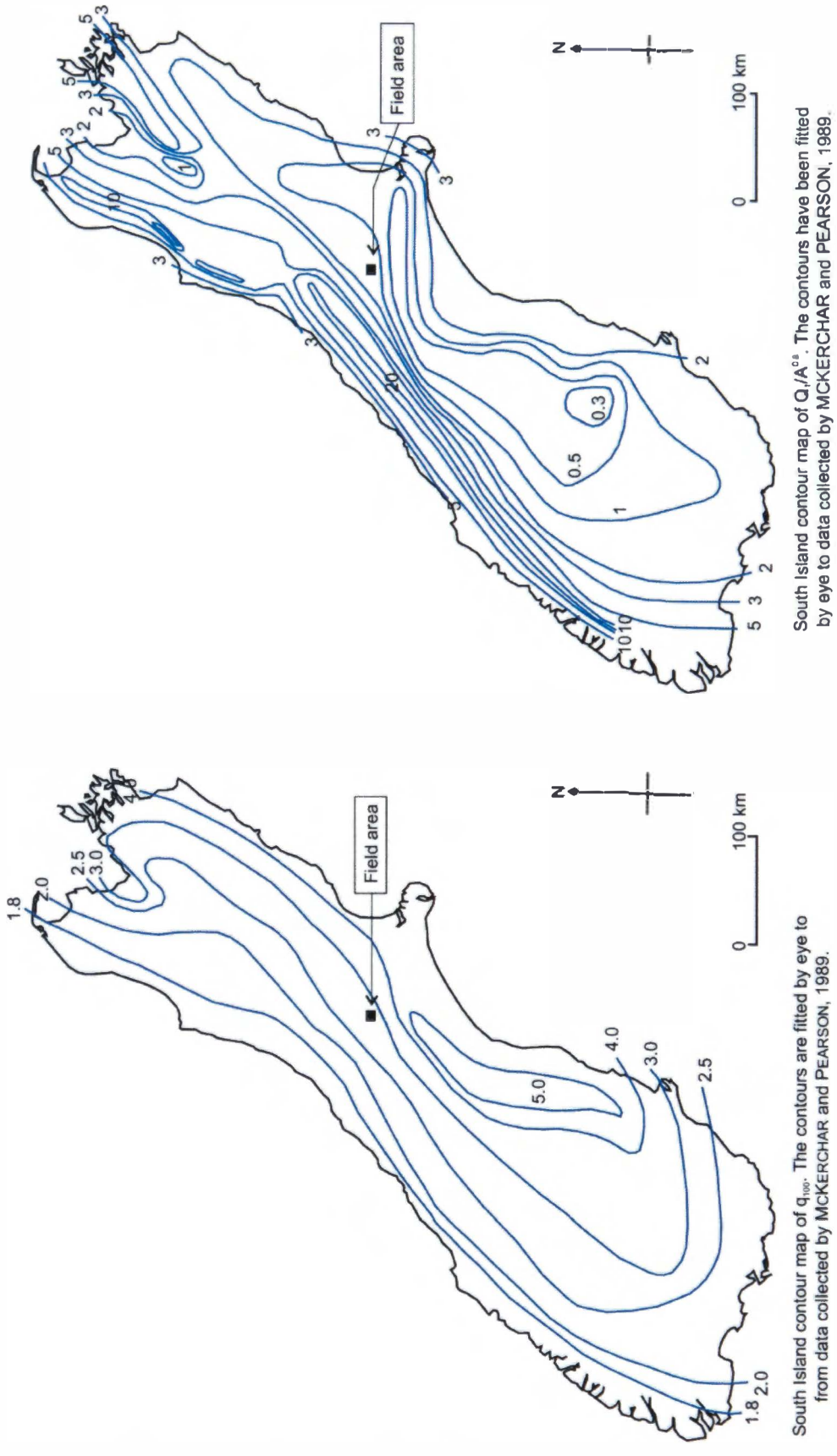

Figure 5.6: South Island contour maps of a) 100 year flood (q_{100}) (left diagram) and b) annual flood ($Q_1 / A^{0.8}$) (right diagram). Modified from MCKERCHAR and PEARSON, 1989.

5.3.3.3 Dam-Break Flood

The secondary hazard associated with damming the Ryton River is the dam-break flood that usually results after the barrier has been overtopped. The maximum peak flood discharge (m^3s^{-1}) from "dam" height and stored water volume can be calculated as:

$$Q_{max} = 181(HV)^{0.43};\ r^2 = 0.76,\ SE = 129\%$$

where H = dam height in metres, V = volume of stored water in $m^3 \times 10^6$ (DAVIES and SCOTT, 1997). The maximum peak flood discharge for scenario 2 is ~250 m^3s^{-1} (actual figure 266 m^3s^{-1}), which is almost 7 times greater than the calculated 100 year flood for the Ryton River (Table 5.4). The duration of flooding would extend over an *estimated* 30 minute period. The flood waters would attenuate significantly downstream due to the broad riverbed, however the camping ground (which is only ~1 m above present day river level) will be flooded. It is considered unrealistic to estimate the flood water height during the dam-break flood waters at the camping ground. Evacuation of the area below the "dam" is essential, including the camping ground, while the Ryton River is dammed by rock avalanche debris.

5.3.4 Mitigation of Effects from a Small Rock Avalanche

5.3.4.1 Scenario 1

A scenario 1 rock avalanche event will cause only minor disturbance to the Ryton River system. In a scenario 1 event the camping ground, the Ryton Bay Road and access further up valley via the Harper Road will not be affected. The EM response plan should be implemented immediately after the event has been detected (figure 5.2). As discussed in Section 5.3.2, cultural features located within the rock avalanche runout path will be destroyed (e.g. fences and the water supply for the Ryton Homestead), and some stock losses could occur if they are grazing in the runout area. The containment of the deposit within the Ryton riverbed, however, dramatically reduces the hazard potential from this rock avalanche event. Regardless of size, the event is life-threatening if people are within the source, runout and/or depositional zone at the time of failure.

The long-term management plan for the scenario 1 rock avalanche event is minimal. Due to the smallness of the deposit within the Ryton riverbed, the "dam"

structure will be overtopped in minutes with no obvious flooding either upstream or downstream. As the generalised long-term management plan shown in figure 5.3 highlights, for a small rock avalanche "dam" (like the scenario 1 event) within the riverbed, there is no real need for further mitigation after the event but some bed changes will occur downstream as the "dam" is progressively removed. This would make the camping ground more vulnerable.

5.3.4.2 Scenario 2

Mitigation for the scenario 2 rock avalanche event involves the same initial emergency response as outlined in figure 5.2. Due to the increase in size of the deposit, a more substantial blockage within the Ryton riverbed is likely to occur. Although the "dam" height is estimated at ~7 m, due to either spreading or localised thickening of the deposit, this height may vary significantly and the characteristics of the "dam" are solely dependent on this. An "artificial" spillway may be required to reduce the flooding potential of the ponded water, both upstream and downstream, as after the rock avalanche event the dam-break flood is considered to be the major threat to the lower Ryton River and adjoining floodplain areas.

Long-term effects for the camping ground due to scenario 2, will be the increased flooding frequency for the lower portions of the Ryton River due to the increased input of sediment by the rock avalanche. This may become a serious problem with the aggradation of the riverbed and subsequent avulsion of the Ryton River. The long-term management plan shown in figure 5.3 provides a guideline of what will be required, after the rock avalanche event. Although the creation of more permanent protection along the riverbanks would reduce the flooding risks as noted in figure 5.3, this should be done with caution. Flood-protection structures such as stop-banks actually increase the future vulnerability of the riverbed and adjacent floodplain areas, and over time may lead to the construction of more permanent structures being built within the camping ground, which is not recommended (Dr T. DAVIES, University of Canterbury, *pers. comm.*, 2004).

5.4 Scenario 3

5.4.1 Introduction

Scenario 3 evaluates the effects on the lower Ryton River section and surrounding area (including the effects to cultural features) of a moderate size rock avalanche

event (~1 x 10^6 m^3 source volume). As discussed in earlier Chapters (e.g. Section 1.1) 1 x 10^6 m^3 is considered to be the "low-end" size for a rock avalanche, however due to the location relative to cultural features, its effects upon the lower portions of the Ryton River will be very significant. The failure headscarp will be larger than for the previous two smaller scenarios, and there will be some debris overtopping the levees towards the lower section of the runout zone (figure 5.1).

A rock avalanche event of 1 x 10^6 m^3 (source volume) within the LCRAD site poses a significant hazard both to human lives and cultural features. The immediate concern is that debris will not be contained within the Ryton River section, which was the case for the first two smaller scenarios. Immediate impacts of a rock avalanche event of this volume depositing into the lower portion of the Ryton River will again be the destruction of fences, possible loss of stock, and disconnection of the Ryton Homestead water supply. However, with a rock avalanche event of this magnitude (1.2 x 10^6 m^3 deposit volume if there is 20 % bulking), these are minor concerns compared to the serious risk to human lives. Events of this size will infill the Ryton River section and continue "flowing" towards the southeast (figure 5.1). The Ryton Bay Road will be buried by rock avalanche debris, and if people are on the road at the time of the event they are in serious danger, as the rock avalanche event will only take tens of seconds to reach the road from the source area as shown by DAN analysis of the LCRA1 event (Section 3.4.6). The burial of the Ryton Bay Road also isolates road access to and from the camping ground, meaning that evacuation of the camping ground will have to use an alternative route, possibly on foot.

5.4.2 Footprint Blockage

The debris runout will not be constrained by the Ryton River Section, infilling the riverbed, overriding the associated cliffs, and engulfing the low topographic zone occupied by the LCRA2 and LCRA3 deposits (figure 5.7). The runout debris will be forced to stop or divert both upstream and downstream when it impacts the cliffs of the LCRA1 deposit, but rock avalanche material is likely to run-up these cliffs in a similar manner to the LCRA2 event, creating a prominent brandung feature. However, it is considered unlikely that debris will overtop the surface of the LCRA1 deposit to any significant extent. This is due to the eroded hollow of the Ryton River section significantly reducing the amount of material reaching the opposing cliffs of the LCRA1 deposit (figure 5.1). From the estimated area of runout displayed in figure

5.1, the average thickness of the deposit within the riverbed is calculated to be ~15 m, while on the south-eastern side of Ryton River the material that overrides the LCRA2 and LCRA3 deposits is calculated to be ~5 m (incorporating the 20% bulking factor for debris).

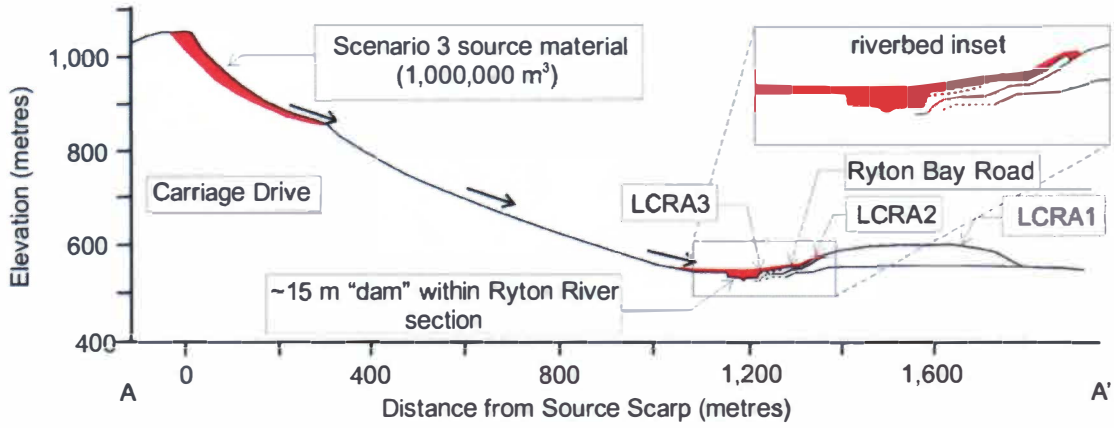

Figure 5.7: Schematic cross section for the scenario 3 rock avalanche event with a source volume of 1 x 10^6 m^3. The debris is not confined within the Ryton River section, infilling the riverbed and flowing over the Ryton Bay Road to 5 m depth. The debris creates a 15 m "dam" within the riverbed section.

5.4.3 Upstream Inundation

From the estimated thickness calculations for a scenario 3 event, the "dam" within the riverbed and river section will have an approximate height of ~15 m. This "dam" height is sufficient for ponded water to submerge the Harper Road abutments to the Harper Bridge, possibly the bridge itself, and also the turnoff to the Ryton Bay Road. Gradual inundation of the upstream riverbed and the Harper Bridge will isolate the inhabitants further up the valley; however this flooding would occur gradually and would allow evacuation of the upper valley residents if considered necessary.

The development of a temporary lake behind the rock avalanche "dam", will take longer than for the scenario 2 event. With a "dam" height of 15 m (taking the assumptions mentioned in Section 5.3.3.2 into consideration) it is estimated to take approximately 21 days under normal flow conditions (Table 5.3). Immediately following emplacement of the rock avalanche event, upstream flooding will begin to occur. The lake will have an estimated volume of ~3,700,000 m3 (calculated figure 3,660,000 m3), if there is no creation of a "natural" spillway through the rock avalanche deposit. This was estimated by using an R.L of 545 m (a.s.l) and the

present-day topography. As mentioned above, assumptions for the calculation of lake statistics can be found in Section 5.3.3.2.

Table 5.3: Lake Statistics for the Scenario 3 event. Rainfall, catchment area, mean annual flow, mean annual flood and 100 year flood data as for Table 5.2

Lake Statistics for the Temporary Lake development for Scenario 3	
(R.L. of 545 m)	
Dam height (H)	15 m
Planimetric surface of water body(S)	0.565 km²
Water Volume (V)	3,660,000 m^3
Length of time for lake to fill under mean annual flow	21.18 days
Length of time to for lake to fill under mean annual flood	2.65 days
Length of time for lake to fill under ~100 year flood	1.06 days
Landslide dam-break flood $Q_{max} = 181(HV)^{0.43}$ (DAVIES and SCOTT, 1997)	1,006 m^3s^{-1}

*Value read off South Island contour map of $Q_f / A^{0.8}$ (refer to figure 5.6).

**Value read of South Island contour map of q_{100} (refer to figure 5.6).

5.4.4 Dam-Break Flood

If there is little or no spillway created (either "natural" or "artificial" as discussed below) the dam-break flood after the structure has been overtopped by the Ryton River will be extremely large (Table 5.3). The maximum peak flood discharge from Ryton River water overtopping the "dam" and rapidly incising is calculated to be ~1,000 m^3s^{-1} (with a calculated value of 1,006 m^3s^{-1} in Table 5.3; with a "dam" height of 15 m and a water volume of 3,660,000 m^3; refer to equation in Section 5.3.3.3; DAVIES and SCOTT (1997)). This is a *catastrophic* flooding hazard for the downstream portion of the Ryton River and surrounding low-lying area. The camping ground is under direct threat of rapid, severe flooding with sediment rich-floodwaters. Flooding would attenuate significantly after *approximately* 1 hour.

5.4.5 Mitigation of Effects from a Large Rock Avalanche

Immediately following the detection of the rock avalanche event the EM response (figure 5.2) needs to be initiated. Due to the extended area of runout compared to the earlier two scenarios, it is more important to account for people that were located around the area. Once the source area has been assessed and deemed safe, the

excavation of an "artificial" spillway is the most likely option to mitigate against the severe flood risk.

The long-term management plan as shown in figure 5.3, indicates that temporary flood protection could be constructed, however working downstream of the "dam" may be highly dangerous depending on the stability of the structure (i.e. the width to height ratio and height of dammed water on the upstream side). Immediate removal of the caravans via paddocks to the south, or if necessary abandonment of the camping ground, may be required.

If a "natural" or an "artificial" spillway is created, the immediate flooding from the breach of the "dam" will be considerably less severe than otherwise. Long-term effects, to the riverbed, however as discussed in Section 5.2.6, will still significantly endanger the camping ground from the massive influx of sediment from the rock avalanche deposit, which will increase active channel avulsion and increase flood frequency. Relocation of the camping ground is believed to be the most feasible option for mitigation of scenario 3. Once again it is stressed that construction of flood protection (e.g. stopbanks) is not recommended due to the potential of the increased future vulnerability to the low lying area of the camping ground site and also their on-going maintenance that will be required.

5.5 Summary

The potential exists for a further rock avalanche at the LCRAD site, and it poses a serious hazard to the immediate area and to users of the lower Ryton River. This assessment is based on the knowledge that three rock avalanches have occurred at this site during the last 10,000 years, and there is evidence that another failure is likely from the crest of Carriage Drive from a displaced wedge block of ~ 35,000 m^3 ± 5,000 m^3 identified during fieldwork. It is not known when the failure will occur, however an earthquake is the most likely source of a triggering mechanism. Section 2.5 highlighted active faults within the area, and of particular note are the two major strike-slip faults; the Alpine Fault has a recurrence interval of c. 250 years, with the last rupture occurring ~253 years B.P. (YETTON *et al.*, 1998), and the PPAFZ ruptured c. 650 years B.P. and before that at ~1,500 years B.P. Ruptures along both of these

faults are believed to be capable of producing earthquake magnitudes of M>7, which could trigger a further substantial rock avalanche event from Carriage Drive.

Three scenarios of varying magnitudes were chosen to model the effects and hazards involved in a rock avalanche event of differing volumes. Although calculations have been made using potential volumes of material which will detach and fail as a rock avalanche from Carriage Drive, an earthquake event is likely to cause additional collapse of the source area strata. Therefore, the three scenarios are intended to provide realistic descriptions of the hazards associated with a future rock avalanche event from Carriage Drive, and to provide an EM response and long-term management plan to the scale that is necessary for the size of the event.

From modelling scenarios 1 and 2, it is believed that due to the "catch ditch capability" of the Ryton River section, rock avalanche events with debris volumes of up to 100,000 m^3 will be contained within the Ryton River, which limits the immediate rock avalanche emplacement hazard to within the source area, runout path and riverbed. Increases in volumes from the scenario 1 to 2 events increase the depositional runout of the debris, and the flooding hazards both upstream and downstream.

The scenario 3 event showed that the associated hazards of a ~1,200,000 m^3 deposit volume significantly increase, due to the extent of the runout burying the Ryton Bay Road, with the extensive flooding both upstream and downstream of the resultant "dam". Upstream flooding has the real potential to inundate the Harper Road abutments for the Ryton Bridge, and also the Ryton Bay Road. The Ryton Bridge is unlikely to be damaged by the flood waters due to the ponding and stillness of the water body, and therefore access further up-valley will be the only consequence. Dam-break flooding is a severe threat to the camping ground, as flooding is estimated to be many times greater than the predicted 100 year flood for the river if the structure survives until overtopping. A "natural" spillway could develop which will significantly reduce the volume of stored water behind the "dam", and therefore, the flood risk both upstream and downstream.

An EM response plan was designed to enable an efficient staged response to an otherwise chaotic natural geomorphological event. A rock avalanche event occurs very rapidly, taking seconds from initiation to deposition, which obviously poses a great risk to inhabitants in the immediate area. Depending on the size and nature of the rock avalanche event, a long-term management plan is also provided to mitigate the effects of a rock avalanche occurring within the Ryton riverbed.

Chapter 6

Summary and Conclusions

6.1 Project Scope and Objectives

The Lake Coleridge Rock Avalanche Deposits (LCRADs) are located in the middle Rakaia Valley, near the shores of Lake Coleridge. This study has shown that the LCRAD consists of three separate rock avalanche deposits termed the LCRA1, LCRA2 and LCRA3 deposits respectively. Previous studies of the site conducted by WHITEHOUSE (1981, 1983) and WHITEHOUSE and GRIFFITHS (1983) identified only one rock avalanche, and therefore failed to provide accurate dates for the Lake Coleridge rock avalanche events.

The definition of a rock avalanche used in this study is from HSÜ (1975), who defined a rock avalanche as being a *large bulk of predominantly dry, massive rock which instantaneously detaches from a mountainside, and travels downslope at very high velocities, depositing out onto the valley floor*. The main aim of this project was to reconstruct the events at and around the LCRAD site, since the Acheron 3 ice withdrawal from the middle Rakaia Valley, which has been dated to ~11,650 ± 200 years B.P.(NZ1290) by BURROWS and RUSSELL (1975). This aim was achieved by mapping and analysis of the rock avalanche deposits and the surrounding area. Excavating trenches to study internal structures and importantly to locate organic matter provided three radiocarbon dates (including one AMS date), and one optically stimulated luminescence date, to temporally constrain the rock avalanche events.

GPS surveying enabled geomorphic interpretation of terrace development along the lower portion of the Ryton River, from between Mt Hennah and Round Hill to the mouth of the river at Lake Coleridge. This was vital in reconstructing the effects the rock avalanche events had on the river.

6.2 Geological and Geomorphological Setting

The LCRAD, located to the south east of Carriage Drive which is the source of the rock avalanche debris, occurs within the middle Rakaia Valley adjacent to Lake Coleridge. The basement and cover geology within the Lake Coleridge area is solely Torlesse Supergroup "greywacke" and "argillite", and derived materials. Outcrop of bedrock is largely restricted to parts of hill slopes, because of the extensive glacial and postglacial cover materials blanketing the valley floors, and the widespread development of screes. The wide valley floors and steep-sided hills reflect both the active tectonic history of the area and glacial action within the Rakaia Valley.

Within the rock avalanche source area on Carriage Drive the basement strata typically strike towards the north-northwest, with dips ranging from 42° to sub-vertical and changing from east- to west-facing across the source area. Characteristically, the Torlesse Supergroup strata display varying scales of bedding between the alternating sandstone and mudstone (or argillite) beds within the field area. The near-surface rock mass has undergone significant physical alteration, predominantly by freeze-thaw processes and seismic ground motion, which has caused the strata to become highly disaggregated, although only limited chemical alteration has occurred. Ridge rents or "anti-scarps" are located along the northeastern ridge on Carriage Drive, with one ridge rent on the south western ridge, and these show the dilation of the rock mass which is thought to have occurred preferentially along the mudstone layers.

Glacial ice tongues, particularly from the Wilberforce Glacier, are believed to have affected the Cottons Sheep Range including Carriage Drive a number of times during the Pleistocene; SOONS (1963) recognised the Woodlands, Tui Creek, Bayfield and Acheron Advances within the Rakaia Valley. The present project has focused on the Acheron 3 Advance because of its influence on the LCRAD site and surrounding area. It is thought that the ancestral Ryton River was blocked by Acheron 3 glacial ice and was diverted around the northeastern flank of Round Hill. A fluvial fan developed from the diverted meltwaters, and subsequently followed the receding ice margin back towards "Greater Lake Coleridge". "Greater Lake Coleridge" achieved a maximum elevation of ~530 m within the Coleridge Trough, between the receding snout of the Wilberforce Glacier and its terminal moraine. Two beach deposits

located within the Acheron 3 terminal moraine near the Lake Coleridge Homestead represent two still-stands of the lake during progressive lowering of "Greater Lake Coleridge" towards the pre-Lake Coleridge Power Station elevation of ~508 m. Fluvial changes between glacial events within and surrounding the LCRAD site are significant, particularly with meltwater channels becoming abandoned.

Tectonic shortening of the inland Canterbury region has left a strong imprint over the landscape causing mountain range development, and also the presently active major thrust and thrust/strike-slip faults that surround Lake Coleridge. Studies of the major faults within the area, such as the; Porters Pass-Amberley Fault Zone, Harper Fault, Cheeseman Fault, Torlesse Fault Zone and the Craigieburn Fault Zone and also the Alpine Fault situated ~55 km to the northwest of the LCRAD site, all indicate that these faults have the potential to produce earthquakes with magnitudes of >M6. The potential for the faults within the Lake Coleridge area to produce M>6 earthquakes at any time, and therefore their potential as triggering mechanisms for a rock avalanche event at the LCRAD site was clearly recognised in this study.

Regional "clustering" of rock avalanche deposits is a phenomenon that was initially studied in New Zealand by WHITEHOUSE (1981, 19830) and WHITEHOUSE and GRIFFITHS (1983), and has previously been used to help reconstruct regional seismicity on the assumption that earthquakes are the dominant triggering mechanism for rock avalanche initiation. With more in-depth studies of individual rock avalanche sites, such as this project and SMITH'S (2003) study of the Acheron rock avalanche, a better understanding of the inland Canterbury seismic history is developing. Brief summaries of the Craigieburn rock avalanche studied by WHITEHOUSE (1981) and ORWIN (1998), and the Acheron rock avalanche studied by SMITH (2003), are also provided in this thesis.

6.3 The Lake Coleridge Rock Avalanche 1 Deposit

The LCRA1 deposit is interpreted to have failed approximately 9,720 ± 750 years B.P., after the withdrawal of Acheron 3 ice from the valley. The deposit fell from Carriage Drive, which is the southern-most peak of the Cottons Sheep Range, and the source, runout path and deposit are hourglass-shaped in plan form. The calculated volume for the LCRA1 deposit is 12.5×10^6 m^3, however a large portion of the debris

has been eroded by the Ryton River, leaving an estimated 5.1 x 10^6 m^3 present today. The planimetric surface area of the present-day deposit is 0.261 km^2.

The LCRA1 deposit has a Fahrböschung of 15.5° and has a calculated excess travel distance (L_e) of 1,030 m. When compared to European rock avalanches the LCRA1 deposit displays high mobility, and DAN modelling suggests emplacement of debris onto the valley floor with velocities up to ~100 ms^{-1}. Internally, the rock avalanche is highly compacted and has chaotic structures, which are both typical characteristics of rock avalanche deposits studied elsewhere.

The LCRA1 deposit is thought to have dammed the Ryton River for a substantial period of time (of the order of years), before the river began to significantly erode the dam. A lake beach at 557 m (a.s.l) is unrelated to higher levels of "Greater Lake Coleridge", and suggests a significant period of damming of the Ryton River by the LCRA1 deposit. The lake that developed from the ponded Ryton River covered an area of ~1.1 km^2 and had a volume of ~17 M m^3, assuming present day valley topography. Overtopping failure is calculated to have occurred within ~100 days using the formula of DAVIES and SCOTT (1997), and making the following assumptions:

- There was no significant seepage of water through the "dam".
- Mean annual flow conditions (Mar) were assumed to represent actual flow conditions, and to be a realistic estimation for overtopping calculations.
- The 100 year flood provided the worst case scenario for the flow of the Ryton River.

6.4 The Lake Coleridge Rock Avalanche 2 and 3 Deposits

The LCRA2 and LCRA3 deposits are discussed together due to both their small size relative to the LCRA1 deposit, and more importantly because they are believed to have occurred very close together in time.

The LCRA2 deposit was dated at 668 ± 36 years B.P. from a piece of mānuka taken from the rock avalanche debris within the recently-eroded cliffs that line the Ryton River. Like the LCRA1 event, the source area was the southern flank of Carriage Drive. The debris failed from the summit of Carriage Drive and followed the

runout path of the preceding rock avalanche, although the runout width of the LCRA2 debris was constricted by levees and it may have actually enhanced or created the levee deposits during runout. The debris crossed the Ryton River and was confined within the low-lying topography formed by erosion of the Ryton River into LCRA1 debris. Topographic constraint of the LCRA2 runout is clearly indicated by the well-developed "brandung" feature, where the debris has run up the river-eroded cliffs of the preceding rock avalanche deposit.

The calculated volume for the LCRA2 deposit is 0.66 x 10^6 m^3, but like the LCRA1 deposit a significant portion of the debris has been eroded by the Ryton River, leaving an estimated 0.4 x 10^6 m^3 present today. The planimetric surface area of the present day deposit is ~50,000 m^2, the LCRA2 event has a Fahrböschung of 19°, and a calculated excess travel distance (L_e) of 639 m. The LCRA2 was also compared to European rock avalanches, and like the LCRA1 deposit shows high mobility. Internally, the rock avalanche displays "inverse stratification", which resembles the alternating bedding characteristic of the Torlesse Supergroup source strata.

The LCRA2 event is believed to have created a temporary dam within the Ryton riverbed, after the emplacement of the debris. The maximum "dam" height of ~7 m is thought to have been at or about R.L 540 m (a.s.l), and ponding of the Ryton River was therefore less significant than the LCRA1 damming. The planimetric surface of the temporary lake calculated using present-day valley topography was 0.46 km^2, with a volume of ~2.3 M m^3. The water is estimated to have overtopped the dam structure after approximately two weeks, with a subsequent dam-break "outwash" flood recorded by the presence of three dam-break "outwash" terraces directly downstream of the LCRA2 deposit.

The existence of the LCRA3 deposit provides evidence for a third rock avalanche event from Carriage Drive. The deposit is only clearly defined on the surface within the cliffs eroded by the Ryton River, where the deposit has a thickness of ~2 m. Away from the cliff locality there are no geomorphological features that define the deposit, and the absence of morphology combined with the obvious smallness in size prevented any statistical study on the LCRA3 deposit.

The LCRA3 event is interpreted to have occurred very soon after the LCRA2 event because of both the size and its location within the same runout area as the LCRA2 deposit. The LCRA3 deposit may well represent a lag deposit from the second rock avalanche event, and the Ryton River is believed to have already been "dammed" by the LCRA2 deposit at the time.

6.5 Failure Causes and Chronology

An objective of this study was to determine whether the three rock avalanche events at the LCRAD site were coseismic, although it is acknowledged that there are other triggering mechanisms for rock avalanche events, such as oversteepening of slopes and progressive dilation of the rock mass which incorporates weathering and storm effects. However, considering the regional seismicity, the most likely single triggering mechanism identified for rock avalanche initiation is seismic shaking.

From the optically stimulated luminescence date of 9,720 ± 750 years B.P. obtained from sandy "loess" underlying the LCRA1 deposit, and from other evidence such as the lack of organic material and a proper soil development within this horizon, the LCRA1 event was interpreted to have failed shortly after the retreat of Acheron 3 glacial ice. Glacially steepened slopes on Carriage Drive, combined with rapid internal stress changes within the rock mass from the removal of ice support on the valley walls and the unfavourably oriented bedding and defect sets, may have initiated the LCRA1 failure by dilation. A seismic trigger is also a possible cause of failure of the dilated rock mass, but this study has been unable to identify such an earthquake event.

The age of the LCRA2 deposit was established from a radiocarbon date of 668 ± 36 years B.P. (Wk14221). Dilation of the rock mass is thought to have been the precursor condition within Carriage Drive due to continued gravitational toppling to depths of tens of metres. However the LCRA2 event occurred during a period of high seismicity, which numerous authors have identified between 500 and 700 years B.P. This seismic activity occurred both along the western segment of the PPAFZ, with rupture dates of 1,152 ± 51 years and 600 ± 100 years B.P. (SMITH, 2003), and the Alpine Fault whose most recent ruptures are considered to be well constrained at 850 years B.P., 500 years B.P., 330 years B.P. and 253 years B.P. (YETTON *et al.*, 1998).

Dating of organic material dragged into a fault plane across the Carriage Drive Fault also indicated that the last rupture on the Carriage Drive Fault post-dated 755 ± 46 years B.P. The rupture along the Carriage Drive Fault may also be a potential trigger for the LCRA2 event. Therefore, given both the age of the LCRA2 deposit and its proximity to major active fault systems, seismicity is the preferred triggering mechanism.

As discussed both above and elsewhere in this thesis, the LCRA3 deposit is considered to have failed soon after the LCRA2 event. Although limited in geographic extent and geomorphological expression, the deposit is interpreted to be a lag deposit of the LCRA2 event. If this is the case, then further source area collapse and/or seismic aftershocks from the main rupture which initiated the LCRA2 event are probable triggering mechanisms for the LCRA3 event.

6.6 Future Hazards at the Lake Coleridge Rock Avalanche site

Within the source area for the Lake Coleridge Rock Avalanche deposits on Carriage Drive, a future potential rock avalanche has been identified. Continued dilation by gravitational toppling-style failure is occurring along the sub-vertical argillite beds on the two main ridgelines of Carriage Drive, and has produced a wedge-block of material which has become detached from the *in situ* rock mass. This block is estimated to be ~35,000 ± 5,000 m^3 in volume. However, in the event of an earthquake, seismic shaking may initiate additional detachment of *in situ* bedrock from the source area, and the subsequent rock avalanche could potentially be very much larger.

A hazard assessment of a future rock avalanche at the LCRAD site was conducted for two main reasons. The identification of the detached block at the summit of Carriage Drive indicates that continued dilation of the rock mass is occurring, and that there is the *real* potential for a further rock avalanche event. The site is also vulnerable with respect to the location of the depositional zone in an area of human activity.

Three different-sized failure scenarios were applied to a future rock avalanche event at the site, termed scenarios 1, 2 and 3 respectively. Scenario 1 is a very small

rock avalanche with a source volume of 10,000 m^3. The deposit of the scenario 1 event would be contained within the Ryton riverbed, and would cause minimal disturbance to the Ryton River, with the debris "dam" lasting only minutes. Scenario 2 has a source volume of 100,000 m^3 and is also contained within the riverbed. However, depending on the characteristics of the debris deposition, the blockage within the river could be quite significant with a "dam" height of ~7 m or even higher, but if spreading and/or a "natural" spillway develop the effects of damming the Ryton River will obviously be smaller. Scenario 3 is believed to represent a serious scenario for a rock avalanche event at the site, with a source volume of 1,000,000 m^3. A rock avalanche with this order of magnitude will not only create a serious hazard (as would the first two events), but will not be contained within the riverbed and will bury the Ryton Bay Road with rock avalanche debris.

An emergency (EM) response plan was devised to cover all three scenarios, as the approach to deal with the immediate aftermath of a rock avalanche event at the site remains the same. Long-term management strategies for the riverbed after a rock avalanche event of varying magnitude were also developed. Scenario 1 required little mitigation (if any), but scenario 2 will require either the development of an "artificial" spillway and/or possible flood protection of the camping ground. Scenario 3 showed that such an event would have a catastrophic effect at the site, and relocation of the camping ground is recommended before a future rock avalanche occurs.

6.7 Future Work

There is potential for further work within the Lake Coleridge rock avalanche deposit area, specifically:

- Although a model has been presented within this study, the nature of the Carriage Drive Fault is still uncertain and should be further investigated.
- Fundamental glacial studies undertaken within the Rakaia Valley, such as those by SOONS (1963) and subsequent workers, have not considered the glacial sequences or chronology within the tributary valleys surrounding the LCRAD site. These warrant investigation to identify meltwater channels and other glacial geomorphological features, as will the detailed history or ice advance and retreat.

- As highlighted by the hazard analysis associated with the LCRAD site, the relocation of the camping ground from Ryton Bay is considered a prudent option which should be considered seriously *before* a future rock avalanche event occurs. This is because of the severe flooding risk from a dam-break flood and/or the long-term increased risk of flooding after a rock avalanche event due to changes in the river behaviour.

References

Adams, J. (1981). Earthquake-Triggered Landslides Form Lakes in New Zealand. *Division of Seismology and Geothermal Studies*, Earth Physics Branch Department of Energy, Mines, and Resources, Ottawa KIA OY3, Canada.

Anderson, M. (1963). *A River rules my Life*. **In:** Eiby, G. (1990). The Lake Coleridge Earthquakes of 1946. *Bulletin of the New Zealand National Society for Earthquake Engineering,* 23: (2), 150-158.

Angeli, M.G.; Gasparetto, P.; Menotti, R.M.; Pasuto, A.; Silvano, S.; Soldati, M. (1996). **In:** Dikau, R.; Brunsden, D.; Schrott, L.; Ibsen, M. (editors) (1996). *Landslide Recognition: Identification, Movement and Causes.* Report No. 1 of the European Commission Environment Programme Contract No. EV5V-CT94-0454. John Wiley & Sons, New York, U.S.A.

Aitken, M.J. (1994). Optical Dating: A Non-Specialist Review. *Quaternary Geochronology (Quaternary Science Reviews),* 13: 503-508.

Aitken, M.J. (1998). An introduction to optical dating: the dating of Quaternary sediments by the use of photon-stimulated luminescence. **In:** Burbank, D.W. and Anderson, R.S. (2001). *Tectonic Geomorphology.* Blackwell Science Ltd, U.S.A.

Augustinus, P.C. (1992). The influence of rock mass strength on glacial valley cross-profile morphometry, a case study from the Southern Alps, New Zealand. *Earth Surface Processes and Landforms*, 17: 39-51.

Augustinus, P.C. (1995a). Rock mass strength and the stability of some glacial valley slopes. **In:** Ballantyne, C.K. (2002). Paraglacial Geomorphology. *Quaternary Science Reviews*, 21: 1935-2017.

Augustinus, P.C. (1995b).Glacial valley cross-profile development: the influence of in situ rock stress and rock mass strength, with examples from the Southern Alps, New Zealand. *Geomorphology*, 14: 87-97.

Ballantyne, C.K. (2002). Paraglacial Geomorphology. *Quaternary Science Reviews*, 21: 1935-2017.

Beck, A.C. (1967). Gravity faulting as a mechanism of topographic adjustment. *New Zealand Journal of Geology and Geophysics*, 11: 191-199.

Berryman, K.R.; Beanland, S.; Cooper, A.F.; Cutten, H.N.; Norris, R.J.; Wood, P.R. (1992). The Alpine fault, New Zealand: variations in Quaternary structural style and geomorphic expression. **In:** Pettinga, J.R.; Yetton, M.D.; Van Dissen, R.J.; Downes, G. (2001). Earthquake source identification and characterisation for the Canterbury region, South Island, New Zealand. *Bulletin of the New Zealand Society for Earthquake Engineering*, 34: 282-317.

Beschta, R.L. (1983). Channel changes following storm-induced hillslope erosion in the Upper Kowai Basin, Torlesse Range, New Zealand. *Journal of Hydrology (New Zealand).* 22: 93-111.

Bierman, P.R. (1994). Using *in situ* produced cosmogenic isotopes to estimate rates of landscape evolution; a review from the geomorphic perspective. *Journal of Geophysical Research,* 99: 13,885-13,896.

Bishop, D.G.; Bradshaw, J.D.; Landis, C.A. (1985). Provisional Terrane map of the South Island, New Zealand. **In**: Howell, D.G. (editor), *Tectonostratigraphic Terranes in the Circum-Pacific region.* Council for Minerals and Energy, Houston, Texas, pages 515-521.

Bock, C.G. (1977). Martinez Mountain rock avalanche. **In:** Hewitt, K. (2002). Styles of rock-avalanche depositional complexes conditioned by very rugged terrain, Karakoram Himalaya, Pakistan. *Geological Society of America Reviews in Engineering Geology*. 15: 345-377.

Boggs, S. (Jr). (1995). *Principles of Sedimentology and Stratigraphy* (2nd Edition). Prentice Hall, New Jersey, United States of America.

Boore, D. (1973). The effect of simple topography on seismic waves: Implications for the accelerations recorded at Pacoima dam, San-Fernando valley, California. **In:** Zaslavsky, Y. and Shapira, A. (2000). Experimental study of topographic amplification using the Israel seismic network. *Journal of Earthquake Engineering,* 4: (1), 43-65.

Boot, L. (1933). Map of part of the Southern Alps. *The Canterbury Mountaineer,* 2: (frontispiece).

Bovis, M.J. (1982). Uphill-facing (antislope) scarps in the coast mountains, southwest British Columbia. *Geological Society of America Bulletin,* 93: 804-812.

Bovis, M.J. (1990). Rock-slope deformation at Affliction Creek, southern Coast Mountains, British Columbia. *Canadian Journal of Earth Sciences,* 27: 243-254.

Bowden, M.J. (1983). *A Rakaia River and Catchment: A Resource Survey.* North Canterbury Catchment Board and Regional Water Board, 1-3. Christchurch, New Zealand.

Bowman, S. (1990). *Radiocarbon Dating: Interpreting the Past: Los Angeles.* University of California Press, London. England.

Bradshaw, J.D. (1989). Cretaceous geotectonic patterns in the New Zealand Region. *Tectonics,* 8: 803-820.

Bradshaw, J.D.; Adams, C.J.; Andrews P.B. (1981). Carboniferous to Cretaceous on the Pacific margin of Gondwana: the Rangitata phase of New Zealand. **In:** Cresswell, M. M. and Vella, P. (editors), *Gondwana Five; Selected Papers and Abstracts of Papers Presented at the Fifth International Gondwana Symposium,* p. 217-221.

Brady, B.H.G. and Brown, E.T. (1985). Rock Mechanics for Underground Mining. **In:** Kinakin, D. and Stead, D. (2004). Analysis of the distributions of stress in natural ridge forms: implications for the deformation mechanisms of rock slopes and the formation of *sackung. Geomorphology,* (Article in Press).

Britten, R. (2000). *Lake Coleridge: The Power, the People, the Land.* Hazard Press Ltd, Christchurch. New Zealand.

Brodzikowski, K. and Van Loon, A.J. (1987). A systematic classification of glacial and periglacial environments, facies and deposits. *Earth Science Reviews,* 24: 297-381.

Brooks, G.R. and Hickin, E.J. (1991). Debris avalanche impoundments of Squamish River, Mount Cayley area, southwestern British Columbia. *Canadian Journal of Earth Science,* 28: (9), 1375-1385.

Bull, W.B. (1996). Prehistoric earthquakes on the Alpine Fault, New Zealand. *Journal of Geophysical Research,* 101: (B3), 6037-6050.

Bull, W.B. (2000). Lichenometry: A New Way of Dating and Locating Prehistorical Earthquakes. **In:** *Quaternary Geochronology: Methods and Applications,* edited by Noller, J.S.; Sowers, J.M.; Lettis, W.R. AGU Reference Shelf, (2000) 4: 261-272.

Bull, W.B. and Brandon, M.T. (1998). Lichen dating of earthquake-generated regional rockfall events, Southern Alps, New Zealand. *Geological Society of America Bulletin,* 110: (1), 60-84.

Bull, W.B.; King, J.; Kong, F.; Moutoux, T.; Phillips, W.M. (1994). Lichen dating of coseismic landslide hazards in alpine mountains. *Geomorphology,* 10: 253-264.

Burbank, D.W. and Anderson, R.S. (2001). *Tectonic Geomorphology.* Blackwell Science Ltd, U.S.A.

Burrows, C.J. (1975). A 500–Year–Old Landslide in the Acheron River Valley, Canterbury. *New Zealand Journal of Geology and Geophysics,* 18: 357-360.

Burrows, C.J. (1979). A chronology for cool-climate episodes in the Southern Hemisphere 12,00 – 10,000 yr B.P. *Palaeogeography, Palaeoclimatology, Palaeoecology,* 27: (3-4), 287-347.

Burrows, C.J. (1983). Radiocarbon dates from Late Quaternary deposits in the Cass District, Canterbury, New Zealand. *New Zealand Journal of Botany,* 21: 443-454.

Burrows, C.J. (1995). A macrofossil flora from sediments in a lagoon marginal to Lake Coleridge, Canterbury, New Zealand. *New Zealand Journal of Botany,* 33: 519-522.

Burrows, C.J. (1996). Radiocarbon dates for Holocene fires and associated events, Canterbury, New Zealand. *New Zealand Journal of Botany*, 34: 111-121.

Burrows, C.J. and Maunder, B.R. (1975). The Recent Moraines of the Lyell and Ramsay Glaciers Rakaia Valley, Canterbury. *Journal of the Royal Society of New Zealand*, 5: (4), 479-491.

Burrows, C.J. and Russell, J.B. (1975). Moraines of the Upper Rakaia Valley. *Journal of the Royal Society of New Zealand*, 5: (4), 463-477.

Burrows, C.J. and Russell, J.B. (1990). Aranuian Vegetation history of the Arrowsmith Range, Canterbury I. Pollen diagrams, plant macrofossils, and buried soils from Prospect Hill. *New Zealand Journal of Botany*, 28: 323-345.

Carryer, S.J. (1967). The glacial deposits along the northern flank of the Mount Hutt Range. *New Zealand Journal of Geology and Geophysics*, 10: (4), 1136-1144.

Cerling, T.E. and Craig, G. (1994). Geomorphology and in-situ cosmogenic isotopes. *Annual Review of Earth and Planetary Sciences*, 22: 273-317.

Chamberlain, C.G. (1996). Seismic Hazard from Cross-Faulting in North Canterbury: Broader Implications from the Arthur's Pass Earthquake Sequence of 18 June 1994. Master's thesis, University of Canterbury. Christchurch, New Zealand.

Chigira, M. (1992). Long-term gravitational deformation of rocks by mass creep. *Engineering Geology*, 32: 157-184.

Chinn, T.J. (1981). Use of rock weathering rind thickness for Holocene absolute age dating in New Zealand. *Arctic and Alpine Research*, 13: 33-45.

Coates, G. (2002). *The Rise and Fall of the Southern Alps*. Canterbury University Press. Christchurch, New Zealand.

Colman, S.M. (1977). The development of weathering rinds on basalts and andesites and their use as a Quaternary dating method western United States. **In:** Chinn, T.J. (1981). Use of rock weathering rind thickness for Holocene absolute age dating in New Zealand. *Arctic and Alpine Research*, 13: 33-45.

Conner, H.E. (1965). Tussock Grasslands in the Middle Rakaia Valley, Canterbury, New Zealand. **In:** Bowden, M.J. (1983). *A Rakaia River and Catchment: A Resource Survey*. North Canterbury Catchment Board and Regional Water Board, 1-3. Christchurch, New Zealand.

Costa, J.E. (1988). Floods from Dam Failures. **In:** *Flood Geomorphology*, Baker, V.R.; Kochel, C.; Patton, P.C. (editors), John Wiley & Sons, New York p. 503.

Costa, J.E., Schuster, R.L. (1988). The formation and failure of natural dams. *Geological Society of America Bulletin*, 100: 1954-1068.

Cotton, C.A. (1950). Tectonic scarps and fault valleys. *Geological Society of America Bulletin*, 61: 717-758.

Cowan, H.A. (1992). Structure, Seismicity and Tectonics of the Porter's Pass-Amberley Fault Zone, North Canterbury, New Zealand. PhD thesis, University of Canterbury, New Zealand.

Cowan, H.A.; Nicol, A.; Tonkin, P. (1996). A comparison of historical and paleoseismicity in a newly formed fault zone and a mature fault zone, North Canterbury, New Zealand. *Journal of Geophysical Research*, 101: 6021-6036.

Cox, P.T. (1926). Geology of the Rakaia Gorge District. *Transactions of the New Zealand Institute,* 56: 91-111.

Coyle, S.A. (1988). The Porters Pass Fault. Master's thesis, University of Canterbury. Christchurch, New Zealand.

Crozier, M. (1991). Determination of palaeoseismicity from landslides. **In:** *Landslides.* Bell, D.H. (editor), Proceedings of 6th International Symposium on Landslides, Christchurch. Balkema, Vol. 12. pp. 1173-1180.

Cruden, D.M. (1982). The Brazeau Lake slide, Jasper National Park, Alberta. **In:** Hewitt, K. (2002). Styles of rock-avalanche depositional complexes conditioned by very rugged terrain, Karakoram Himalaya, Pakistan. *Geological Society of America Reviews in Engineering Geology*. 15: 345-377.

Cruden, D.M. and Varnes, D.J. (1996). Landslide types and processes. **In**: *Landslides: Investigations and Mitigation.* Turner, A.K. and Schuster, R.L. (editors), Transportation Research Board, Special Report 247, National Research Council, Washington, D.C., pp. 36-75.

Davies, T.R. (2002). Landslide-dambreak floods at Franz Josef Glacier township, Westland, New Zealand: a risk assessment. *Journal of Hydrology (NZ),* 41: (1), 1-17.

Davies, T.R.; McSaveney, M.J. (1999). Runout of dry granular avalanches. *Canadian Geotechnical Journal*, 36: 313-320.

Davies, T.R. and McSaveney, M.J. (2002). Dynamic simulation of the motion of fragmenting rock avalanches. *Canadian Geotechnical Journal*, 39: (4), 789-798.

Davies, T.R.; McSaveney, M.J.; Hodgson, K.A. (1999). A fragmentation-spreading model for long-runout rock avalanches. *Canadian Geotechnical Journal*, 36: (6), 1096-1110.

Davies, T.R. and Scott, B.K. (1997). Dambreak flood hazard from the Callery River, Westland, New Zealand. *Journal of Hydrology (NZ)*, 36: (1), 1-13.

DeMets, C.; Gordon, R.G.; Argus, D.F.; Stein, S. (1990). "Current plate motions". *Geophysical Journal International*, 101: 425-478.

DeMets, C.; Gordon, R.G.; Argus, D.F.; Stein, S. (1994). Effect of recent revisions to the geomagnetic time scale on estimates of current plate motions. *Geophysical Research Letters*, 21: 2191-2194.

Dikau, R.; Brunsden, D.; Schrott, L.; Ibsen, M. (editors) (1996). *Landslide Recognition: Identification, Movement and Causes.* Report No. 1 of the European Commission Environment Programme Contract No. EV5V-CT94-0454. John Wiley & Sons, New York, U.S.A.

Dobson, A.D. and Speight, R. (1924). The so-called "Railroad" at Rakaia Gorge. *Transactions of the New Zealand Institute,* 55: 627-630.

Eiby, G. (1990). The Lake Coleridge Earthquakes of 1946. *Bulletin of the New Zealand National Society for Earthquake Engineering,* 23: (2), 150-158.

Eisbacher, G.H. and Clague, J.J. (1984). *Destructive Mass Movement in High Mountains: Hazard Management*: Geological Survey of Canada, Ottawa. Canada.

Elvy, J.M. (1999). Tectonic Geomorphology and Palaeoseismic Investigations, Mount Hutt District, Canterbury. Master's thesis. University of Canterbury. Christchurch, New Zealand.

Evans, S.G. (1989). Rock avalanche runup record. **In:** Hewitt, K. (2002). Styles of rock-avalanche depositional complexes conditioned by very rugged terrain, Karakoram Himalaya, Pakistan. *Geological Society of America Reviews in Engineering Geology*. 15: 345-377.

Evans, S.G.; Hungr, O.; Enegren, E.G. (1994). Landslides in the Vancouver-Fraser Valley-Whistler region. **In:** Hewitt, K. (2002). Styles of rock-avalanche depositional complexes conditioned by very rugged terrain, Karakoram Himalaya, Pakistan. *Geological Society of America Reviews in Engineering Geology*. 15: 345-377.

Evans, S.; Hungr, O.; Clague, J.J. (2001). Dynamics of the 1984 rock avalanche and associated distal debris flow on Mount Cayley, British Columbia, Canada; implications for landslide hazard assessment on dissected volcanoes. *Engineering Geology,* 61: 29-51.

Fitzsimons, S.J. (1997). Late-Glacial and Early Holocene Glacier activity in the Southern Alps, New Zealand. *Quaternary International*, 38/39: 69-76.

Gage, M. (1951). The dwindling glaciers of the Upper Rakaia Valley, Canterbury, New Zealand. *Journal of Glaciology*, 1: (9), 504-507.

Gagnepain-Beyneix, J.; Lepine, J.C.; Nercessian, A.; Hirn, A. (1995). Experimental study of site effects in the Fort-de-France area (Martinique Island). **In:** Zaslavsky, Y. and Shapira, A. (2000). Experimental study of topographic amplification using the Israel seismic network. *Journal of Earthquake Engineering,* 4: (1), 43-65.

Gerber, E. (1980). Geomorphic and geological effects of stresses, geomorphological problems in the alps. *Rock Mechanics.* Supplementum, 9: 93-107.

Govi, M.; Gullà, G.; Nicoletti, P.G. (2002). Val Pola rock avalanche of July 28, 1987, in Valtellina (Central Italian Alps). *Geological Society of America Reviews in Engineering Geology*, 15: 71-89.

Gregg, D.R. (1964). *Sheet 18. Hurunui. Geological Map of New Zealand.* Department of Scientific and Industrial Research. Wellington, New Zealand.

Haast, J.V. (1866). *Report on the headwaters of the River Rakaia.* Christchurch, New Zealand.

Hadley, J.B. (1964). Landslides and related phenomena accompanying the Hebgen Lake earthquake of August 17, 1959. **In:** Hewitt, K. (2002). Styles of rock-avalanche depositional complexes conditioned by very rugged terrain, Karakoram Himalaya, Pakistan. *Geological Society of America Reviews in Engineering Geology*. 15: 345-377.

Hancox, G.T.; Chinn, T.J.; McSaveney, M.J. (1991). Immediate report – Mt Cook rock avalanche, 14 December 1991. DSIR Geology and Geophysics, Lower Hutt, New Zealand.

Hancox, G.T.; Perrin, N.D.; Dellow, G.D. (2002). Recent studies of historical Earthquake-Induced Landsliding, Ground Damage, and MM Intensity in New Zealand. *Bulletin of the New Zealand Society for Earthquake Engineering*, 35: (2), 59-95.

Harrison, J.V. and Falcon, N.L. (1938). An ancient landslip at Saidmarreh in south-western Iran. **In:** Hewitt, K. (2002). Styles of rock-avalanche depositional complexes conditioned by very rugged terrain, Karakoram Himalaya, Pakistan. *Geological Society of America Reviews in Engineering Geology*. 15: 345-377.

Heim, A. (1882). Der Bergsturz von Elm. **In:** Hsü, K.J. (1975). Catastrophic debris streams (Sturzstroms) generated by rockfalls. *Geological Society of America Bulletin*, 86: 129-140.

Heim, A. (1932). *Bergsturz and Menschenleben*. Fretz and Wasmuth Verlag, Zürich, Switzerland, 218 p. (Translated in 1989 by N. Skermer as Landslides and human lives. Bitech Publishers Vancouver, B.C.).

Heuberger, H.; Masch, L.; Preuss, E.; Schrocker, A. (1984). Quaternary landslides and rock fusion in Central Nepal and the Tyrolean Alps. **In:** Hewitt, K. (2002). Styles of rock-avalanche depositional complexes conditioned by very rugged terrain, Karakoram Himalaya, Pakistan. *Geological Society of America Reviews in Engineering Geology*. 15: 345-377.

Hewitt, K. (1998). Catastrophic landslides and their effects on the Upper Indus streams, Karakoram Himalaya, northern Pakistan. *Geomorphology*, 26: 47-80.

Hewitt, K. (2002). Styles of rock-avalanche depositional complexes conditioned by very rugged terrain, Karakoram Himalaya, Pakistan. *Geological Society of America Reviews in Engineering Geology*. 15: 345-377.

Hoek, E. (2000). *Rock Engineering: Course notes by Evert Hoek*. http://www.rocscience.com/hoek/PracticalRockEngineering.asp (10/03/2003).

Hogg, A.G. (1982). *Radiocarbon Dating At University of Waikato, New Zealand*, University of Waikato, Hamilton.

Hovius, N.; Stark, C.P.; Allen, P.A. (1997). Sediment flux from a mountain belt derived by landslide mapping. *Geology*, 25: 231-234.

Howard, M.E. (2001). Holocene Surface-Faulting Earthquakes Along the Porters Pass Fault. Master's thesis. University of Canterbury. Christchurch, New Zealand.

Howell, D.G. (1981). Submarine fan facies in the Torlesse terrane, New Zealand. *Journal of the Royal Society of New Zealand,* 13: 107-127.

Hsü, K.J. (1975). Catastrophic debris streams (Sturzstroms) generated by rockfalls. *Geological Society of America Bulletin,* 86: 129-140.

Hungr, O. (1990). Mobility of Rock Avalanches. *Report of the National Research Institute for Earth Science and Disaster Prevention.* No. 46: 11-19.

Hungr, O. (1995). A model for the runout analysis of rapid flow slides, debris flows, and avalanches. *Canadian Geotechnical Journal,* 32: 610-623.

Hungr, O.; Evans, S.G.; Bovis, M.J.; Hutchinson, J.N. (2001). A review of the classification of landslides of the flow type. *Environmental and Engineering Geoscience,* 7: 221-238.

Hutchinson, J.N. (1988). General Report: Morphological and geotechnical parameters of landslides in relation to geology and hydrology. **In:** Bonnard (ed) Landslides, Proceedings, 5th International Symposium on Landslides, Lausanne, Volume 1, p. 3-35.

Imbrie, J.; Hays, J.D.; Martinson, D.G.; McIntrye, A.; Mix, A.C.; Morley, J.H.; Prell, W.L.; Shackleton, N.J. (1984). The orbital theory of Pleistocene climate: Support from a revised chronology of the marine δ18O record. **In:** *Milankivitch and Climate.* Berger, A.L., (editor), p. 269-305. Riedel, Dordrecht.

Issler, N.A. (2004). Deformation of the Torlesse Terrane in the Mt Hutt Range, Central Canterbury, New Zealand. Master's thesis, University of Canterbury. Christchurch, New Zealand.

Jacoby, G.C. (2000). Dendrochronology. **In:** *Quaternary Geochronology: Methods and Applications,* Noller, J. S. Sowers, J.M. Lettis, W.R. (editors), AGU Reference Shelf, 4: 11-20.

Jibson, R.W. (1996). Use of landslides for paleoseismic analysis. *Engineering Geology,* 43:291-323.

Jones, L.S. and Schumm, S.A. (1999). Causes of avulsion: an overview. **In:** *Fluvial Sedimentology.* Smith, N.D. and Rogers, J. (editors), VI: International Association of Sedimentologists Special Publication. Vol. 28. Blackwell, Oxford, pp. 171-178.

Keffer, D.K. (1984). Rock avalanches caused by earthquakes: source characteristics. *Science,* 223: 1288-1289.

Kent, P.E. (1966). The transport mechanism in catastrophic rock falls. *Journal of Geology,* 74: 79-83.

Kilburn, C.R.J. and Sorensen, S.A. (1998). Runout lengths of Sturzstroms: the control of initial conditions and of fragment dynamics. *Journal of Geophysical Research,* 103: 17877-17884.

Kinakin, D. and Stead, D. (2004). Analysis of the distributions of stress in natural ridge forms: implications for the deformation mechanisms of rock slopes and the formation of *sackung*. *Geomorphology,* (Article in Press).

Korup, O. (2002). Recent research on landslide dams – a literature review with special attention to New Zealand. *Progress in physical Geography*, 26: (2), 206-235.

Korup, O. (2004). Landslide-induced river channel avulsions in mountain catchments of southwest New Zealand. *Geomorphology*, 63: 57-80.

Korup, O.; McSaveney, M.J.; Davies, T.R.H. (2004). Sediment generation and delivery from large historic landslides in the Southern Alps, New Zealand. *Geomorphology*, 64: (1-2), 189-207.

Kramer, S.L. (1996). *Geotechnical Earthquake Engineering*. Prentice Hall, Upper Saddle River, N.J.

Lal, D. (1991). Cosmic ray labelling of erosion surfaces: *in situ* nuclide production rates and erosion. *Earth and Planetary Science Letters*, 104: 424-439.

Lang, A.; Moya, J.; Corominas, J.; Schrott, L.; Dikau, R. (1999). Classic and new dating methods for assessing the temporal occurrence of mass movements. *Geomorphology*, 30: 33-52.

Lauder, W.R. (1962). Teschenites from Acheron River, Mid-Canterbury, New Zealand, with Notes on the Geology of the Surrounding Country. *Transactions of the Royal Society of New Zealand (Geology)*, 1: (1), 109-127.

Li, T. (1983). A mathematical model for predicting the extent of a major rockfall. **In:** Hungr, O. (1990). Mobility of Rock Avalanches. *Report of the National Research Institute for Earth Science and Disaster Prevention*. No. 46: 11-19.

Lian, O.B. and Shane, P.A. (2000). Optical dating of paleosols bracketing the widespread Rotoehu tephra, North Island, New Zealand. *Quaternary Science Reviews*, 19, 1649-1662.

Lintott, W.H. and Burrows, C.J. (1973). A pollen diagram and macrofossils from Kettlehole Bog, Cass, South Island, New Zealand. *New Zealand Journal of Botany*, 11: 269-282.

Locke, W.W. (III) Andrews, J.T., Webber, P.J. (1979). A manual for lichenometry. **In:** Burbank, D.W. and Anderson, R.S. (2001). *Tectonic Geomorphology*. Blackwell Science Ltd, U.S.A.

Lowe, J.J. and Walker, M.J.C. (1997). *Reconstructing Quaternary Environments* (2nd Edition). Addison Wesley Longman Limited, Harlow, Essex, England.

Lucchitta, B.K. (1979). Landslides in Valles Marineris, Mars. **In:** Hewitt, K. (2002). Styles of rock-avalanche depositional complexes conditioned by very rugged terrain, Karakoram Himalaya, Pakistan. *Geological Society of America Reviews in Engineering Geology*. 15: 345-377.

MacBeth, I.L. (1988). Coastal analogies?: Beaches of Lake Coleridge. Master's thesis, University of Canterbury. Christchurch, New Zealand.

MacKinnon, T.C. (1983). Origin of the Torlesse terrane and coeval rocks, South Island, New Zealand. *Geological Society of America Bulletin*, 94: 967-985.

McConnell, R.G. and Brook, R.W. (1904). Report on the great landslide at Frank, Alberta, Canada. **In:** Hewitt, K. (2002). Styles of rock-avalanche depositional complexes conditioned by very rugged terrain, Karakoram Himalaya, Pakistan. *Geological Society of America Reviews in Engineering Geology*. 15: 345-377.

McFadgen, B.G. (1982). Dating New Zealand archaeology by radiocarbon. *New Zealand Journal of Science,* 25: (4), 379-392.

McKerchar, A.I. and Pearson, C.P. (1989). *Flood Frequency in New Zealand.* Publication No. 20 of the Hydrology Centre, Christchurch, New Zealand.

McSaveney, M.J. (1978). Sherman Glacier rock avalanche, Alaska, U.S.A. **In:** Voight, B. (editor) *Rockslides and avalanches*, 1. Vol 14A, Dev. Geotech. Eng, 197-258.

McSaveney, M.J. (1992). A manual for weathering-rind dating of grey sandstones of the Torlesse Supergroup, New Zealand. *Institute of Geological and Nuclear Sciences, Science Report*, Report: 92/4, 52 pp.

McSaveney, M.J. (1992). The Mount Fletcher rock avalanche of 2 May 1992. Immediate Report, New Zealand Department of Scientific and Industrial Research, *Geology and Geophysics*, pp 22.

McSaveney, M.J. (1993). Rock avalanches of 2 May and 6 September 1992, Mount Fletcher, New Zealand. *Landslide News*, 7: 2-4.

McSaveney, M.J. (2002). Recent rockfalls and rock avalanches in Mount Cook National Park, New Zealand. *Geological Society of America Reviews in engineering Geology*, 15: 35-70.

Melosh, H.J. (1987). The mechanics of large rock avalanches. *Reviews in Engineering Geology,* 7: 41-49.

Mitchell, W.A.; Dunning, S.; Taylor, P.J.; McSaveney, M.J.; Strom, A. (2001). Investigation of rock avalanches in high mountains. *Geological Society of America and Geological Society of London, International (III)*

Moar, N.T. (1971). Contributions to the Quaternary history of the New Zealand flora. *New Zealand Journal of Botany,* 9: 80-145.

Mollard, J.D. (1977). Regional landslide types in Canada. **In:** Hewitt, K. (2002). Styles of rock-avalanche depositional complexes conditioned by very rugged terrain, Karakoram Himalaya, Pakistan. *Geological Society of America Reviews in Engineering Geology*. 15: 345-377.

Morris, J.D. (1991) Applications of ^{10}Be to problems in the earth sciences. *Annual Review of Earth and Planetary Sciences,* 19: 181-187.

Murck, B.W.; Skinner, B.J.; Porter, S.C. (1997). *Dangerous Earth: An Introduction to Geologic Hazards*. John Wiley & Sons, INC. New York, USA.

Murray-Wallace, C.V.; Banerjee, D.; Bourman, R.P.; Olley, J.M.; Brooke, B.P. (2002). *Quaternary Science Reviews,* 21:1077-1086.

Nash, T.R. (2003). Engineering Geological Assessment of Selected Landslide Dams Formed from the 1929 Murchison and 1968 Inangahua Earthquakes. Master's thesis, University of Canterbury. Christchurch, New Zealand.

New Zealand Meteorological Service. (1980). Summaries of climatological observations to 1980. NZ Meteorological Service Miscellaneous Publication. 177.

Nicholson, C. and Seeber, P.W. (1989). Evidence for Contemporary Block Rotation in Strike-Slip Environments: Examples from the San Andreas Fault System, Southern California. **In:** Kissel, C. and Laj, C. (editors), *Paleomagnetic Rotations and Continental Deformation.* Kluwer Academic Publishers, pp. 247-280.

Nicholson, C.; Seeber, P.W.; Sykes, L.R. (1986). Seismicity and Fault Kinematics Through the Eastern Traverse Ranges, California: Block Rotation, Strike-Slip Faulting and Low-Angle Thrusts. *Journal of Geophysical Research,* 91: (B5), 4891-4908.

Nicol, A.; Howard, M.; Campbell, J.; Pettinga, J. (2001). Paleoearthquakes on the Porters Pass Fault. Christchurch, IGNS, p. 28.

Nicoletti, P.G. and Sorriso-Valvo, M. (1991). Geomorphic controls of the shape and mobility of rock avalanches. *Geological Society of America Bulletin,* 103: 1365-1373.

Noller. J.S.; Sowers, J.M.; Lettis, W.R. (editors). (2000). *Quaternary Geochronology: Methods and Applications.* American Geophysical Union, Washington, D.C, America.

Norris, R.J. and Cooper, A.F. (1995). Origin of small-scale segmentation and transpressional thrusting along the Alpine Fault, New Zealand. *Geological Society of America Bulletin,* 107: (2), 231-240.

Norris, R.R.; Koons, P.O.; Cooper, A.F. (1990). The obliquely convergent plate boundary in the South Island of New Zealand: Implications for ancient collision zones. *Journal of Structural Geology,* 12: 715-725.

Noverraz, F. and Bonnard, C. (1991). L'écroulement rocheux de Randa, près de Zermatt. **In:** *Landslides.* Bell, D.H. (editor), Proceedings of 6th International Symposium on Landslides, Christchurch. Balkema, Vol. 12. pp. 165-170.

Orwin, J.F. (1998). The application and implications of rock weathering-rind dating to a large rock avalanche, Craigieburn Range, Canterbury, New Zealand. *New Zealand Journal of Geology and Geophysics,* 41: 219-223.

Pearce, A.J. and Watson, A.J. (1986). Effects of earthquake-induced landslides on sediment budget and transport over a 50-yr period. *Geology,* 14: 52-55.

Pettinga, J.R.; Yetton, M.D.; Van Dissen, R.J.; Downes, G. (2001). Earthquake source identification and characterisation for the Canterbury region, South Island, New Zealand. *Bulletin of the New Zealand Society for Earthquake Engineering,* 34: 282-317.

Porter, S.C. (1969). Relative dating of alpine drift sheets using weathering rinds. *Geological Society of America, Abstracts for 1968, Special Paper*, 121: p. 545

Porter, S.C. (1975). Glaciation limit in New Zealand's Southern Alps. *Arctic and Alpine Research*, 7: 33-37.

Porter, S.C. and An, Z. (1995). Correlation between climatic events in the North Atlantic and China during the last glaciation. *Nature (London)*, 375 (6529): 305-308.

Prebble, W.M. (1995). Landslides in New Zealand. Bell, D (ed). **In:** Proceedings of the International Symposium on Landslides. 6: 2101-2123.

Prescott, J.R. and Robertson, G.B. (1997). Sediment Dating by Luminescence: A Review. *Radiation Measurements*, 27: (5/6), 893-922.

Rains, R.B. (1967). The Late Pleistocene glacial sequence of the High Peak Valley, Canterbury. *New Zealand Journal of Geology and Geophysics*, 10: 1145-1158.

Reyners, M.; Robinson, R.; Pancha, A.; McGinty, P. (2002). Stresses and strains in a twisted subduction zone – Fiordland, New Zealand. *Geophysical Journal International,* 148: 637-648.

Ricker, K.E.; Chinn, T.J.; McSaveney, M.J. (1993). A Late Quaternary moraine sequence dated by rock weathering rinds, Craigieburn Range, New Zealand. *Canadian Journal of Earth Sciences,* 30: (9), 1861-1869.

Rogers, G.M. and McGlone, M.S. (1989). A postglacial vegetation history of the sourthern-central uplands of North Island, New Zealand. *Journal of the Royal Society of New Zealand*, 19: 229-248.

Ross, J. (1954). The physiography of the Selwyn catchment. Master's thesis, University of Canterbury. Christchurch, New Zealand.

Ruhe, R.V. (1965). Quaternary paleopedology. **In:** Lowe, J.J. and Walker, M.J.C. (1997). *Reconstructing Quaternary Environments* (2nd Edition). Addison Wesley Longman Limited, Harlow, Essex, England.

Scheidegger, A.E. (1963). On the tectonic stresses in the vicinity of a valley and a mountain range. Proceedings of the Royal Society of Victoria, 76: 141-143.

Schoeneich, Ph. (1991). La datation des glissements de terrain. **In:** *Landslides.* Bell, D.H. (editor), Proceedings of 6th International Symposium on Landslides, Christchurch. Balkema, Vol. 12. pp. 205-212.

Schuster, R.L. (1983). Landslide dams – a worldwide phenomenon. *Annual Symposium of the Japan Landslide Society, Kansai Branch, Osaka.* p. 1-23.

Schuster, R.L.; Logan, R.L.; Pringle, P.T. (1992). Prehistoric Rock Avalanches in the Olympic Mountains, Washington. *Science*, 258: 1620-1621.

Shreve, R.L. (1966). Sherman landslide, Alaska. *Science*, 154: 1639-1643.

Shreve, R.L. (1968). The Blackhawk landslide. *Geological Society of America, Special Paper*, 108: 47 p.

Simpson, C. and Schmid, S.M. (1983). An evaluation of criteria to deduce the sense of movement in sheared rocks. *Geological Society of America Bulletin,* 94: (11), 1281-1288.

Simpson, G.D.H.; Cooper, A.F.; Norris, R.J. (1994). Late Quaternary evolution of the Alpine Fault Zone at Paringa, South Westland, New Zealand. *New Zealand Journal of. Geology and Geophysics.* 37: 49–58.

Smith, G.M. (2003). The Coseismicity and Morphology of the Acheron Rock Avalanche Deposit in the Red Hill Valley, New Zealand. Master's thesis, University of Canterbury. Christchurch, New Zealand.

Soons, J.M. (1963). The Glacial Sequence in Part of the Rakaia Valley, Canterbury, New Zealand. *New Zealand Journal of Geology and Geophysics,* 6: 735-756.

Soons, J.M. and Burrows, C.J. (1978). Dates for Otiran deposits, including plant microfossils and macrofossils, from Rakaia Valley. *New Zealand Journal of Geology and Geophysics,* 21: (5), 607-615.

Soons, J.M. and Gullentops, F.W. (1973). Glacial advances in the Rakaia Valley, New Zealand. *New Zealand Journal of Geology and Geophysics,* 16: (3), 425-438.

Speight, R. (1910). The Mount Arrowsmith District. *Transactions of the New Zealand Institute,* 43: 315-378.

Speight, R. (1926). Varved Silts from the Rakaia Gorge. *Rec. Canterbury (N.Z) Mus.,* 3: 55-81.

Speight, R. (1933). The Rakaia Valley. *Transactions of the New Zealand Institute.,* 63: 457-496

Stirling, M.W.; McVerry, G.H.; Berryman, K.R. (2002). A New Seismic Hazard Model for New Zealand. *Bulletin of the Seismological Society of America,* 92: (5), 1878-1903.

Suggate, R.P. (1990). Late Pliocene and Quaternary Glaciations of New Zealand. *Quaternary Science Reviews,* 9: 175-197.

Stewart, J.P. (2004). Analysis of Topographic Effects On Ground Motions At The Pleasant Valley Pumping Plant, California. http://erp-web.er.usgs.gov/reports/annsum/vol40/nc/G0038.htm (27/04/04).

Terzaghi, K. (1950). Mechanism of Landslides. *The Geological Society of America Engineering Geology (Berkey) Volume,* 83-123.

Tonkin, P.J. and Basher, L.R. (1990). Soil-stratigraphic techniques in the study of soil and landform evolution across the Southern Alps, New Zealand. *Geomorphology,* 3: 547-575.

Trifunac, M.D. and Hudson, D.E. (1971). Analysis of the Pacoima Dam accelerogram, San Fernando, California, earthquake of 1971. **In:** Zaslavsky, Y. and Shapira, A. (2000). Experimental study of topographic amplification using the Israel seismic network. *Journal of Earthquake Engineering,* 4: (1), 43-65.

Turner, A.K. and Jayaprakash, G.P. (1996). Introduction. **In:** *Landslides: Investigation and Mitigation*, Special Report 247. Turner, A.K. and Schuster, R.L. (editors). National Academy Press, Washington D.C. pp. 3-11.

Turney, C.S.M.; McGlone, M.S.; Wilmshurst, J.M. (2003). Asynchronous climate change between New Zealand and the North Atlantic during the last deglaciation. *Geological Society of America,* 31: (3), 223-226.

Twiss, R.J. and Moores, E.M. (1992). *Structural Geology.* W.H. Freeman and Company, United States of America.

Varnes D.J. (1978). Slope movement types and processes. **In:** *Landslides; analysis and control.* Schuster, R.L. and Krizek, R.J. (editors). Special Report – Transportation Research Board, National Research Council, no 176: 11-33.

Voight, B. (1978). Rockslides and Avalanches: an introduction. **In:** *Rockslides and Avalanches: 1. Natural Phenomena,* Voight, B. (editor), Elsevier, New York, p. 833.

Voight, B. and Pariseau, W.G. (1978). Rockslides and avalanches – An introduction. **In:** *Rocksli des and Avalanches: 1. Natural Phenomena,* Voight, B. (editor), Elsevier, Amsterdam, 14A, p. 1-67.

Von Haast, J. (1879). *Geology of Canterbury and Westland.* The Times, Christchurch, New Zealand.

Wardle, P. and Campbell, A.D. (1976). Seasonal cycle of tolerance to low temperatures is three native woody plants, in relation to their ecology and post-glacial history. **In:** Burrows, C.J. and Russell, J.B. (1990). Aranuian Vegetation history of the Arrowsmith Range, Canterbury I. Pollen diagrams, plant macrofossils, and buried soils from Prospect Hill. *New Zealand Journal of Botany,* 28: 323-345.

Whitehouse, I.E. (1981). A large rock avalanche in the Craigieburn Range, Canterbury. *New Zealand Journal of Geology and Geophysics,* 24: 415-421.

Whitehouse, I.E. (1983). Distribution of large rock avalanche deposits in the central Southern Alps, New Zealand. *New Zealand Journal of Geology and Geophysics,* 26: 271-279.

Whitehouse, I.E. and Griffiths. G.A. (1983). Frequency and hazard of large rock avalanches in the central Southern Alps, New Zealand. *Geology,* 11: 331-334.

Whitehouse, I.E.; Knuepfer, P.L K.; McSaveney, M.J.; Chinn, T.J.H. Growth of weathering rinds on Torlesse Sandstone, Southern Alps, New Zealand. **In:** *Rates of chemical weathering of rocks and minerals,* Colman, S. M. and Dethier, D. P. (editors). Academic Press, Orlando, USA.

Williams, M.; Dunkerley, D.; Deckker, P.; Kershaw, P.; Chappel, J. (1998). *Quaternary Environments.* Arnold, Sydney, Australia.

Wintle, A.G. (1997). Luminescence Dating: Laboratory Procedures and Protocols. *Radiation Measurements,* 27: (5/6), 769-817.

Yetton, M.D.; Wells, A.; Traylen, N.J. (1998). The probability and consequences of the next Alpine Fault earthquake. EQC Research Project 95/193. Geotech Consulting Christchurch. p. 161.

Young, D.A. (1997). Structure and Tectonic Geomorphology of the Craigieburn Rangefront, Castle Hill Basin, North Canterbury. BSc(Hons) Thesis. University of Canterbury. Christchurch, New Zealand.

Zaslavsky, Y. and Shapira, A. (2000). Experimental study of topographic amplification using the Israel seismic network. *Journal of Earthquake Engineering,* 4: (1), 43-65.

Appendix A

A Geometric and geomorphologic characteristics of large rock avalanches in central Southern Alps from Whitehouse and Griffiths, 1983

APPENDIX A

Geometric and geomorphologic characteristics of large rock avalanches in central Southern Alps from WHITEHOUSE and GRIFFITHS (1983).

	Locality*	Deposit Area ($10^4 m^2$)	Thickness (metres)	Volume ($10^6 m^3$)	Volume Eroded ($10^6 m^3$)	Age (years B.P)	Dating Method
1	Poulter River (Thompson Stream)	48	10	5	0.7	21	1
2	Poulter River (Lake Minchin)	76	35	27	3	?	
3	Poulter River (Casey Hut)	228	10	23	9	4020 ± 90	2(1824)
4	Poulter River (Mt Binser)	55	10	5	-	?	
5	Taramakau River (Otehake River)	190	30	57	5	21	1
6	Waimakariri River (Hawdon Stream)	30	40	12	-	2750 ± 710	3
7	Waimakariri River (Mt Binser)	81	50	40	-	9000 ± 2340	3,4
8	Otira River	43	100	43	10	2000 ± 90	2(4258)
9	Taipo River (Hunts Creek)	63	50	35	2	3600 ± 940	3
10	Taipo River (Hunts Creek)	21	20	4	-	2750 ± 710	3
11	Waimakariri River (Crow River)	29	100	29	4	6100 ± 1580	3
12	Harper River (Cass Saddle)	22	10	2	-	5750 ± 1490	3
13	Taipo River (Julia Creek)	22	15	3	0.3	2750 ± 710	3
14	Broken River (Leith Hill)	90	5	4	-	3800 ± 990	3,5
15	Wilberforce River (Weka Stream)	38	50	19	5	2140 ± 560	3
16	Wilberforce River (Burnett Stream)	36	20	7	-	7270 ± 70	2,6(5509)
17	Avoca River	121	50	60	16	5500 ± 1430	3
18	Craigiebum Range	387	130	500	-	350 ± 90	3
19	Acheron River	61	10	6	0.6	532 ± 50	2(532)
20	Wilberforce River (Griffiths Stream A)	95	10	9	16	7870 ± 120	2(5009)
21	Wilberforce River (Griffiths Stream B)		25	24		10250 ± 150	2(5010)
22	**Lake Coleridge**	**23**	**20**	**4**	**0.7**	**150 ± 40**	**3**
23	Mathias River (Boundary Creek)	280	100	280	86	1500 ± 390	7
24	Mathias River (Mistake Creek)	54	20	11	2	2750 ± 710	3
25	Mathias River (Moraine Creek)	22	20	4	1	4400 ± 1140	3
26	Mathias River	37	10	4	1	3000 ± 780	7
27	Ashburton River (North Branch)	75	15	11	-	1560 ± 400	3
28	Ashburton River (North Branch)	5	30	1	0.3	150 ± 40	3
29	Ashburton River (South Branch)	70	10	7	3	5280 ± 105	2(1289)

	Locality*	Deposit Area ($10^4 m^2$)	Thickness (metres)	Volume ($10^6 m^3$)	Volume Eroded ($10^6 m^3$)	Age (years B.P)	Dating Method
30	Lawrence River	31	10	3	2	100 ± 260	3
31	Lawrence River	70	15	6	0.5	800 ± 210	3
32	Clyde River (McCoy Stream)	31	50	15	8	4900 ± 1280	3,8
33	Clyde River	50	20	10	3	356 ± 34	2(4902)
34	Rangitata River (Lake Camp)	38	5	2	-	1600 ± 420	3
35	Rangitata River (Pudding Valley)	122	10	10	-	1700 ± 440	3
36	Havelock River (Fan Stream)	26	35	9	4	1560 ± 400	3
37	Havelock River (Cloudy Stream)	35	30	10	-	3370 ± 880	3
38	Havelock River	38	20	8	3	?	
39	Havelock River (Forbes River)	13	10	1	0.4	550 ± 140	3
40	Rangitata River (Forest Creek)	81	10	7	-	1560 ± 400	3
41	Rangitata River ((Bush Stream)	330	30	99	-	3370 ± 880	3
42	Godley River (MacKinnon Stream)	26	40	10	2	150 ± 40	3
43	Godley River (Bloody Point)	84	25	21	4	1700 ± 440	3
44	Cass River	36	10	4	0.8	1200 ± 310	3
45	Jollie River	23	20	4	0.3	2750 ± 710	3
46	Jollie River	110	70	77	31	1700 ± 440	3

*Number refers to location on figure 1.6

1 Historical record: probably fell in 1929 Arthur's Pass earthquake

2 Radiocarbon date using new ^{14}C half-life. Corrected for secular variation. New Zealand Radiocarbon Dating Laboratory number given

3 Dated from thickness of weathering rinds on surface clasts using method of CHINN (1981). Rinds measured to 0.2 mm

4 Near maximum age datable by weathering rinds. May be older

5 Minimum age: weathering rinds from scree on avalanche scar

6 Minimum age: wood in silts from rock-avalanche-dammed lake

7 Weathering rinds measured to nearest 0.5 mm

8 Minimum age: rinds from moraine on top of avalanche deposit. Buried rinds indicate avalanche is at least 1,000 years older

Refer to WHITEHOUSE (1983) and WHITEHOUSE and GRIFFITHS (1983) for further details

Appendix B

B1 Raw dip and dip direction data collected on Carriage Drive for bedding

B2 Raw dip and dip direction data collection on Carriage Drive for joints

APPENDIX B1

Raw Data Collected On Carriage Drive for Bedding. Refer to figure B1 for locations.

ID	Dip direction	Dip
B1	032	74
B2	062	78
B3	050	68
B4	061	82
B5	041	77
B6	035	62
B7	030	42
B8	014	52
B9	022	56
B10	170	71
B11	038	84
B12	040	68
B13	090	80
B14*	248	59

*Overturned bedding measurement taken by CHAMBERLAIN (1996) and not included on Stereographic Plot (figure 2.2). Bedding with equivalent strike and dip recordings can also be found in figure 3.22.

Appendix B2

Raw Data Collected On Carriage Drive for Joints. Refer to figure B1 for locations.

ID	Dip direction	Dip
J1	094	88
J2	140	80
J3	118	76
J4	270	43
J5	285	60
J6	148	59
J7	224	50
J8	130	60
J9	276	70
J10	235	74
J11	296	82
J12	252	84
J13	066	70
J14	70	86
J15	130	90
J16	302	30
J17	330	30
J18	56	52
J19	290	34
J20	40	70
J21	204	48
J22	92	16

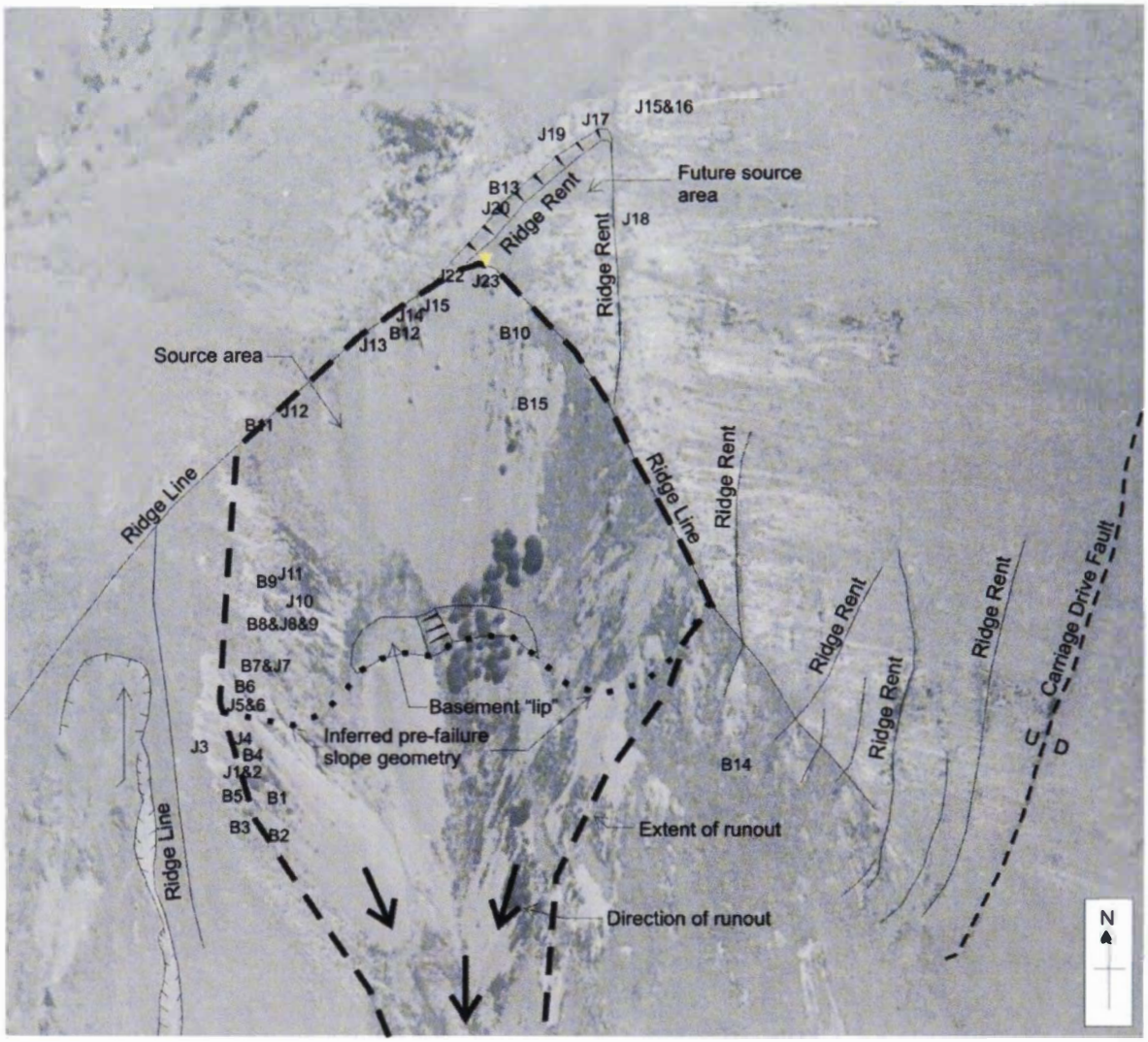

Figure B1: Bedding and Joint measurement locations on Carriage Drive. Refer also to figure 3.22.

Appendix C

C Oxygen isotope stages for China, North Atlantic and the Rakaia Valley in ELVY (1999) adopted from WILLIAMS *et al.* (1998) after PORTER and AN (1995)

APPENDIX C

Oxygen Isotope Stages for China, North Atlantic and the Rakaia Valley in ELVY (1999) from WILLIAMS *et al.* (1998) after PORTER and AN (1995)

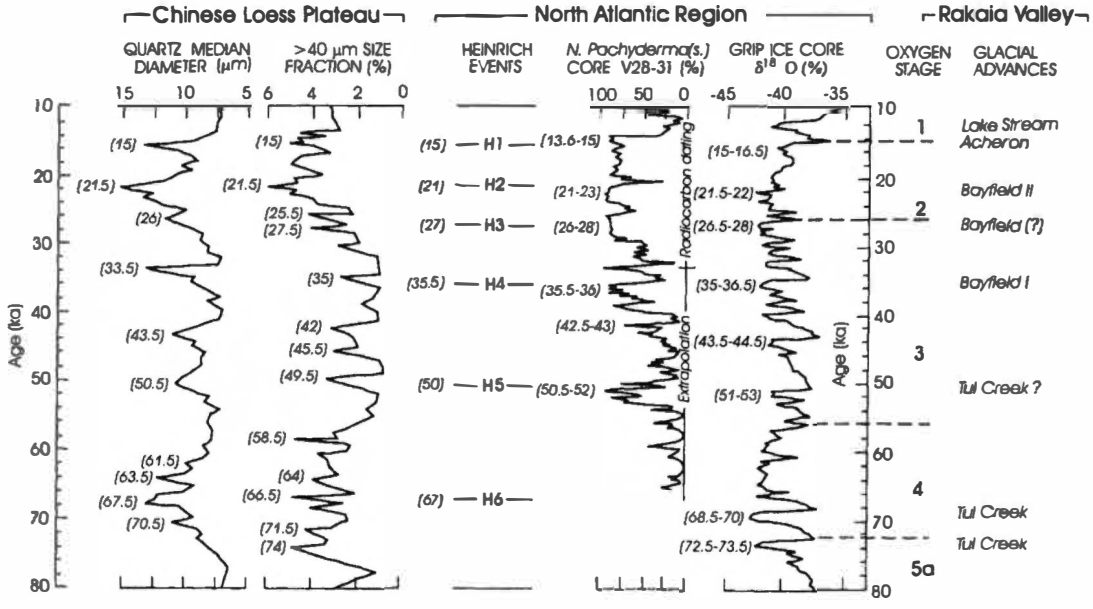

Record spanning the bulk of the last glacial. Loess data, including grain-size fluctuations taken to represent wind strength, are on the left. Records from the North Atlantic region, including the marine record of Heinrich events, and the GRIP (Greenland ice-core project) ice core O^{18} record are on the right. Commonly used oxygen isotope stages are tentatively correlated with the Rakaia Valley Glacial sequence by ELVY (1999).

Appendix D

D Limits of successive glacial advances in the Rakaia Valley from SOONS (1963)

APPENDIX D

Limits of Successive Glacial Advances in the Rakaia Valley from SOONS (1963)

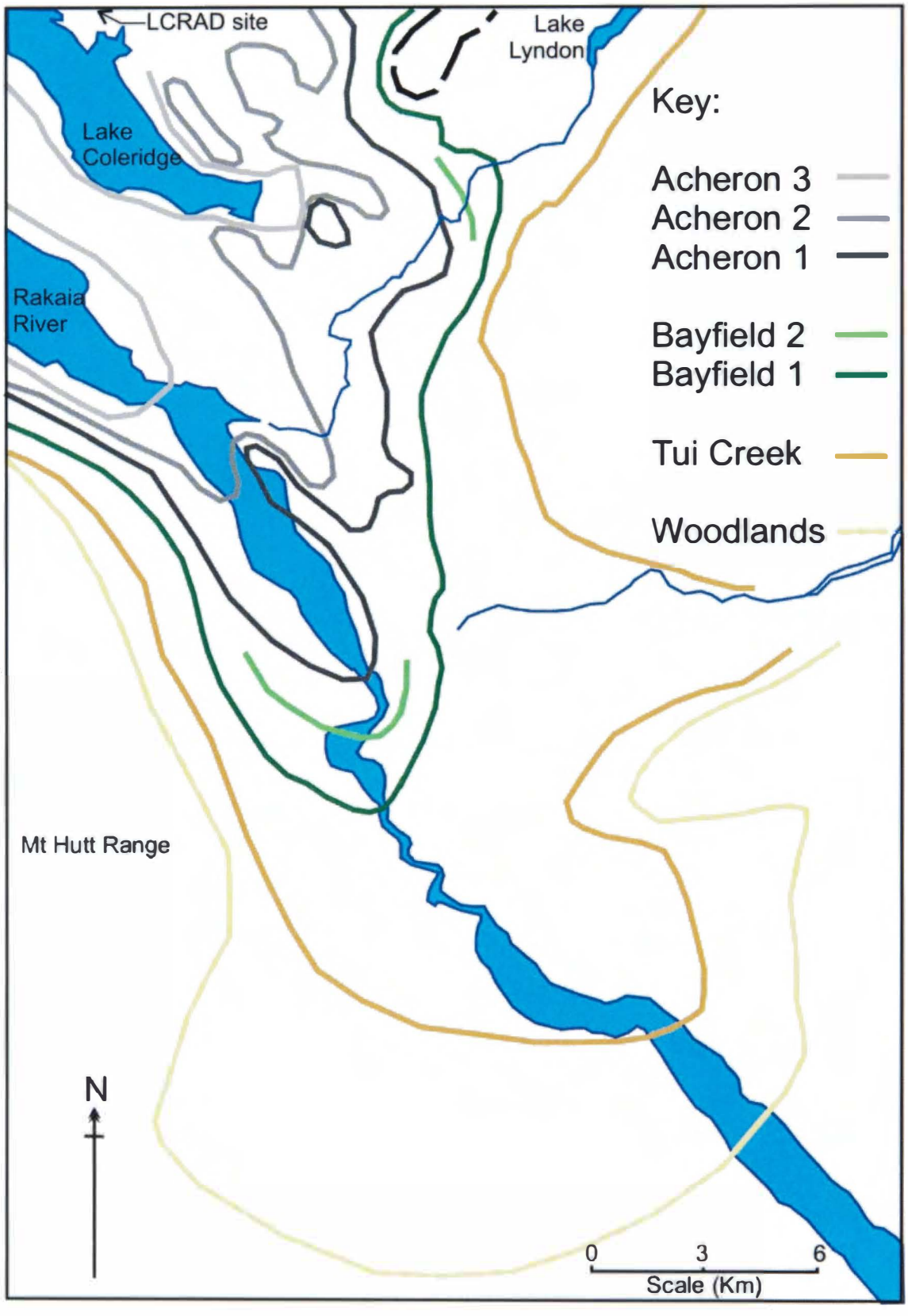

Appendix E

E Carriage Drive Fault Discussion

APPENDIX E

Carriage Drive Fault Discussion

The existence of the Carriage Drive Fault as a normal fault within a structural domain dominated by strike-slip transfer faults, oblique thrusts and/or reverse faults (PETTINGA *et al.*, 2001) is unusual. Therefore a brief discussion of the Carriage Drive Fault is necessary.

Limited information on the Carriage Drive Fault exists, which is possibly due to its small extent and apparent regional insignificance. However, due to the proximity of the Carriage Drive Fault to the source area for the Lake Coleridge Rock Avalanches it was necessary for this project to investigate it. The Carriage Drive Fault strikes at 140° and is ~900 m in exposure length. The southern end of the scarp intersects the ridgeline at an elevation of ~660 m where it disappears on the southern flank of Carriage Drive underneath scree slopes. The northern extent of the scarp is buried beneath younger fan deposits (figure 2.11) at an elevation of ~600 m, and it is not found again to the north.

The development of the Carriage Drive Fault, which is a normal fault within this widely documented compressional tectonic regime, is unusual. It is located in an area of oblique collision between the Australian and Pacific tectonic plates east of the Alpine Fault. In addition, within the North Canterbury region the change from oblique subduction to oblique continental collision is associated with tectonic shortening, thus causing crustal thickening and uplift (PETTINGA *et al.*, 2001). During the PETTINGA *et al.* (2001) study structural domains were assigned to the Canterbury region, and the Lake Coleridge area was placed in a domain which has hybrid strike-slip and thrust faulting. All the faults included in the PETTINGA *et al.* (2001) study found structures within the Lake Coleridge area were strike-slip, reverse, or a combination of both.

During the present study a trench (T_5) was excavated across the fault scarp, and a small basin or graben structure found between the bedrock footwall and the hanging wall consisting of colluvial gravel sheetwash (figure 2.12). Two horizons containing charcoal displayed drag deformation into the main fault plane with a visible maximum vertical displacement of ~1.8 m and a horizontal displacement of ~1.2 m. Two smaller normal faults located within the lower central portion of the trench

provide only centimetres of displacement within the sequence. As discussed in Chapters 2 and 4 the charcoal was dated at 755 ± 46 years B.P. (WK15118) for the upper horizon and 4,428 ± 35 years B.P. (Wk15119) for the lower horizon. This indicates rupture along the Carriage Drive Fault which post-dates the (WK15118) 755 ± 46 years B.P. charcoal horizon. However, little else could be gleaned from the excavation to provide information on the rupture history of the Carriage Drive Fault.

As discussed in Section 2.5.1 a regional northwest to southeast structural trend appears to control the major drainage patterns, for example the Wilberforce and Rakaia Rivers and the Lake Coleridge Trough (figure 2.5). Supporting this argument, SPEIGHT (1933) believed that the Rakaia Valley's alignment was caused by faulting rather than solely by glacial erosion. SOONS (1963) also pointed to evidence for such faulting from the straight flanks of the Mount Hutt and Big Ben Ranges which overlook the Valley, however no surface fault ruptures are identifiable which may be due to the presence of river, colluvial or outwash gravel deposits.

The appearance or surface expression of the Carriage Drive Fault, and trench excavations across the scarp (refer to figures 2.11 and 2.12), suggests that it is a normal fault, which appears to be somewhat of an anomaly in this area. A possible explanation for this occurrence can be taken from southern California. NICHOLSON *et al.* (1986) and NICHOLSON and SEEBER (1989) found evidence for contemporary block rotation in strike-slip environments (figure E1). Empirical evidence of block rotation by strike-slip faulting can occur on many different scales (figure E1) from millimetres to kilometres (NICHOLSON *et al.*, 1989). It is therefore possible to find localised normal fault extension, which is approximately perpendicular to the major through-going strike-slip faults, within a tectonically compressional regime. This pattern of faulting is similar to S-C foliation[♦] that is found in ductile shear zones (Mrs J. CAMPBELL, University of Canterbury, *pers. comm.*, 2004). Large-scale cross faulting has been identified in the northern region of the South Island, New Zealand, with numerous geological maps locating it in the Marlborough Fault Zone (MFZ).

[♦] S and C foliations are commonly found in ductile shear zones. S-foliation is a continuous coarse foliation which is defined by the preferred orientation of crystals and its dominant orientation is oblique to the ductile shear zone. C-foliation (C comes from the French term *cisaillement*, meaning, "shear") is a set of shear bands that develop subparallel to the boundaries of shear zones (TWISS and MOORES, 1992).

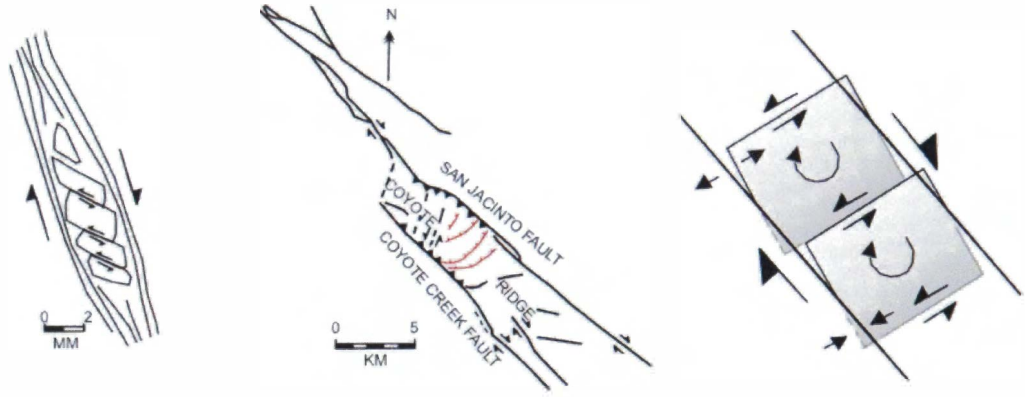

Figure E1: Two geological examples of block rotation by strike-slip faulting on scales from millimetres to kilometres, modified from NICHOLSON *et al.* (1986) **in** NICHOLSON and SEEBER, 1989. a) Fracture and rotation (or bookcasing) of a feldspar crystal along cleavage planes in a ductile matrix (SIMPSON and SCHMID, 1983 **in** NICHOLSON and SEEBER, 1989. b) Rotating blocks which are defined by secondary *cross faults* between an overlapping right-step from the two major strike-slip faults. **NB** arrows indicate slip movement and red lines indicate normal faulting. c) Schematic representation of block rotation. NICHOLSON *et al.* (1986) notes that during the interseismic period, the major through going strike-slip faults become locked which causes small blocks to rotation (modified from NICHOLSON *et al.* (1986)).

To compare the Carriage Drive Fault with the California example, the major through-going strike-slip faults are the Alpine Fault ~55 km to the northwest of the Carriage Drive Fault and the PPAFZ which is located ~9 km to the southeast of the Fault. The PPAFZ is believed to terminate on the western banks of the Rakaia River. Therefore, the similarities demonstrated from the Californian example from NICHOLSON *et al.* (1986), and NICHOLSON and SEEBER (1989), could be used to explain the presence of the Carriage Drive Fault in an otherwise strike-slip and thrust dominated tectonic regime.

Further evidence perhaps for extensional features within the area is the "Railroad" landform (grid reference K35: 993 473). Early investigations by VON HAAST (1879) suggested that the "Railroad" feature was glacial in origin, while DOBSON and SPEIGHT (1924) identified a number of aeolian features associated with the structure but deduced that it had to be tectonic in origin. It is a northwest to southeast trending depression which GREGG (1964) mapped as two sub-parallel active fault traces (in ELVY, 1999). In the most recent study of the "Railroad" structure, undertaken by ELVY (1999), the distinction between aeolian or tectonic (glacial origin had been discarded) was still not made as ELVY put forward two models for the development of the landform; 1) the "Railroad" structure is a tectonic graben like structure that was

enhanced by wind action, or 2) a landform purely created by wind action (ELVY, 1999).

The Carriage Drive Fault is a normal fault and perhaps the cross faulting examples from California and the MFZ provide a possible model for the occurrence of the fault.

Appendix F

F1 Data for 40 Rock Avalanches considered in NICOLETTI and SORRISO-VALVO (1991) and the LCRA1 and LCRA2 deposits from this study

F2 Relation of Travel Distance to size of Fallen Mass (modified from HSÜ, 1975)

APPENDIX F1

Data for 40 Rock Avalanches considered in NICOLETTI and SORRISO-VALVO (1991) and the LCRA1 and LCRA2 deposits from this study

Geo-morph* Control	Name and Date	Rock(s)	Breakaway Structures	V (10^6 m^3)	L (m)	D† (m)	H (m)	Le (m)	Le/L	H/L	Wm (m)	Wa (m)	Wm/Wa	Wm/L	Wm/D†	Wa/L	Wa/D†	Ice on path	Bends§ <<90°(-90°)	Stopping	Fall-back Ridges	Moraine	Seismic Trigger	Site	Main reference(s)
L	Pandemonium Cr., 1959	Gneiss	Fractures	6.7	8,600	-	2,000	5,400	0.63	0.23	250	780	0.32	-	0.03	-	0.09	Y	5(1)	Spontaneous	N	-	N	Coast Mts, B.C., Canada	Evans and other, 1989
L	Twin Slides (W), unk.	Carbon. r.	Dipsl. 25°	7	4,670	-	900	3,230	0.69	0.19	100	520	0.19	-	0.02	-	0.11	-	3	Spont.	N	-	Possible	Mackenzie Mts, N.W. Canada	Eisbacher, 1978, 1979
L	Twin Slides (E), unk.	Carbon. r.	Dipsl. 25°	7	4,400	-	820	3,080	0.70	0.19	100	460-	0.22	-	0.02	-	0.10	-	1(1)	Part. forced	N?	-	Possible	Mackenzie Mts, N.W.Canada	Eisbacher, 1978, 1979
	Antronapiana, 1642	Gneiss	Fractures	12	4,190	-	1,650	2,640	0.37	0.39	380	380	1.00	-	0.09	-	0.09	N	1	Spont.	N	-	N	West. Alps, Italy	Eisbacher and Clague, 1984
L	Huascaran, 1962	Grandodior.	Fractures 70°-80°	13	15,520	-	3,600	9,760	0.63	0.23	240	1,600	0.15	-	0.02	-	0.11	Y	2(1)	Spont.	N?	-	N	Cordillera Blanca, Peru	Plafker and Ericksen, 1978
L	Sherman, 1964	Sandstone Siltstone	Fractures	13.3	5,950	-	1,080	4,220	0.71	0.18	1,970	3,260	0.60	-	0.33	-	0.55	Y	1	Spont.	N	Y	Y	Chugach Mts., AK, USA	Shreve, 1966; McSaveney, 1978
L	Triolet Glac., 1717	Granite	Fractures	18	6,900	-	1,860	3,920	0.57	0.27	500	500	1.00	-	0.07	-	0.07	Y	1(1)	Spont.	N	-	N	Mt. Blanc Massif, Italy	Porter and Orombelli, 1980
L	Steller I, 1964	-	Fractures 40°-45°	20	6,700	-	1,200	4,780	0.71	0.18	1,610	2,000	0.81	-	0.24	-	0.30	Y	-	Spont.	N	-	Y	Chugach Mts., AK, USA	Post, 1967; Lucchitta, 1978
L	Allen 4, 1964 or 1965	-	Fractures -50°	23	7,700	-	1,300	5,620	0.73	0.17	1,140	1,430	0.80	-	0.15	-	0.19	Y	-	Spont.	N	-	Doubtful	Chugach Mts., AK, USA	Post, 1967; Lucchitta, 1978
L	Fairweather, 1964 or 1965	-	Fractures -45°	26	10,000	-	3,300	4,720	0.47	0.33	860	1,500	0.57	-	0.09	-	0.15	Y	4	Spont.	N	-	Doubtful	Chugach Mts., AK, USA	Post, 1967; Lucchitta, 1978
L	Schwan, 1964	-	Fractures -50°	27	6,100	-	1,550	3,620	0.59	0.25	1,670	2,000	0.83	-	0.27	-	0.33	Y	-	Spont.	N	-	Y	Chugach Mts., AK, USA	Post, 1967; Lucchitta, 1978
L	Devastation Gl., 1975	Soft volc, r.	Fractures?	27	6,100	-	1,190	4,200	0.69	0.20	-	-	-	-	-	-	-	Y	2	Spont.	N	-	N	Coast Mts., B.C., Canada	Mokievsky-Zubok, 1977
L	Diablerets, 1749	Limestone	Scarpsl.	30	5,500	-	1,200	3,580	0.65	0.22	650	1,910	0.34	-	0.12	-	0.35	N	2	Spont.	N	-	N	Valais, Switzerland	Heim, 1932; Eisbacher and Clague, 1984
L	Rubble Cr., 1855 or 1856	Dacite	Fractures -35°	33	6,900	-	1,040	5,240	0.76	0.15	180	1,500?	0.12?	-	0.03	-	0.22?	N	3	Spont.	N	Y	Possible	Coast Mts., Canada	Moore and Mathews, 1978
L	Nozzle, unk.	Carbon. r.	Dipsl. 27°	67	6,420	-	1,050	4,740	0.74	0.46	180	1,500	0.12	-	0.03	-	0.23	-	1(1)	Spont.	N	-	Possible	Mackenzie Mts., N.W. Canada	Eisbacher, 1979
L	Huascaran, 1970	Granodior.	Fractures 70°-80°	75	15,600	-	3,850	9,440	0.60	0.25	1,810	6,400	0.28	-	0.12	-	0.41	Y	-	Part. forced	Y	-	Y	Cordillera Blanca, Peru	Plafker and Ericksen, 1978
L	**Lake Coleridge Rock Avalanche 1, ~9,700 B.P.**	**Greywacke**	**Fractures/ Dipsl.**	**10**	**1,780**	**1,725**	**495**	**1,031**	**0.58**	**0.28**	**320**	**880**	**0.36**	**0.20**	**0.19**	**0.49**	**0.51**	**N**	**-**	**Spont.**	**N**	**-**	**Possible**	**Lake Coleridge, Ryton Station, Inland Canterbury, New Zealand**	**Whitehouse, 1981; Whitehouse and Griffiths 1983**
L	**Lake Coleridge Rock Avalanche 2, ~668 B.P.**	**Greywacke**	**Fractures/ Dipsl.**	**0.5**	**1,350**	**1,350**	**470**	**639**	**0.47**	**0.35**	**230**	**510**	**0.45**	**0.17**	**0.17**	**0.39**	**0.38**	**N**	**-**	**Part. forced**	**Y**	**-**	**Highly prob.**	**Lake Coleridge, Ryton Station, Inland Canterbury, New Zealand**	**None**
M	Dusty Cr., 1963	Dacite Pyrocl.r.	Fractures -30°	7	2,490	-	970	940	0.38	0.39	310	300	10.4	-	0.13	-	0.12	N	2	Spont.	N	-	Unlikely	Coast Mts., B.C., Canada	Clague and Souther, 1982
M	Elm, 1881	Slate	Fractures -50°	10	2,300	-	600	1,340	0.58	0.26	240	530	0.46	-	0.11	-	0.23	N	2	Spont.	N	Y	N	Glarus, Switzerland	Heim, 1932
M	Sasso Englar, unk.	Resistant volc. r.	Fractures -60°	13	1,680	-	370	1,100	0.65	0.22	990	1,010	0.98	-	0.59	-	0.60	N	-	Spont.	N	-	-	Eastern Alps, Italy	Fuganti, 1969
M	Drinov, unk.	Gneiss	Fractures -35°	18.5	1,560	-	410	900	0.58	0.26	330	320	1.03	-	0.21	-	0.21	-	1	Spont.	N	-	-	Krusne Hory Mts., Czechoslovakia	Spurek, 1974
M	Damocles, unk.	Carbon. r.	Dipsl. 17°	27	3,400	-	550	2,520	0.74	0.16	370	250	1.48	-	0.11	-	0.07	-	1	Spont.	N	-	Possible	Mackenzie Mts., N.W. Canada	Eisbacher, 1979
M	Mystery Cr., unk.	Diorite	Fractures	35	4,000	-	1,250	2,000	0.50	0.31	700	1,350	0.52	-	0.18	-	0.34	-	-	Spont.?	N	-	Possible	Coast Mts., B.C., Canada	Eisbacher, 1983
M	Goldau, 1806	Conglom.	Dipsl. 20°	35	6,100	-	1,120	4,300	0.70	0.18	1,660	3,700	0.45	-	0.27	-	0.61	N	1	Spont.	N	-	N	Schwyz, Switzerland	Heim, 1932
M	Frank, 1903	Limestone	Comp. sur. -45°	36.5	3,290	-	800	2,00	0.61	0.24	1,320	2,050	0.65	-	0.40	-	0.62	N	-	Spont.	N	Y	N	Front Ranges, Alberta, Canada	Cruden and Krahn, 1978; Strahler, 1984
M	Low. Gros Ventre, 1925	Landstone Limestone Soft sed. r.	Dipsl. 20°	38	4,350	-	660	3,300	0.76	0.15	960	910	1.05	-	0.22	-	0.21	N	(1)	Spont.?	Y?	-	Highly prob	Gros Ventre Range, WY, USA	Voight, 1978
M	Stalk Lakes, unk.	Clastic r.	Dipsl.30°?	53	3,000	-	700	1,880	0.63	0.23	640	1,880	0.34	-	0.21	-	0.63	-	-	Spont.	N	Y	-	Skeena Mts., B.C., Canada	Mollard, 1977
M	Lavini di Marco, 883	Carbon. r.	Dipsl. 20°	200	5,650	-	1,170	3,780	0.67	0.21	1,870	1,910	0.98	-	0.33	-	0.34	N	-	Spont.	N	-	N	Eastern Alps, Italy	Fuganti, 1969
M	Mont Granier, 1248	Limestone Marl	Dipsl. 12°	210	7,690	-	1,520	5,260	0.68	0.20	2,540	4,310	0.59	-	0.33	-	0.56	N	2	Spont.	N	Y	N	Western Alps, France	Cruden and Antoine, 1984; Eisbacher and Clague, 1984
M	Silver Reef, unk.	Marble	Fractures	227	6,670	-	760	5,460	0.82	0.11	2,120	2,820	0.75	-	0.32	-	0.42	N	-	Part. forced?	Y	-	-	S. Bernardino Mts., CA, USA	Shreve, 1968
M	Blackhawk, unk.	Marble	Fractures	283	9,860	-	1,100	8,100	0.82	0.11	2,140	2,720	0.79	-	0.22	-	0.28	N	-	Spont.	N	-	-	S. Bernardino Mts., CA, USA	Shreve, 1968
M	Martinez Mt., unk.	Gneiss	Fractures -30°	380	8,560	-	1,850	5,590	0.65	0.22	1,100	1,370	0.80	-	0.13	-	0.16	N	-	Spont.	N	-	-	S. Rosa Mts., CA, USA	Bock, 1977; Baldwin II, 1984
M	Rockslide Pass, unk.	Dolostone Limestone	Dipsl. 14°	493	6,330	-	1,000	4,730	0.75	0.16	1,280	1,720	0.74	-	0.20	-	0.27	N	1	Spont.	N	-	Possible	Mackenzie Mts., N.W. Canada	McLellan and Kaiser, 1984
M	Maligne Lake, unk.	Carbon r. Chert Shale	Dipsl. 25°	667	5,470	-	980	3,900	0.71	0.18	2,560	4,110?	0.62?	-	0.47	-	0.47?	N	-	Spont.	N	Y	-	Queen Elizabeth R., Alberta, Canada	Cruden, 1976; Mollard, 1977
M	Mayumarca, 1974	Sandstone Siltstone	Dipsl. 25°	1,600	8,000	-	1,800	5,120	0.64	0.22	1,380	3,800	0.38	-	0.17	-	0.48	N	(1)	Part. forced	Y	Y?	N	Cordillera Occidental, Peru	Lee and Duncan, 1975; Kojan and Hutchinson, 1978
H	Costantino, 1973	Gneiss	Fractures -25°	20	2,240	1,880	940	740	0.33	0.42	470	950	0.50	0.21	0.25	0.42	0.50	N	(1)	Forced	Y	N	N	Aspromonte R., South. Italy	Guerricchio and Melidoro, 1973; Nicoletti and Sorriso-Valvo, unpub. data
H	Madison Canyon, 1959	Geness Schist Dolostone	Fractures -30°	28	1,680	1,280	430	990	0.59	0.26	830	1,420	0.58	0.49	0.65	0.85	1.11	N	(1)	Forced	Y?	-	Y	Madison Range, MT, USA	Hadley, 1964, 1978
H	Monte Zandilla, 1987	Dior. gabbro Orthoquartz.	Fractures -35°	40	3,950	2,250	1,390	1,730	0.44	0.35	750	3,080	0.24	0.19	0.33	0.78	1.37	N	(1)	Forced	Y	N	N	Valtelina, Central Alps, Italy	Govi, written. commun., 1988; Nicoletti and Sorriso-Valvo, unpub. data
H	Hope, 1965	Basic metavolc. r.	Fractures -30°	47	4,240	2,800	1,220	2,280	0.54	0.29	1,200	3,720	0.32	0.28	0.43	0.88	1.33	N	(1)	Forced	Y?	Y	Highly prob.	Cascade Mts. B.C., Canada	Bruce and Cruden, 1977; Mathews and McTaggart, 1978
H	Triple Slide, unk.	Carbon r.	Dipsl. 15°	47	3,970	3,440	550	3,090	0.78	0.14	490	1,940	0.25	0.12	0.14	0.49	0.56	-	1(1)	Forced?	-	-	Possible	Mackenzie Mts., N.W. Canada	Eisbacher, 1979
H	Parpan, unk.	Dolostone crystal. r.	Scarpsl.?	400	6,550	4,200	1,340	4,410	0.67	0.20	1,600	6,350	0.25	0.24	0.38	0.97	1.51	-	1(1)	Forced	Y?	-	-	Graubunden, Switzerland	Heim, 1932; Abele, 1974

*L = low-energy-dissipative, M = moderate-energy-dissipative, H = high-energy-dissipative.
†In high-energy-dissipative conditions, D=L; consequently Wm/D>Wm/L and Wa/D>Wa/L; in low-energy- and moderate-energy-dissipative conditions, D=L
§Have been considered as "bends" the place where the broken line representing L forms angles.

APPENDIX F2

Relation of Travel Distance to size of Fallen Mass (modified from HSÜ, 1975)

Locality of event	Fahrböschung (degrees)	Equivalent coefficient of friction	Excessive travel distance L_e (km)	Volume (10^6 m^3)
Tsiolkosky (Moon)	3.5	0.06	?	1,200,000
Saidmarreh (Iran)	4.5	0.08	16.5	20,000
Fernpass (Austria)	5	0.09	13.3	1,000
Tamins	5.5	0.095	11.4	1,300
Deyen, Glarus	6.25	0.11	5.4	600
Silver Reef (U.S.A)	7.5	0.13	?	220
Blackhawk (U.S.A)	7.5	0.13	7.6	280
Flims	7.5	0.13	12.3	12,000
Siders	8	0.14	13.5	1,000 to 2,000
Gros Ventre (U.S.A)	10	0.17	2.5	38
Kandertal	11	0.19	6.9	140
Apollo 17 (Moon)	11	0.2	?	200
Sherman (U.S.A)	12	0.21	4	30
Goldau	12	0.21	4	30 to 40
Engelberg	12.5	0.22	4.8	2,500 to 3,000
Pamir	14	0.24	3.8	2,000
Frank (Canada)	14	0.25	2.1	30
Glarnisch	14	0.25	4.5	800
Madison	15	0.27	0.9	29
Scima da Saoseo	15	0.27	3.1	80
Lake Coleridge Rock Avalanche 1	**15.5**	**0.28**	**1.0**	**10**
Huascaran	17	0.3	11.8	2
Elm	17	0.31	1.15	10
Corno di Dosdé	18	0.32	1.8	20
Voralpsee	18	0.33	1.6	30

Locality of event	Fahrböschung (degrees)	Equivalent coefficient of friction	Excessive travel distance L_e (km)	Volume (10^6 m^3)
Diablerets	19	0.34	2.5	50
Vaiont (Italy)	19	0.34	0.7	250
Lake Coleridge Rock Avalanche 2	**19**	**0.35**	**0.6**	**0.5**
Disentis	20	0.36	0.9	10 to 20
Obersee GL	20	0.36	2.1	120
Poschivo	20	0.36	1.7	150
Wengen (2)	23	0.42	0.45	5 to 6
Val Lagone	24	0.44	0.7	0.5 to 0.8
Wengen (1)	24	0.45	0.3	2 to 3
Mombiel	23	0.47	0.2	0.8
Schächental	30	0.58	0.2	0.5
Airolo	33	0.64	0	0.5

Appendix G

G Grain size distribution of granule, sand, silt and clay size fractions shown as percentage of sample by weight from sandy "loess" horizon above glacial till from within T_1 and T_4

APPENDIX G

Grain size distribution of granule, sand, silt and clay size fractions shown as percentage of sample by weight from within sandy "loess" horizon above glacial till from within T_1 and T_4

T_1 – refer to figures 3.7, 3.10 and 3.11. Grid reference K35: 150 700. Samples A, B, C and D refer to location of sample within the sandy "loess" horizon (figure G1).

Sample 1/A	%	Sample 1/B	%
Granule	1.13	Granule	1.39
Sand	58.93	Sand	47.99
Silt	37.12	Silt	48.00
Clay	2.82	Clay	2.62

Sample 1/C	%	Sample 1/D	%
Granule	3.02	Granule	1.06
Sand	55.69	Sand	49.71
Silt	39.20	Silt	46.10
Clay	2.02	Clay	3.13

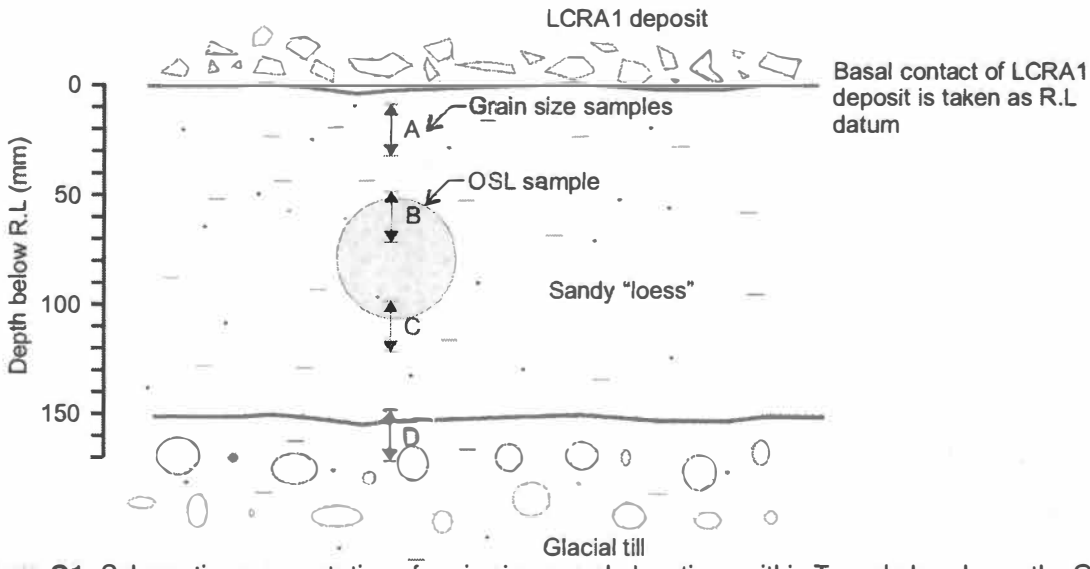

Figure G1: Schematic representation of grain size sample locations within T_1 and also shows the OSL sample taken from the sandy "loess" horizon.

T_4 – refer to figures 3.12 and 3.13. Grid reference K35: 655 295. Samples A, B, C and D refer to location of sample within the sandy "loess" horizon (figure G2).

Sample 4/A	%	Sample 4/B	%
Granule	9.90	Granule	0.54
Sand	41.91	Sand	51.87
Silt	42.46	Silt	43.26
Clay	5.73	Clay	4.33

Sample 4/C	%	Sample 4/D	%
Granule	9.38	Granule	2.95
Sand	52.50	Sand	47.94
Silt	34.70	Silt	42.32
Clay	3.42	Clay	6.79

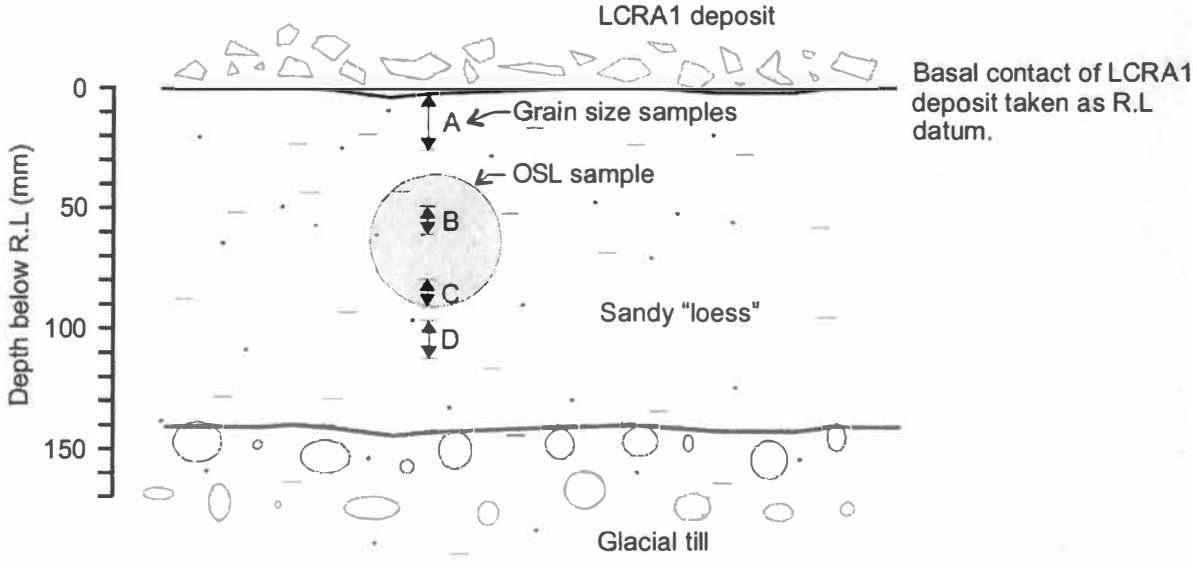

Figure G2: Schematic representation of grain size sample locations within T_4 and also shows the OSL sample taken from the sandy "loess" horizon.

Appendix H

H1 Radiocarbon dating Report by Dr HOGG (University of Waikato) on sample WK 14221.

H2 Radiocarbon dating Report by Dr HOGG (University of Waikato) on sample WK 15118.

H3 Radiocarbon dating Report by Dr HOGG (University of Waikato) on sample WK 15119.

H4 OSL Report by Dr RIESER (University of Victoria) on sandy "loess" located directly underneath the LCRA1 deposit.

APPENDIX H1

Report on Radiocarbon Age Determination for Wk 14221 to date the LCRA2 deposit. Mānuka sample located in cliffs lining the Ryton River. Grid reference K35: 440 575.

The University of Waikato

Radiocarbon Dating Laboratory

Private Bag 3105
Hamilton,
New Zealand.
Fax +64 7 838 4192
Ph +64 7 838 4278
email c14@waikato.ac.nz
Head: Dr Alan Hogg

Report on Radiocarbon Age Determination for Wk- 14221

Submitter	J Lee
Submitter's Code	L.Coleridge RA 1/5
Site & Location	Ryton Station, Lake Coleridge, New Zealand
Sample Material	Wood
Physical Pretreatment	Surfaces scraped clean. The wood was chopped up into small splinters and washed in ultrasonic bath.
Chemical Pretreatment	Sample was washed in hot 10% HCl, rinsed and treated with hot 1% NaOH. The NaOH insoluble fraction was treated with hot 10% HCl, filtered, rinsed and dried.

$d^{14}C$	-79.2 ± 4.2	‰
$\delta^{13}C$	-24.7 ± 0.2	‰
$D^{14}C$	-79.7 ± 4.2	‰
% Modern	92.0 ± 0.4	%
Result	**668 ± 36 BP**	

Comments

AG Hogg
26/8/04

- Result is *Conventional Age or % Modern* as per Stuiver and Polach, 1977, Radiocarbon 19, 355-363. This is based on the Libby half-life of 5568 yr with correction for isotopic fractionation applied. This age is normally quoted in publications and must include the appropriate error term and Wk number.
- Quoted errors are 1 standard deviation due to counting statistics multiplied by an experimentally determined Laboratory Error Multiplier of 1
- The isotopic fractionation, $\delta^{13}C$, is expressed as ‰ wrt PDB.
- Results are reported as *% Modern* when the conventional age is younger than 200 yr BP.

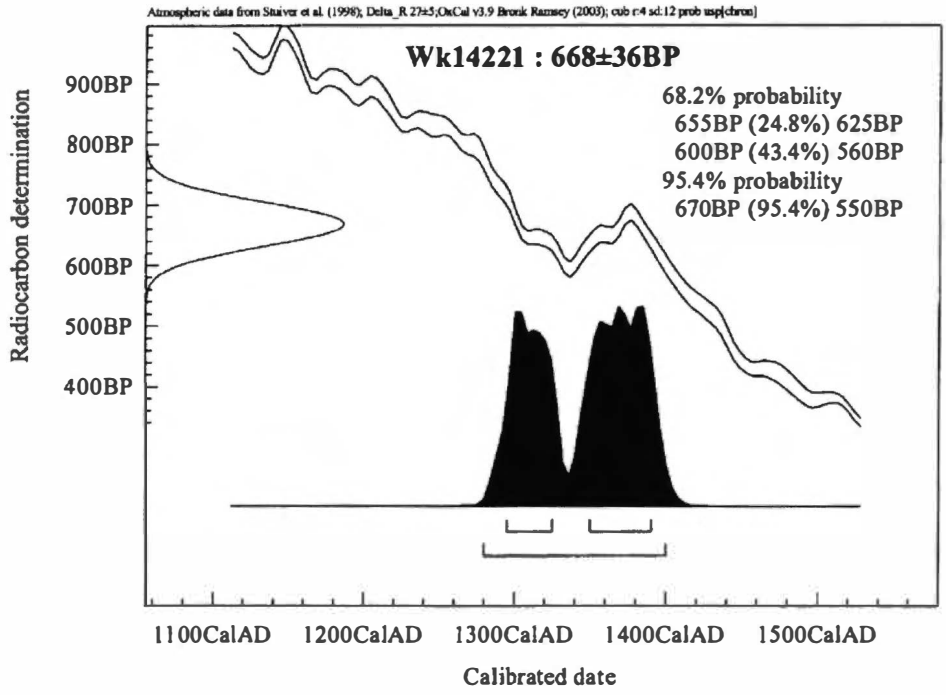
Atmospheric data from Stuiver et al. (1998); Delta_R 27±5;OxCal v3.9 Bronk Ramsey (2003); cub r:4 sd:12 prob usp[chron]
Wk14221 : 668±36BP
68.2% probability
655BP (24.8%) 625BP
600BP (43.4%) 560BP
95.4% probability
670BP (95.4%) 550BP
Radiocarbon determination
900BP
800BP
700BP
600BP
500BP
400BP
1100CalAD
1200CalAD
1300CalAD
1400CalAD
1500CalAD
Calibrated date

APPENDIX H2

Report on Radiocarbon Age Determination for Wk 15118 to date the upper ruptured charcoal horizon within T_5 across the Carriage Drive Fault. Grid reference K35: 985 850.

The University of Waikato

Radiocarbon Dating Laboratory

Private Bag 3105
Hamilton,
New Zealand.
Fax +64 7 838 4192
Ph +64 7 838 4278
email c14@waikato.ac.nz
Head: Dr Alan Hogg

Report on Radiocarbon Age Determination for Wk- 15118

(AMS measurement by IGNS [NZA-20567])

Submitter	J Lee
Submitter's Code	CDF3
Site & Location	Carriage Drive Fault, Lake Coleridge, Canterbury,, New Zealand
Sample Material	Charcoal
Physical Pretreatment	Possible contaminants were removed. Washed in ultrasonic bath.
Chemical Pretreatment	Sample washed in hot 10% HCl, rinsed and treated with hot 0.5% NaOH. The NaOH insoluble fraction was treated with hot 10% HCl, filtered, rinsed and dried.

$d^{14}C$	-80.4 ± 4.9	‰
$\delta^{13}C$	-23.5 ± 0.2	‰
$D^{14}C$	-89.8 ± 5.1	‰
% Modern	91.0 ± 0.5	%
Result	**755 ± 46 BP**	

Comments

AGHogg

26/8/04

- Result is *Conventional Age or % Modern* as per Stuiver and Polach, 1977, Radiocarbon 19, 355-363. This is based on the Libby half-life of 5568 yr with correction for isotopic fractionation applied. This age is normally quoted in publications and must include the appropriate error term and Wk number.
- Quoted errors are 1 standard deviation due to counting statistics multiplied by an experimentally determined Laboratory Error Multiplier of 1
- The isotopic fractionation, $\delta^{13}C$, is expressed as ‰ wrt PDB.
- Results are reported as *% Modern* when the conventional age is younger than 200 yr BP.

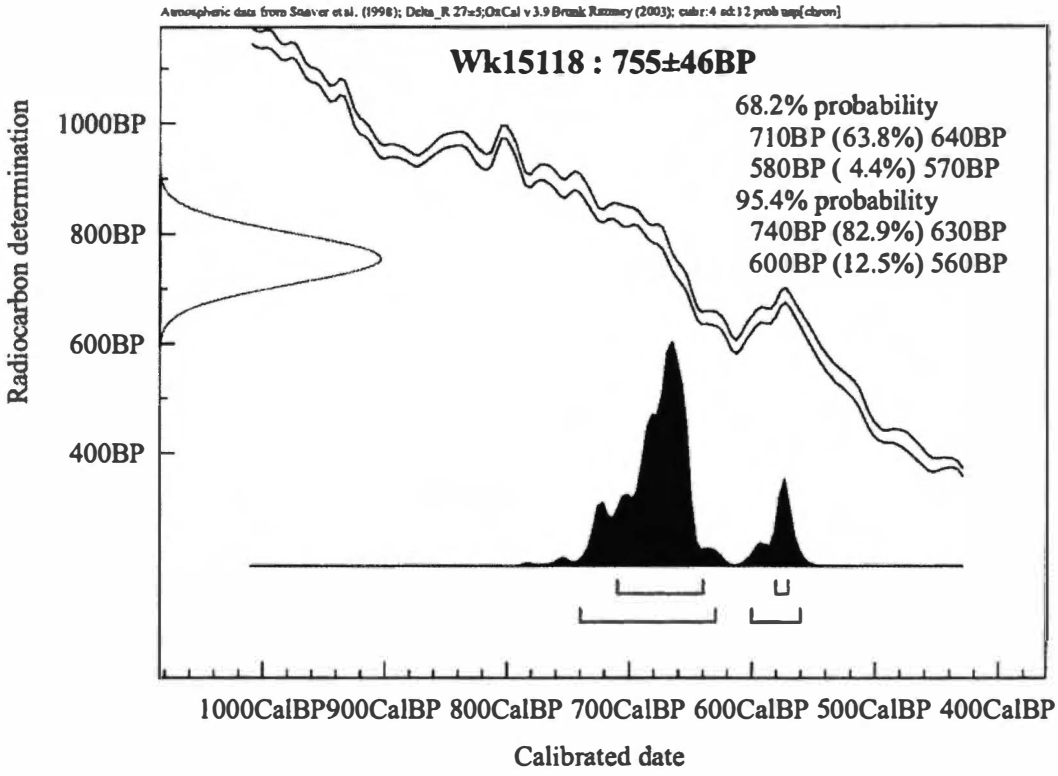
Atmospheric data from Stuiver et al. (1998); Delta_R 27±5;OxCal v 3.9 Bronk Ramsey (2003); cub r:4 sd:12 prob usp[chron]
Wk15118 : 755±46BP
68.2% probability
710BP (63.8%) 640BP
580BP (4.4%) 570BP
95.4% probability
740BP (82.9%) 630BP
600BP (12.5%) 560BP
Radiocarbon determination
1000BP
800BP
600BP
400BP
1000CalBP 900CalBP 800CalBP 700CalBP 600CalBP 500CalBP 400CalBP
Calibrated date

APPENDIX H3

Report on Radiocarbon Age Determination for Wk 15119 to date the lower ruptured charcoal horizon within T_5 across the Carriage Drive Fault. Grid reference K35: 985 850.

The University of Waikato

Radiocarbon Dating Laboratory

Private Bag 3105
Hamilton,
New Zealand.
Fax +64 7 838 4192
Ph +64 7 838 4278
email c14@waikato.ac.nz
Head: Dr Alan Hogg

Report on Radiocarbon Age Determination for Wk- 15119

Submitter	J Lee
Submitter's Code	CDF4
Site & Location	Carriage Drive Fault, Lake Coleridge, Canterbury,, New Zealand
Sample Material	Charcoal
Physical Pretreatment	Possible contaminants were removed. Washed in ultrasonic bath.
Chemical Pretreatment	Sample washed in hot 10% HCl, rinsed and treated with hot 1% NaOH. The NaOH insoluble fraction was treated with hot 10% HCl, filtered, rinsed and dried.

$d^{14}C$	-422.0 ± 2.5	‰
$\delta^{13}C$	-23.4 ± 0.2	‰
$D^{14}C$	-423.8 ± 2.5	‰
% Modern	57.6 ± 0.2	%
Result	**4428 ± 35 BP**	

Comments

AGHogg

26/8/04

- Result is *Conventional Age or % Modern* as per Stuiver and Polach, 1977, Radiocarbon 19, 355-363. This is based on the Libby half-life of 5568 yr with correction for isotopic fractionation applied. This age is normally quoted in publications and must include the appropriate error term and Wk number.
- Quoted errors are 1 standard deviation due to counting statistics multiplied by an experimentally determined Laboratory Error Multiplier of 1
- The isotopic fractionation, $\delta^{13}C$, is expressed as ‰ wrt PDB.
- Results are reported as *% Modern* when the conventional age is younger than 200 yr BP.

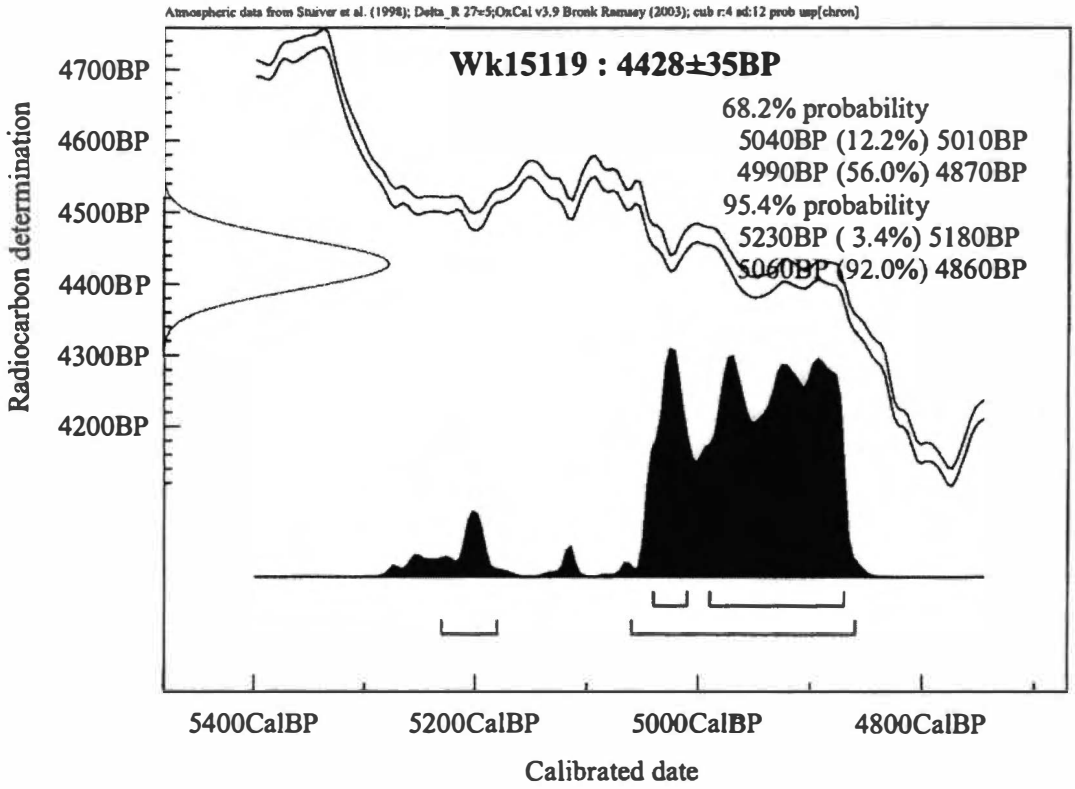
Atmospheric data from Stuiver et al. (1998); Delta_R 27±5;OxCal v3.9 Bronk Ramsey (2003); cub r:4 sd:12 prob usp[chron]
Wk15119 : 4428±35BP
68.2% probability
5040BP (12.2%) 5010BP
4990BP (56.0%) 4870BP
95.4% probability
5230BP (3.4%) 5180BP
5060BP (92.0%) 4860BP
Radiocarbon determination
4700BP
4600BP
4500BP
4400BP
4300BP
4200BP
5400CalBP
5200CalBP
5000CalBP
4800CalBP
Calibrated date

APPENDIX H4

Determination of sediment deposition ages by Optically Stimulated Luminescence dating of sandy "loess" sampled from T_4 underlying the LCRA1 deposit (figures 3.12, 3.13 and G2). Grid reference K35: 655 295.

VICTORIA UNIVERSITY OF WELLINGTON
Te Whare Wānanga o te Ūpoko o te Ika a Māui

Determination of sediment deposition ages by Luminescence Dating

Dr. Uwe Rieser

04/11
Technical Report
22th May 2004

SCHOOL OF EARTH SCIENCES
Te Kura Tātai Aro Whenua
P.O. Box 600, Wellington, New Zealand
Telephone +64-4-463-5337, Facsimile +64-4-463-5186

Luminescence Dating of 1 sample / Lake Coleridge

report by: Dr. Uwe Rieser
Luminescence Dating Laboratory / School of Earth Sciences
Victoria University of Wellington
e-mail: uwe.rieser@vuw.ac.nz
tel: 0064-4-463-6125
fax: 0064-4-463-5186

Summary
1 sample (laboratory code WLL389) was submitted for Luminescence Dating by Jenny Lee (University of Canterbury). The deposition age has been determined using the silt fraction. The palaeodose, i.e. the radiation dose accumulated in the sample after the last light exposure (assumed at deposition), was determined by measuring the blue luminescence output during infrared optical stimulation (which selectively stimulates the feldspar fraction). The doserate was estimated on the basis of a low level gammaspectrometry measurement.
All measurements were done in Victoria Universities Dating Laboratory.

Procedure / Luminescence measurements
Sample preparation was done under extremely subdued safe orange light in a darkroom. Outer surfaces, which may have seen light during sampling, were removed and discarded.
The actual water content and the saturation content were measured using 'fresh' inside material.
The sample was treated with 10%HCl to remove carbonates until the reaction stopped, then carefully rinsed with distilled water. Thereafter, all organic matter was destroyed with 10%H_2O_2 until the reaction stopped, then carefully rinsed with distilled water. By treatment with a solution of sodium citrate, sodium bicarbonate and sodium dithionate iron oxide coatings were removed from the mineral grains and then the sample was carefully rinsed again.
The grain size 4-11µm was extracted from the sample in a water-filled (with added dispersing agent to deflocculate clay) measuring cylinder using Stokes' Law. The other fractions were discarded. The sample then was brought into suspension in pure acetone and deposited evenly in a thin layer on 70 aluminum discs (1cm diameter).
Luminescence measurements were done using a standard Riso TL-DA15 measurement system, equipped with Kopp 5-58 and Schott BG39 optical filters to select the luminescence blue band. Stimulation was done cw at about 30mW/cm^2 with infrared diodes at 880Δ80nm. β-irradiations were done on a Daybreak 801E ^{90}Sr,^{90}Y β-irradiator, calibrated against SFU, Vancouver, Canada to about 3% accuracy. α-irradiations were done on a ^{241}Am irradiator supplied and calibrated by ELSEC, Littlemore, UK.

The Paleodose was estimated by use of the multiple aliquot additive-dose method (with late-light subtraction). After an initial test-measurement, 30 aliquots were β-irradiated in six groups up to six times of the dose result taken from the test. 9 aliquots were α-irradiated in three groups up to three times of the dose result taken from the test. These 39 disks were stored in the dark for four weeks to relax the crystal lattice after irradiation.
After storage, these 39 disks and 9 unirradiated disks were preheated for 5min at 220C to remove unstable signal components, and then measured for 100sec each, resulting in 39

shinedown curves. These curves were then normalized for their luminescence response, using 0.1s shortshine measurements taken before irradiation from all aliquots.
The luminescence growth curve (β-induced luminescence intensity vs added dose) is then constructed by using the initial 10 seconds of the shine down curves and subtracting the average of the last 20 sec, the so called late light which is thought to be a mixture of background and hardly bleachable components. The shine plateau was checked to be flat after this manipulation. Extrapolation of this growth curve to the dose-axis gives the equivalent dose D_e, which is used as an estimate of the Paleodose.
A similar plot for the alpha-irradiated discs allows an estimate of the α-efficiency, the a-value (Luminescence/dose generated by the α-source divided by the luminescence/dose generated by the β-source).

Fading test
Samples containing feldspars in rare cases show an effect called anomalous fading. This effect inhibits accurate dating of the sample, as the electron traps in the crystal lattice of these feldspars are unable to store the age information over longer periods of time.
Your sample did not give an indication of this problem so far, but a routine test must be carried out after 6 months storage of an irradiated subsample to be sure. Thus, the age reported below must be seen as preliminary until the fading test has been carried out. You will be notified by e-mail about the result.

Procedure / Gamma spectrometry
The dry, ground and homogenised soil sample was encapsuled in an airtight perspex container and stored for at least 4 weeks. This procedure minimizes the loss of the short-lived noble gas ^{222}Rn and allows ^{226}Ra to reach equilibrium with its daughters ^{214}Pb and ^{214}Bi.

The sample was counted using high resolution gamma spectrometry with a broad energy Ge detector for a minimum time of 24h. The spectrum was analysed using GENIE2000 software. The doserate calculation is based on the activity concentration of the nuclides ^{40}K, ^{208}Tl, ^{212}Pb, ^{228}Ac, ^{214}Bi, ^{214}Pb, ^{226}Ra.

Results

Table1: Doserate contribution of cosmic radiation

Sample no.	depth below surface (m)	dD_e/dt (Gy/ka)[1]	Field code
WLL389	2	0.1732±0.0087	LCRA1

[1] Contribution of cosmic radiation to the total doserate, calculated as proposed by Prescott & Hutton (1994), Radiation Measurements, Vol. 23.

Table2: Radionuclide and water content

Sample no.	Water content δ^1	U (µg/g) from ^{214}Th	U (µg/g)[2] from ^{226}Ra, ^{214}Pb, ^{214}Bi	U (µg/g) from ^{210}Pb	Th (µg/g)[2] from ^{208}Tl, ^{212}Pb, ^{228}Ac	K (%)	Field code
WLL389	1.200	4.00±0.50	2.62±0.05	3.24±0.47	12.93±0.19	2.78±0.06	LCRA1

[1] Ratio wet sample to dry sample weight. Errors assumed 50% of (δ-1).
[2] U and Th-content is calculated from the error weighted mean of the isotope equivalent contents
All numbers marked in red: Minor radioactive disequilibrium (significant on 2σ-level), between 234Th and 226Ra (likely due to removal of solved 226Ra from the site, caused by groundwaterflow).

Table3: Measured a-value and equivalent dose, doserate and luminescence age

Sample no.	a-value	D_e (Gy)	dD/dt (Gy/ka)	**OSL-age (ka)**	Field code
WLL389	0.041±0.003	45.2±1.6	4.65±0.29 (4.42±0.29)	**9.72±0.75 (10.2±0.8)**	LCRA1

* The sample showed a radioactive disequilibrium (see table 2), and the given age was corrected accordingly. As the level of disequilibrium over time is unknown, this age is only a better estimate and cannot be seen as the 'true' age. In brackets the uncorrected doserate and age is given, calculated under the invalid assumption that the sample was in radioactive equilibrium (226Ra content used for calculation).

Comment:
The sample originates from a relatively thin layer of Loess (~20cm thickness), so some of the absorbed gamma-radiation originates from the under- and overlying Greywacke. As the radionuclide contents of the Greywacke may vary from the Loess, there is a slight uncertainty in the doserate calculation (which was done under the assumption of an infinite homogenous Loess matrix). However, given the relatively high radioactivity of the Loess, this problem is probably negligible.